

University of Dundee

DOCTOR OF PHILOSOPHY

Functional analysis of the Argonaute family proteins during early embryonic and germ cell development in the mouse

Comazzetto, Stefano

Award date:
2013

Awarding institution:
University of Dundee

[Link to publication](#)

General rights

Copyright and moral rights for the publications made accessible in the public portal are retained by the authors and/or other copyright owners and it is a condition of accessing publications that users recognise and abide by the legal requirements associated with these rights.

- Users may download and print one copy of any publication from the public portal for the purpose of private study or research.
- You may not further distribute the material or use it for any profit-making activity or commercial gain
- You may freely distribute the URL identifying the publication in the public portal

Take down policy

If you believe that this document breaches copyright please contact us providing details, and we will remove access to the work immediately and investigate your claim.

Download date: 17. Feb. 2017

DOCTOR OF PHILOSOPHY

Functional analysis of the Argonaute family proteins during early embryonic and germ cell development in the mouse

Stefano Comazzetto

2013

University of Dundee

Conditions for Use and Duplication

Copyright of this work belongs to the author unless otherwise identified in the body of the thesis. It is permitted to use and duplicate this work only for personal and non-commercial research, study or criticism/review. You must obtain prior written consent from the author for any other use. Any quotation from this thesis must be acknowledged using the normal academic conventions. It is not permitted to supply the whole or part of this thesis to any other person or to post the same on any website or other online location without the prior written consent of the author. Contact the Discovery team (discovery@dundee.ac.uk) with any queries about the use or acknowledgement of this work.



**“Functional analysis of the Argonaute
family proteins during early
embryonic and germ cell development
in the mouse”**

S. Comazzetto

**“Functional analysis of the Argonaute family
proteins during early embryonic and germ cell
development in the mouse”**

**Stefano Comazzetto MSc, BSc
EMBL Mouse Biology Unit, Rome**

**Submitted for the degree of Doctor of Philosophy at the
University of Dundee**

College of Medicine, Nursing and Dentistry

Supervisors: Dr. Dónal O’Carroll

Pr. Stephen M. Keyse

December 2013

Table of content

Table of content	1
List of Tables and Figures	4
Acknowledgement	6
Declaration	8
Summary	9
Abbreviation	10
Chapter 1: Introduction	15
1.1 Argonaute proteins bind distinct classes of small non-coding RNAs	15
1.2 Argonaute protein family: Ago and Piwi subclades	17
1.3 Structural domains of the Argonaute family proteins	19
1.4 The miRNA and siRNA pathways	21
1.4.1 miRNA biogenesis	21
1.4.2 siRNA biogenesis.....	22
1.4.3 Determinants of miRNA-target interaction	25
1.4.4 miRNAs silence target RNAs through multiple mechanisms.....	27
1.4.5 siRNAs silence target genes both at the transcriptional and post-transcriptional levels	28
1.4.6 Regulation of miRNA activity	30
1.5 Argonaute 2: central component of miRNA and siRNA silencing pathways in mammals	32
1.5.1 Physiological relevance of Ago2 in mouse	32
1.5.2 Regulation of Ago2 activity by post-translational modifications.....	34
1.6 The piRNA pathway	37
1.6.1 piRNA biogenesis	37
1.6.2 piRNA-mediated silencing mechanisms.....	42
1.7 Physiological relevance of piRNAs in flies and mouse germ cell development	43
1.8 PIWI proteins contribute to stem cell maintenance in different organisms	47
1.9 The quest for the identification of the spermatogonial stem cell	48
1.9.1 The “A single” and the “reserve stem cell” models for spermatogonial stem cells	48
1.9.2 Identification of spermatogonial stem cells: methods and markers	52
Chapter 2: Materials and methods	55
2.1 Generation of <i>Ago2</i>^{S388A} and <i>Miwi2</i>^{tdTomato} alleles	55
2.1.1 <i>Ago2</i> ^{S388A} targeting strategy	55
2.1.2 <i>Miwi2</i> ^{tdTomato} targeting strategy	55
2.2 Generation of mice using homologous recombination in mouse embryonic stem cells	56
2.3 PCR genotyping of <i>Ago2</i> and <i>Miwi2</i> mouse alleles	57
2.3.1 Genotype protocol for <i>Ago</i> ^{Neo-S388A} allele	57
2.3.2 Genotype protocol for <i>Ago</i> ^{S388A} , <i>Ago2</i> ^{FL} and <i>Ago2</i> ⁻ allele.....	58
2.3.2 Genotype protocol for <i>Miwi2</i> ^{tdTomato} allele	60
2.4 Southern Blot on restriction enzyme-digested genomic DNA	61

2.4.1 Isolation of DNA for Southern Blot	61
2.4.2 Preparation of Southern Blot probes	61
2.4.3 Southern Blot.....	62
2.5 Sequencing of wild type and <i>Ago2</i>^{S388A} alleles.....	63
2.6 Isolation and PCR genotyping of mouse embryos from <i>Ago2</i>^{S388A/+} intercrosses	65
2.6.1 Isolation and genotyping of embryos at embryonic day from E6.5 to E12.5	65
2.6.2 Isolation of embryos at embryonic day E3.5	65
2.6.3 PCR genotyping of embryos isolated at E3.5 by nested PCR	66
2.7 Analysis of fertility in <i>Ago2</i>^{S388A} mutant animals	67
2.8 Isolation of cells from bone marrow, spleen, testis and thymus for flow	
cytometry	68
2.8.1 Isolation of single cell suspension from bone marrow	68
2.8.2 Isolation of single cell suspension from spleen and thymus	69
2.8.3 Erythrolysis of bone marrow and splenic single cell suspensions.....	69
2.8.4 Isolation of single cell suspension from juvenile male testis.....	70
2.8.5 Isolation of single cell suspension adult male testis.....	71
2.9 Poly I:C and lypopolysaccharide treatment	71
2.10 Generation of chimeric mice by bone marrow transplantation	72
2.11 Quantitative analysis of peripheral blood	72
2.12 Immunostaining of hematopoietic and testicular cells for flow cytometry	
analysis and sorting.....	73
2.12.1 General immunostaining protocol for erythroid, lymphoid and myeloid lineages.....	73
2.12.2 Immunostaining protocol for hematopoietic stem cell and early progenitor	
populations.....	74
2.12.3 Immunostaining of testicular cells for flow cytometry analysis and sorting.....	75
2.12.4 List of antibodies used in this study	76
2.12.5 Definition of hematopoietic cell populations during this study	79
2.13 Generation and purification of a phospho-specific S388 <i>Ago2</i> antibody (in	
collaboration with Sabin Antony and Maria Placentino).....	80
2.14 Overexpression of wild type and S388A mouse <i>Ago2</i> in cultured cells (in	
collaboration with Maria Placentino)	81
2.15 Western Blot.....	82
2.15.1 Production of a phosphorylated L2 linker domain in vitro (in collaboration with Dr.	
Philipp Selenko, FMP Berlin)	82
2.15.2 Protein extracts preparation from transfected HEK293T cells	83
2.15.3 Resolution of proteins by SDS-PAGE	83
2.15.4 Blotting of proteins onto membranes.....	83
2.15.5 Blocking and antibody staining	84
2.15.6 Stripping of membrane for immunoblot.....	84
2.16 Immunofluorescence staining of human cells and mouse tissues	85
2.16.1 Staining of transfected HeLa cells.....	85
2.16.2 Staining of embryonic day E3.5 mouse blastocyst (in collaboration with Maria	
Placentino).....	86
2.16.3 Staining of testis section from embryonic day E16.5 male mouse (In collaboration	
with Dr. Claudia Carrieri)	87
2.17 Quantitative real-time PCR.....	88
2.17.1 RNA isolation from sorted testis cells.....	88
2.17.2 Reverse transcription and real time PCR from isolated RNA	89
2.18 Data analysis	91
Annex 1: Media and solution	91

Chapter 3: Phosphorylation of Ago2 serine 388 is necessary for embryonic development depending on the genetic background.....	95
3.1 Results.....	95
3.1.1 Generation of a non-phosphorylatable Ago2 allele <i>in vivo</i>	95
3.1.2 Homozygous phosphomutant mice are lethal in a mixed genetic background	100
3.1.3 Ago2 S388 phosphorylation is dispensable for hematopoiesis	103
3.1.4 Ago2 S388 phosphorylation is dispensable for female fertility.....	110
3.1.5 Ago2 S388 phosphorylation is not necessary for Ago2-dependent processes in the C57Bl/6N genetic background	112
3.1.6 Ago2 S388 phosphorylation is dispensable for endotoxic stress response	118
3.1.7 Ago2 S388 phosphorylation is necessary for embryonic development in the 129S2 genetic background.....	121
3.1.8 Differential phenotype of Ago2 S388 mutation between C57Bl/6N and 129S2 genetic backgrounds depends on loci close to the Ago2 locus.....	124
3.1.9 Development of an Ago2 phospho-serine 388 specific antibody.....	126
3.2 Discussion.....	130
3.2.1 Ago2 S388 phosphorylation and hematopoietic development.....	130
3.2.2 Ago2 S388 phosphorylation significance during oocyte maturation.....	132
3.2.3 Ago2 S388 phosphorylation in embryonic development: a background-dependent effect.....	135
3.2.3.1 Lack of Ago2 phosphorylation at serine 388 causes embryonic defects at the peri-implantation stage.....	135
3.2.3.2 Mutation of Ago2 serine 388 reveals the importance of genetic background on the phenotypic consequences of post-translational modification site mutations	139
3.2.3.3 Embryonic lethality of Ago2 S388A mutants points to other kinases involved in Ago2 phosphorylation	144
3.3 Conclusions and future plans.....	148
Chapter 4: Miwi2 expression marks a population of spermatogonia with stem cell characteristics	151
4.1 Results.....	151
4.1.1 Generation of reporter allele to mark Miwi2-expressing cells <i>in vivo</i>	151
4.1.2 The <i>Miwi2^{tdTomato}</i> allele labels two distinct populations of germ cells in juvenile mice	154
4.1.3 The tdTomato ⁺ c-Kit ⁻ cellular fraction has cell cycle and gene-expression profile typical of a stem cell population.....	160
4.1.4 Comparison of tdTomato ⁺ c-Kit ⁻ cellular fraction from adult and juvenile testis shows similar surface marker profile	164
4.2 Discussion.....	167
4.2.1 Miwi2 is expressed in the testis of juvenile male mice.....	167
4.2.2 The <i>Miwi2^{tdTomato}</i> allele marks a population of germ cells presenting several stem cell properties.....	168
4.2.3 Miwi2 marks two similar cell populations in both adult and juvenile mouse testes.....	172
4.3 Conclusions and future plans.....	175
Bibliography	177

List of Tables and Figures

Figure 1.	pp.24	miRNA and siRNA biogenesis.
Figure 2.	pp.41	piRNA biogenesis.
Figure 3.	pp.46	Germ cell development in mouse testis.
Figure 4.	pp.51	Spermatogonia organization in the murine testis.
Figure 5.	pp.97	Targeting strategy and validation of the <i>Ago2</i> ^{Neo-S388A} allele.
Figure 6.	pp.99	Breeding strategy of the <i>Ago2</i> ^{S388A/+} animals employed during this study.
Figure 7.	pp.102	<i>Ago2</i> ^{S388A/S388A} homozygous mutants are lethal in a mixed genetic background.
Figure 8.	pp.104	No defects in adult hematopoietic development in <i>Ago2</i> ^{S388A/FL} ; <i>Mx-Cre</i> mice upon Cre-induction.
Figure 9.	pp.107	Ago2 S388 phosphorylation is not necessary for erythroid development in a cell-autonomous fashion.
Figure 10.	pp.109	Ago2 S388 phosphorylation is not necessary for lymphoid and myeloid development in a cell-autonomous fashion.
Figure 11.	pp.111	Ago2 S388 phosphorylation is dispensable for oogenesis.
Figure 12.	pp.113	<i>Ago2</i> ^{S388A/S388A} animals are viable and fertile in a C57Bl/6N genetic background.
Figure 13.	pp.114-115	No defects in adult hematopoietic development in <i>Ago2</i> ^{S388A/S388A} animals in a C57Bl/6N genetic background.
Figure 14.	pp.117	No defects in HSC and early hematopoietic progenitors in <i>Ago2</i> ^{S388A/S388A} animals in a C57Bl/6N genetic background.
Figure 15.	pp.120	Ago2 phosphorylation at S388 is not necessary for MK2-dependent endotoxic response.
Figure 16.	pp.123	<i>Ago2</i> ^{S388A/S388A} homozygous mutants are lethal in 129S2 genetic background.
Figure 17.	pp.124	<i>Ago2</i> ^{S388A/S388A} homozygous mutants are viable in a reverse F ₂ genetic background.
Figure 18.	pp.127	No differences in phosphorylation levels of Ago2 S388

		between 129S2 and C57Bl/6N at blastocyst stage.
Figure 19.	pp.153	Targeting strategy and validation of the <i>Miwi2</i> ^{tdTomato} allele.
Figure 20.	pp.155	Miwi2 expression marks two populations of spermatogonia in juvenile mouse testis.
Figure 21.	pp.157	TdTomato ⁺ c-Kit ⁻ cell population possesses a surface marker profile reminiscent of SSCs.
Figure 22.	pp.159	TdTomato ⁺ c-Kit ⁺ cell population possesses a surface marker profile of more differentiated spermatogonia.
Figure 23.	pp.161	Cell cycle profile of tdTomato ⁺ c-Kit ⁻ and tdTomato ⁺ c-Kit ⁺ cells.
Figure 24.	pp.163	Expression profile of tdTomato ⁺ c-Kit ⁻ reveals a stem cell signature.
Figure 25.	pp.166	Adult and juvenile tdTomato ⁺ c-Kit ⁻ cells share similar surface marker expression profiles.
Table 1.	pp.37	Post-translational modification of the human Ago2 protein.

Acknowledgement

My sincere thanks go to Dr. Dònal O'Carroll. He was an invaluable source of ideas, comments and technical suggestions during my PhD in his lab. It was a great opportunity to learn from him to thoroughly think and analyse every single experiment, without losing the focus on the main target of the project. Furthermore, I would like to express my gratitude to all the members of my Thesis Advisory Committee, and in particular to Prof. Stephen M. Keyse, for their valuable and beneficial suggestions.

I would like to acknowledge the people in the several EMBL Facilities that helped and supported me in this thesis work. In particular, I would like to thank Dr. Giulia Bolasco from the EMBL Monterotondo Microscopy Facility and Dr. Pedro Moreira from the EMBL Monterotondo Transgenic Facility for their assistance with microscopes and the generation of transgenic mice, respectively. In addition, my gratitude goes to Dr. Philip Hublitz from the EMBL Monterotondo Gene Expression Facility for his services in the creation of the targeting constructs as well as to the numerous suggestions during my PhD. Finally, I would like to thank Dr. Daniel Bilbao-Cortes from the EMBL Flow Cytometry facility for his enormous help and support during the several hours spent at the flow cytometer.

My immense gratitude goes to all the previous and present members of the O'Carroll group and the members of the Buonomo group. In particular, I would like to acknowledge Dr. Claudia Carrieri for the help and the data sharing for the Miwi2 project (Fig. 19). Furthermore, my special thanks go to Maria Placentino: her hard work was endlessly in the purification and testing of the phospho-specific antibody as well as in the final characterization of the Ago2 phenotype (Fig. 16 and 18). Finally, I would like to thank the PhD and post-doc community in EMBL Monterotondo that made my years in the lab much more acceptable, and sometimes funny too.

Last, the biggest thanks go to my family, my dad Carlo, my mom Sonia and my little sister Chiara. They have been always supportive during the darkest periods and helped

me to continue on my journey to become a scientist when I was discouraged. I would not reach the end of my PhD without their constant care and affection.

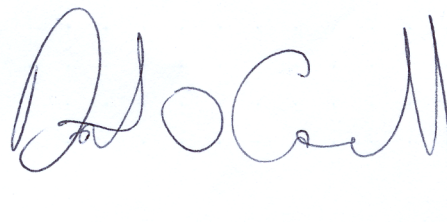
Declaration

I hereby declare that the following thesis is based on the results of investigations conducted by myself and that this thesis is of my own composition. Work other than my own is clearly indicated in the text by reference to the original publications. This dissertation has not in whole, or in part, been previously submitted for a higher degree.

A handwritten signature in black ink, appearing to read 'Stefano Comazzetto', with a long horizontal stroke extending to the right.

Stefano Comazzetto

I certify that Stefano Comazzetto has spent the equivalent of eight terms in research work at the Mouse Biology Unit, EMBL Monterotondo, and that he has fulfilled the conditions of the Ordinance General No. 14 of the University of Dundee and is qualified to submit the accompanying thesis in application for the degree of Doctor of Philosophy.

A handwritten signature in blue ink, appearing to read 'Dónal O'Carroll', with a long vertical stroke extending downwards from the end.

Dr. Dónal O'Carroll

Summary

Argonaute proteins are known regulators of gene expression through their association with small non-coding RNAs. Specifically in mammals, microRNAs (miRNA) and short interfering RNAs (siRNAs) bind to Ago-like subclade of the Argonaute family to regulate gene expression, while Piwi-interacting RNAs (piRNAs) associate with PIWI proteins to silence transposons in the germ line.

In mammals, genetic experiments revealed that Ago2 is the central effector for both siRNA and miRNA silencing pathways in several developmental processes. Phosphorylation of serine 388 of murine protein is dependent on the MK2 and Akt/PKB pathways and regulates Ago2 localization. I created a nonphosphorylatable *Ago2*^{S388A} allele to study this phosphorylation event during mouse development. Lack of Ago2 phosphorylation is dispensable for adult hematopoiesis, oogenesis, and for the MK2-dependent endotoxic stress response. Furthermore, I discovered a partially penetrant lethal phenotype of *Ago2*^{S388A/S388A} embryos at peri-implantation in mixed 129P2xC57Bl6N and 129S2 genetic backgrounds, but not in C57Bl/6N background. In conclusion, I demonstrated for the first time that mutation of a post-translational modification site has a differential phenotypic outcome depending on the genetic background.

Genetic ablation of PIWI-proteins in the mouse leads to a block in male meiosis. Strikingly, loss of Miwi2 causes an additional progressive loss of germ cells, reminiscent of a stem cell phenotype. However, Miwi2 levels are high in fetal testis and become undetectable soon after birth. I generated a *Miwi2*^{tdTomato} transcriptional reporter allele and proved that Miwi2 expression marks a subpopulation of spermatogonial cells that possesses surface markers, cell cycle and gene expression profile reminiscent of stem cells in juvenile testis. Comparison of juvenile and adult Miwi2-expressing cells revealed a significant difference in Thy-1 surface expression, which could be indicative of a higher self-renewal capacity in young cells. In summary, these data posit that Miwi2 expression defines a population of *bona fide* stem cells in the mouse testis.

Abbreviation

ADAR	Adenosine deaminase acting on RNA
ADP	Adenosine diphosphate
Ago1	Argonaute 1
Ago2	Argonaute 2
Ago3	Argonaute 3
Akt/PKB	Protein kinase B
A _{al}	A aligned spermatogonia
A _{pr}	A paired spermatogonia
A _s	A single spermatogonia
As	Arsenite trioxide
Aub	Aubergine
C3PO	Tanslin/Component 3 of promoter of RISC
CFU-E	Colony forming unit erythroid
c-Kit	V-Kit Hardy-Zuckerman 4 feline sarcoma viral oncogene homolog
CNV	Copy number variant
C-P4H(I)	Type I collagen prolyl-4-hydroxylase
c-Ret	Proto-oncogene tyrosine-protein kinase receptor
DAPI	4',6-diamidino-2-phenylindole
D-Gal	D-Galactose
DCL-3	Endoribonuclease Dicer homolog 3
DCL-4	Endoribonuclease Dicer homolog 4
DGCR8	DiGeorge syndrome critical region 8
DP	Double-positive T cell progenitor
<i>Drosophila</i>	<i>Drosophila melanogaster</i>
dsRNA	Double stranded RNA
DTA	Diphtheria toxin A
E-cad	Cadherin 1

EGFR	Epidermal growth factor receptor
endo-siRNA	Endogenous short interfering RNA
EpCAM	Epithelial cell adhesion molecule
ERK	Extracellular signal-regulated kinase
ESC	Embryonic stem cell
FACS	Fluorescent-activated cell sorting
GDNF	Glial cell line-derived neurotrophic factor
GFP	Green fluorescent protein
GFRA1	GDNF-family receptor alpha 1
GMP	Granulo-monocyte precursor
GSC	Germline stem cell
GWAS	Genome-wide association studies
H3K9	Histone 3 lysine 9
H3K9me3	Histone 3 lysine 9 trimethylated
Hb	Hemoglobin
hc-siRNA	Heterochromatin-associated siRNA
HCT	Hematocrit
HDAC1	Histone deacetylase 1
Hen1	Helix-loop-helix protein 1
HMGA2	High mobility group AT-hook protein 2
hnRNP A1	Heterogenous nuclear ribonucleoprotein A1
HSC	Hematopoietic stem cell
ICM	Inner cell mass
IL-6	Interleukin 6
In	Intermediate spermatogonia
IRES	Internal ribosomal entry site
kb	Kilobase
KSRP	KH-type slicing regulator protein
Lgr5	Leucine-rich repeat-containing G-protein coupled receptor
Lin28	Protein lin-28
LMPP	Lymphoid-primed multipotent progenitor cell

LPS	Lypopolysaccharide
LT-HSC	Long-term hematopoietic stem cell
MAPK	Mitogen-activated protein kinase
MitoPLD	Mitochondrial cardiolipin hydrolase
MACS	Magnetic-activated cell sorting
MCH	Mean cell hemoglobin
MCHC	Mean corpuscular hemoglobin concentration
MCV	Mean cell volume
MHC-I	Major hystocompatibility complex I
MK2	Mitogen-activated protein kinase activated protein kinase 2
MK3	Mitogen-activated protein kinase activated protein kinase 3
MK5	Mitogen-activated protein kinase activated protein kinase 5
MKK3	Dual-specificity mitogen-activated protein kinase kinase 3
MKK6	Dual-specificity mitogen-activated protein kinase kinase 6
miRNA	MicroRNA
MPP	Multiple progenitor cell
mRNA	Messenger RNA
MT	Mouse transcript
mTORC2	Target of rapamycin complex 2
Mx	Interferon-induced GTP-binding protein Mx1
Ngn3	Neurogenin 3
Neo	Neomycin
NRIF	Neurotrophin receptor-interacting factor
nt	Nucleotide
Oct-4	POU domain, class 5, transcription factor 1
p68/Ddx5	Probable ATP-dependent RNA helicase DDX5
p72/Ddx17	Probable ATP-dependent RNA helicase DDX17
PGC	Primordial germ cell
PDK1	Pyruvate dehydrogenase kinase isoform 1
PI3K	Phosphatidylinositide 3-kinases
PI(3,4,5)P ₃	Phosphatidylinositol 3,4,5 triphosphate

piRNA	Piwi-interacting RNA
PLZF	Promyelocytic leukaemia zinc finger
PND	Post-natal day
P-bodies	Processing bodies
PARP	Poly(ADP-ribose) polymerase
Poly I:C	Polyinosinic:polycytidylic acid
Pre-B	Precursor B cell
Pre-CFU-E	Pre-colony forming unit erythroid precursor
Pre-GM	Pre-granulo monocyte precursor
Pre-MegE	Premegakaryocyte/erythroid precursor
pre-miRNA	Precursor microRNA
pri-miRNA	Primary microRNA
Pro-B	Progenitor B cell
PTGS	Post-transcriptional gene silencing
RBC	Red blood cell count
Rdp1	RNA-dependent RNA polymerase 1
RDR2	RNA-dependent RNA polymerase 2
RDR6	RNA-dependent RNA polymerase 6
RDW	Red blood cell distribution width
RF ₁	Reverse F ₁ generation
RF ₂	Reverse F ₂ generation
RISC	RNA-induced silencing complex
RITS	RNA-induced transcriptional silencing complex
RLC	RISC-loading complex
RNAi	RNA interference
RNA Pol II	RNA polymerase II
RNA Pol IV	RNA polymerase IV
Sca-1	Stem cell antigen 1
SG	Stress granules
SINE	Short interspersed repetitive sequence
siRNA	Short interfering RNA

SNP	Single nucleotide polymorphism
SSC	Spermatogonial stem cell
ssRNA	Single stranded RNA
tasiRNA	Trans-acting short interfering RNA
TGF β 1	Transforming growth factor beta 1
TNF- α	Tumour necrosis factor alpha
TRBP	Tar-binding protein
TRIM71/Lin41	E3 ubiquitin-protein ligase TRIM71
UTR	Untranslated region
Zp3	Zona pellucida 3 protein
XRN1	5'-3' exoribonuclease 1
XRN4	5'-3' exoribonuclease 4

Chapter 1: Introduction

1.1 Argonaute proteins bind distinct classes of small non-coding RNAs

Over the past years the study of gene expression revealed a new layer of regulation through the discovery of several classes of small non-coding RNAs. These short RNA molecules are able to mediate both transcriptional and post-transcriptional silencing in a variety of organisms by the association with a class of conserved proteins, the Argonaute protein family (reviewed in Hutvagner, 2008; Meister, 2013). So far, three classes of small RNA molecules were discovered in association with Argonaute polypeptides: microRNAs (miRNAs), short interfering RNAs (siRNAs) and Piwi-interacting RNAs (piRNAs) (Hammond, 2001; Hutvagner, 2002; Martinez, 2002; Aravin, 2006; Girard, 2006).

siRNAs are ~22 nucleotide (nt) RNA molecules derived from long double-strand RNA (dsRNA) precursors and represent the principal triggers of the silencing mechanism called RNA interference (RNAi) (Hamilton, 1999; Zamore, 2000; Bernstein, 2001; reviewed in Carthew, 2009). RNAi is considered a surveillance mechanism against genomic parasites such as transposable elements and viruses, which generate dsRNA molecules during their replication cycle in plants and some animals (Ratcliff, 1997; Li, 2002). This silencing mechanism was first described in the nematode *Caenorhabditis elegans*, where the introduction of different dsRNAs was able to silence the expression of the complementary target genes (Fire, 1998). Similar phenomena were discovered also in plants and fungi and were termed post-transcriptional gene silencing (PTGS) and quelling, respectively (Napoli, 1990; Lindbo, 1992; Cogoni, 1996; English, 1996; Dalmay, 2000; Bartel, 2004). The conservation of the components of the RNAi pathway across the eukaryotic domain indicates the functional importance of this regulatory mechanism (Cerutti, 2006). Nonetheless, particular organisms such as *Saccharomyces cerevisiae* and parasites *Leishmania major* and *Trypanosoma cruzi* are refractory to dsRNA-induced silencing (Robinson, 2003; DaRocha, 2004; Ullu, 2004). Thus, the

RNAi mechanism represents a conserved, but non-essential, defence mechanism against genomic parasites (Cerutti, 2006).

miRNA is a class of 21-23nt non-coding RNAs that are present in plants and metazoans (Cerutti, 2006; Grimson, 2008; reviewed in Carthew, 2009). They are genome-encoded and regulate several physiological processes both in plants and animals (Brennecke, 2003; Johnston, 2003; Emery, 2003; Chen, 2004a; reviewed in Bartel, 2004). The first miRNA, *lin-4*, was discovered in *C. elegans* as a post-transcriptional regulator of the heterochronic gene *lin-14* (Lee, 1993; Wightman, 1991; Wightman, 1993). The identification of a second RNA with similar features in worms, *let-7*, and its homologs in flies and human genomes opened to the hypothesis of a conserved silencing mechanism (Pasquinelli, 2000; Reinhart, 2000; Slack, 2000). Small RNA sequencing studies have then identified miRNA molecules in a broad spectrum of plants and animals (Lagos-Quintana, 2001; Lau, 2001; Lee, 2001; Berezikov, 2006; Ruby, 2006; Chiang, 2010; Kuchen, 2010). However, the absence of any miRNA in fungi and several unicellular eukaryotes such as *Trypanosoma brucei* suggests a later development of this silencing pathway during eukaryotic evolution (Djikeng, 2001; Reinhart, 2002). In addition, differences in biogenesis and mechanisms of action as well as the lack of conservation between plant and metazoan miRNAs indicate that this pathway has evolved independently in these two phyla during evolution (Bartel, 2004; Cerutti, 2006). Nonetheless, comparative analysis between metazoan miRNAs showed that a consistent group (~30) of these molecules are conserved among Bilaterians (Pasquinelli, 2000; Hertel, 2006; Sempere, 2006; Prochnick, 2007; Christodoulou, 2010). In addition, it is believed that bilaterian complexity might, in part, be due to miRNA regulation due to the increased number of miRNA families in higher animals (Sempere, 2006; Prochnick, 2007; Grimson, 2008). As such, miRNAs represent a class of small regulatory RNAs that greatly contribute to the evolution and physiology of plants and animals.

The third conserved class of Argonaute-bound RNAs is represented by piRNAs. They are 24-30nt long RNAs, which are highly expressed in germ cells where they control transposable element activity (reviewed in Ishizu, 2012; Luteijn, 2013). As miRNA, they are genome-encoded, deriving by piRNA producing clusters or transposable elements present in the genome (Aravin, 2006; Brennecke, 2007; Kuramochi-

Miyagawa, 2008; Li, 2013). piRNAs were first described in mouse germ cells, but small RNA sequencing identified them also in zebrafish and *Drosophila* gonads (Aravin, 2006; Girard, 2006; Lau, 2006; Brennecke, 2007; Houwing, 2007). Even though it has been demonstrated that piRNAs are essential for fertility in many bilaterians, they are not expressed in plants and fungi (Lin, 1997; Deng, 2002; Kuramochi-Miyagawa, 2004; Carmell, 2007; Grimson, 2008; De Fazio, 2011; Reuter, 2011; Di Giacomo, 2013). On the other hand, the sponge *Amphibedon queenslandica* and the sea anemone *Nematostella vectensis* express a class of small RNAs with characteristic similar to piRNAs (Grimson, 2008). These data suggest that piRNAs were present in the common eukaryotic ancestor, and their expression was lost during the evolution of plants and fungi.

1.2 Argonaute protein family: Ago and Piwi subclades

The Argonaute protein family is defined by the presence of two conserved motifs: the PAZ, named after fly Piwi and plant Ago1 and Zwiille proteins, and the PIWI domains (Cox, 1998; Cerutti, 2000; Lingel, 2004; Cerutti, 2006). Three paralogous groups can be distinguished among Argonaute family members: Argonaute-like proteins, which are similar to *Arabidopsis thaliana* Ago1 and bind miRNAs and siRNAs; PIWI-like proteins, which are related to *Drosophila melanogaster* Piwi and associate with piRNAs; and group 3 Argonaute proteins, which contains 18 proteins specific for the nematode *Caenorhabditis elegans* (Lin, 1997; Bohmert, 1998; Yigit, 2006; reviewed in Hutvagner, 2008). The number of Argonaute genes in different species varies: for instance, four Argonaute- (Ago1-4) and 3 PIWI-like proteins (Mili, Miwi and Miwi2) are present in mouse, *Drosophila melanogaster* instead contains 2 Ago-like and 3 PIWI-like coding genes, while *C. elegans* encodes for 5 Ago-like, 3 PIWI-like and 18 group 3 Argonaute genes (Cerutti, 2006; Hutvagner, 2008). Sequence alignment revealed that several bacteria and archaea encodes for proteins with a PIWI domain (Cerutti, 2000; Anantharaman, 2002; Ullu, 2004). Indeed, the first crystal structure of Ago-like polypeptides were obtained in *Pyrococcus furiosus* and *Aquifex aeolicus* and revealed the presence of a PIWI domain fused to variant PAZ-like motifs (Song, 2004; Yuan,

2005). Strangely, parasites like *Leishmania major* and *Trypanosoma cruzi* that do not present a functional RNAi pathway have Argonaute proteins which may have lost the PAZ domain and retained only the PIWI domain (Ullu, 2004). The functional role of these proteins have not been elucidated yet.

Comparative computational analysis of the Argonaute family members in the five eukaryotic supergroups revealed that the last eukaryotic common ancestor possessed at least one Ago-like and one PIWI-like protein (Cerutti, 2006; Yigit, 2006; Grimson, 2008). However, lineage-specific loss of one or both Argonaute components has occurred during evolution: *Saccharomyces cerevisiae* has no Argonaute proteins while *Schizosaccharomyces pombe* contains only 1 Ago-like protein (Volpe, 2002; Sigova, 2004; Cerutti, 2006). Nonetheless, this Ago-Piwi silencing system has likely evolved as an innate immune pathway to protect organisms against foreign nucleic acids such as transposable elements and viruses (Cerutti, 2006; Hutvagner, 2008; Joshua-Tor, 2011). The ancestral PIWI protein might localize in the nucleus and control transposable element expression, while the ancient Argonaute protein would be localized in the cytoplasm and protect against viral infections. Indeed, in plants the Ago clade proteins form a protective system against virus infection by recognition of double-strand intermediates in virus replication (Ratcliff, 1997; Hamilton, 1999; Mlotshwa, 2008). Similar mechanisms were described for *D. melanogaster* and *C. elegans* in the animal kingdom (Lu, 2005; Wang, 2006). In mammals, even though there are no evidences of an Ago-mediated antiviral response, PIWI-like proteins are necessary to repress transposable elements in male germ cells (Deng, 2002; Kuramochi-Miyagawa, 2004; Carmell, 2007; De Fazio, 2011; Reuter, 2011; Di Giacomo, 2013). This duality of Ago- and PIWI-like proteins was further developed through the duplication of genes encoding for the two subclade members, which in turn lead to diversification of their functional roles. In fact, Ago-like proteins execute gene regulation through binding of miRNAs and siRNAs, while PIWI-like proteins bind to piRNAs and regulate genome-encoded transposable elements in germ cells (Hammond, 2001; Hutvagner, 2002; Martinez, 2002; Aravin, 2006; Girard, 2006; Lau, 2006).

1.3 Structural domains of the Argonaute family proteins

Argonaute proteins are characterized by four different domains: amino-terminal (N), PAZ (Piwi-Argonaute-Zwille), MID and PIWI domains. Two linker domains, indicated as L1 and L2, connect the N to PAZ domain and the PAZ to the MID domain, respectively.

During siRNA and miRNA biogenesis (described in more details in the following sections “miRNA biogenesis” and “siRNA biogenesis”), both small RNAs are loaded as duplexes in a multiprotein complex called RNA-induced silencing complex (RISC) (Hammond, 2000; Elbashir, 2001; Nykänen, 2001; Martinez, 2002; Schwarz, 2002). Argonaute proteins bind directly the RNA duplex, and only one of the two strands is kept in the complex, referred as guide strand, while the other is released (passenger strand). The N domain is required for small RNA loading onto the protein and it facilitates the unwinding of small RNA duplexes (Kwak, 2012). *In vitro* biochemical assays revealed that mutation of conserved residues in the N domain of human Argonaute 2 impedes the maturation of the RISC complex. These mutations result in a higher retaining of passenger strand in RISC complexes in cell culture, suggesting a role in the unwinding process of siRNA and miRNA duplexes (Kwak, 2012).

The PAZ and the MID domains of the Argonaute proteins play essential roles in the binding of the small RNA guide. The Argonaute-bound non-coding RNAs have two important common biochemical features due to their biogenesis: they have a phosphate group at their 5' end and a hydroxyl group at their 3' end (reviewed in Bartel, 2004; Carthew, 2009). The PAZ domain assumes an oligonucleotide binding fold, which creates a hydrophobic pocket for the binding of the 3' end of the guide RNA (Song, 2004; Ma, 2004; Jinek, 2009). The 5' end of the small RNA interacts with several residues of the MID and PIWI domains (Schirle, 2012; Elkayam, 2012). Importantly, the 5' phosphate group of the first nucleotide is inserted in a pocket of the MID domain, forming a plethora of interactions with the three oxygens of the phosphate (Ma, 2005; Parker, 2005; Frank, 2010; Schirle, 2012; Elkayam, 2012). The MID domain was additionally suggested to possess the ability to bind the 5' m⁷G cap structure of target mRNAs and be important for post-transcriptional repression of target genes (Kiriakidou,

2007). However, compelling evidences from biochemical and functional assays on mutated Argonaute proteins as well as structural data demonstrated that the MID domain does not bind directly the cap structure of mRNAs (Eulalio, 2008; Boland, 2010; Frank, 2010; Frank, 2011).

The PIWI domain presents an RNase-H-like fold and some Argonaute proteins are capable of cutting or slicing the target RNA between residue 10 and 11 of the guide small RNA in case of perfect complementarity (Liu, 2004; Song, 2004; Parker, 2004). This cleavage releases products with a 3'-hydroxyl and a 5'-phosphate, another characteristic feature of RNase-H enzymes (Martinez, 2004; Schwarz, 2004). A catalytic triad composed of Asp-Asp-His (DDH) residues was believed to be necessary for the endonuclease activity of Argonaute family members (Song, 2004; Ma, 2005; Parker, 2005; Yuan, 2005). The crystal structure of the first eukaryotic Argonaute protein from the budding yeast *Kluyveromyces polysporus* instead revealed the presence of an invariant glutamate residue in the catalytic pocket, turning the catalytic centre in a tetrad (DEDH) (Nakanishi, 2012). The crystal structure of human Ago2 protein further confirmed the formation of a catalytic tetrad in the mammalian protein (Elkayam, 2012; Schirle, 2012). Interestingly, the presence of an intact catalytic tetrad in the PIWI domain is not sufficient to create a functional endonuclease. Indeed, human Ago3 has a functional catalytic centre but no endonucleolytic activity (Liu, 2004; Meister, 2004). Several independent works have recently showed that additional residues in both the N and PIWI domains are involved in the slicing of target RNAs (Faehnle, 2013; Hauptmann, 2013; Nakanishi, 2013; Schurmann, 2013). The endonuclease activity in the PIWI domain is not a distinctive characteristic of Argonaute protein families. For example, Ago2 is the only Argonaute-like protein in mouse and humans, which retains the capability to slice, target RNAs in case of perfect complementarity (Liu, 2004; Song, 2004; Meister, 2004). Among the mouse PIWI-like protein, mutation of the catalytic triad in Miwi or Mili leads to male sterility due to transposon derepression, while a similar mutation in the Miwi2 protein has no phenotypic consequences (De Fazio, 2011; Reuter, 2011; Di Giacomo, 2013). In conclusion, the endonuclease activity is necessary for the function of only some Ago- and PIWI-like proteins, allowing them to directly slice target mRNAs in the case of nearly perfect complementarity.

1.4 The miRNA and siRNA pathways

1.4.1 miRNA biogenesis

miRNAs are usually transcribed by RNA polymerase II from miRNA-producing loci, and transcripts are capped and polyadenylated (Cai, 2004; Lee, 2004; Xie, 2005; Ozsolak, 2008; Corcoran, 2009) (Fig. 1). These transcripts can contain one or several miRNAs in the same transcriptional unit (Altuvia, 2005; Baskerville, 2005). Primary miRNA transcripts (pri-miRNAs) have a characteristic stem-loop structure with long 5' and 3' tails, that are cleaved in the nucleus by a protein complex, the Microprocessor (Lee, 2003; Denli, 2004; Gregory, 2004; Landthaler, 2004). This complex is composed of the RNase type III enzyme Drosha and the double-stranded RNA-binding domain protein DGCR8: DGCR8 binds the junction between the single stranded RNA (ssRNA) and the double stranded RNA (dsRNA) stem of the pri-miRNA and allows Drosha to cleave ~11 bp downstream the junction (Gregory, 2004; Han, 2004; Landthaler, 2004; Han, 2006). This enzymatic reaction releases a ~60 nt long precursor miRNA (pre-miRNA) that harbors two peculiar features: a phosphate at the 5' end and a 2nt 3'-overhang at the base of the stem structure. Pre-miRNAs are subsequently exported to the cytoplasm by Exportin 5 and further processed by a second RNase type III enzyme, Dicer (Bernstein, 2001; Grishok, 2001; Hutvagner, 2001; Ketting, 2001; Yi, 2003). Dicer associates with other two proteins, TRBP (Tar RNA Binding Protein) and Ago2, as well as other polypeptides, in the RISC loading complex (RLC) (Chendrimada, 2005; Maniataki, 2005; Macrae, 2008). Within the RLC Dicer cleaves the pre-miRNA into 21-23nt long double-stranded miRNAs. Finally, only one strand of the duplex is loaded into a ribonucleic complex named RNA-induced silencing complex (RISC) (Hammond, 2000; Elbashir, 2001; Nykänen, 2001; Martinez, 2002; Schwarz, 2002). An important determinant for strand selection depends on the miRNA duplex: the strand with less stable paired 5' end is preferentially loaded into the RISC (asymmetry rule) (Khvorova, 2003; Schwarz, 2003; Tomari, 2004). The central components of the RISC complex are composed of an Argonaute-like protein, that binds directly to the single-stranded

miRNA, and GW182, which interacts with Ago2 and is necessary for mRNA silencing (Liu, 2005; Meister, 2005; Behm-Ansmant, 2006; Till, 2007). The miRNA will then direct the RISC complex to target genes to mediate their silencing (Hammond, 2000; Elbashir, 2001; Nykänen, 2001; Martinez, 2002; Schwarz, 2002).

Several exceptions have been described to this canonical biogenetic pathway, in which miRNAs are produced independently of either Drosha or Dicer enzymatic activity (Meister, 2013). miRNAs whose generation is Drosha-independent are referred to as mirtrons (Okamura, 2007; Ruby, 2007; Babiarz, 2008). Mirtrons are often derived from the splicing process of mRNAs from protein-coding genes. Spliced intron folds in a structure that mimics a pre-miRNAs, thus being exported from the nucleus for subsequent Dicer-mediated processing in the cytoplasm (Okamura, 2007; Ruby, 2007; Babiarz, 2008). Dicer activity has also been shown to be dispensable for miRNA biogenesis. The only example so far is represented by miR-451 (Cheloufi, 2010; Cifuentes, 2010; Rasmussen, 2010; Yang, 2010). Pre-miR-451 presents an unusual structure with the guide strand of the miRNAs that is part of both the stem and the short loop (Cheloufi, 2010; Cifuentes, 2010; Yang, 2010). Indeed, Ago2 endonuclease activity is required both in mouse and zebrafish to cut the pre-miRNA, which is further processed by an unknown nuclease into the mature miR-451 (Cheloufi, 2010; Cifuentes, 2010; Rasmussen, 2010; Yang, 2010).

1.4.2 siRNA biogenesis

dsRNA molecules are known to trigger RNAi silencing in animals, plants and fungi (Napoli, 1990; Lindbo, 1992; Cogoni, 1996; English, 1996; Fire, 1998; Dalmay, 2000; reviewed in Bartel, 2004). dsRNA precursors can derive from endogenous sources, such as transposable element, convergent mRNA transcripts and sense-antisense mRNA duplexes, or exogenous sources, such as viral replication intermediates (Fire, 1998; Cogoni, 1999; Ketting, 1999; Dalmay, 2000; Mourrain, 2000; Smardon, 2000; Aravin, 2001; Li, 2002) (Fig. 1). siRNAs are structurally similar to miRNAs: they are ~22 nt long and exhibits a phosphate at the 5' end and a 3' hydroxyl at the 3' end. Indeed, siRNAs are produced by the RNase type III enzyme Dicer (Bernstein, 2001; Zhang,

2004; Macrae, 2006). These long dsRNAs are bound by Dicer through its PAZ domain and cleaved in 21-23nt RNA duplexes (Hamilton, 1999; Hammond, 2000; Zamore, 2000; Grishok, 2001; Kettings, 2001; Knight, 2001). The RNA duplex is then loaded into the RISC complex: a catalytically active Argonaute protein cuts one of the two strands, and the nicked strand is further removed by the endonuclease C3PO (Matranga, 2005; Miyoshi, 2005; Liu, 2009; Ye, 2011).

Since siRNAs often share high complementarity with their targets, the outcome of siRISC-RNA interaction results in the cleavage of targets (Hamilton, 1999; Elbashir, 2001; Vance, 2001; Pickford, 2002). In plants and some animals, such as *C. elegans* and planarians, the sliced RNA product could become the substrate for a RNA-dependent RNA polymerase (RdRPs) (Sijen, 2001; Newmark, 2003; Baulcombe, 2004; Allen, 2005; Yoshikawa, 2005; Cerutti, 2006). As such, RdRPs contribute to the production of secondary siRNAs from target RNAs, thus amplifying the silencing of the targets (Sijen, 2001; Baulcombe, 2004; Wassenegger, 2006). Plants and worms use this system to mount a highly specific immune response against viral infections (Silhavy, 2002; Blevins, 2006; Deleris, 2006). Indeed, siRNA-mediated silencing is spread across tissues nearby the site of delivery of the dsRNA template (Fire, 1998; Newmark, 2003; Tretter, 2008). Notably, a similar pathway is exploited in plants for the generation of *trans*-acting siRNAs (tasiRNAs) (Allen, 2005; Xie, 2005; Yoshikawa, 2005; Dunoyer, 2007). In fact, in *Arabidopsis thaliana* miRNAs mediate the cleavage of specific *TAS* non-coding RNAs, which are then transformed by the polymerase RDR6 in dsRNA precursor for the processing of a Dicer-like homolog, DCL4 (Allen, 2005; Xie, 2005; Yoshikawa, 2005). However, RdRPs proteins are absent in mammals and *Drosophila*, even though they are conserved among the eukaryotic supergroups (Cerutti, 2006). As such, RdRPs and the amplification cycle of siRNAs might be ancillary for the mounting of an effective RNAi pathway.

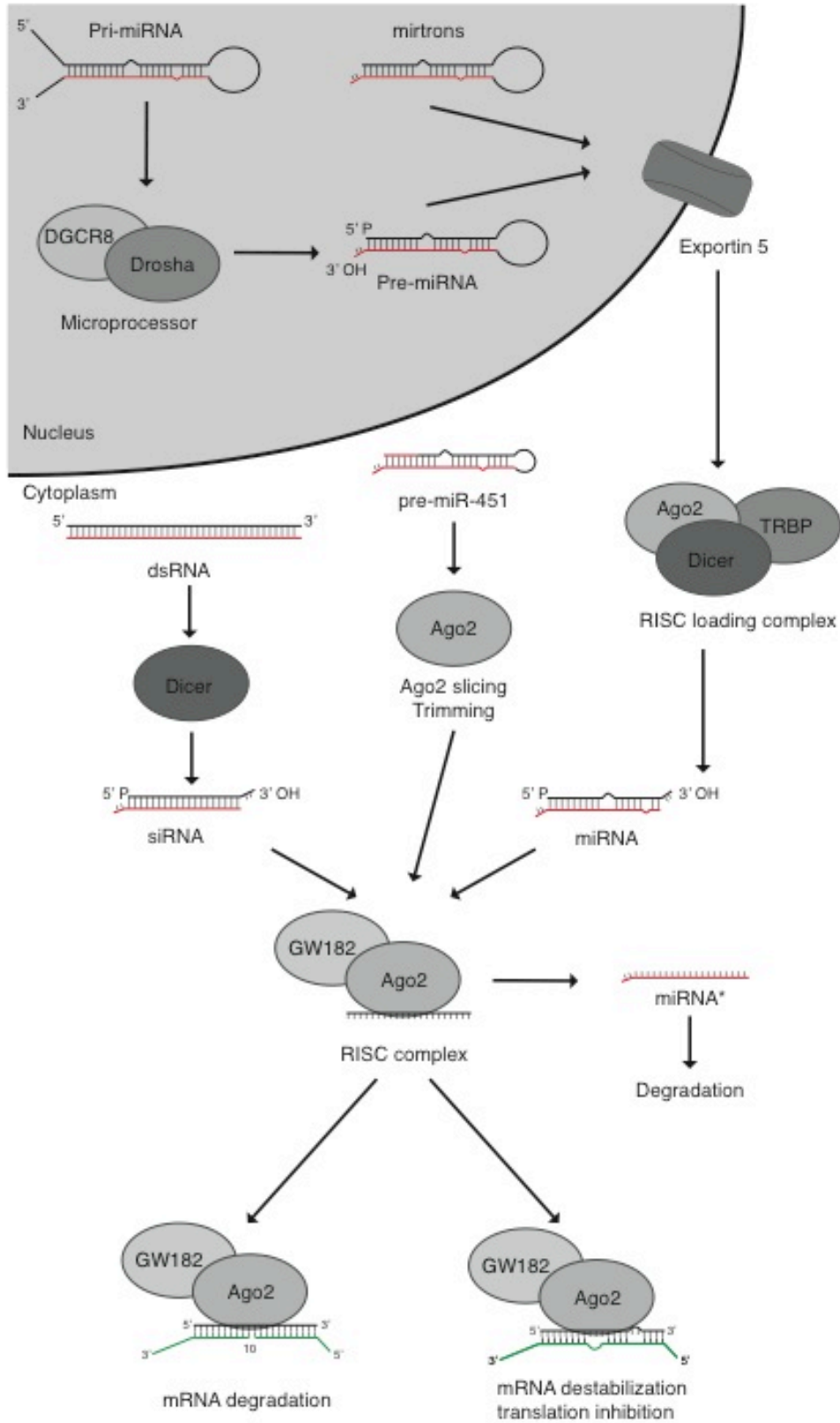


Figure 1. miRNA and siRNA biogenesis.

The biogenesis of miRNAs and siRNAs is schematically depicted in here. For further details please refer to the main text.

1.4.3 Determinants of miRNA-target interaction

The RISC complex is able to mediate the silencing of target genes through complementarity between the guide small RNA and the target gene. In case of perfect complementarity, a catalytically active Ago protein cleaves the target molecule through its endonuclease activity; if the complementarity is only partial, RISC promotes silencing through RNA destabilization and translational inhibition (reviewed in Bartel, 2009; Ameres, 2013). In plants, miRNA-mediated silencing is believed to rely mainly on endonucleolytic cleavage due to perfect match between the RNA and the target mRNA (Llave, 2002; Tang, 2003; Dunoyer, 2004; Souret, 2004; Addo-Quaye, 2008). Nonetheless, experimental data derived from *mad* mutants and evaluation of protein and mRNA levels in *A. thaliana* suggest that plant miRNAs also induce translational repression of target mRNAs (Palatnik, 2007; Brodersen, 2008; Lanet, 2009). On the other hand, only a few examples of perfect complementarity between the miRNA and the target mRNAs have been discovered in the mouse (Yekta, 2004; Hornstein, 2005; Karginov, 2010).

Since animal miRNAs often bind to target RNAs through partial complementarity, extensive efforts were made to identify motifs in the sequence that affect miRNA activity. Experimental studies on miRNA-target RNA interactions proved that the specificity of miRNA silencing depends on the miRNA *seed sequence* (Lewis, 2003; Doench, 2004; Brennecke, 2005; Lewis, 2005). The *seed sequence* consists of nucleotides 2-8 of the miRNA guide strand and a perfect pairing between guide and target RNA in this region is essential for RISC action (Grimson, 2007; Bartel, 2009). Additional pairing at position 1 and at nucleotide 13-16 at the 3' end of the miRNA strengthens the miRNA-mRNA interaction, enhancing target repression (Grimson, 2007; Nielsen, 2007; Wee, 2012). The structures of human Ago1 and Ago2 proteins confirmed the importance of the seed sequence since nucleotides 2-6 of the guide RNA are exposed

with Watson-Crick faces to the solvent, reducing the energy cost due to nucleic acid pairing (Elkayam, 2012; Schirle, 2012; Faehnle, 2013).

Seed sequence matches can occur in any region of target mRNAs. Indeed, sites at the 5' untranslated region (5' UTR) and in the coding sequence of target mRNAs have been reported (Forman, 2008; Grey, 2010; Hafner, 2010; Reczko, 2012; Helwak, 2013). However, miRNA binding silences more efficiently target RNAs when it happens in the 3' untranslated region (3' UTR) (Farh, 2005; Lewis, 2005; Lim, 2005; Grimson, 2007; Gu, 2009). Indeed, even though identification of miRNA-mRNA targets through ultraviolet (UV) induced crosslinking pinpoints that a large fraction of these interactions takes place in the coding region of mRNAs, seed sequence pairing mediates a higher silencing in binding sites present at the 3' UTR (Hafner, 2010; Helwak, 2013).

Recent works have discovered alternative modes of interaction that still trigger a functional miRISC-mRNA association. First, the *seed sequence* of miRNAs could harbor bulged or mismatched nucleotides (Lal, 2009; Chi, 2012; Helwak, 2013; reviewed in Ameres, 2013). Indeed, in mouse brain a set of miR-124 targets contains one bulged nucleotide across position 5 and 6 of the seed sequence that is not paired to the miRNA seed (Chi, 2012). These sites were confirmed also for let-7 targets in nematodes and from *in vitro* analysis of Ago protein in the eubacterium *Thermus thermophilus* (Vella, 2004; Long, 2007; Wang, 2008). Second, a stretch of 11-12 base pairing at the centre of the miRNA is able to silence target transcripts even in the absence of seed pairing (Shin, 2010). Central pairing sites are able to mediate cleavage of target mRNAs at high concentration of magnesium *in vitro*, but sequencing analysis of degraded RNA failed to detect slicing products for these miRNA-mRNA interaction sites *in vivo*, suggesting that they likely repress mRNA translational in physiological conditions (Shin, 2010). Third, the implementation of a new crosslinking strategy coupled with high-throughput sequencing showed that extensive base-pairing interaction in the 3' end of the miRNA can efficiently mediate target silencing (Helwak, 2013). These sites were validated through luciferase reporter assays, but the strength of miRNA-mediate repression was lower compared to a perfect *seed sequence* complementarity (Helwak, 2013).

1.4.4 miRNAs silence target RNAs through multiple mechanisms

As discussed in the previous section, miRNAs can silence their target genes at the post-transcriptional level by Ago-mediated slicing in case of perfect Watson-Crick base pairing along the miRNA sequence (Llave, 2002; Tang, 2003; Dunoyer, 2004; Souret, 2004; Yekta, 2004; Hornstein, 2005; Addo-Quaye, 2008; Karginov, 2010). Endonucleolytic cleavage occurs at the phosphodiester bond between nucleotide 10 and 11 of the miRNA (Liu, 2004; Meister, 2004; Miyoshi, 2005; Rivas, 2005). The exosome together with exoribonucleases Xrn4 and Xrn1 subsequently degrade the sliced mRNA fragments in plants and animals, respectively (Souret, 2004; Orban, 2005).

In case of only partial complementarity, miRNA-bound RISC can inhibit protein production from coding mRNAs through translational inhibition and mRNA destabilization (reviewed in Bartel, 2009; Ameres, 2013). Studies using ribosome profiling and internal ribosomal entry sites (IRES) in the mRNA of reporter genes showed that block of the translation process can take place both at the initiation and post-initiation stages (Seggerson, 2002; Humphrey, 2005; Pillai, 2005; Maroney, 2006; Nottrott, 2006; Mathonnet, 2007; Wakiyama, 2007). On the other hand, effects of miRNA binding could be readily detected at the transcriptional level, supporting experimental data of a destabilization of target mRNAs (Bagga, 2005; Krutzfeldt, 2005; Lim, 2005; Baek, 2008; Selbach, 2008; Hendrickson, 2009). The destabilization process involves the recruitment of the CCR4-NOT deadenylase complex through interaction with the GW182, a central component of the RISC complex (Behm-Ansmant, 2006; Giraldez, 2006; Wu, 2006). This interaction induces the deadenylation of target transcripts, followed by decapping and degradation through cellular exonucleases (Souret, 2004; Orban, 2005; Behm-Ansmant, 2006; Giraldez, 2006; Wu, 2006). In addition, shortening of the poly-A tail of mRNA targets can in turn reduce the rate of translational initiation by preventing the recircularization of the mRNA (Behm-Ansmant, 2006; Giraldez, 2006; Wu, 2006). Recent studies shed new light on this controversy. Ribosome profiling demonstrated that in mammals more than 84% of the miRNA-directed repression depends on mRNA destabilization (Baek, 2008; Guo, 2010). In addition, a study in zebrafish showed that in early embryos miR-430 initially

suppresses translation of target RNAs and only after the maternal-to-zygotic transition triggers mRNA destruction (Bazzini, 2012). These data suggest a model in which miRNA binding first induces translational repression and only later causes mRNA destabilization of target mRNAs.

Translationally inactive mRNAs often accumulate in subcellular cytoplasmic structures called processing bodies (P-bodies) (reviewed in Anderson, 2006; Parker, 2007). P-bodies contain high concentrations of RNA turnover complexes, such as the deadenylase CCR4-NOT complex and the decapping enzymes Dcp1/Dcp2 (Ingelfinger, 2002; Sheth, 2003; Cougot, 2004; Behm-Ansmant, 2006; Eulalio, 2007). Notably, components of the RISC complex such as Argonaute and GW182 proteins are found in P-bodies, suggesting that miRNA-dependent silencing of target mRNAs takes place in these granules (Liu, 2005; Ding, 2005; Meister, 2005; Behm-Ansmant, 2006). However, a study on Ago2 localization in mammalian cells revealed that only 1-2% of the protein is localized in P-bodies in normal culture conditions (Leung, 2006). In addition, depletion of certain P-bodies components results in P-bodies disassembly without any effect on miRNA activity (Eulalio, 2007). A possible explanation would be that RISC interacts with RNA degradation complexes in the cytoplasm, and it is then recruited to P-bodies.

1.4.5 siRNAs silence target genes both at the transcriptional and post-transcriptional levels

siRNAs have been described to regulate the expression of target genes both at the transcriptional and post-transcriptional level (reviewed in Tomari, 2005 and Carthew, 2009). They can regulate the RNA levels of targets through Argonaute-dependent slicing and further degradation through cellular exonucleases, since they often present a complete match with their target RNAs (Elbashir, 2001; Liu, 2004; Meister, 2004; Miyoshi, 2005). However, siRNAs with partial mismatches or loaded into a Slicer-inactive Ago protein can mediate silencing of target mRNAs through post-transcriptional mechanisms similar to animal miRNAs (Jackson, 2003; Scacheri, 2004).

siRNAs have also the ability to regulate gene expression at the level of RNA transcription (reviewed in Carthew, 2009; and Grewal, 2010). In *S. pombe*, siRNAs

deriving from heterochromatic regions associate with Ago1, the only Argonaute protein, and together with other factors form the RNA-induced transcriptional silencing (RITS) complex (Volpe, 2002; Noma, 2004; Verdel, 2004). RITS uses the loaded siRNAs to recognize nascent transcripts at complementary loci, inducing the recruitment of histone methyltransferases to promote methylation on lysine 9 of histone H3 (H3K9) (Volpe, 2002; Noma, 2004; Buhler, 2006). In addition, RITS associates with the Rdp1, an RNA-dependent RNA polymerase, facilitating the production of secondary siRNA from nascent transcripts and the subsequent spreading of histone modifications to nearby genomic regions (Motamedi, 2004; Sugiyama, 2005). In plants, a similar mechanism involves a specific class of siRNAs called heterochromatin-associated siRNAs (hc-siRNAs) (reviewed in Melnyk, 2011). hc-siRNAs are transcribed by the plant-specific RNA Pol IV, forming dsRNAs due to the activity of RDR2 RNA polymerase (Xie, 2004; Herr, 2005; Onodera, 2005; Pontes, 2006). These intermediates are further processed by one of the four Dicer homologs, DCL-3, into 24nt siRNAs which are specifically loaded into Ago4, Ago6 and Ago9 (Zilberman, 2003; Xie, 2004; Zilberman, 2004; Herr, 2005; Qi, 2006; Eun, 2011). This complex finally recognizes nascent transcripts from targeted loci in the nucleus, promoting both histone and DNA methylation (Zilberman, 2003; Wierzbicki, 2008; Havecker, 2010).

In animals compelling works in flies and worms confirmed the presence of a siRNA-mediated transcriptional regulation (Pal-Bhadra, 2002; Sijen, 2003; Vastenhouw, 2003; Pal-Bhadra, 2004; Guang, 2008). However, the existence of a functional transcriptional regulation by siRNAs in mammals is still debatable. Indeed, evidences for siRNA-directed chromatin modifications were collected in transfection experiments with siRNAs directed to promoter sequences in human cell lines (Kim, 2006; Janowski, 2006; Schwartz, 2008; Chu, 2010). Furthermore, nuclear localization of Argonaute proteins has been reported (Robb, 2005; Rudel, 2008; Ohrt, 2008; Weinmann, 2009). Nonetheless, other studies using tagged Ago2 protein as well as data from our lab suggested that Ago2 is localized only in the cytoplasm (Meister, 2005; Leung, 2006; Leung, 2011; Horman, 2013; Fig. 16 and 18). Further experiments using gene ablation techniques are necessary to shed light on this controversy.

1.4.6 Regulation of miRNA activity

Since miRNA interaction with target RNAs is largely but not exclusively based on a 6-8 nucleotide seed sequence, a single miRNA is predicted to regulate the expression of hundreds of genes (Farh, 2005; Krek, 2005; Lewis, 2005; Lim, 2005; Giraldez, 2006; Helwak, 2013). Since this small non-coding RNAs could modulate a vast realm of targets, it is fundamental for the cell to regulate miRNA function according to several cellular cues. Different steps of the miRNA biogenesis pathway, such as transcription and precursor cleavage, are amenable for the regulation of levels of miRNAs at a global or individual scale (reviewed in Siomi, 2010 and Kim, 2010). Transcription factors and DNA methylation at the promoters restrict the expression of particular miRNAs to specific tissues (Aboobaker, 2005; He, 2007; Zhou, 2007; Dore, 2008). In addition, the availability of Drosha and Dicer could regulate the global levels of mature miRNAs (Wulczyn, 2007; Forman, 2008; Han, 2009; Levy, 2010). Indeed, a double negative feedback loop regulates the two Microprocessor components. DGCR8 interaction with Drosha stabilizes the protein levels of the endonuclease (Yeom, 2006). On the other hand, Drosha recognizes and cleaves two hairpin structures in the 5' untranslated region of DGCR8 mRNA, which in turn targets the mRNA for degradation (Han, 2009). A similar autoregulatory feedback loop mechanism involves let-7 miRNA and Dicer: let-7 targets Dicer mRNA within its coding region, thus modulating the total rate of miRNA biogenesis (Forman, 2008).

Microprocessor-dependent cleavage represents an additional point of miRNA regulation. RNA editing by ADAR (adenosine deaminase acting on RNA) protein reduces processing of pri-miR-142 and pre-miR-151 by Drosha and Dicer, respectively (Yang, 2006; Kawahara, 2007). On the other hand, the association with accessory factors, such as p68 and p72 helicases, could regulate the Microprocessor function. In fact, transforming growth factor beta (TGF- β) and estrogen signaling pathways modulate Drosha-mediated pri-miRNAs processing through association with p68 and p72 (Davis, 2008; Yamagata, 2009). Furthermore, the interaction of p53 with p68 and Drosha after DNA damage enhances Microprocessor-mediated processing of a subset of miRNAs (Suzuki, 2009).

Several RNA binding proteins control the maturation process of miRNAs. In fact, the peculiar stem-loop structure of miRNA precursors presents a binding platform for numerous cofactors (reviewed in Siomi, 2010). hnRNP A1 protein binds pri-miRNA-18a in two regions within the terminal loop and the stem, thus favouring binding and cleavage by the Microprocessor complex (Guil, 2007; Michlewski, 2008). In addition, binding of KH-type splicing regulator protein (KSRP) to G-rich sequences in the terminal loop of a subset of miRNAs promotes both Drosha- and Dicer-mediated cleavage steps (Trabucchi, 2009). Furthermore, LIN28 binding to a GGAG motif of let-7 and other miRNAs reduces both pri-miRNA and pre-miRNA processing (Heo, 2008; Heo, 2009; Newman, 2008; Rybak, 2008; Viswanathan, 2008). Two Lin28 homologs are found in mammals. LIN28b sequesters let-7 pri-miRNA to the nucleoli, thus preventing Drosha cleavage (Piskounova, 2011). In the cytoplasm, LIN28a instead recruits the terminal uridylyl transferase 4 or 7 (TUT4-7) to the pre-let-7 RNA, which adds a uridine tail to the pre-let-7 (Hagan, 2009; Heo, 2009). Polyuridylation of let-7 precursor inhibits Dicer cleavage and targets it for degradation. On the other hand, in the absence of Lin28, TUT4-7 mediate the addition of only one uridine residue to a subset of pre-let-7s and other pre-miRNAs. This creates a classical 2nt 3' overhang in the precursor miRNA, promoting Dicer processing (Heo, 2012).

In order to regulate the activity of protein in the miRNA pathway after cellular stresses, a fast and highly controlled means is represented by post-translational modification. For example, KSRP function is regulated by phosphorylation events after DNA damage response and BMP signaling (Zhang, 2011; Pasero, 2012). In addition, deacetylation of DGCR8 by histone deacetylase 1 (HDAC1) enhances association to pri-miRNAs, thus promoting miRNA maturation (Wada, 2012). Furthermore, TRBP phosphorylation by the ERK signaling pathway enhances miRNA production through stabilization of the Dicer-TRBP complex (Paroo, 2009). Argonaute proteins also undergo several post-translational modifications in response to stress stimuli. A better description of such modification as well as their regulatory relevance is described in details in the next section.

1.5 Argonaute 2: central component of miRNA and siRNA silencing pathways in mammals

1.5.1 Physiological relevance of Ago2 in mouse

Argonaute proteins in plants and animals have undergone a series of gene duplications, resulting in a variable number of proteins in each species (Cerutti, 2006; Hutvagner, 2008). In mouse and humans, 4 Ago-like proteins, called Ago1-4, are present in the genome (Cerutti, 2006; Hutvagner, 2008). Among them, Ago2 is the only member of the family, which retains the capability to slice target RNAs in case of perfect complementarity (Liu, 2004; Song, 2004; Meister, 2004). All four Agos are able to mediate post-transcriptional silencing through miRNA-target interaction, suggesting the possibility of an overlapping function (Liu, 2004; Meister, 2004; Pillai, 2004; Wu, 2008; Su, 2009). Furthermore, all Ago proteins bind similar populations of miRNAs (Azuma-Mukai, 2008; Dueck, 2012; Wang, 2012). However, Ago1, Ago2 and Ago3 are likely expressed in all murine tissues, while Ago4 seems to have a less broad expression pattern (Petri, 2011). Genetic ablation of single Ago proteins in mice shed light to the possible physiological roles of these proteins. Ago4 is highly expressed in the testis, and male mice lacking Ago4 show mild defects in meiotic entry and division, but are nonetheless fertile (Modzelewski, 2012). On the other hand, Ago1- and Ago3-mutant animals are viable and fertile, but Ago1-Ago3 double knockout animals show lower resistance to pulmonary flu infection (O'Carroll, 2007; Van Stry, 2012).

The lack of Ago2 in mouse models has shown much more severe phenotypes compared to loss of the other single Ago proteins. Indeed, Ago2 is the only Ago-like protein with a functional endonuclease activity (Liu, 2004; Song, 2004; Meister, 2004). This function is not only important for siRNA mediated silencing, but it is also necessary for the few miRNAs that show perfect complementarity with their targets and for miR-451 maturation (Elbashir, 2001; Liu, 2004; Yekta, 2004; Meister, 2004; Hornstein, 2005; Cheloufi, 2010; Cifuentes, 2010; Karginov, 2010; Rasmussen, 2010; Yang, 2010). Even though Ago1 and Ago2 were shown to be loaded with siRNA with higher efficiency than Ago3 and Ago4, slicing of the siRNA duplex precursor by Ago2 enhances the

loading of the guide strand in a functional RISC complex (Matranga, 2005; Miyoshi, 2005; Liu, 2009; Su, 2009). Furthermore, Ago2 endonuclease activity is required for the maturation of pre-miR-451, and slicing-inactive Ago2 mutants die perinatally (Cheloufi, 2010). Finally, *in vitro* and *in vivo* studies demonstrated that Ago2 is necessary for Dicer-mediated cleavage of a subset of miRNAs (Diederich, 2007; O'Carroll, 2007).

Since Ago2 is a central component of the RISC complex, germ line ablation of Ago2 causes embryonic lethality as early as embryonic day 10.5 (E10.5) (Liu, 2004; Alisch, 2007; Morita, 2007). The phenotypic outcome of gene ablation varied between the studies due to differences in the insertion of the mutagenic cassette and in the mouse strain used (Liu, 2004; Alisch, 2007; Morita, 2007). Similar embryonic lethality results from the ablation of the central miRNA components DGCR8 and Dicer (Bernstein, 2003; Wang, 2007)

Conditional loss-of-function approaches demonstrated the importance of Ago2 in several adult tissues. Depletion of Ago2 in hematopoietic stem cells (HSCs) causes a cell-autonomous impairment in erythroid and B-cell development (O'Carroll, 2007). Mice reconstituted with Ago2-deficient bone marrow showed a severe anaemia and splenomegaly due to impairment in orthochromatophilic erythroid progenitors. This is in part due to the lack of miR-451, which needs a slicing-competent Argonaute protein for the maturation of the pre-miRNA (Rasmussen, 2010). In addition, the number of mature B cells is reduced due to a partial block in the pro-B-to-pre-B progenitor cell differentiation (O'Carroll, 2007).

Ago2 was demonstrated to be essential also for female fertility. Conditional ablation of Ago2 during oogenesis blocks oocyte maturation at meiosis due to spindle organization defects (Kaneda, 2009). Interestingly, a similar phenotypic effect arises from the elimination of Dicer in growing oocytes, but not DGCR8 (Murchison, 2007; Tang, 2007; Suh, 2010; Ma, 2010). Since Dicer is essential for both siRNA and miRNA biogenesis while DGCR8 is involved only in miRNA maturation, these genetic observations suggest that siRNA activity is fundamental for oogenesis, while miRNA function is dispensable. Indeed, gene expression profiles and luciferase reporter assays demonstrated that mature miRNAs are present in oocytes but are not functional (Suh, 2010; Ma, 2010). On the other hand, endogenous siRNAs are active in this cell type and

are likely to be central for gene regulation (Watanabe, 2006; Watanabe, 2008; Suh, 2010; Ma, 2010).

Finally Ago2 has been shown to be necessary for miRNA function in the skin and the nervous system. In fact, Ago2 loss in dopaminergic neurons revealed a role for miRNAs in cocaine addiction (Schaefer, 2011). Furthermore, ablation of Ago2 together with Ago1 specifically in the skin provokes severe skin defects such as hair follicle degeneration and a thickened epidermis (Wang, 2012). In conclusion, Ago2 is necessary for the execution of miRNA and siRNA functions in several physiological processes.

1.5.2 Regulation of Ago2 activity by post-translational modifications

The central role of Ago2 in both miRNA and siRNA silencing pathways make it an amenable target to control the activity of these two post-transcriptional regulators. Several post-translational modifications of Ago2 protein have been described in human and mouse (Table 1) (reviewed in Kim, 2010, and Siomi, 2010). These modifications can impact the stabilization of the protein or its silencing activity during normal and stress conditions. Reduction of Ago2 protein levels has an impact on the stability and overall expression levels of miRNAs, which are not protected by degradation (Diederich, 2007). In addition, post-translational modification of Ago2 allows integrating miRNA and siRNA-mediated silencing into the signaling network during stress responses.

The protein TRIM71 (also known as Lin41) is a E3 ubiquitin ligase and targets Ago2 protein for degradation in mice (Rybak, 2009). Another TRIM-NHL family member, NHL-2, regulates miRNA-RISC and target interaction in *C. elegans* (Hammell, 2009). A second modification that interferes with Ago2 protein stability is prolyl-hydroxylation (Qi, 2008; Wu, 2011). In fact, hypoxic conditions increase the levels of type I collagen prolyl-4-hydroxylase (C-P4H(I)) in human cell lines. This enzyme associates with Ago2 and mediates the hydroxylation of Proline 700. This in turn increases both miRNA- and siRNA-mediated silencing of mRNA in reporter assays (Qi, 2008; Wu, 2011).

Poly-ADP-ribosylation and phosphorylation are instead post-translational modifications used to modulate Ago2 function in response to external cues. For example, after

induction of cellular stress, Ago2 and other miRNA components are assembled in cytoplasmic structures called stress granules (SGs), which contain stalled translation preinitiation complexes (Kedersha, 2002; Kimball, 2003; reviewed in Anderson, 2006). There, poly(ADP-ribose) polymerases (PARPs) mediate the addition of multiple ADP-ribose molecules to Ago2 and other proteins, thus inhibiting both miRNA and siRNA function (Leung, 2011). Knockdown of the poly(ADP-ribose) glycohydrolase, an enzyme that destroys poly-ADP-ribose chains, achieved a similar reduction of RISC function in untreated cells (Leung, 2011). Even though the mechanism of inhibition is not clear yet, it is possible that Ago2 activity is reduced due to steric hindrance, blocking interaction with target mRNAs and/or other protein complexes.

Phosphorylation represents one of the most common protein modifications. Mass spectrometry approaches identified several phosphorylated sites in the Ago2 protein that are present throughout the entire length of the protein (Zheng, 2008; Huttlin, 2010; Rudel, 2011). Only few of these post-translational modification sites were characterized in details. Tyrosine 529 is phosphorylated in human cell lines in normal culture conditions (Rudel, 2011). It is present in the MID domain, which is important for the binding of the 5' end of the guide RNA (Ma, 2005; Parker, 2005; Frank, 2010; Schirle, 2012; Elakayan, 2012). Phosphorylation of Y529 or mutation of the tyrosine in a glutamate (Y529E) reduces the binding of small RNA guides to the Ago2 protein (Rudel, 2011). Recent structural data showed that tyrosine 529 forms a hydrogen bond with the 5' base of the miRNA bound to Ago2, and the presence of a negative charge destroys this interaction (Schirle, 2012; Elakayan, 2012). More recently, epidermal growth factor receptor (EGFR) was identified as the kinase responsible for phosphorylation of tyrosine 393 of the human Ago2 (Shen, 2013). Tyrosine 393 lies on the linker L2 domain of the Argonaute protein, away from the miRNA and mRNA binding sites and the PIWI domain. Interestingly, a subset of miRNAs with a long loop structure showed a reduced Dicer processivity after EGFR-mediated tyrosine phosphorylation. This is probably due to a reduced interaction between Ago2 and the other components of the RISC loading complex, namely Dicer and TRBP (Shen, 2013). Another phosphorylation event interests the serine 387 of the human Ago2 (Zeng, 2008; Horman, 2013). Mass spectrometry on overexpressed and endogenous Ago2 protein

revealed basal level of phosphorylation in normal cell culture conditions (Zeng, 2008). Phosphorylation of serine 387 was found to be increased after stress induction with sodium arsenite and anisomycin, which are known to stimulate the p38 mitogen-activated protein kinase (MAPK) pathway. The p38-MAPK kinase pathway is a well-studied signaling pathway that is activated in response to several stress stimuli, ranging from oxidative stress, translational inhibition and DNA damage (Rouse, 1994; Freshney, 1994; Manke, 2005; reviewed in Ono, 2000). Use of the SB203580 specific inhibitor of p38 kinase demonstrated that activation of this pathway leads to phosphorylation of Ago2. However, an *in vitro* approach pinpointed that a kinase downstream of p38, called mitogen-activated protein kinase activated protein kinase 2 (MAPKAPK2 or MK2), but not p38 itself could phosphorylate Ago2 at serine 387. Functional studies with a non-phosphorylatable Ago2 protein, where serine 387 was replaced by an alanine residue, demonstrated that Ago2 mutant localizes less efficiently to P-bodies during resting culture conditions compared to the wild type protein. However, no differences in subcellular localization were seen between the wild type and phosphomutant protein after induction of stress (Zeng, 2008). A recent study identified a second kinase, Akt3/PKB γ , as capable of Ago2 phosphorylation at serine 387 (Horman, 2013). Further biochemical and functional characterization showed a reduction of interaction between GW182 and the phospho-deficient Ago2 protein, which could explain a decrease in Ago2 localization to P-bodies. This in turn leads to a reduced capability of mutant Ago2 to mediate miRNA-based silencing of reporter genes. Surprisingly, the phosphomutant protein possessed a higher endonuclease ability and thus an enhanced siRNA-mediated silencing of target genes (Horman, 2013). A more thorough characterization of the outcome of serine phosphorylation on endogenous Ago2 protein is needed to appreciate the meaning of this modification on miRNA and siRNA silencing pathways. In addition, the importance of any of the aforementioned Ago2 post-translational modifications was not tested *in vivo* thus far. Interestingly, a proteomic approach from several mouse tissues discovered very low amount of Ago2 phosphorylation only at serine 387 in brain, liver, lung and spleen (Huttlin, 2010). This points to Ago2 serine 387 phosphorylation as a promising target to understand the significance of miRNA and siRNA pathways regulation at an organismal level.

Modification	Residue	Function	Reference
Ubiquitination	Unknown	Destabilizes the Ago2 protein	Leung, 2011
Prolyl 4-hydroxylation	P700	Enhances stability of Ago2 protein	Qi, 2008; Wu, 2011
Poly-ADP-rybosilation	Unknown	Reduced miRNA- and siRNA-mediated silencing	Rybak, 2009
Phosphorylation	Y529	Impairs miRNA binding	Rudel, 2011
Phosphorylation	Y393	Regulation of maturation of miRNA subset	Shen, 2013
Phosphorylation	S387	Regulation of P-body localization	Zeng, 2008; Horman, 2013

Table 1: Post-translational modifications of the human Ago2 protein.

1.6 The piRNA pathway

1.6.1 piRNA biogenesis

piRNAs represent the third class of silencing Argonaute-bound small non-coding RNAs. They are 24-30nt long and are bound to the PIWI subclade of the Argonaute proteins (Aravin, 2006; Girard, 2006; Grivna, 2006; Lau, 2006). In *D. melanogaster*, three PIWI proteins, Ago3, Aubergine (Aub) and Piwi, execute piRNA function; in mouse, Mili, Miwi and Miwi2 participate to piRNA-mediate silencing (reviewed in Hutvagner, 2008). Similarly to miRNAs, piRNAs can repress the expression of target genes through both transcriptional and post-transcriptional mechanisms. Their expression is mainly restricted to germ cells, where they control the activity of transposable elements. In fact, mutation of any of the PIWI proteins in mouse and fly causes male sterility due to meiotic defects (Cox, 1998; Schmidt, 1999; Deng, 2002; Kuramochi-Miyagawa, 2004;

Carmell, 2007; Li, 2009). More recent works have opened the possibility that piRNAs can be expressed in other tissues, where they act as regulators of coding mRNAs, but they have not been described as ubiquitously as miRNAs (Lee, 2011; Rajasethupathy, 2012).

piRNA biogenesis has been studied extensively in flies and mouse (Fig. 2). Conversely to miRNAs and siRNAs, piRNA maturation is independent of RNase III enzymes Droscha and Dicer (Vagin, 2006; Brennecke, 2007; Houwing, 2007). They are generated by ssRNA molecules derived from intergenic regions in the genome (Aravin, 2007; Brennecke, 2007; Li, 2013). Two distinct pathways of piRNA production have been discovered so far: the primary processing pathway and the secondary amplification pathway, which generate primary and secondary piRNAs, respectively (Fig 2A-B). In *Drosophila*, the primary processing pathway starts from the transcription of RNA transcripts from piRNA clusters. These clusters are a few kilobases to 100 kilobases long and they are processed into many different piRNAs (Brennecke, 2007). On the contrary, two different sets of piRNAs are expressed during male germ cell development in the mouse: pre-pachytene piRNAs, which are expressed during early testis development and derive from transposable elements scattered throughout the genome; pachytene piRNAs, which are expressed in adult testis and derive from piRNA clusters similarly to *Drosophila* (Aravin, 2006; Girard, 2006; Grivna, 2006; Lau, 2006; Aravin, 2007; Aravin, 2008). Recent works are starting to pinpoint the promoter regions and transcription factors necessary for the transcription of piRNA clusters both in flies and mammals (Brennecke, 2007; Li 2013).

These long ssRNA precursors are processed in smaller fragments by cellular endonucleases in perinuclear granules known as nuage or inter-mitochondrial cement (Aravin, 2009; Shoji, 2009; Huang, 2011) (Fig. 2A). Several lines of work in *Drosophila* suggest that the protein Zucchini is necessary for primary piRNA biogenesis (Pane, 2007; Saito, 2009; Haase, 2010; Olivieri, 2010; Saito, 2010). Zucchini is a member of the phospholipase D superfamily and its mammalian homolog, MitoPLD, is able to produce the signaling molecule phosphatidic acid from lipids present in the mitochondrial membrane (Choi, 2006; Huang, 2011; Watanabe, 2011). In addition, crystallographic studies and *in vitro* nuclease assays demonstrated that

Zucchini/MitoPLD possess a three-dimensional fold of a nuclease and they are capable of cleaving single stranded DNA and RNA molecules (Ipsaro, 2012; Nishimasu, 2012; Voigt, 2012). It is proposed that Zucchini/MitoPLD play a dual role in primary RNA formation: they produce phosphatidic acid, which recruit the components for the assembly of nuage, and cleave long piRNA precursors in smaller fragments. It is although unclear why primary piRNAs presents a strong bias towards a uracil in position 1 (1-U) (Brennecke, 2007; Aravin, 2008). Indeed, Zucchini/Mito-PLD do not show any preference to cut before a uracil residue, opening to the possibility that additional factors associate with them to determine the cleavage site. Another possibility consists in a later selection of the generated fragments by binding to PIWI proteins.

After the generation of short RNA fragments from piRNA precursor, primary piRNAs are loaded onto specific PIWI proteins, which correspond to Piwi and Aub in *Drosophila* and Mili and Miwi in mouse (Li, 2009; Malone, 2009; Saito, 2009). The 3' end of the piRNA is then formed through an unknown exonuclease, usually referred to as Trimmer (Kawaoka, 2011; Vourekas, 2012). Indeed, deep-sequencing data of piRNA associated with PIWI proteins showed a broad size distribution with a peak at length that varies between the different PIWI proteins (Aravin, 2006; Grivna, 2006; Brennecke, 2007; Carmell, 2007; Li, 2009). In addition, 3'-5' endonucleolytic activity was detected on longer RNA molecules loaded into PIWI proteins in cell extracts *in vitro* (Kawaoka, 2011). After 3' end maturation, piRNAs are 2'-O-methylated at their 3' end by the RNA methylase Hen1 (Horwich, 2007; Saito, 2007; Kamminga, 2010; Kawaoka, 2011). This modification enhances the piRNA stability by protecting it from the addition of a poly-U tail and consequent degradation (Horwich, 2007; Saito, 2007; Kamminga, 2010).

The mature primary piRNAs are then used to directly silence transposable elements at the transcriptional and post-transcriptional level. In addition, they act as templates for the formation of secondary piRNA through the secondary amplification pathway, also known as the ping-pong cycle (Brennecke, 2007; Gunawardane, 2007; Aravin, 2008) (Fig. 2B). Indeed, primary piRNAs, especially mouse pre-pachytene piRNAs and *Drosophila* piRNA clusters, are enriched for transposon sequences with an antisense orientation (Aravin, 2007; Brennecke, 2007; Aravin, 2008). This permits the recognition of sense transposon transcripts through base pairing, which triggers the cleavage of the

transposon mRNA (Saito, 2006; Gunawardane, 2007; Nishida, 2007). Flies and mice employ two similar but distinguishable amplification pathways to produce secondary piRNAs. In *Drosophila*, Aub is responsible for the cleavage of target transcripts through its Slicer activity in the cytoplasm (Gunawardane, 2007; Nishida, 2007). The sense transposon mRNA is then further processed by an unknown mechanism into smaller fragments that are loaded into Ago3 (Brennecke, 2007; Gunawardane, 2007; Li, 2009; Malone, 2009). These secondary piRNAs have a characteristic sense orientation and present a strong bias for an adenine in position 10 (10-A) due to the endonucleolytic activity of Argonaute proteins (Brennecke, 2007). Secondary piRNAs can bind to antisense transcripts derived from repetitive elements or piRNA cluster and catalyze their cleavage. This in turn creates a new substrate for the generation of piRNAs in the sense orientation, allowing the amplification of piRNAs highly specific towards the most expressed transposons. The first evidences of the ping-pong cycle were uncovered in *Drosophila*, where Aub binds mainly to antisense piRNAs derived from primary processing containing a 1-U, while Ago3 is loaded with secondary sense piRNAs with a 10-A bias (Brennecke, 2007). Since both Aub and Ago3 participate to this two-steps amplification process, *Drosophila* ping-pong cycle is referred as heterotypic.

In mouse, a similar mechanism exists, and it was believed to involve both Mili and Miwi2 proteins (Aravin, 2008). However, a recent genetic study with endonucleolytic dead proteins demonstrated the presence of a homotypic ping-pong cycle interesting only Mili (De Fazio, 2011). Indeed, deep-sequencing analysis of Mili-bound piRNAs highlighted the presence of a characteristic ping-pong signature, which is missing between Mili-Miwi2 piRNA populations (De Fazio, 2011).

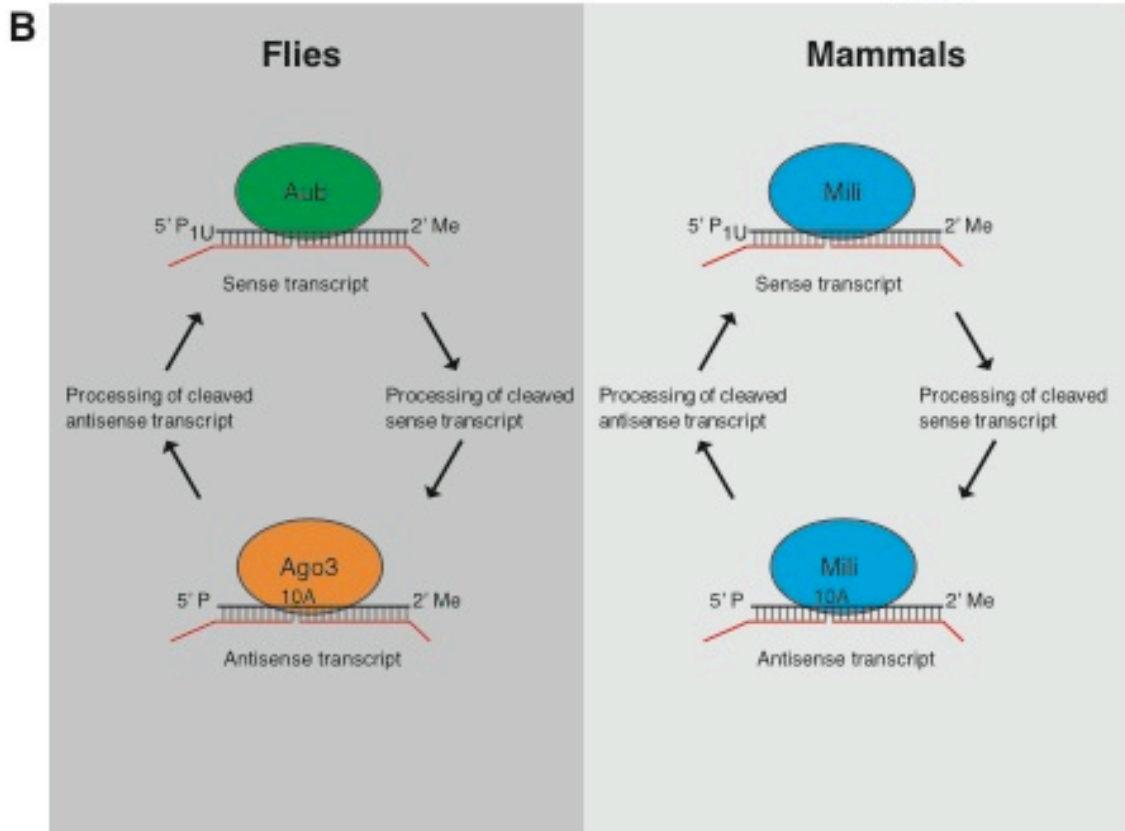
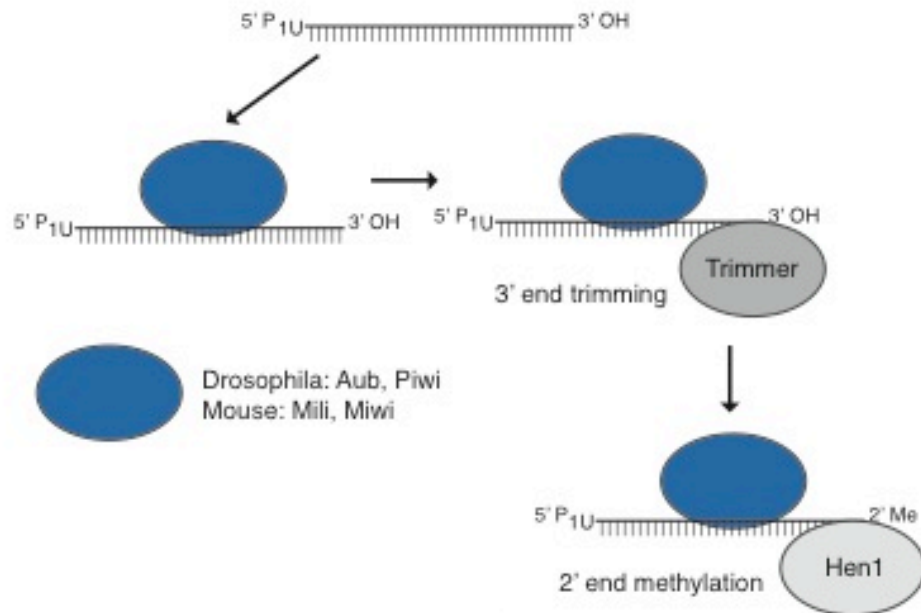
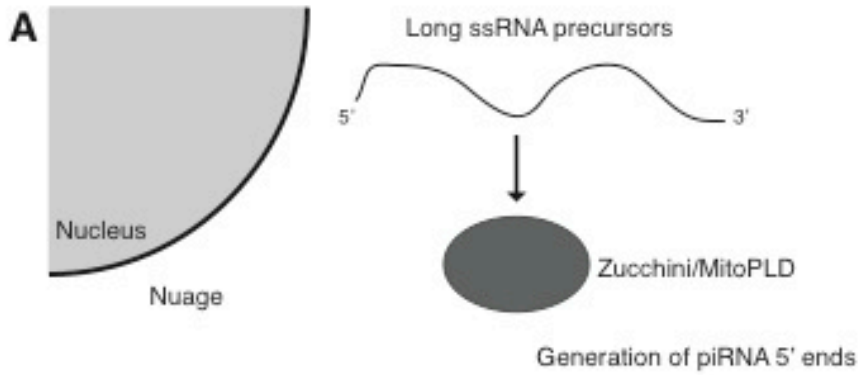


Figure 2. piRNA biogenesis.

(A) Generation of primary piRNAs from endogenous long ssRNA precursors is depicted in here. (B) Graphical description of the “ping-pong” amplification cycle for the generation of secondary piRNAs and amplification of specific piRNA classes in *Drosophila* and mouse. For further details please refer to the main text.

1.6.2 piRNA-mediated silencing mechanisms

piRNAs can silence their targets both at the transcriptional and post-transcriptional level. At the post-transcriptional level, PIWI proteins loaded with primary and secondary piRNAs are able to slice their targets in case of nearly perfect complementarity (Reuter, 2011). The sequence modules necessary for the recognition are not known yet. This renders harder the identification of targets for most of mouse pachytene piRNAs, which do not show perfect base pairing with any RNA transcript (Aravin, 2006; Girard, 2006; Lau, 2006). However, data from flies and mammals indicate that PIWI proteins do not tolerate high degree of mismatches (Reuter, 2011; Huang, 2013).

Transcriptional silencing of transposable elements requires the presence of PIWI proteins in the nucleus. *Drosophila* Piwi and mouse Miwi2 proteins are able to translocate to the nucleus and silence transposon elements present in the genome (Cox, 2000; Brennecke, 2007; Carmell, 2007; Aravin, 2008). In *Drosophila*, loss of Piwi reduces the levels of histone H3 lysine 9 trimethylated (H3K9me3) at the euchromatin regions targeted by Piwi. This in turn increases RNA Polymerase II occupancy on these regions, thus augmenting transcription (Sienski, 2012; Le Thomas, 2013; Rozhkov, 2013). It is not clear if Piwi recognizes target loci through displacement of one of the two DNA strands or by recognition of the transcribed RNA. However, it seems that Piwi silencing at specific transposon loci requires RNA Pol II transcription, supporting the latter hypothesis (Sienski, 2012).

In mammals, Miwi2 is the only PIWI protein that localizes in the nucleus (Aravin, 2008). Lack of Miwi2 induces transposon derepression during early stages of male germ cell development (Carmell, 2007; Kuramochi-Miyagawa, 2008). This is due to a defective cytosine methylation at the promoter of retrotransposons (Carmell, 2007;

Aravin, 2008; Kuramochi-Miyagawa, 2008). Similar to Piwi, the endonuclease activity of Miwi2 is dispensable for its functions (De Fazio, 2011; Darricarrère, 2013). The exact mechanism by which Miwi2 operates has not been elucidated yet. However, DNA methylation complex has been shown to be necessary for transposon silencing in male gonads (Bourc'his, 2004; Kaneda, 2004; Webster, 2005).

1.7 Physiological relevance of piRNAs in flies and mouse germ cell development

Genetic studies revealed the central function of the piRNA pathway in the regulation of transposon in germ cells. In *Drosophila*, Aub, Ago3 and Piwi take part to piRNA-mediated regulation of transposable elements in the female germ line (reviewed in Hutvagner, 2008). Flies ovaries are divided into functional units called ovarioles. Each ovariole presents at the apical part of the structure a germarium, that contains a group of 2-3 germline stem cells (GSCs) surrounded by a niche formed by somatic cells (Brown, 1962; Brown, 1964; Wieschaus, 1979; Lin, 1993). When GSCs divide asymmetrically, only the daughter cell adjacent to the niche is retained as a stem cell, while the other daughter cell initiates the differentiation process into a cystoblast. The cystoblast undergoes 4 incomplete divisions to form a cyst of 16 cells interconnected through intracellular bridges. The cyst is then enveloped by follicle cells in the centre of the germarium, forming an egg chamber. This is afterwards released from the germarium and develops into a mature egg (reviewed in Spradling, 1993). Aub and Ago3 are localized in the cytoplasm of germ cells, while Piwi is expressed both in germ and surrounding somatic cells and is localized mainly in the nucleus (Cox, 2000; Harris, 2001; Brennecke, 2007; Li, 2009) As such, germ cells rely on both primary piRNAs and secondary piRNAs derived from the ping-pong cycle to silence transposable elements: Aub and Ago3 deficient animals are sterile (Wilson, 1996; Harris, 2001; Li, 2009). On the contrary, *Drosophila* somatic cells rely only on primary piRNAs and Piwi to regulate transposable element expression. Indeed, Piwi mutants present transposon derepression both in somatic and germ cells, causing sterility due to defects in germ cells as well as in GSCs niche (Lin, 1997; Cox, 1998; Cox, 2000; Szakmary, 2005). The

nuclear localization of Piwi is essential for its activity, while its endonuclease activity is dispensable (Klenov, 2011; Darricarrère, 2013).

In mammals, the piRNA pathway is fundamental for the control of transposon activity and expression during male germ cell development (Deng, 2002; Kuramochi-Miyagawa, 2004; Carmell, 2007; Aravin, 2008; Kuramochi-Miyagawa, 2008; De Fazio, 2011; Reuter, 2011; Di Giacomo, 2013). Spermatogenesis is a highly organized process that takes place in the seminiferous tubules of the testis (Fig. 3). The first germ cell lineage consists of primordial germ cells (PGCs), which are specified from epiblast cells at embryonic day E7.0 in the mouse embryo (Chiquoine, 1954; Ginsburg, 1990; Lawson, 1992; Ohinata, 2005). During development, PGCs migrate from the base of the allantois to finally reach the genital ridges at embryonic day 10.5. These cells are then engulfed within the chords formed by Sertoli cells and surrounded by peritubular cells, becoming gonocyte or prospermatogonia (Clermont, 1957; Sapsford, 1962). Sertoli cells and peritubular cells represent the major somatic components in the seminiferous tubules. After entering the genital chords, gonocytes proliferate until embryonic day E16.5, and then they arrest at the G₁ phase of the cell cycle until 3 days after birth (PND 3) (Sapsford, 1962; Kluin, 1981; Vergouwen, 1991; Nagano, 2000). During this developmental window, a genome-wide DNA demethylation process takes place, followed by *de novo* DNA methylation to establish silencing epigenetic marks on transposon elements and male-specific imprinted genes (Walsh, 1998; Davis, 1999). Gonocytes start to proliferate again just after birth, and proliferation is accompanied by relocation of cells from the centre of the tubules towards the basement membrane (McGuinness, 1992; Nagano, 2000). Between PND 3-5, gonocytes are specified into spermatogonia stem cells (SSCs) (Huckinss, 1968; Kluin, 1981; McLean, 2003; Drumond, 2011). SSCs are part of the spermatogonia population, which represents the mitotic stages of germ cell development. After specification, SSCs are believed to proliferate to enlarge the stem cell pool and to differentiate to give rise to the first spermatogenic cycle (de Rooij, 2000). The first round of spermatogenesis is a highly synchronized process: the first meiotic cells, called spermatocytes, are produced at PND 10, while haploid cells such round spermatids first appear at PND 20-21 (Fig. 3). Mature sperm is then released commencing from PND 35 (Sapsford, 1962; Kluin, 1982; Sung,

1986; Vergouwen, 1991). This process continues throughout the life of the individual in highly organized manner in the lumen of the tubules: spermatogonia reside at the basement, while meiotic cells are moving towards the lumen during the differentiation process (Bellve, 1977; de Rooij, 2000).

The three PIWI proteins have distinctive expression patterns during embryonic and adult germ cell development (Fig. 3). Mili expression initiates in PGCs at embryonic day E12.5, and Mili protein is detected in almost all differentiating cells in the adult testis (Aravin, 2008; Di Giacomo, 2013). Miwi2 is highly expressed commencing from E14.5-E15.5; its protein level declines gradually after birth, becoming undetectable at PND 4 (Carmell; 2007; Aravin, 2008; Kuramochi-Miyagawa, 2008). Miwi is instead detected only in adult testis in late meiotic stages and in round spermatids (Deng, 2002; Di Giacomo, 2013). Loss-of-function genetic studies have demonstrated the roles of murine PIWI proteins, which mirror their expression patterns. In fact, loss of Miwi or its endonuclease activity causes male sterility due to transposon expression in round spermatids (Deng, 2002; Reuter, 2011). On the other hand, defects in Mili and Miwi2 lead to sterility due to impairment of early meiotic processes (Kuramochi-Miyagawa, 2004; Carmell, 2007; De Fazio, 2011). Both proteins are indeed needed for the reestablishment of DNA methylation on the promoter of transposable elements (Aravin, 2008; Kuramochi-Miyagawa, 2008). In addition, a recent study revealed a role of Mili during meiotic development: conditional ablation of Mili or its endonuclease activity after DNA methylation induces derepression of transposons during pachytene stage of the meiotic division, leading to sterility (Di Giacomo, 2013).

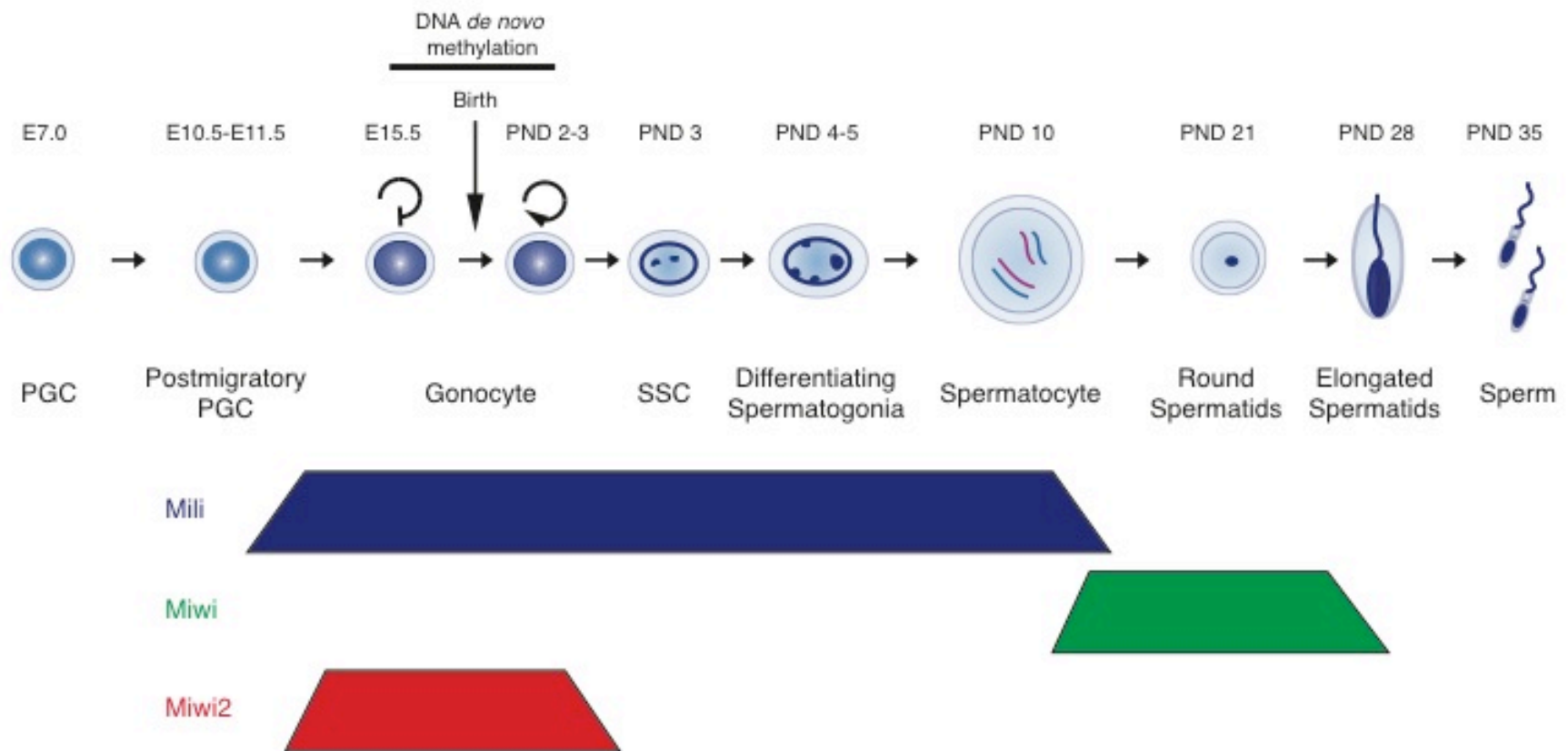


Figure 3. Germ cell development in mouse testis.

The generation and development of male germ cells is depicted. Primordial germ cells (PGCs) development is indicated until the cells are specified into spermatogonial stem cells (SSCs). For the meiotic and haploid cell types, the developmental time point of their first appearance in the mouse testis is also indicated. Expression profile of the three murine PIWI-like proteins (Mili, Miwi and Miwi2) is

1.8 PIWI proteins contribute to stem cell maintenance in different organisms

As for piRNAs, PIWI proteins are well-conserved throughout evolution, and it is hypothesized that the common eukaryotic ancestor encoded for one Ago-like and one PIWI-like protein (Cerutti, 2006; Grimson, 2008). Studies in bilaterian and non-bilaterian metazoan organisms revealed that PIWI proteins are not expressed only in germ cells, arguing to a possible role in somatic tissues (Reddien, 2005; Lee, 2011; Rajasethupathy, 2012; reviewed in Juliano, 2011). In particular, in cnidarians and sponges, PIWI orthologs are expressed in germ cells and in adult stem cells (Seipel, 2004; Denker, 2008; Funayama, 2010). In addition, work in the tunicate *Botrylloides leachi* showed that PIWI ortholog is expressed and is essential for the function of totipotent stem cells during regeneration (Brown, 2009; Rinkevich, 2010).

More detailed studies in planarians, which are protostomes like *Drosophila* and *C. elegans*, confirmed the physiological importance of piRNAs and PIWI proteins in adult stem cells (Reddien, 2005; Rossi, 2006; Palakodeti, 2008; De Mulder, 2009). Flatworms possess a pool of adult stem cells, called neoblasts, which represent ~30% of total cells in adult planarians and have the ability to differentiate in somatic and germ cells. Neoblasts participate to the generation of differentiated cells both during homeostasis and regeneration (Baguna, 1989; Newmark, 2002). Deep-sequencing of small RNA libraries discovered the presence of a class of small RNAs with features similar to animal piRNAs in the flatworm *Schmidtea mediterranea* (Palakodeti, 2008). Analysis of the expression of the three PIWI paralogs encoded in the *S. mediterranea* genome (SMEDWI-1, -2 and -3) revealed that these proteins are mainly expressed in neoblasts (Reddien, 2005; Palakodeti, 2008). Specific RNAi against *Smedwi-2* and *Smedwi-3*, but not *Smedwi-1*, demonstrated that these two proteins are necessary for tissue maintenance in adult animals during homeostatic and regenerative conditions, leading to lethality (Reddien, 2005; Palakodeti, 2008). This is likely due to defects in the differentiation of neoblasts, which in turn triggers a gradual depletion of stem cell pool (Reddien, 2005). In addition, piRNA levels are reduced after *Smedwi-2* and *Smedwi-3* knockdown,

suggesting that piRNA-PIWI complexes work to regulate expression profiles in neoblasts (Palakodeti, 2008).

In flies and mice, only Piwi and Miwi2 mutants displayed a phenotypic outcome that suggests a role in germ stem cell maintenance (Cox, 1998; Cox, 2000; Szakmary, 2005; Carmell, 2007). Indeed, lack of functional Piwi lead to sterility due to a reduction of GSCs and egg chambers. However, this is due to defects in somatic cells in the stem cell niche and not to a cell-autonomous defect in GSCs lacking Piwi (Cox, 1998; Cox, 2000; Szakmary, 2005; Klenov, 2011). On the other hand, genetic ablation of Miwi2 in mouse not only blocks spermatogenic differentiation during early meiosis, but it also induces the gradual loss of germ cells in the seminiferous tubules (Carmell, 2007; De Fazio, 2011). The latter defect does not depend on functional impairment of the somatic environment in the tubules, since transplantation of wild type germ cells in Miwi2-null testis reconstitutes complete spermatogenesis (Carmell, 2007). These results demonstrate a cell-autonomous role of Miwi2 in spermatogonia stem cell pool in mammals. In fact, the phenotypic consequences of Miwi2 depletion are reminiscent of genetic ablation of other proteins, such as Nanos2 and PLZF, which are used as markers for stem cell population (Tsuda, 2003; Buaas, 2004; Costoya, 2004; Nakagawa, 2007). Nonetheless, Miwi2 expression becomes undetectable soon after birth (Carmell, 2007; Aravin, 2008; Kuramochi-Miyagawa, 2008). More detailed studies on Miwi2 expression and function are needed to evaluate the physiological relevance of this protein in stem cells in mammals.

1.9 The quest for the identification of the spermatogonial stem cell

1.9.1 The “A single” and the “reserve stem cell” models for spermatogonial stem cells

Spermatogenesis is a highly regulated process that produces male haploid gametes from diploid germ cells in the testis. In mammals, spermatogenic development takes place in the seminiferous tubules of the testis, which comprise both somatic and germ cells (reviewed in Russell, 1990 and Eddy, 2002). The two principal somatic cell components

are peritubular cells and Sertoli cells. Peritubular cells cover the outside of the basal membrane present at the base of the tubules. Sertoli cells instead form an epithelium on the luminal part of the basal membrane. These cells form tight junctions between each other, providing a physical barrier between the tubule lumen and the other tissues called blood-testis barrier (Russell, 1990; Yoshida, 2010). In addition, Sertoli cells support germ cell development through nurturing and differentiating signals (Dym, 1970; Russell, 1990). Germ cells are localized in an ordered fashion in the lumen of the tubules, and their position correlates with the stage of differentiation (Fig. 4). Indeed, diploid germ cells, referred as spermatogonia, are found at the base of the tubules between Sertoli cells and the basal membrane. Spermatogonia cells form syncytia during cell division due to incomplete cytokinesis, allowing the synchronization of later division. As such, spermatogonia are typically found as isolated cells or syncytia of 2^n cells (Fawcett, 1959; Huckins, 1971a; Weber, 1987). Two classes of spermatogonia can be distinguished by morphological features: undifferentiated spermatogonia, which consist of single cells (A single or A_s) or syncytia of 2 (A paired or A_{pr}), 4, 8, 16 or 32 cells (A aligned or A_{al}); differentiated spermatogonia, which derive from undifferentiated spermatogonia and comprise stages A_1 , A_2 , A_3 , A_4 , Intermediate (In) and B spermatogonia (Huckins, 1971a; Huckins, 1978; de Rooij, 2000). B spermatogonia undergo the meiotic division, giving rise to spermatocytes. These cells translocate across the tight junction into the adluminal compartment (Bellve, 1977; de Rooij, 2000).

As in many other adult tissues, the existence of a stem cell population in mouse testis has been postulated. Two models have been proposed to describe the identity and behaviour of this spermatogonial stem cell (SSC) population (reviewed in de Rooij, 2000). The “ A_s model” hypothesizes that single isolated A_s spermatogonia are bona-fide SSCs (Huckins, 1971a; Oakberg, 1971). This theory is sustained by morphological observation on whole-mount testis sections and considers spermatogonia syncytia as terminally committed towards differentiation (Huckins, 1971a-b; Oakberg, 1971; de Rooij, 1973; Lok, 1983). As such, A_s spermatogonia are believed to be the true stem cell reservoir, with the possibility to divide asymmetrically for the formation of a stem cell and a daughter cell that will then form syncytia (Huckins, 1971a; de Rooij, 2000). A

second model, the “A₀ theory” or “reserve stem cell theory”, asserts that stem activity does not reside only in the population of A_s cells but also in spermatogonia syncytia (Clermont, 1968; Bartmanska, 1983). This scheme envisions the possibility that spermatogonia syncytia can dissociate and replenish the SSC pool. In fact, A_{al} spermatogonia are not distinguished in this model, and are believed to be part of the A₁-A₄ population. In normal homeostatic conditions, A₁ spermatogonia become A₄ without any change in their stemness capacity; A₄ cells can then either differentiate to In spermatogonia or divide to reform a chain of A₁ cells. The A_s and A_{pr} are believed to represent A₀ cells or reserve stem cells: these cells do not contribute to spermatogenesis in homeostatic conditions, but during regeneration. This model is supported by the presence of a constant number of A_s-A_{pr} cells, which rarely divide during homeostasis but actively cycle in response to irradiation (Clermont, 1968; Dym, 1970; de Rooij, 1973; Clermont, 1975; Erickson, 1978; Erickson, 1981). However, kinetics studies using H³-thymidine incorporation revealed that A_s and A_{pr} cells are actively cycling even in homeostatic conditions (Huckins, 1971b; de Rooij, 1973; Lok, 1983).

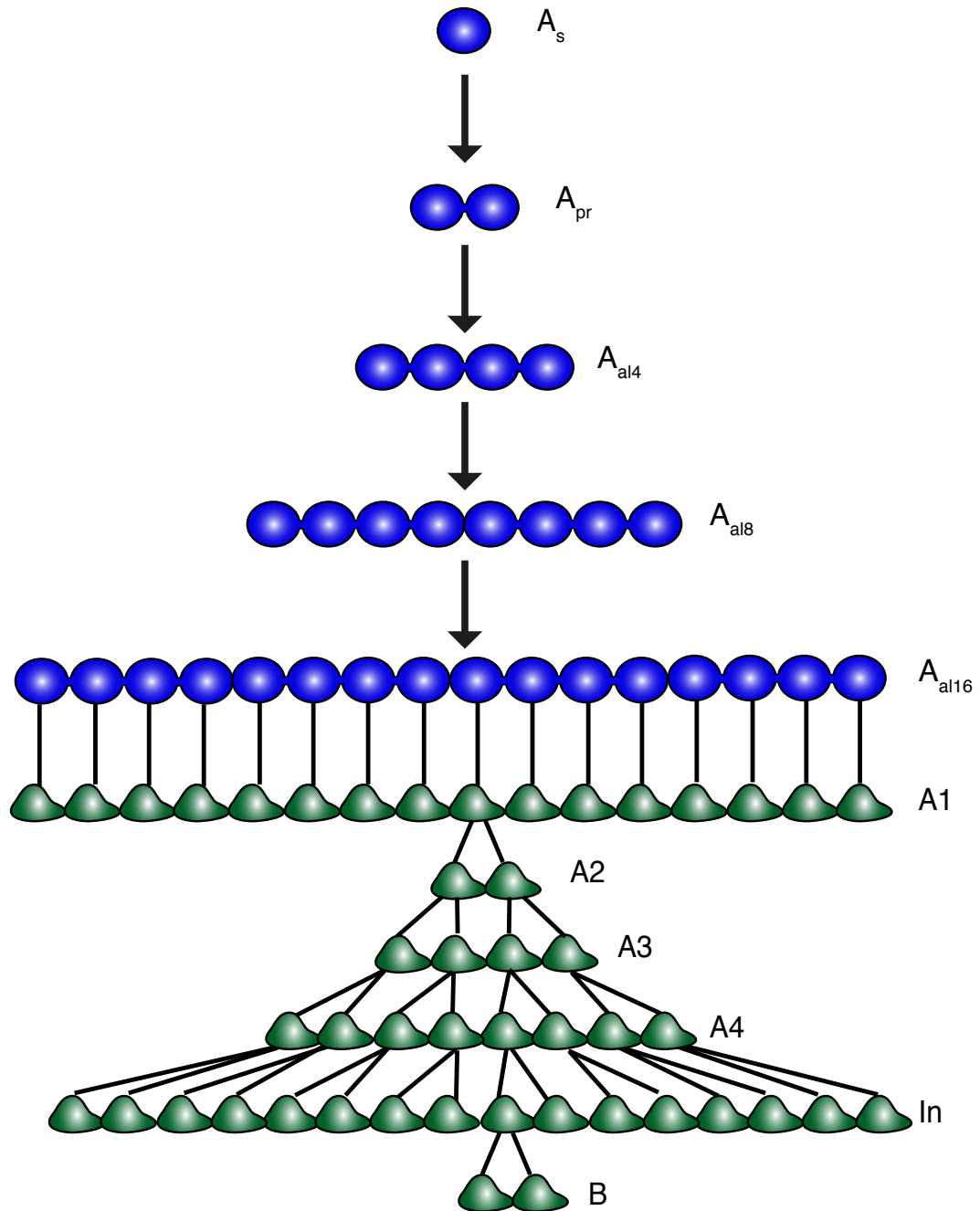


Figure 4. Spermatogonia organization in the murine testis.

The organization and classification of the different spermatogonia cells is schematically represented in here. For further details please refer to the main text.

1.9.2 Identification of spermatogonial stem cells: methods and markers

The first attempts to identify the SSC population in mouse testis were based on the discovery of markers for the different spermatogonia populations. Based on the assumption that A_s spermatogonia represent a population of bona-fide SSCs, immunofluorescence and live imaging experiments from whole mount seminiferous tubules were used to identify proteins selectively expressed in these cells. Glial cell line-derived neurotrophic factor receptor α 1 (GFRA1) and the receptor kinase c-Ret were first used as stem cell markers, and they have been shown to be necessary for spermatogonia maintenance both *in vitro* and *in vivo* (Meng, 2000; Kanatsu-Shinohara, 2003; Kubota, 2004; Buageaw, 2005; Hofmann, 2005; Naughton, 2006; He, 2007; Tokuda, 2007). Immunofluorescence experiments further demonstrated that the transcription factor PLZF and the RNA binding proteins Lin28 and Nanos2 are expressed in specific subsets of undifferentiated spermatogonia (Tsuda, 2003; Buaas, 2004; Costoya, 2004; Tokuda, 2007; Sada, 2009; Suzuki, 2009; Zheng, 2009). Transgenic mice expressing the fluorescent GFP protein under the promoter of Oct4 and Neurogenin 3 (Ngn3) genes have further enriched the number of available markers for spermatogonial cells (Ohbo, 2003; Yoshida, 2004). However, combination of these proteins revealed that A_s spermatogonia represent an heterogeneous cell population (Tokuda, 2007; Sada, 2009; Suzuki, 2009; Nakagawa, 2010). For example, GFRA1⁺ Nanos2⁺ PLZF⁺ Ngn3⁻ cells contains a high fraction of A_s and A_{pr} spermatogonia, while GFRA1⁻ Nanos2⁻ PLZF⁺ Ngn3⁺ cells largely contain all the A_{al} spermatogonia (Sada, 2009; Suzuki, 2009; Nakagawa, 2010). Interestingly, it was also reported that some Ngn3⁺ cells are able to become GFRA1⁺ and act as stem cells (Nakagawa, 2007; Nakagawa, 2010). Even though A_s spermatogonia heterogeneity is well-described, it has been recently shown that Id4 is expressed exclusively in A_s cells (Oatley, 2011). Combination of the enlisted proteins as well as the discovery of new spermatogonia markers are needed to understand if A_s spermatogonia are the only stem cell population in mammalian testis.

Transplantation assay represents the golden standard to test the stem cell potential of purified cell populations in many tissues (Spangrude, 1988; Stingl, 2006; Shackleton,

2006). Transplantation of testis cells is possible and gives the opportunity to test the self-renewal capacity of isolated cell populations (Brinster, 1994a-b). The intracellular localization of the aforementioned markers used for the identification of SSCs halted their use in transplantation assays. In addition, transfer of single cell suspension renders impossible to relate stem cell activity to the positional information that defines the different undifferentiated spermatogonia. As such, transplantation technique was initially used in unsorted mouse testis preparations to evaluate the effects of age on stem cells activity (Brinster, 1994b; Shinohara, 2001; McLean, 2003). First transplantation data showed that testis cells from pups (PND 5-12) have a much higher capacity to repopulate donor testis than neonatal (PND 0-2) cells and preparation from almost adult mice (PND 21-28) (Brinster, 1994b; Shinohara, 2001). A more detailed analysis demonstrated that cells from PND 10-12 possess the highest stem cell activity compared to both neonatal and adult testicular cells (McLean, 2003). However, cell preparation from adult cryptorchid testis, in which only spermatogonia and somatic components are present in the seminiferous tubules, displays the higher repopulating capacity (Shinohara, 2001; Kubota, 2004). Further studies coupled transplantation technique to cell population sorted by flow cytometry based on specific surface markers. Adhesion proteins such integrin $\alpha 6$ (CD49f) and $\beta 1$ (CD29) and morphological features as low side scatter were used to enrich for stem cell activity (Shinohara, 2000 and 2001; Kubota, 2003). On the other hand, c-Kit and integrin αv (CD51) levels negatively correlate with repopulating activity (Shinohara, 2000 and 2001; Kubota, 2003). Comparison with other stem cell populations such as hematopoietic and neural stem cells highlighted the differences and similarities on surface marker profiles (Kubota, 2003). A 25 fold enrichment is achieved over unsorted cells from cryptorchid testis when MHC-I⁺ Thy-1⁺ CD49f⁺ cells were transplanted into recipient mice, with an estimated stem cell concentration of 1 out 15 cells (Kubota, 2003). Additional surface markers, like the tetraspanin CD9 and the adhesion molecule EpCAM, were used alone to select cells through Magnetic-activated Cell Sorting (MACS) for stem cell activity (Kanatsu-Shinohara, 2004; Kanatsu-Shinohara, 2011). Recent applications of MACS- and FACS-based cell purification methods allowed for the analysis of GFRA1⁺ and PLZF⁺ cell population in transplantation assays (Buageaw, 2005; Grisanti, 2009; Hobbs,

2010). Reconstitution with GFRA1-enriched cells gave opposing results, with either increase or reduction of donor-derived colonies (Buageaw, 2005; Grisanti, 2009). However, analysis of PLZF-expressing cells by flow cytometry revealed that these cells are mainly CD45⁻ CD51⁻ Thy-1⁺ c-Kit⁻. Sorting and reconstitution of donor testis with this cell population gives a 25 fold increase in the cologenic activity compared to unsorted cells (Hobbs, 2010). This sorting strategy yields a population in which 1 out of 80 cells is estimated to have self-renewal capacity (Hobbs, 2010). Further detailed analysis on gene expression is needed to identify the real SSCs population.

Chapter 2: Materials and methods

2.1 Generation of *Ago2*^{S388A} and *Miwi2*^{tdTomato} alleles

2.1.1 *Ago2*^{S388A} targeting strategy

The strategy to create a nonphosphorylatable *Ago2* allele consists in the insertion of two nucleotide exchanges in exon 10 of the endogenous *Ago2* locus to convert the AGT codon for serine 388 into a GCT codon for an alanine residue. The two nucleotide mutations introduced maintain the codon usage to avoid alteration of translational rate of the mutant protein (Codon Usage Database, species *Mus musculus*, www.kazusa.or.jp). The targeting vector (*pDTA-Ago2Neo-S388A*) contains homology arms and a *neomycin* (*neo*) resistance cassette flanked by two LoxP sites between exon 8 and 9. Cre-mediated recombination of the *neo* element allows the creation of a transcriptionally competent *Ago2*^{S388A} knock-in allele. The targeting vector *pDTA-Ago2Neo-S388A* was constructed by Dr. Philip Hublitz from the Gene Expression Facility of EMBL Monterotondo.

2.1.2 *Miwi2*^{tdTomato} targeting strategy

A fluorescently-labeled *Miwi2* transcriptional reporter allele was created by the direct insertion of a tdTomato expression cassette in the endogenous *Miwi2* locus. The targeting vector (*pDTA-Miwi2-Neo-tdTomato*) carries homology arms to the *Miwi2* locus and a *neomycin* (*neo*) resistance cassette flanked by two FRT sites to allow an FLP-dependent excision. The tdTomato expression cassette is fused to the coding region of exon 1 of the *Miwi2* locus, followed by a strong poly-A signal derived from the Simian virus 40 (Carswell and Alwine, 1989) to prevent expression of downstream *Miwi2* regions. A synthetic intron is inserted between the 5' untranslated region and the translated part of exon 1 to aid correct nuclear processing and export. The targeting vector *pDTA-Ago2Neo-S388A* was constructed by Dr. Philip Hublitz from the Gene Expression Facility of EMBL Monterotondo.

2.2 Generation of mice using homologous recombination in mouse embryonic stem cells

The targeting constructs pDTA-Ago2Neo-S388A was electroporated into IB10 mouse embryonic stem cells (ESCs) (Passage 14) derived from the 129P2 genetic mouse background (Robanus-Maandag, 1998). In contrast, the pDTA-Miwi2-Neo-tdTomato targeting construct was electroporated into A9 ESCs (Passage 11) derived from a F₁ hybrid of C57Bl/6 and 129 mouse genetic backgrounds (Kind gift of A. Wutz). IB10 and A9 ESCs were routinely maintained in standard ES cell medium (See Appendix “Buffers and Media solutions”) on a monolayer of Mitomycin C (MMC)(Sigma, M4287)-treated primary mouse embryonic fibroblasts (pMEF). Approximately 10⁷ ESCs were electroporated with a given targeting construct and plated onto neomycin resistant MMC-treated pMEFs. 24h after electroporation, selection for ESC clones carrying the *neo* resistance was started by adding G418 (250ug/ml active concentration)(GIBCO, 11811) to the ES cell medium. After 5 and 6 days of selection for A9 and IB10 ESCs respectively, 200 ES cell colonies were picked for each electroporation and expanded and frozen in ES cell freezing medium. Southern blot screening was used to identify clones undergone to homologous recombination. Depending on the construct, the targeting efficiency ranged between 1-10%. For generation of *Ago2*^{Neo-S388A/+} chimeric animals, two independent clones were expanded and injected in embryos at the blastocysts stage. For the generation of ESC mice from *Miwi2*^{Neo-tdTomato/+} A9 cells, two independent clones were expanded and injected in embryos at the morula stage. Upon confirmed germ-line transmission of the targeted allele by Southern blot, the mice were crossed either to Deleter-Cre mice (Schwenk, 1995) or to the Flp-expressing transgenic mice (FLPeR) (Farley, 2000) to remove the *neo* cassette from the *Ago2* and *Miwi2* targeted loci, respectively. These genetic manipulations resulted in the generation of *Ago2*^{S388A} and *Miwi2*^{tdTomato} alleles. For the *Ago2* phosphomutant allele, the resulting *Ago2*^{S388A/+}; *Tg*^{DelCre} animals were backcrossed for one generation with C57Bl/6N mice to remove the Cre transgene. Mice in this 129P2xC57Bl/6N mixed genetic background were employed for the first experimental sets. In addition, *Ago2*^{S388A/+} or *Ago2*^{Neo-S388A/+} heterozygotes in a 129P2xC57Bl/6N

mixed background were mated with *Ago2^{FL/FL}*; *Mx-Cre* (O’Carroll, 2007; Kuhn, 1995) and *Ago2^{FL/FL}*; *Zp3-Cre* (De Vries, 2000) for the analysis of hematopoietic and oocyte development, respectively. Two co-isogenic lines were created by backcrossing *Ago2^{S388A/+}* animals for at least 8 generation with C57Bl/6N and 129S2 inbred mice from Harlan. *Miwi2^{tdTomato/+}* animals employed for the analysis were backcrossed at least twice with C57Bl/6N mice before analysis.

All of the mice were bred and maintained in EMBL Mouse Biology Unit, Monterotondo, in accordance with Italian legislation (Art. 9, 27. Jan 1992, no116) under license from the Italian Ministry of Health.

2.3 PCR genotyping of Ago2 and Miwi2 mouse alleles

To perform the genotype of the different mouse alleles, standard PCR reagents and protocols were used from DNA derived from mouse tail biopses. DNA isolation consists of the lysis of tails biopses in 200µl of 0.05M NaOH for 40 minutes at 95°C. Subsequently, 20µl of 1M Tris-HCl pH 7.5 was added to equilibrate the pH of the solution and 1µl of this solution was use for each PCR reaction as a template. TAQ polymerase was acquired from the PEPCF Facility in EMBL Heidelberg.

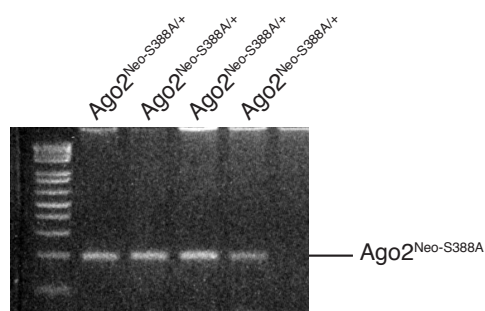
Components	Final concentration	Volume (µl)
KT Buffer (10X)	1X	2.5
dNTPs (20mM)	200µM	0.25
Primer Mix (20µM)	200nM	0.25
Genomic DNA	N/A	1
Taq Polimerase	N/A	0.25
PCR-grade ddH ₂ O		Up to 25

2.3.1 Genotype protocol for Ago^{Neo-S388A} allele

Primers:

Ago2-S388A-Tgeno-F1	5'-cctgccacgatccataacttc-3'
Ago2_T-geno_R1	5'-tgtccagcaactatgttacagacc-3'

Expected length:



Ago2^{Neo-S388A} 195bp

PCR program:

Step	Temperature (°C)	Time (s)	Cycles
Denaturation	95	180	1X
Denaturation	95	30	35X
Annealing	62	30	
Elongation	72	30	
Final elongation	72	300	1X
Pause	12	Forever	1X

Resolve PCR in a 3.5% Agarose gel run at 200V for 20 minutes.

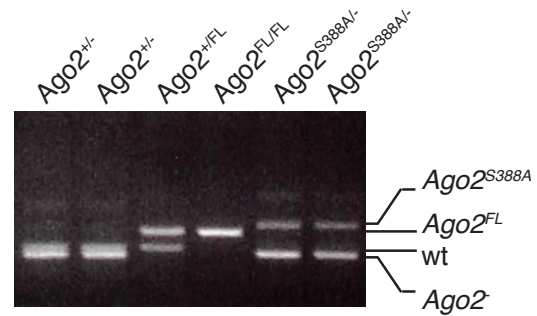
2.3.2 Genotype protocol for *Ago2*^{S388A}, *Ago2*^{FL} and *Ago2*⁻ allele

Primers:

Ago2_Geno_F38096	5'-gtgagccactcactgcac-3'
Ago2_Geno_R38376	5'-tgatcatggttgaggtctga-3'
Ago2_Geno_NR1	5'-cctgccaatctgaggtcagtc-3'

Expected length:

Wt	301bp
<i>Ago2</i> ⁻	273bp
<i>Ago2</i> ^{FL}	351bp
<i>Ago2</i> ^{S388A}	376bp



PCR program:

Step	Temperature (°C)	Time (s)	Cycles
Denaturation	94	180	1X
Annealing	58.4	60	1X
Elongation	72	120	1X
Denaturation	94	30	34X
Annealing	58.4	40	
Elongation	72	30	
Final elongation	72	180	1X
Pause	12	Forever	1X

Resolve PCR in a 3.5% Agarose gel run at 200V for 40 minutes using thin comb for a proper separation of bands.

2.3.2 Genotype protocol for *Miwi2^{tdTomato}* allele

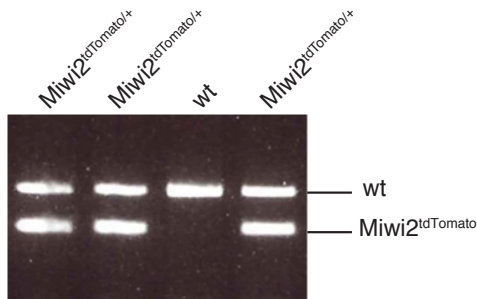
Primers:

Miwi2_Geno_FW1	5'-tactcccaaactccgagtc-3'
Miwi2_Geno_R1	5'-gtgcctatcagaaacgcaa-3'
Miwi2_Geno_R2	5'-ctcctagccagagtgcctt-3'

Expected length:

Wt 329bp

Miwi2^{tdTomato} 230bp



PCR program:

Step	Temperature (°C)	Time (s)	Cycles
Denaturation	94	180	1X
Denaturation	94	30	35X
Annealing	63	30	
Elongation	72	40	
Final elongation	72	300	1X

Pause	12	Forever	1X
-------	----	---------	----

Resolve PCR in a 3.5% Agarose gel run at 200V for 20 minutes.

2.4 Southern Blot on restriction enzyme-digested genomic DNA

2.4.1 Isolation of DNA for Southern Blot

Tail biopses or single cell suspensions were digested by incubation in 500µl of Tail Digestion Buffer (see Annex 1) at 56°C overnight. 500µl of phenol-chloroform mixture (Sigma, 77617) were added to the samples: tubes were shaken vigorously for 10 seconds and centrifuged at 10,000RPM for 3 minutes in a table-top centrifuge (Eppendorf, Centrifuge 5424). The upper aqueous phase was then removed and transferred in a clean 1.5ml tube. This operation was repeated twice. Subsequently, a 1:1 volume of chlorophorm (Merck, K33534645) was added to samples. After shaking and centrifugation as previously described, the aqueous phase was transferred to a clean 1.5ml tube. Then a 1:1 volume of isopronanol (Sigma, 33539) and a 1:10 volume of 3M sodium acetate (Sigma, S2889) were added to each sample and the purified DNA was precipitated by centrifugation at maximum speed for 5 minutes. The supernatant was removed and the DNA washed with 1ml of 70% ethanol. After centrifugation at maximum speed for 5 minutes, the ethanol was carefully removed and the pellet left to air-dry for 5 minutes. DNA was resuspended in 50µl of PCR-grade ddH₂O and store at 4°C. DNA content was quantified with a NanoDrop 8000 spectrophotometer (Thermo Scientific).

2.4.2 Preparation of Southern Blot probes

Southern blot probes for both Ago2 (Probe 12i) and Miwi2 (Miwi2 3' probe) were synthesized by PCR reaction from tail-derived DNA. The following primers were used for the production of the probes:

Primers	Sequence	Probe length
---------	----------	--------------

Ago2_probei12_F	5'-cccaaagcctgtaaagtctagc-3'	458bp
Ago2_probei12_R	5'-gtgggtgtagtctcggaaca-3'	
Miwi2_Ex3_probe_F	5'-aaggaaggatagtcgcgtgtt-3'	352bp
Miwi2_Ex3_probe_R	5'-acaccaactcttcgaagtcc-3'	

PCR program:

Step	Temperature (°C)	Time (s)	Cycles
Denaturation	95	180	1X
Denaturation	95	30	35X
Annealing	59	40	
Elongation	72	60	
Final elongation	72	300	1X
Pause	12	Forever	1X

PCR products were resolved in a 1% Agarose gel run at 120V for 1 hour. Fragments of the correct size of the probes were excised from the gel using a scalpel under a transilluminator and purified using the QIAquick Gel Extraction Kit (Qiagen, 28704) following manufacturer instructions. The DNA was eluted in 50µl of PCR-grade ddH₂O and store at -20°C. DNA content was quantified with a NanoDrop 8000 spectrophotometer (Thermo Scientific).

2.4.3 Southern Blot

10µg of purified DNA was digested overnight at 37°C with 40U of BamHI (NEB, R0136S) or AseI (NEB, R0526S) for *Ago2* or *Miwi2* alleles screening, respectively. For the separation of *Ago2* alleles, samples were loaded in a 1.2% Agarose gel and run at 130V for 5 hours; for the distinction of *Miwi2* alleles, a 0.8% Agarose gel was run at 130V for 3 hours. The DNA fragments were successively transferred overnight to a Hybond™-N+ Nylon Membrane (GE healthcare, RPN203B) in a classic blotting sandwich using passive capillary transfer in alkaline solution (0.4M NaOH, 1.5M NaCl).

After transfer completed, the membrane was rinsed twice with 0.2M SSC, dried at 37°C for 20 minutes, and the DNA UV-linked at 150mJ/cm².

30ng of purified probe were marked with α -[32P]-dGTP using the Random primers labeling kit (Invitrogen, 18187-013) according to manufacturer instructions. The membrane was first incubated for 2 hours at 65°C in Southern hybridization buffer (See Annex 1), then the labeled probe was added to the solution and left for hybridization overnight. Membrane was thoroughly washed three times with Southern washing solution pre-heated at 65°C (See Annex 1), each wash step taking 20 minutes at 65°C. Finally, the membrane was wrapped in Saran wrap and exposed to a phosphoscreen for 24 hours. Phosphoscreen was scanned using the Fluorescent Image Analysis System FLA-5100 (Fujifilm).

2.5 Sequencing of wild type and *Ago2*^{S388A} alleles

Sequencing of tail-DNA from two wild type and two *Ago2*^{S388A}/*S388A* littermates in a 129P2xC57Bl/6N mixed genetic background was used to confirm the presence of two point mutations (AGT to GCT) for the conversion of serine 388 to an alanine codon. DNA was isolated with phenol-chlorophorm mixture as previously described, and a 403bp fragment encompassing exon 9 to 10 of the *Ago2* locus was amplifying using the following primer set:

Ago2_Exon9-10_F	5'-aagagcacttggcctgtc-3'
Ago2_Exon9-10_R	5'-aggtctgtaacatagttgctgga-3'

PCR program:

Step	Temperature (°C)	Time (s)	Cycles
Denaturation	95	180	1X
Denaturation	95	30	35X
Annealing	61	40	

Elongation	72	60	
Final elongation	72	300	1X
Pause	12	Forever	1X

PCR fragments were purified using the PCR purification kit (QIAgen, 28104) and 40ng of amplicon were used for the following sequencing reaction.

Components	Final concentration	Volume (μl)
BigDye Terminator Buffer (AB, 4339843) 5X	1X	3
BigDye Terminator Buffer (AB, 4337454)	N/A	2
Primer Ago2_Exon9-11_F (2 μ M)	160nM	1.6
PCR fragment	40ng	1-2
PCR-grade ddH ₂ O		Up to 20

Sequencing program

Step	Temperature ($^{\circ}$C)	Time (s)	Cycles
Denaturation	95	300	1X
Denaturation	95	15	25X
Annealing	52	15	
Elongation	60	180	
Pause	12	Forever	1X

Fragments from sequencing reaction were precipitated with ethanol and resuspended in 10 μ l of PCR-grade ddH₂O. 4 μ l of this solution were then crosslinked with formamide HiDi (AB, 4311320) for 3 minutes at 95 $^{\circ}$ C. Samples were then sequenced using the ABI310 sequencer from Applied Biosystem.

2.6 Isolation and PCR genotyping of mouse embryos from *Ago2*^{S388A/+} intercrosses

2.6.1 Isolation and genotyping of embryos at embryonic day from E6.5 to E12.5

Ago2^{S388A/+} heterozygous animals from a 129P2xC57Bl/6N mixed and 129S2 genetic background were intercrossed for embryogenetic studies. Vaginal plug was checked for 1-4 days after mating: the day of the appearance of vaginal plug was considered as embryonic day E0.5. At the day of isolation, pregnant females were sacrificed by cervical dislocation and the isolated uterus was transferred on ice-cold 1X PBS (Gibco, 14190-094). Single deciduas were then separated and the embryos were isolated from maternal tissues under a stereomicroscope. Embryos were transferred in clean ice-cold 1X in a 10mm dish (Falcon, 351029) to take pictures using a Leica stereomicroscope (Leica MZ12). For DNA isolation from E9.5-E12.5 embryos, a small piece of the embryo was taken and digested in 100µl of embryo lysis buffer (See Annex 1) in a 1.5ml tube. Whole embryos isolated at E6.5-E7.5 were transferred in a 1.5ml containing 25µl of embryo lysis buffer. Samples were incubated for 2 hours at 54°C and then passed at 72°C for 20 minutes to inactivate the proteinase K activity. 1-2µl of embryo lysis buffer was employed to genotype the embryos by PCR as described in the previous section.

2.6.2 Isolation of embryos at embryonic day E3.5

Ago2^{S388A/+} heterozygous animals from a 129S2 genetic background were intercrossed for embryogenetic studies. Vaginal plug was checked for 1-4 days after mating: the day of the appearance of vaginal plug was considered as embryonic day E0.5. At E3.5, pregnant females were sacrificed by cervical dislocation and the uterus was carefully isolated and cleaned under a stereomicroscope. Blastocysts were flushed out from the uterus using 1ml of M2 medium and 1ml syringe with a 26 ½ G needle (BD Plastipack, 300015) in a 6mm plastic dish (Falcon, 353001). Each embryo was then transferred in 10µl of embryo lysis buffer in a 1.5ml tube. Samples were incubated for 2 hours at 54°C and then passed at 72°C for 20 minutes to inactivate the proteinase K activity. 2µl of

embryo lysis buffer was employed to genotype the embryos by PCR as described in the next section.

2.6.3 PCR genotyping of embryos isolated at E3.5 by nested PCR

To genotype embryos at the E3.5 stage, two consecutive PCR reactions were employed to amplify distinctive fragments for wild type and *Ago2*^{S388A} alleles. This two-step protocol allows the specific amplification of the *Ago2* locus from low content DNA samples and limits the presence of contaminant bands. Indeed, a first PCR reaction amplifies specifically the region of interest from the genomic DNA, while the second reaction employs internal primers that anneal within the DNA fragment amplified during the first reaction. The cumulative number of amplification cycles (55 cycles) permits the amplification of the desire band from low quantities of DNA samples.

First PCR reaction primer set:

Ago2_Geno_F38096	5'-gtgagccactcactgcac-3'
Ago2_Geno_R38376	5'-tgatcatggtgaggtctga-3'

Wild type 301bp
Ago2^{S388A} 376bp

PCR program for the first reaction:

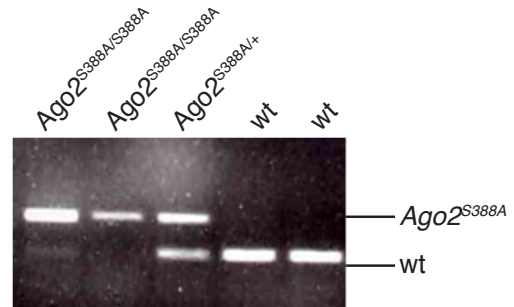
Step	Temperature (°C)	Time (s)	Cycles
Denaturation	95	180	1X
Denaturation	95	30	30X
Annealing	58	40	
Elongation	72	30	
Final elongation	72	300	1X

Pause	12	Forever	1X
-------	----	---------	----

Second PCR reaction:

SC_Ago2_Nest2_FW	5'-tcatgccagggttacctacaa-3'
SC_Ago2_Nest2_RV	5'-agggagatttcagaggctgag-3'

Wild type 104bp
Ago2^{S388A} 180bp



PCR program for the second reaction:

Step	Temperature (°C)	Time (s)	Cycles
Denaturation	95	180	1X
Denaturation	95	30	25X
Annealing	59	40	
Elongation	72	30	
Final elongation	72	180	1X
Pause	12	Forever	1X

Resolve in a 3.5% Agarose gel at 200V for 20 minutes.

2.7 Analysis of fertility in *Ago2*^{S388A} mutant animals

Ago2^{S388A/FL}; *Zp3-Cre* and *Ago2*^{+/FL}; *Zp3-Cre* females in a mixed genetic background were mated with wild type C57Bl/6N male animals of known fertility. Females used for

testing were 2-4 months old. The presence of a vaginal plug was evaluated 1-4 days after mating, and the males were removed from the cage after the appearance of the plug. The size of the litter was evaluated both at birth and at weaning. Pups were genotyped by PCR at weaning to confirm the efficiency of Cre recombination.

Wild type and *Ago2*^{S388A/S388A} animals in a C57Bl/6N genetic background were mated with wild type C57Bl/6N mice of the opposite sex. The mice used for testing were 2-4 months old. The presence of a vaginal plug was evaluated 1-4 days after mating, and the males were removed from the cage after the appearance of the plug. The size of the litters was evaluated both at birth and at weaning.

2.8 Isolation of cells from bone marrow, spleen, testis and thymus for flow cytometry

2.8.1 Isolation of single cell suspension from bone marrow

Bone marrow cells were isolated from the femur and tibia of adult mice (2-4 months old if not indicated). The procedure is as follows:

1. Sacrifice the mouse with CO₂.
2. Isolate the whole femur and tibia from the adult mouse. Remove the foot by cutting it near the joint. Place it in a 15ml falcon tube with ice-cold 10ml of BSS+2%FCS (See Annex 1).
3. Carefully clean the femur and the tibia from the muscular and cartilaginous tissues by using forceps and clean paper towel.
4. Transfer the clean tibia and femur in a 250ml porcelain mortar. Add 10ml of ice-cold BSS+2%FCS and use a 21cm pestle to crush the sample. Continue until all the red pulp of the bone marrow is separated from the rest.
5. Further disrupt disembedded marrow by pipetting with a 10ml pipette.
6. Filter the solution with a 70µm cell strainer (BD Falcon, 352350) directly in a 50ml falcon tube.
7. Rinse with additional 10ml of ice-cold BSS+2%FCS the mortar and filter it through the same 70µm cell strainer.

8. Centrifuge cells at 1,200RPM for 5 minutes at 4°C (Eppendorf 5810R, swinging bucket rotor)
9. Remove supernatant and resuspend cells in 10ml of ice-cold BSS+2%FCS.

2.8.2 Isolation of single cell suspension from spleen and thymus

Spleen and thymus cells were isolated from adult 2-4 months old mice:

1. Sacrifice the mouse with CO₂.
2. Isolate the spleen and the thymus from the animal. For spleen, carefully remove from adjacent tissues with a forceps. For the thymus, open the thoracic cavity without damaging the lungs and the heart, and remove carefully the thymus without breaking the veins near it. Transfer the organ in a 15ml falcon tube containing 5ml of ice-cold BSS+2%FCS.
3. Place a 70µm cell strainer in a 6mm dish. Transfer the spleen or the thymus along with the 5ml BSS+2%FCS on top of the cell strainer. Smash the tissue through the grid by using the sterile plunger of a 1ml syringe. Rinse the cell strainer with 1ml BSS+2%FCS.
4. Resuspend cells repeatedly with a 10ml pipette to ensure the formation of a single cell suspension. Rinse the 6mm dish with 1ml of ice-cold BSS+2%FCS. Transfer the solution to a 15ml falcon tube.
5. Centrifuge cells at 1,200RPM for 5 minutes at 4°C.
6. Remove the supernatant and resuspend cells in 10ml of ice-cold BSS+2%FCS.

2.8.3 Erythrolysis of bone marrow and splenic single cell suspensions

In order to analyse the different leukocyte population, samples derived from bone marrow and spleen need to be depleted from erythroid cells. This is achieved by inducing the lysis of enucleated cells through hypotonic stress. The protocol is as follows:

1. Centrifuge bone marrow and spleen samples at 1,200RPM for 5 minutes at 4°C.
2. Remove supernatant. Resuspend cells in 1ml of ACK lysis buffer (See Annex 1) and incubate for 2 minutes at room temperature.
3. Add 20ml of ice-cold BSS+2%FCS to restore the osmotic conditions.

4. Centrifuge at 1,200RPM for 5 minutes at 4°C.
5. Remove supernatant. Repeat lysis in case the cell pellet has still a red colour. In case of a successful red blood cell lysis, resuspend cells in 10ml of ice-cold BSS+2%FCS.

2.8.4 Isolation of single cell suspension from juvenile male testis

Cells from juvenile (post-natal day 14) mice were isolated as follow:

1. Sacrifice the mouse by cervical dislocation;
2. Isolate both testes and remove the tunica albuginea. Place testes in 1ml of Goni-MEM medium (See Annex 1) in a 1.5ml tube.
3. Let the testes sediment by gravity, then remove the supernatant and add 1ml of fresh Goni-MEM to the tube.
4. Add 40µl of collagenase (12.5mg/ml, Sigma, c7657). Incubate in shaking for 10 minutes at 32°C.
5. Centrifuge the sample at 1,000RPM for 5 minutes in a table-top centrifuge (Eppendorf, Centrifuge 5424).
6. Remove supernatant and wash with 1ml fresh Goni-MEM.
7. Centrifuge the sample at 1,000RPM for 5 minutes in a table-top centrifuge.
8. Remove supernatant. Add 1ml of 0.05% trypsin+EDTA (Invitrogen, 25300-054). Incubate in shaking for 5 minutes at 32°C.
9. Neutralize trypsin by addition of 200µl of FCS. Centrifuge at 1,000RPM for 5 minutes in a table-top centrifuge.
10. Remove supernatant, then add 100µl of Goni-MEM containing 0.05mg/ml of DnaseI (Sigma, DN-25-100µg). Pipette thoroughly the sample several times to help the fragmentation of the DNA released from dead cells.
11. Add 1ml of Goni-MEM and centrifuge at 1,000RPM for 10 minutes in a table-top centrifuge.
12. Remove supernatant. Resuspend cells in 1ml of fresh Goni-MEM. Keep cells on ice for immunostaining for flow cytometry.

2.8.5 Isolation of single cell suspension adult male testis

1. Sacrifice the mouse by cervical dislocation;
2. Isolate both testes and remove the tunica albuginea. Place testes in 25ml of Goni-MEM medium in a 50ml Falcon tube.
3. Let the testes sediment by gravity, then remove the supernatant and add 24ml of fresh Goni-MEM to the tube.
4. Add 1ml of collagenase (12.5mg/ml, Sigma, c7657). Incubate in a water bath shaking for 10 minutes at 32°C.
5. Let the testes sediment by gravity, then remove the supernatant and add 25ml of fresh Goni-MEM to the tube.
6. Let the testes sediment by gravity, then remove the supernatant. Add 5ml of 0.05% trypsin+EDTA (Invitrogen, 25300-054). Incubate in a water bath shaking for 5 minutes at 32°C.
7. Neutralize trypsin by addition of 1ml of FCS. Centrifuge at 1,000RPM for 5 minutes (Eppendorf 5810R, swinging bucket rotor).
8. Remove supernatant, then add 1ml of Goni-MEM containing 0.05mg/ml of DnaseI (Sigma, DN-25-100µg). Pipette thoroughly the sample several times to help the fragmentation of the DNA released from dead cells.
9. Add 20ml of Goni-MEM and filter cells with a 70µm cell strainer. Centrifuge at 1,000RPM for 5 minutes (Eppendorf 5810R, swinging bucket rotor).
10. Remove supernatant. Resuspend cells in 20ml of fresh Goni-MEM. Keep cells on ice for immunostaining for flow cytometry.

2.9 Poly I:C and lypopolysaccharide treatment

Adult *Ago2*^{+/*FL*}; *MxCre* and *Ago2*^{*S388A/FL*}; *Mx-Cre* between 2-3 months old were injected intraperitoneally with 250µg of polyinosinic:polycytidylic acid (poly I:C, Amersham Biosciences, 27-4732) for a total of three times, with an interval of 3 days between each administration.

Administration of 30µg/Kg of lypopolysaccharide from *Escherichia Coli 0111:B4* (LPS, Sigma, 4391) with 800mg/Kg of D-galactose (D-gal, Sigma, G0750) was performed on

adult mice through intraperitoneal injection. The survival rate of each cohort of injected animals was scored up to 24 hours after injection. 7 mice per cohort were employed in a C57Bl/6N genetic background, while 10 recipient mice after 3 months from bone marrow transplantation were administered with LPS+D-gal for each experimental group.

2.10 Generation of chimeric mice by bone marrow transplantation

Bone marrow cells isolated from *Ago2*^{+/*FL*}; *Mx-Cre*; *Ly5.2* and *Ago2*^{S388A/*FL*}; *Mx-Cre*; *Ly5.2* adult mice in a mixed genetic background were used for transplantation in lethally irradiated C57Bl/6N recipients. Each control and experimental donor mouse was used to transplant 5 recipient animals. Three independent transplantations were completed with three different donors for both *Ago2*^{+/*FL*}; *Mx-Cre*; *Ly5.2* and *Ago2*^{S388A/*FL*}; *Mx-Cre*; *Ly5.2* animals. The procedure is listed below:

1. 6-8 weeks old *Ly5.1* females in a C57Bl/6N genetic background were irradiated with 875rad 16-24 hours before transplantation.
2. Bone marrow cells from *Ago2*^{+/*FL*}; *Mx-Cre*; *Ly5.2* and *Ago2*^{S388A/*FL*}; *Mx-Cre*; *Ly5.2* animals were isolated as previously described, without lysis of red blood cells.
3. Cells were washed 3 times with 20ml of ice-cold PBS to remove any minimal contamination of FCS and other contaminants to avoid an immune reaction by centrifugation at 1,200RPM for 5 minutes at 4°C.
4. Cells were resuspended at a density of 10⁷ nucleated cells/ml in ice-cold PBS.
5. Recipient mice were briefly heated under a red bulb lamp and transplanted with 2x10⁶ nucleated cells through the tail vein.

Recipient animals were under treatment with medicated water (Baytril, Bayer) for 4 weeks after the transplantation, and they were analysed 12 to 16 weeks after reconstitution.

2.11 Quantitative analysis of peripheral blood

Quantitative analysis of blood parameters was performed on facial vein-derived blood collected in heparin-coated microcapillary tubes (Brand, 1303430). Samples were placed

in agitation before analysis, which was conducted with an automated flow cytometry-based haematology (Hemavet HV950FS, Drew Scientific).

2.12 Immunostaining of hematopoietic and testicular cells for flow cytometry analysis and sorting

2.12.1 General immunostaining protocol for erythroid, lymphoid and myeloid lineages

A common protocol for the staining of erythroid and B cell progenitors, T cell and myeloid populations is described:

1. 1×10^6 cells from bone marrow, spleen and thymus single cell suspension were transferred in a well of a round-bottomed 96-well plate;
2. Centrifuge at 1,200RPM for 5 minutes at 4°C.
3. Remove supernatant by inverting the plate on the sink and gently tapping the bottom of it. Remove the remaining liquid on the wells by laying the plate on a paper towel.
4. Add 25 μ l of 1X PBS+3%FCS supplemented with 1/50 dilution of purified CD16/32 antibody (see “*List of antibodies used in this study*” at the end of this session). Mix the plate by gentle vortexing to resuspend the cells and incubate on ice for 10 minutes.
5. Add 25 μ l of 1X PBS+3%FCS containing the appropriate antibody mixture. Mix by gentle vortexing and incubate on ice for 20 minutes. Protect cells from light until analysis of the samples at the flow cytometer.
6. Wash cells by adding 200 μ l of 1X PBS+3%FCS.
7. Centrifuge at 1,200RPM for 5 minutes at 4°C.
8. Remove supernatant as step 3.
9. Resuspend cells in 300 μ l 1X PBS+3%FCS supplemented with 1 μ g/ml of 7-actinomycin (7AAD) (Sigma, A9400) and transfer them in a FACS tube (12x75mm round bottom) after filtering with a 50 μ m filcon (BD Falcon, 340632).

All the cells were acquired using a two-laser BD FACSCanto™ Flow Cytometer or a five-laser BD FACSAria™ II Sorp cell sorter under the guidance of Dr. Daniel Bilbao in

the EMBL Flow Cytometry Facility. Data was analysed off-line using FlowJo® Flow Cytometry analysis software (TreeStar, Inc.)

Immunostainings performed with this protocol:

1. Late erythroid progenitor: Ter119-APC, CD71-PE.
2. Late B cell progenitors: CD45R-APC, IgM-PE, CD43-FITC.
3. Immature B cells: CD45R-APC, IgM-PE, IgD-FITC.
4. T cells: CD3-APC, CD8-PE, CD4-FITC.
5. Myeloid cells: Gr-1-APC, CD11b-PE.
6. For transplanted animals, CD45.1-PE-Cy7 and CD45.2-Pacific Blue conjugated antibodies were added to staining 2-5.

2.12.2 Immunostaining protocol for hematopoietic stem cell and early progenitor populations

A common protocol for the staining of early hematopoietic progenitor populations is described:

1. 1×10^7 cells from bone marrow single cell suspension were transferred in a 1.5ml tube;
2. Centrifuge at 1,200RPM for 5 minutes at 4°C.
3. Resuspend cells in 100µl of 1X PBS+3%FCS supplemented with 1/100 dilution of lineage-specific antibody mixture. Incubate 10 minutes on ice.
4. Wash cells by adding 1ml of 1X PBS+3%FCS and centrifuge at 1,200RPM for 5 minutes at 4°C.
5. Remove supernatant, and add 100µl of 1X PBS+3%FCS containing 1/200 dilution of GAR-TC tricolour reagent. Incubate 10 minutes on ice. Protect cells from light until analysis of the samples at the flow cytometer.
6. Wash cells by adding 1ml of 1X PBS+3%FCS and centrifuge at 1,200RPM for 5 minutes at 4°C.
7. Remove supernatant and add 50µl of 1X PBS+3%FCS supplemented with 1/50 dilution of purified CD16/32 antibody. Incubate on ice for 10 minutes.

8. Add 50µl of 1X PBS+3%FCS containing the appropriate antibody mixture. Mix by gentle vortexing and incubate on ice for 20 minutes.
9. Wash cells by adding 1ml of 1X PBS+3%FCS and centrifuge at 1,200RPM for 5 minutes at 4°C.
10. Centrifuge at 1,200RPM for 5 minutes at 4°C.
11. Remove supernatant, then resuspend cells in 300µl 1X PBS+3%FCS supplemented with 1µg/ml of 7-actinomycin (7AAD) and transfer them in a FACS tube after filtering with a 50µm filcon.

All the cells were acquired using a five-laser BD FACSAria™ II Sorp cell sorter under the guidance of Dr. Daniel Bilbao in the EMBL Flow Cytometry Facility. Data was analysed off-line using FlowJo® Flow Cytometry analysis software (TreeStar, Inc.)

Immunostainings performed with this protocol:

1. HSC and LMPP: Lineage cocktail (CD4, CD5, CD8, CD11b, CD45R, Gr-1, Ter119), c-Kit-APC-Alexa 750, Sca-1-PE-Cy7, CD150-APC, Flt-2/Flk-3-PE. (Kiel, 2005; Adolfsson, 2005)
2. Early megakaryocytic-erythroid and myeloid progenitors: Lineage cocktail (CD4, CD5, CD8, CD11b, CD45R, Gr-1, Ter119, Sca-1, IL7Ra), c-Kit-APC-Alexa 750, CD41-PE, CD150-APC, CD105-Bio, Streptavidin-PE-Cy7. (Socolovsky, 2001)
3. Early progenitor B cells: Lineage cocktail (CD11b, Gr-1, Ter119), BP-1-Alexa 647, CD45R-APC-eFluor780, CD43-FITC, IgM-PE, CD93-PE-Cy7, CD24-Pacific Blue. (Hardy, 1991; Hardy, 1996)

2.12.3 Immunostaining of testicular cells for flow cytometry analysis and sorting

A common protocol for the staining of testis cell populations is described:

1. $3-5 \times 10^6$ cells from adult or juvenile testis single cell suspension were transferred in a 1.5ml tube;
2. Centrifuge at 1,000RPM for 5 minutes at 4°C.
3. Resuspend cells in 25µl of 1X PBS+3%FCS supplemented with 1/50 dilution of purified CD16/32 antibody. Incubate 10 minutes on ice.

4. Add 25µl of 1X PBS+3%FCS containing a mixture of CD45 and CD51 antibodies conjugated with biotin. Incubate 10 minutes on ice.
5. Wash cells by adding 1ml of 1X PBS+3%FCS and centrifuge at 1,000RPM for 10 minutes at 4°C (Eppendorf 5810R, swinging bucket rotor).
6. Remove supernatant, and resuspend cells in 100µl of 1X PBS+3%FCS containing the appropriate antibody mixture. Incubate 20 minutes on ice. Protect cells from light until analysis of the samples at the flow cytometer.
7. Wash cells by adding 1ml of 1X PBS+3%FCS and centrifuge at 1,000RPM for 10 minutes at 4°C.
8. Remove supernatant, then resuspend cells in 300µl 1X PBS+3%FCS supplemented with 1µg/ml of 7-actinomycin (7AAD) and transfer them in a FACS tube after filtering with a 50µm filcon.

For samples used for sorting defined cell population, the whole sample from a *Miwi2^{tdTomato/+}* juvenile mouse was immunostained as described. All the cells were acquired or sorted using a five-laser BD FACSAria™ II Sorp cell sorter under the guidance of Dr. Daniel Bilbao in the EMBL Flow Cytometry Facility. Data were analysed off-line using FlowJo® Flow Cytometry analysis software (TreeStar, Inc.).

2.12.4 List of antibodies used in this study

The table below enlists the antibody (from eBioscience, if not stated) employed for flow cytometry studies:

Antibody	Alternative name	Clone	Fluorophore	Isotype	Catalog number	Dilution
CD4	L3T4	GK1.5	Purified	Rat IgG2a, k	14-0041-85	1/100
CD5	Ly-1	53-7.3	Purified	Rat IgG2a, k	14-0051-85	1/100
CD8a	Ly-2	53-6.7	Purified	Rat IgG2a, k	14-0081-85	1/100
CD11b	Mac-1	M1/70	Purified	Rat IgG2a, k	14-0112-85	1/100
CD45R	B220	RA3-6B2	Purified	Rat IgG2a, k	14-0452-85	1/100
Ter-119	Ly-76	Ter-119	Purified	Rat IgG2a, k	14-5921-85	1/100
Gr-1	Ly-6g	RB6-8C5	Purified	Rat	14-5931-85	1/100

				IgG2a, k		
Sca-1	Ly-6a/E	D7	Purified	Rat IgG2a, k	14-5981-85	1/400
Il-7 Rca chain	CD127	A7R34	Purified	Rat IgG2a, k	14-1271-85	1/400
B2- microglobulin	MHC-I (associated to)	S19.8	Purified	Mouse IgG2b, k	555299 (BD Pharmigen)	1/50
Sca-1	Ly-6a/E	D7	PE-Cy7	Rat IgG2a, k	25-5981-82	1/100
Rat IgG2a, k	Control Isotype		PE-Cy7	Rat IgG2a, k	25-4321-81	
Streptavidin			PE-Cy7		25-4317-82	1/600
CD45.1	SJL, Ly5.1	A20	Pe-Cy7	Mouse IgG2a, k	25-0453	1/50
CD117	c-kit	2B8	Pe-Cy7	Rat IgG2b, κ	25-1171	1/800
CD93	C1qRp	AA4.1	Pe-Cy7	Rat IgG2b, kappa	25-5892-82	1/200
Flk-2/Flt-3	Ly-72	A2F10.1	PE	Rat IgG2a, k	12-1351-83	1/50
CD41	fibrinogen receptor	eBio MWreg30	PE	Rat IgG1, κ	12-0411-83	1/300
CD8a	Ly-2	53-6.7	PE	Rat IgG2a, k	553032 (BD Pharmingen)	1/400
Mac-1	CD11b	M1/70	PE	Rat IgG2b, k	12-0112-83	1/200
IgM	Antimouse μ chain		PE	Goat	115-116-075 (Jackson)	1/200
CD71	Transferrin receptor	R17217	PE	Rat IgG2a, k	12-0711	1/100
Rat IgG2a	Control Isotype	eBR2a	PE	Rat IgG2a	12-4321-81	
Rat IgG2a, k	Control Isotype		PE	Rat IgG2a, k	*12-4724-81	Mouse IgG2a, k
Rat IgG1, κ	Control Isotype	P3	PE	Rat IgG1, κ	*12-4714-81	Mouse IgG1, κ
CD4	L3T4	RM4-5	FITC	Rat IgG2a, k	553047 (BD Pharmingen)	1/200
IgD		11-26c	FITC	Rat IgG2a, k	11-5993-85	1/400
CD43	LY-48, Leukosialin	S7	FITC	Rat IgG2a, k	553270 (BD Pharmigen)	1/100
CD9		KMC8	FITC	Rat IgG2a, k	11-0091	1/50
CD34	mucosialin	RAM34	FITC	Rat IgG2a, k	11-0341-81	1/50
CD49f	integrin alfa-6	GoH3	FITC	Rat IgG2a, k	11-0495-80	1/200
EpCam	CD326	G8.8	FITC	Rat IgG2a, k	11-5791-82	1/100
CD105	Endoglin	MJ7/18	Bio	Rat IgG2a, k	13-1051-85	1/100
CD51		RMV-7	Bio	Rat IgG1,	104104 (Biolegend)	1/50

				k		
CD45	Leukocyte common agent(LCA)	30-F11	Bio	Rat IgG2b, k	13-0451	1/200
c-Kit	CD117	2B8	APC-Alexa750	Rat IgG2b, k	27-1172-82	1/600
Rat IgG2a, k	Control Isotype		Bio	Rat IgG2a, k	13-4321-81	
Rat IgG2b, k	Control Isotype		APC-Alexa750	Rat IgG2b, k	27-4031-81	
Gr-1	Ly-6G	RB6-8C5	APC	Rat IgG2b, k	17-5931-82	1/800
Ter-119	Ly-76	TER-119	APC	Rat IgG2b, k	17-5921	1/200
CD3e		145-2C11	APC	armenian hamster IgG	17-0031-83	1/200
CD45R	B220	RA3-6B2	APC	Rat IgG2a, k	17-0452	1/400
Rat IgG2b, k	Control Isotype	A95-1	APC	Rat IgG2b, k	556924 (BD Pharmingen)	
CD150	SLAMf1	TC15-12F12.2	APC	Rat IgG2a, λ	115910	1/100
BP-1	Ly-51	6C3	Alexa Fluor 647	Rat IgG2a, κ	108312 (Biolegend)	1/200
CD90.2	Thy1	30-H12	AlexaFluor 647	Rat IgG2b, k	105318 (Biolegend)	1/100
CD45.2	Ly-5.2, LCA	104	Pacific Blue	Mouse (SJL) IgG2a, κ	109820 (Biolegend)	1/100
CD24	Heat Stable Antigen (HSA)	M1/69	Pacific Blue	Rat IgG2b, k	101820 (Biolegend)	1/200
CD29	integrin beta1	hmbeta1-1	Pacific Blue	armenian hamster IgG	102224 (Biolegend)	1/200
Rat IgG2b K	Control Isotype	RTK4530	Pacific-blue	Rat IgG2b, κ	400627 (Biolegend)	
Sca-1	Ly-6a/E	D7	Pacific-blue	Rat IgG2a, κ	108119 (Biolegend)	1/100
CD45R	B220	RA3-6B2	APC-eFluor 780	Rat IgG2a, kappa	47-0452-82	1/200
Isotype Control	Rat IgG2a K		APC-eFluor 780	Rat IgG2a, kappa	47-4321-82	
Streptavidin			605NC		93-4317	1/100
GARTC	Goat F(ab') ₂ anti-Rat IgG (H+L)		Tri-Colour		R40106	1/200

2.12.5 Definition of hematopoietic cell populations during this study

The different hematopoietic populations were defined as listed below:

Full name	Abbreviation	Marker profile	References
Long-term hematopoietic stem cells	LT-HSC	Lin ⁻ c-Kit ⁺ Sca-1 ⁺ Flt3 ⁻ CD150 ⁺	Kiel, 2005
Lymphoid-primed multipotent progenitors	LMPP	Lin ⁻ c-Kit ⁺ Sca-1 ⁺ Flt3 ⁺ CD150 ⁻	Adolfsson, 2005
Pre-Granulocyte/Monocyte precursor + Granulocyte/Monocyte precursor	Pre-GM + GMP	LinII ⁻ c-Kit ⁺ CD41 ⁻ CD105 ⁻ CD150 ⁻	Pronk, 2007
Pre-Megakaryocyte/Erythroid precursor	PreMeg-E	LinII ⁻ c-Kit ⁺ CD41 ⁻ CD105 ⁻ CD150 ⁺	Pronk, 2007
Pre-Colony-Forming-Unit Erythroid	Pre-CFU-E	LinII ⁻ c-Kit ⁺ CD41 ⁻ CD105 ⁺ CD150 ⁺	Pronk, 2007
Colony-Forming-Unit Erythroid	CFU-E	LinII ⁻ c-Kit ⁺ CD41 ⁻ CD105 ⁺ CD150 ⁻	Pronk, 2007
Pre-pro-B progenitor	Fr. A'	LinIII ⁻ CD45R ⁺ CD43 ⁺ BP-1 ⁻ CD24 ⁻ CD93 ⁺	Li, 1996
Early pro-B progenitor	Fr. B	LinIII ⁻ CD45R ⁺ CD43 ⁺ BP-1 ⁻ CD24 ⁺	Hardy, 1991
Late pro-B progenitor	Fr. C	LinIII ⁻ CD45R ⁺ CD43 ⁺ BP-1 ⁺ CD24 ^{lo}	Hardy, 1991
Late pro-B	Fr. C'	LinIII ⁻ CD45R ⁺ CD43 ⁺ BP-1 ⁺	Hardy, 1991

progenitor		CD24 ^{hi}	
Pre-B progenitors	Pre-B	CD45R ⁺ CD43 ⁻ IgM ⁻	Mecklenbrauker , 2002
Immature B		CD45R ^{lo} CD43 ⁻ IgM ⁺	Mecklenbrauker , 2002
Recirculating B		CD45R ^{hi} CD43 ⁻ IgM ⁺	Mecklenbrauker , 2002
Double-positive T cells	DP	CD4 ⁺ CD8 ⁺	
CD4 T cells	CD4	CD3 ⁺ CD4 ⁺ CD8a ⁻	
CD8 T cells	CD4	CD3 ⁺ CD4 ⁻ CD8a ⁺	
Proerythroblast	I	Ter119 ^{int} CD71 ^{hi}	Socolovsky, 2001
Basophylic erythroblast	II	Ter119 ^{hi} CD71 ^{hi}	Socolovsky, 2001
Polychromatophylic erythroblast	III	Ter119 ^{hi} CD71 ^{int}	Socolovsky, 2001
Orthochromatophylic erythroblast	IV	Ter119 ^{hi} CD71 ⁻	Socolovsky, 2001

LinI: CD4, CD5, CD8a, CD11b, CD45R, Ter119, Gr-1.

LinII: CD4, CD5, CD8a, CD11b, CD45R, Ter119, Gr-1, IL7Ra, Sca-1.

LinIII: CD11b, Gr-1, Ter119.

2.13 Generation and purification of a phospho-specific S388 Ago2 antibody (in collaboration with Sabin Antony and Maria Placentino)

CD-1 female animals were immunized with a peptide (KLMRSAPSFNTDP) encompassing a phosphorylated serine 388 of the murine Ago2 protein. 500ml of supernatant from culture of antibody-producing hybridoma cells were purified using a 10ml chromatography column (BioRad, Poly-prep Chromatography Column, 731-1550)

coated with protein G resin (GenScript, L00209). The protocol used for antibody purification is as follows:

1. Wash column with 100 ml of Wash/Binding buffer (200mM Na₂HPO₄, 0.15M NaCl, pH 8.0). Let the buffer flow through the column by gravity in a cold room.
2. Add 500ml of supernatant from hybridoma cells secreting a phospho-specific S388 Ago2 antibody. Let the liquid to go through the column by gravity, and collect it in a clean T175 flask (Falcon, 353045).
3. When all the supernatant has passed through the column, repeat step 2 twice.
4. After 3 runs of supernatant flow-through, wash the column three times with 250ml of Wash/Binding buffer. Let the liquid to pass through the column by gravity.
5. Add 8ml of 0.1M glycine pH 2.5 solution to the column to elute all the bound immunoglobulins. Collect the eluted solution in 8 fractions of 1ml each in 1.5ml tubes containing 65µl of 1M Tris-HCl pH 9.5 solution.
6. Quantify protein concentration in the eluted fraction by the Bio-Rad Dc Protein Assay Kit (Bio-Rad, 500-0111) following manufacturer instructions.
7. Combine fractions containing the highest protein content up to a final volume of 3ml. Add the combined fractions (max 3ml) to the Slide-A-Lyzer Dialysis cassette 3.500 MWCO (Thermo Scientific, #66330). Dialyze the antibody against 1X PBS + 20% Glycerol (at least 2L) in the cold room overnight.
8. Collect the purified antibody solution from the dialysis cassette. Add sodium azide to a final concentration of 0.02% to the solution as a preservative.
9. Measure the protein concentration of the purified antibody solution with the Bio-Rad Dc Protein Assay Kit (Bio-Rad, 500-0111) following manufacturer instructions.

The purified phospho-specific S388 Ago2 antibody was employed for immunoblot and immunofluorescence assays.

2.14 Overexpression of wild type and S388A mouse Ago2 in cultured cells (in collaboration with Maria Placentino)

To induce Ago2 overexpression, both HEK293T and HeLa cells have been transfected with a plasmids encoding either the wild type version of murine Ago2 (*pcDNA3.1-Ago2-*

WT) or a mutated S388A Ago2 protein (*pcDNA3.1-Ago2-S388A*). These plasmids were generated in the lab using the pcDNA3.1 vector backbone (Invitrogen, V790-20). HEK293T and HeLa cells were maintained in standard culture medium in incubator at 37°C with 7.5% CO₂ pressure.

Cells were transfected either with pcDNA3.1-Ago2-WT or with pcDNA3.1-Ago2-S388A plasmids or left untransfected as negative control. Moreover, cotransfection with a plasmid encoding for the green fluorescent protein (pCMV-eGFP, Addgene plasmid 11153) was employed to evaluate transfection efficiency. 2.5×10^6 and 4×10^5 cells were transfected with 1 µg of *pcDNA3.1-Ago2-WT/pcDNA3.1-Ago2-S388A* alone or with 8 µg of *pcDNA3.1-Ago2-WT/pcDNA3.1-Ago2-S388A* together with 0.8 µg of pCMV-GFP for protein extracts or immunofluorescence, respectively. Transfection was performed using LipofectamineTM 2000 (Invitrogen, 11668019) according to manufacturer instructions. 24 hours after transfection, cells were either left untreated or incubated with 250 µM of sodium arsenite (AS) for 90 minutes at 37 °C. Untreated and AS-treated cells were then harvested for protein lysis or fixed for immunofluorescence analysis. Transfected efficiency was around 80-85% of total cultured cells as assayed by scoring GFP-positive cells using a two-laser BD FACSCantoTM Flow Cytometer.

2.15 Western Blot

2.15.1 Production of a phosphorylated L2 linker domain in vitro (in collaboration with Dr. Philipp Selenko, FMP Berlin)

A peptide encompassing the L2 linker domain of the mouse Ago2 protein was used to test the specificity of the anti-phosphoserine 388 antibody we developed. The peptide contains residue 354-422 of the murine Ago2 protein, with a Myc tag (EQKLISEEDL) at the C-terminal of the peptide. A mutant peptide was also made by converting S388 into an alanine. Both wild type and S388A peptides were incubated overnight with 1.26 µg of purified MK2 kinase. The phosphorylation at serine 388 was monitored through NMR.

2.15.2 Protein extracts preparation from transfected HEK293T cells

After transfection and AS treatment, cells have been harvested with 0,05% Trypsin (Invitrogen, 25300-054) and pelleted by centrifugation at 1000 rpm for 5 minutes. After centrifugation, cells were resuspended in 10 ml of PBS and counted with a Cellometer™ Auto T4 (Nexcelom Bioscience). Cells were washed twice in PBS and transferred in a 1.5 ml eppendorf tube. The cellular pellet was then resuspended in Protein Lysis Buffer (See Annex 1) at a concentration of 2×10^4 cells/ μ l. The lysis was achieved by incubation on ice for 20 minutes. The protein extracts were then cleared from cellular debris by two steps of centrifugation at 14,000 RPM for 20 minutes at 4°C. Samples were then stored at -20°C. Protein concentration was measured with the Bio-Rad Dc Protein Assay Kit (Bio-Rad, 500-0111) following manufacturer instructions.

2.15.3 Resolution of proteins by SDS-PAGE

Separating gel (7.5% acrylamide for protein extracts and 15% acrylamide for purified Ago2 L2 peptides) and stacking gel (4% acrylamide) were prepared using standard procedures. Before loading into the gel, 4X Laemmli buffer (See Annex 1) was added to each sample to a final concentration of 1X. Samples were boiled at 95 °C for 3 minutes and then cleared by centrifugation. 50 μ g of protein extracts and 5-50ng of purified L2 peptides were loaded onto the gel. Samples and the protein ladder (BioRad 161-0317 Broad range) were loaded and the gel was run at 80V until the samples have reached the separating gel. Then, the run was continued at 120V for 90 minutes.

2.15.4 Blotting of proteins onto membranes

For the immunoblotting, two different membranes have been used: PVDF membrane (Immobilion®-P, Millipore IPVH00010), for protein extracts from HEK293T cells; nitrocellulose (BA83 Protran membrane, Whatman, 10402452), for purified Ago2 L2 peptides. After having assembled the blotting sandwich, the blot was run for 45 minutes at 2,5 mA/cm² (140 mA for one membrane) using a TE 70 ECL Semi-dry Transfer Unit (Amersham Biosciences). After the transfer, the membrane was stained in Ponceau S solution (Sigma Aldrich, P7170) for 3 minutes to assess the transfer quality.

2.15.5 Blocking and antibody staining

The membrane was blocked in 5% milk in TBS-T (137 mM NaCl; 2,7 mM KCl; 20 mM TrisHCl pH 7.5; 0,1% Tween20, Sigma Aldrich P9416) for 1 hour at room temperature. Then, it was incubated with primary antibody either at 4 °C overnight or at room temperature 1 hour, shaking.

The primary antibodies used for Western blot are:

- In-house purified mouse α -phosphorylated Ago2 S388 1:200;
- In-house purified mouse α -Ago2 MA2 1:5,000;
- Commercial mouse α -Tubulin 1:20,000 (Sigma Aldrich, T9026);
- Commercial mouse α -Myc 1:1,000 (Abcam, ab39688).

The phospho-specific antibody was incubated in 5% BSA (Bovine Serum Albumine, Sigma Aldrich, A2153) in TBS-T, whereas the other primary antibodies were incubated in 5% milk in TBS-T. Immunoblot with purified phospho-specific S388 Ago2 and anti-Myc antibodies was performed overnight at 4°C in gentle rocking. Total anti-Ago2 and anti-Tubulin antibodies were incubated for 2 hours at room temperature in gentle rocking.

Membrane was washed 3x5 minutes in TBS-T and incubated with a anti-mouse secondary HRP-conjugated antibody (GE Healthcare, NA931). Secondary antibodies are used at 1:10,000 or 1:20,000 dilutions in TBS-T for 1 hour at room temperature in gentle rocking. Then, membrane was washed 3x5 minutes in TBS-T and 2 ml of 1:1 ECL reagent A and B (GE Healthcare, RPN2106) mixture was added and incubated for 2 minutes at room temperature. After the incubation, the excess of ECL solution was removed from the membrane and placed into a plastic pocket. The immunoblot was developed using ChemiDocTM XRS+ (BioRad, 170-8265).

2.15.6 Stripping of membrane for immunoblot

To probe the same membrane with two different antibodies from the same host, the membrane was washed harshly to remove the binding of antibodies used in precedent immunoblotting. The membrane was first incubated in 50ml of stripping solution (See Annex 1) at 50°C for 30 minutes in gentle shaking and further washed 2x10 minutes

with TBS-T. The membrane can be used again for blocking and primary antibody incubation.

2.16 Immunofluorescence staining of human cells and mouse tissues

2.16.1 Staining of transfected HeLa cells

HeLa cells were transfected with plasmids to overexpress either wild type or S388A murine Ago2 protein. After treatment with arsenite, the culture medium was aspirated and cells were washed twice with PBS. Cells were fixed in 4% paraformaldehyde (PFA) in PBS for 10 minutes at room temperature; then, PFA was removed and cells were washed twice with TBS. Coverslips were stored at 4 °C in TBS + 0.02% NaN₃ (Sigma, S2002) until the moment of staining.

The immunostaining was performed on a humidified chamber to avoid the cells to dry. Coverslips were washed once with TBS and cells were permeabilized with Triton Extraction Buffer (See Annex 1) for 10 minutes at room temperature. Cells were washed twice with TBS and then blocked with TBG (0,2% (v/v) cold water fish gelatine (Sigma G7765); 0,5% (w/v) Bovine Serum Albumine (BSA, Sigma A2153) in TBS 1X) for 1 hour at room temperature.

The primary antibody was put in TBG and incubated for 1 hour at room temperature. The primary antibodies used are:

- In-house purified mouse α -phosphorylated Ago2 S388 1:200;
- In-house purified rabbit α -Ago2 MA2 1:1,000.

Coverslips were washed 3x5 minutes with TBG and the secondary antibody was put in TBG for 1 hour at room temperature protected from light. Secondary antibodies used at 1:1,000 dilution were:

- Alexa Fluor® 488 Goat α -Mouse (Molecular Probes, A11001);
- Alexa Fluor® 546 Goat α -Rabbit (Molecular Probes, A11010).

Coverslips were washed 2x5 minutes with TBG and the nuclei were stained with 2 μ g/ml DAPI (4',6-diamidino-2-phenylindole, Sigma, D1306) in TBG for 5 minutes. Coverslips were then washed twice with TBS and mounted on slide using ProLong® Gold Antifade Reagent mounting medium (Invitrogen P36930). Coverslips were placed on a

microscopy slide and sealed with nail polish and stored at 4 °C in the dark. Images were acquired with Confocal microscope Leica TCS SP5.

2.16.2 Staining of embryonic day E3.5 mouse blastocyst (in collaboration with Maria Placentino)

Wild type C57Bl/6N and 129S2 females were mated with male mice from the same genetic background. Males were segregated from females at the appearance of a vaginal plug, which is considered as embryonic day E0.5. Three days later, pregnant females were sacrificed by cervical dislocation and the uterus was carefully isolated and cleaned under a stereomicroscope. Blastocysts were flushed out from the uterus using 1ml of M2 medium and 1ml syringe with a 26 ½ G needle (BD Plastipack, 300015) in a 6mm plastic dish (Falcon, 353001). Blastocysts were collected in M2 medium drop, and then the zona pellucida was digested with Tyrode's Acidic solution (Sigma, T1788) for 10 seconds. Embryos were then fixed in 4%PFA in 1X PBS for 15 minutes at room temperature, and rinsed with PBS/PVP solution (1X PBS supplemented with 3mg/ml of polyvinyl pyrrolidone, Calbiochem, 529504). Embryos can be stored at 4°C before the immunostaining.

For the staining, collected embryos were first permeabilized with 0.25% Triton-X (Sigma, T8787) in PBS/PVP solution for 30 minutes at room temperature. Blastocysts were then transferred in blocking solution (0.2% Donkey serum (Sigma, D9663), 0.1% BSA, 0.01% Tween20) for 15 minutes at room temperature. Samples were then incubated with primary antibodies diluted in blocking solution and incubated overnight at 4°C. The antibody and dilution employed are as follow:

- In-house purified mouse α -phosphorylated Ago2 S388 1:200;
- In-house purified mouse α -Ago2 MA2 1:1000;
- Commercial rabbit α -Nanog 1:200 (Bethyl, A300-397A).

Embryos were washed 3x15 minutes in blocking solution, and subsequently incubated with Alexa Fluor® 546 Donkey α -Rabbit (Molecular Probes, A10040) and Alexa Fluor® 488 Donkey α -Mouse (Molecular Probes, A21202) secondary antibodies, diluted 1:500 in blocking solution for 1 hour at room temperature. The samples were then rinsed 3x15 minutes in blocking solution. For mounting, embryos were passed

through a series of 25%, 50%, 75% and 100% Vectashield mounting medium with DAPI (Vector Laboratories, H-1500). Blastocysts were then passed on a microscope slide (Thermo Scientific, J1800AMNZ) on top of a small drop of Vectashield mounting medium surrounded by blobs of paraffin to avoid the crushing of the embryos. A 13mm coverslip (VWR, 631-0149) was placed on top and sealed with nail polish and stored at 4°C in the dark. Images were acquired with Confocal microscope Leica TCS SP5.

2.16.3 Staining of testis section from embryonic day E16.5 male mouse (In collaboration with Dr. Claudia Carrieri)

Wild type and *Miwi2^{tdTomato/+}* testes were isolated from male embryos at embryonic day E16.5. Samples were then fixed in 4%PFA in 1X PBS at 4°C for 2 hours. Testes were then washed 2x5 minutes in 1X PBS at room temperature. Samples were subsequently transfer in a 10% sucrose solution in 1X PBS for 2 hours at 4°C; this step was further repeated in a 20% sucrose solution in 1X PBS and in mixture (1:1 ratio) of 20% sucrose in 1X PBS and OCT embedding medium (Tissue-Tek, 4583). Samples were finally embedded in OCT embedding medium in an embedding mould by incubation on dry ice for 20 minutes. Embedded tissues were stored at -80°C.

7µm-thick transversal cryosection of embryonic testis were cut from the embedded samples, put on a microscopy slide and dry at room temperature for 1 hour. Samples were then washed 2x10 minute with 1X PBS, and sections were permeabilized with 0.1% Triton-X in 1X PBS for 30 minutes at room temperature. Samples were incubated with blocking solution (5% Donkey serum (Sigma, D9663), 1% BSA, 0.1% Triton-X in 1X PBS) for 1 hour at room temperature. Sections were then stained overnight at 4°C in 1X PBS+1%BSA solution containing 1:100 mouse monoclonal anti-Miwi2 antibody (produced in house, in collaboration with Sabin Antony) and 1:200 rabbit polyclonal anti-RFP antibody (Rockland, 600-401-379). Sections were washed 3x10 minutes with 0.1% Triton-X in 1X PBS at room temperature. Secondary antibodies (Alexa Fluor® 546 Donkey α-Rabbit and Alexa Fluor® 488 Donkey α-Mouse) were diluted 1:1,000 in 1X PBS supplemented with 1%BSA and 0.1% Triton-X. Samples were incubated with secondary antibodies at room temperature for 1 hour. Sections were washed 3x10 minutes with 0.1% Triton-X in 1X PBS at room temperature and stained with 1µg/ml

DAPI in 1X PBS for 15 minutes. Coverslips were then washed twice with TBS and mounted on slide using ProLong® Gold Antifade Reagent mounting medium (Invitrogen P36930). Coverslips' sides were sealed with nail polish and stored at 4 °C in the dark. Images were acquired with Confocal microscope Leica TCS SP5.

2.17 Quantitative real-time PCR

2.17.1 RNA isolation from sorted testis cells

RNA isolation of FACS-sorted CD45⁻ CD51⁻ tdTom⁺ c-Kit⁻ Thy-1^{lo}, CD45⁻ CD51⁻ tdTom⁺ c-Kit⁺ Thy-1^{lo}, CD45⁻ CD51⁻ tdTom⁺ c-Kit⁺ Thy-1⁺ and CD45⁻ CD51⁻ tdTom⁻ c-Kit⁺ Thy-1⁻ from juvenile *Miw2^{tdTomato/+}* male testis is described below:

1. Cells were collected in 1X PBS+3%FCS during sorting procedure. Cells were then pelleted by centrifugation at 1,000RPM for 10 minutes at 4°C.
2. Lyse sorted cells in 500µl Qiazol reagent (Qiagen, 79306) in 1.5ml DNA low-binding tube (Eppendorf, 22431021). Samples were stored at -80°C at least for 24 hours before RNA isolation.
3. Thaw samples for 15 minutes at room temperature prior to the addition 100µl of chlorophorm (Merck, K33534645).
4. Shake tubes vigorously for 15 seconds and incubate 3 minutes at room temperature.
5. Centrifuge at 12,000g for 15 minutes at 4°C (Eppendorf, Centrifuge 5417R).
6. Remove the aqueous phase of the solution (the lower phase containing phenol has red colour) and transfer it in a new 1.5ml DNA low-binding tube. Usually 320µl of aqueous solution were retrieved for each sample.
7. Add 320µl of isopropanol (Sigma, 33539) and 5µg of RNase-free glycogen (Invitrogen, AM9510). Invert tubes several times and incubate for 10 minutes at room temperature.
8. Centrifuge at 12,000g for 10 minutes at 4°C.
9. Remove carefully supernatant without disturbing the pellet at the bottom of the tube. Wash with 1ml of 75% ethanol.
10. Centrifuge at 7,400g for 5 minutes at 4°C.

11. Remove all the supernatant by using both a p1000 and a p200 pipettes. Let the pellet dry for 5 minutes at room temperature.
12. Resuspend pellet in 15µl of Nuclease-free water (Invitrogen, AM9930). Store at -80°C.

RNA concentration was determined with the Qubit RNA assay kit (Invitrogen, Q32855) using a Qubit® Fluorometer (Invitrogen) following manufacturer instructions.

2.17.2 Reverse transcription and real time PCR from isolated RNA

50ng of total RNA from FACS-sorted cell populations were reverse transcribed with random hexamer primers using Superscript™ II Reverse Transcriptase (Invitrogen, 18064-022) following manufacturer instructions.

A quantitative real-time reaction was performed on a LightCycler 480 PCR instrument (Roche) using 2x SYBR green I master (Roche, 04707516001). All the expression data was normalized to the expression levels of GAPDH (Glyceraldehyde 3-phosphate dehydrogenase) reference gene using the $2^{-\Delta\Delta Ct}$ method (Livak, 2001).

PCR reaction program:

Step	Temperature (°C)	Time (s)	Cycles
Denaturation	95	300	1X
Denaturation	95	10	45X
Annealing	60	15	
Elongation	72	10	
Denaturation	95	5	1X
Annealing	65	60	1X
Denaturation	95	N/A	Continuous
Cooling	40	10	1X

Gene-specific primer sets:

RefSeq	Primers	Sequence	Probe length
NM_001122733.1	c-Kit_FW	5'-tcatcgagtgtgatgggaaa-3'	221bp
	c-Kit_RV	5'-ggtgacttgtttcaggcaca-3'	
NM_009050.2	c-RET_RW	5'-gcttcagtacacggtgtagc-3'	134bp
	c-RET_RV	5'-gcctcttgttactgcacagg-3'	
NM_019448.3	Dnmt3L_FW	5'-gcggtactgagccttttag-3'	118bp
	Dnmt3L_RV	5'-gacatttgacatctccacgt-3'	
NM_010279.2	Gfra1_FW	5'-caccatgttctagccactct-3'	118bp
	Gfra1_RV	5'-tacttggtgctgcagctctgt-3'	
NM_009864.2	E-Cad_FW	5'-tgaaggacggtaacaactg-3'	155bp
	E-Cad_RV	5'-gctcttgaccaccgttctcc-3'	
NM_008532.2	EpCAM_FW	5'-gagtcggaagaaccgacaag-3'	125bp
	EpCAM_RV	5'-agtctgcaagctctgatggtc-3'	
NM_031166.2	ID4_FW	5'-actcaccgctcaaacact-3'	171bp
	ID4_RV	5'-ccggtggcttgttctctta-3'	
NM_145833.1	Lin28_FW	5'-agaccaaccattggagtgc-3'	109bp
	Lin28_RV	5'-aatcgaaacccgtgagacac-3'	
NM_194064.2	Nanos2_FW	5'-aacttctgaagcacaatgg	192bp
	Nanos2_RV	5'-caggtacctcacagggtctca-3'	
NM_194059.2	Nanos3_FW	5'-acaaggcaaagacacaggatg-3'	216bp
	Nanos3_RV	5'-cctaagcaagggtccagtctcc-3'	
NM_009719.6	Ngn3_FW	5'-gctgcttgacactgaccctat-3'	150bp
	Ngn3_RV	5'-cgggaaaagggtgtgtct-3'	
NM_177905.3	Miwi2_FW	5'-cgaccccgatgttcagtt-3'	250bp
	Miwi2_RV	5'-atcaatacccacgaccatca-3'	
NM_013633.3	Oct4_FW	5'-ggcgttctcttgaaagggttc-3'	292bp
	Oct4_RV	5'-ctcgaaccacatccttctct-3'	
NM_001033324.2	PLZF_FW	5'-cccagttctcaaaggaggatg-3'	88bp

	PLZF_RV	5'-ttcccacacagcagacagaag-3'	
NM_008084.2	GAPDH_FW	5'-gagcgagaccccactaacat-3'	154bp
	GAPDH_RV	5'-ttcacacccatcacaacat-3'	

2.18 Data analysis

General data analysis was performed using Microsoft Excel 2008 for Macintosh. Graph and statistical test analysis was performed with Graphpad Prism 5 software. All error bars represent standard deviation (s.d.) or standard deviation of the mean (s.e.m.) as indicated in the figure legend. Control and experimental samples were considered statistically different for p-value<0.05 using the Student's unpaired t-test.

Annex 1: Media and solutions

HEK293T and HeLa S2 culture medium: Dulbecco Modified Eagle Medium (D-MEM, Invitrogen, 41965062);
 10% serum (Fetal Calf Serum, FCS, PAA, A15-104);
 1X Penicillin-Streptomycin (Invitrogen, 15070-063).

Standard ES cell medium: Knockout D-MEM (Invitrogen, 10829-018);
 12.5% Fetal Calf Serum (Hyclone, SH30071.03);
 1X Penicillin-Streptomycin (Invitrogen, 15070-063);
 2mM L-Glutamine (GIBCO, 25030);
 0.1mM 2-Mercapto-Ethanol (GIBCO, 31350-010);
 1X Non-essential amino acid (GIBCO, 11140-035);
 LIF (2µl of 1mg/ml solution per 100ml of media, PEPCF Facility Heidelberg).

10X KT buffer: 670mM Tris-HCl pH 9.1

160mM (NH₄)SO₄
35mM MgCl₂
1.5mg/ml BSA

Tail Digestion Buffer: 50mM Tris-HCl pH 8;
100mM EDTA (Sigma, 03609);
100mM NaCl;
1% SDS (Sigma, L4509);
3mg/ml Proteinase K (Roche, 3115852001) to be added fresh.

Southern Hybridization Buffer: 0.5M Na-Phosphate buffer pH 7.2;
1mM EDTA (Sigma, 03609);
3% BSA;
5% SDS (Sigma, L4509).

Southern Washing Buffer: 40mM Na-Phosphate buffer pH 7.2;
1mM EDTA;
5% SDS.

Embryo lysis buffer: 100mM Tris-HCl pH 8;
0.5% NP-40 (Sigma, 13021);
0.5% Tween-20 (Sigma, P9416);
0.2 mg/ml Proteinase K (Roche, 3115852001).

A stock solution of embryo lysis buffer without Proteinase K was filtered through a 0.22µm filter and stored at 4°C. Proteinase K was added fresh before the lysis of samples.

ACK lysis buffer: 0.15M NH₄Cl;
10mM KHCO₃;
0.1mM Na₂EDTA.

Adjust to pH 7.2 with HCl and pass through a 0.22µm filter. Store at room temperature.

BSS buffer

20X BSS Stock I: D-(+)-Glucose (Sigma, G7021);

KHPO₄ (Sigma, P5655);

Na₂HPO₄ (Sigma, S5136)

0.5% Phenol Red in water.

20X BSS Stock II: CaCl₂ 2H₂O (Sigma, C7902);

KCl (Sigma, P5405);

NaCl (Sigma, S5886);

MgCl₂ 6H₂O (Sigma, M2393);

MgSO₄ (Sigma, M2643);

in water.

Prepare the solutions separately, filter sterile and store at 4°C. To produce BSS+2%FCS solution, dilute the 20X BSS Stock I and 20X BSS Stock II solutions with sterile water. Store at 4°C for up to 4 weeks.

Goni-MEM medium: DMEM (Invitrogen, 41965062);

1X Na-Pyruvate (GIBCO, 11360-039);

1X Non-essential amino acid (GIBCO, 11140-035);

1X Penicillin-Streptomycin (Invitrogen, 15070-063);

Sodium DL-Lactate (16.8µl per 100ml of medium) (Sigma, L4263)

M2 medium: 15µl 1M HEPES (Invitrogen, 15630-056);

10µl 100X Penicillin-Streptomycin (Invitrogen, 15070-063);

up to 1ml with Brinster Med BMOC-3 (Invitrogen, 11126-034).

Protein lysis buffer: 150 mM NaCl;

2 mM MgAc;

5% Glycerol (Sigma Aldrich, 15523);

20 mM Tris HCl pH 7.5;

0.5% NP40 (Sigma Aldrich, I8896);
0.2% Triton-X100 (Sigma Aldrich, T8787);
1X Proteinase Inhibitors (complete Mini EDTA-free, Roche, 05892791001);
2X Phosphatase Inhibitors (PhosSTOP, Roche, 04906837001);
2mM DTT (DL-Dithiothreitol, Sigma Aldrich, 43815);
in water.

A stock solution containing the salt and detergent in water was first made, filtered by a 0.22 μ m filter (Millipore, SCGPT05RE) and stored at 4°C. Proteinase and phosphatase inhibitors were added fresh to the lysis buffer together with DTT.

4X Laemmli Buffer: 183mM TrisHCl pH 6.8;
36% Glycerol (Riedel-De Haen 56-81-5);
3.6% SDS;
1% BBF (free acid fisher biotech BP115-25);
4.2% β -mercaptoethanol (Sigma M3148);
in water.

Western Stripping solution: 62.5mM Tris-HCl pH 6.7;
100mM 2-Mercapto-Ethanol (Sigma, M3148);
2% SDS (Sigma, L4509);
in water.

Triton Extraction Buffer: 0,2% Triton X-100 (Sigma Aldrich, T8787);
20 mM Hepes pH 7.9;
50 mM NaCl;
3 mM MgCl₂;
300 mM sucrose (Sigma Aldrich, S9378);
in water.

Filter the solution with a 0.22 μ m and store at 4°C.

Chapter 3: Phosphorylation of Ago2 serine 388 is necessary for embryonic development depending on the genetic background

3.1 Results

3.1.1 Generation of a non-phosphorylatable Ago2 allele *in vivo*

The miRNA and siRNA pathways have been proved to shape several developmental and physiological processes in both animal and plants (reviewed in Carthew, 2009). In mammals, the central role of Argonaute 2 (Ago2) protein in both miRNA- and siRNA-mediated gene silencing renders it an amenable target for the regulation of these pathways. Indeed, numerous post-translational modification of Ago2 has been described so far in cell lines, such as phosphorylation at serine 387 of the human protein (Table 1) (Zeng, 2008; Horman, 2013). Phosphorylation of serine 387 is triggered by the stress-response p38-MAPK pathway, and the downstream MAPKAPK2 (MK2) kinase is responsible for Ago2 phosphorylation *in vitro*. The phosphorylation event has an impact in Ago2 localization during standard cell culture conditions, which in turns may affect miRNA- and siRNA- activity (Zeng, 2008; Horman, 2013). I sought to determine the physiological relevance of Ago2 phosphorylation at serine 387 by creating a non-phosphorylatable Ago2 allele in the mouse.

The serine 387 of the human Ago2 is well conserved through the animal kingdom to the Amphibian class, corresponding to serine 388 of the mouse protein. Furthermore, the MK2 consensus sequence is also conserved throughout evolution (Fig. 5A). The S388 residue resides in the L2 linker between PAZ and MID domains, that are important for the miRNA and mRNA binding activity of Ago2. To study the role of S388 phosphorylation event, we undertook a loss-of-function approach by converting serine 388 into an alanine in exon 10 of the endogenous Ago2 locus (Fig. 5B). A 129P2 mouse embryonic stem cell line (IB10) (Robanus-Maandag, 1998) was electroporated with a targeting vector containing neomycin resistant cassette (neo) between exon 8 and 9 flanked by two *LoxP* sites (Fig. 5B). I screened for clones that have successfully

recombined to the endogenous Ago2 locus by first selecting cells with G418 and then by Southern blotting using a 3' external probe (Fig. 5C). I further confirmed the conversion of serine 388 into an alanine by sequencing of the endogenous Ago2 locus (Fig. 5D). *Ago2*^{Neo-S388A/+} ESC clones were then used for blastocyst injection for the formation of chimeric founder mice. In order to have a transcriptional-competent *Ago2*^{S388A} knock-in allele, I mated the founder mice with a mouse line bearing the Cre-recombinase maintained in a pure C57Bl/6N genetic background (Fig. 6) (Schwenk, 1995). The *Ago2*^{S388A/+}; *Tg*^{DelCre} animals were then backcrossed one generation with C57Bl/6N mice to obtain experimental *Ago2*^{S388A/+} animals in a 129P2xC57Bl/6N mixed genetic background. Heterozygous mice have been used for a first set of experiments in this genetic background, while two co-isogenic lines were established by backcrossing animals with C57Bl/6N and 129S2 inbred strains (Fig. 6).

A

<i>H. sapiens</i>	ISKLMRSAS F NTDPYV	AA379-394
<i>P. troglodytes</i>	ISKLMRSAS F NTDPYV	AA333-348
<i>R. norvegicus</i>	ISKLMRSAS F NTDPYV	AA380-395
<i>M. musculus</i>	ISKLMRSAS F NTDPYV	AA380-395
<i>O. cuniculus</i>	ISKLMRSAS F NTDPYV	AA360-375
<i>G. Gallus</i>	ISKLMRSAS F NTDPYV	AA376-391
<i>X. Laevis</i>	ISKLMRSAS F NTDPFV	AA382-397
<i>D. Rerio</i>	ISKLMRSAN F NTDPYV	AA393-408
<i>D. melanogaster Ago1</i>	INNLVKRA D FN N DSYV	AA488-503
Consensus	ISKLMRSAS F NTDPYV	

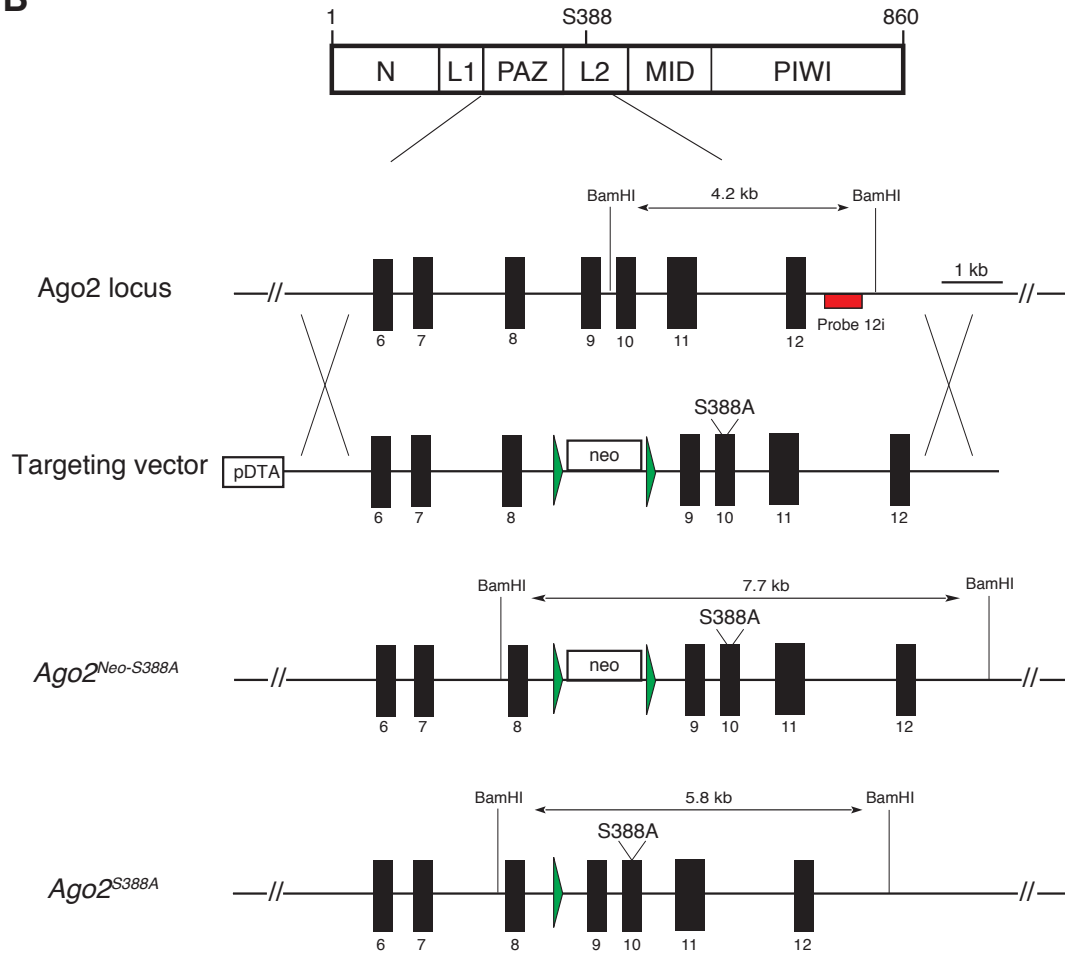
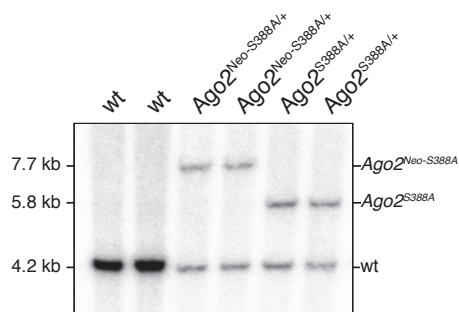
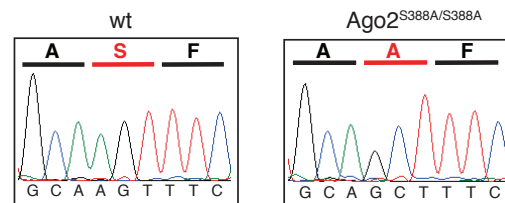
B**C****D**

Figure 5. Targeting strategy and validation of the *Ago2*^{Neo-S388A} allele.

(A) Sequence alignment of a portion of the human Ago2 protein with its orthologs from several species of the animal kingdom. In grey it is highlighted the residue S387 of the human Ago2, which corresponds to S388 of the mouse ortholog. The MK2-consensus sequence is highlighted in green. (B) Schematic representation of the Ago2 locus and targeting strategy for the creation of a nonphosphorylatable *Ago2*^{S388A} allele. Squared boxes indicate the position of *Neomycin* (*neo*) and *Diphtheria Toxin A* (pDTA) selection marker genes. Green triangles mark the position of *LoxP* sites for the Cre-mediated excision of the *neo* cassette to retrieve a transcriptionally competent *Ago2*^{S388A} allele. BamHI sites and the 3' probe used for Southern blot screen of mESC clones after electroporation are indicated. The size of the fragments for the wild type, *Ago2*^{Neo-S388A} and *Ago2*^{S388A} alleles are shown. (C) Representative Southern blot image from tail-derived DNA confirms the effective targeting of the Ago2 locus and the Cre-mediated recombination of the *neo* cassette. (D) Sequencing of tail-derived genomic DNA from wild type and *Ago2*^{S388A/S388A} animals validates the conversion of serine 388 into an alanine by two nucleotide mutations.

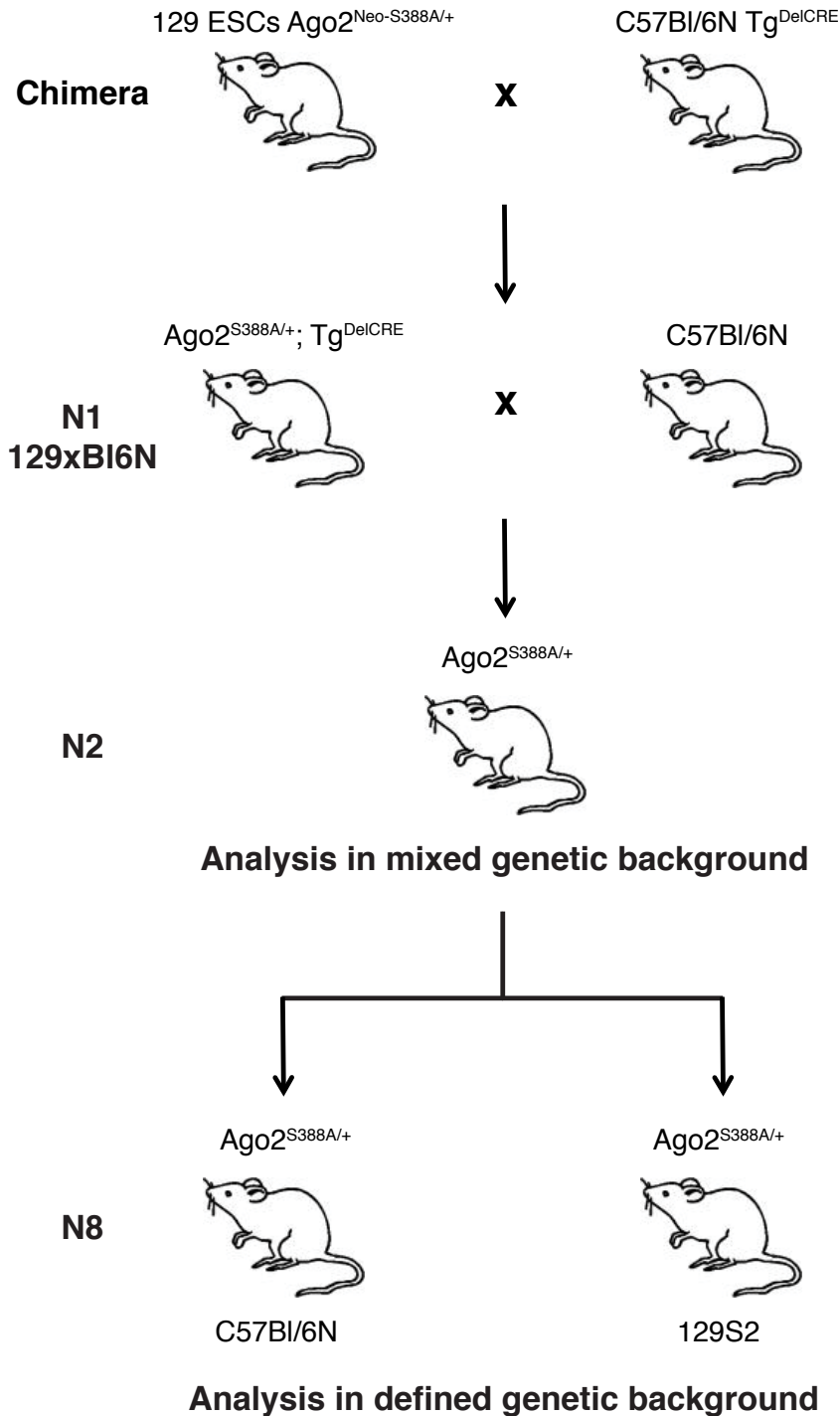


Figure 6. Breeding strategy of the $Ago2^{S388A/+}$ animals employed during this study. After the electroporation of 129P2 mouse embryonic stem cells (IB10), positive clones were used to create chimeric animals. $Ago2^{Neo-S388A/+}$ chimeras were crossed to a mouse

line bearing the *Deleter-Cre* transgene in a C57Bl/6N genetic background (Schwenk, 1995) for the formation of a transcriptionally active *Ago2*^{S388A/+} allele *in vivo*. A second cross with wild type C57Bl/6N animals allowed the separation of the Cre-transgene from the *Ago2* mutant allele. As such, *Ago2*^{S388A/+} heterozygotes in a 129P2xC57Bl/6N genetic background were employed for a first set of experiments. In parallel, two co-isogenic mouse lines were obtained by mating *Ago2*^{S388A/+} animals with C57Bl/6N and 129S2 mice for at least 8 generations.

3.1.2 Homozygous phosphomutant mice are lethal in a mixed genetic background

Compelling evidence demonstrated the importance of a functional miRNA pathway during embryonic development. Indeed, DGCR8- and Dicer-deficient embryos show significant growth defects as early as embryonic day E6.5 (Bernstein, 2003; Wang, 2006; Suh, 2010). On the other hand, loss of *Ago2* causes different phenotypic outcomes depending on the localization of the insertion cassette used for gene inactivation, even though *Ago2*^{-/-} embryos do not survive after E10.5 (Liu, 2004; Alisch, 2007; Morita, 2007). To pinpoint a putative role of serine 388 phosphorylation during embryonic development, heterozygous *Ago2*^{S388A/+} mutants in a mixed 129P2xC57Bl/6N genetic background were intercrossed. The genotype of pups at weaning revealed that only 5.37% of newborn were *Ago2*^{S388A/S388A}, much lower than the expected 25% Mendelian ratio (Figure 7A). The surviving homozygotes developed normally until adulthood, without any gross morphological defect. This is suggestive of the presence of at least one point during embryogenesis when *Ago2* S388 phosphorylation is essential for the survival of the embryo, and phospho-deficient animals that are capable of going through this step could develop normally. The ability to overcome this developmental time point can be stochastic, depending on the physiological conditions each embryo experiences during early stages of development. On the other hand, one or more predetermined genetic variants present in the mouse genome could influence the response to a lack of *Ago2* phosphorylation. Indeed, the use of a mixed 129P2xC57Bl/6N genetic background could support this hypothesis: animals carrying the 129 variant of one or more allele(s) might be more susceptible to die due to the lack of S388 phosphorylation, while the

C57Bl6N variants of the same alleles might render the animal resistant to the lack of this modification. Such phenomenon has been ascribed to determine the outcome of loss-of-function mutation during normal and disease development (reviewed in Gerlai, 1996; Wolfer, 2002) For example, *EGFR*^{-/-} animals die at different time point during embryonic development depending on the genetic background (Sibilia, 1995; Threadgill, 1995; Strunk, 2004). TGFβ1-deficient animals die prenatally in a C57Bl/6J/Ola background, while they survive up to birth in a NIH/Ola genetic background (Shull, 1992; Kulkarni, 1993; Dickson, 1995; Bonyadi, 1997; Kallapur, 1999). To test the possibility of a background-dependent lethality upon Ago2 S388A mutation, I mated heterozygous *Ago2*^{S388A/+} animals for at least 8 generations with wild type 129S2 and C57Bl/6N mice respectively to create two congenic mouse lines (Fig. 6). In parallel, I sought to use the individuals in a 129P2xC57Bl/6N mixed genetic background to identify at which embryonic stage Ago2 S388 phosphorylation might be essential. At mid-gestation, no morphologically normal homozygous mutant embryos were isolated (Fig. 7B). Indeed, while wild type and *Ago2*^{S388A/+} heterozygous embryos were present at the expected Mendelian ratio, the percentage of resorption with characteristic blood infiltration was similar to the number of expected homozygous mutant (Fig. 7B). At E9.5, embryos isolated from reabsorbing deciduas were much smaller compared to normal embryos (Fig. 7C). Analysis of embryos at E6.5-E7.5 revealed a reduced number of morphologically normal *Ago2*^{S388A/S388A} embryos compared to wild type, with a percentage similar to the one of pups present at weaning (Fig. 7A-B). Almost one fourth of the total embryos were morphologically abnormal, with no clear distinction between the embryonic and the extraembryonic part, and most of these embryos were genotyped as *Ago2*^{S388A/S388A} (Fig. 7C). These data indicate that Ago2 phosphorylation at serine 388 is important for embryonic development likely at the peri-implantation stage.

A

	Matings	Wild type	<i>Ago2</i> ^{S388A/+}	<i>Ago2</i> ^{S388A/S388A}	Total
At weaning	18	112 (33.43%)	205 (61.20%)	18 (5.37%)	335
	Expected	84	167	84	

B

	Wild type	<i>Ago2</i> ^{S388A/+}	<i>Ago2</i> ^{S388A/S388A}	Abnormal	Total
E12.5	8 (15.69%)	27 (52.94%)	0	16 (31.37%)	51
E9.5	10 (22.72%)	21 (47.73%)	0	13 (29.55%)	44
E7.5	16 (25.40%)	27 (42.86%)	5 (7.93%)	15 (23.81%)	63
E6.5	14 (27.45%)	15 (29.41%)	3 (5.88%)	19 (37.25%)	51

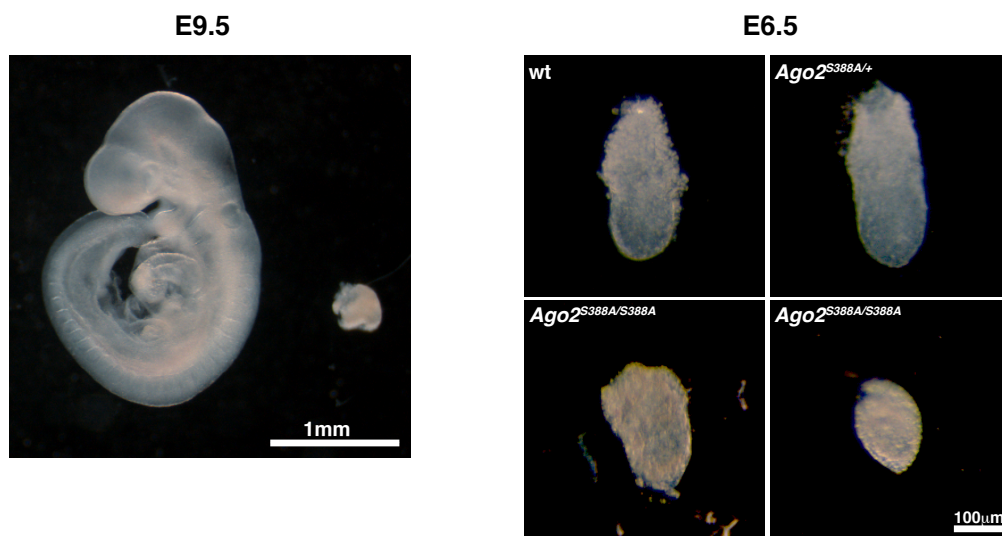
C

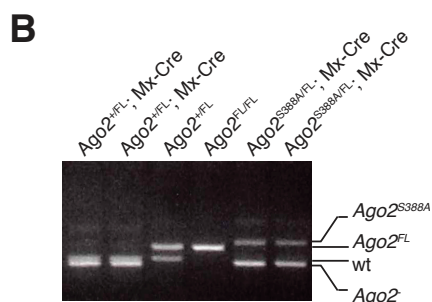
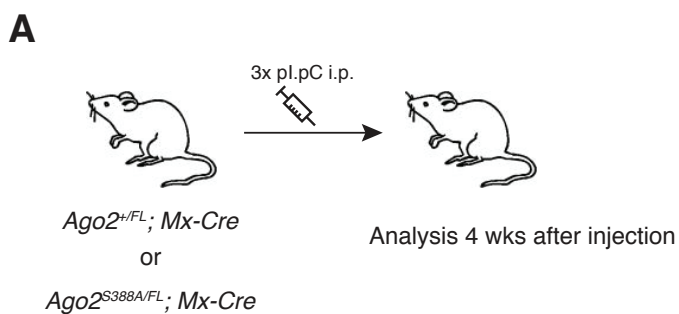
Figure 7. *Ago2*^{S388A/S388A} homozygous mutants are lethal in a mixed genetic background.

(A) *Ago2*^{S388A/+} heterozygous animals in a 129P2xC57Bl/6N mixed genetic background were intercrossed and the resulting litters were genotyped at weaning. The numbers of pups born and the expected numbers for each genotype are represented in the table. A significant lethality is shown for the *Ago2*^{S388A/S388A} mutants ($X^2 < 0.0001$, chi-square test). (B) The table shows the number of embryos isolated at embryonic day E6.5-E12.5

from *Ago2*^{S388A/+} intercrosses for each genotype. Representative images of morphologically normal and abnormal deciduas isolated at E9.5 (C) and E6.5 (D) are shown.

3.1.3 Ago2 S388 phosphorylation is dispensable for hematopoiesis

The activity of Ago2 during adulthood has been shown to be important for several processes, such as hematopoiesis, oogenesis and skin development (O'Carroll, 2007; Kaneda, 2009; Schaefer, 2011; Wang, 2012). In particular, a conditional allele of Ago2 in combination with an inducible Mx-Cre mouse line was employed to show that lack of this protein impacts on erythroid and B cell development in a cell-autonomous fashion (O'Carroll, 2007). Lethally irradiated mice transplanted with bone marrow from *Ago2*^{FL/FL}; *Mx-Cre* upon Cre induction developed a severe anaemia and splenomegaly in the periphery, due to defects of erythroblast differentiation at the orthochromatophilic stage. In addition, B-cell development was impaired in the bone marrow of the transplanted animals, with impaired pro-B-to-pre-B stage of differentiation (O'Carroll, 2007). Since in a mixed genetic background the *Ago2*^{S388A/S388A} mutant animals are almost completely lethal, we employed a similar strategy to investigate the function of S388 phosphorylation during adult hematopoiesis. Heterozygous *Ago2*^{S388A/+} animals were bred with *Ago2*^{FL/FL}; *Mx-Cre* mice to obtain experimental *Ago2*^{S388A/FL}; *Mx-Cre* and control *Ago2*^{+/FL}; *Mx-Cre* animals. Adult mice were injected with poly I:C to induce the Cre-mediated conversion of the *Ago2*^{FL} into a null allele and the hematopoietic system was analysed after 4 weeks from the last injection (Fig. 8A). Analysis of DNA extracted from bone marrow of injected mice verified the conversion of the *Ago2*^{FL} into the non-functional *Ago2*⁻ allele (Fig. 8B). I did not detect any signs of anaemia nor splenomegaly between control and experimental *Ago2*^{S388A/FL}; *Mx-Cre* mice (Fig. 8C). A detailed analysis of erythroid development in the bone marrow and spleen highlighted the absence of any developmental defects both in the percentages and cell numbers of erythroblast populations (Fig. 8D). No significant differences for B cell progenitors were present in *Ago2*^{S388A/FL}; *Mx-Cre* mice compared to control littermates in the bone marrow. These data suggest that Ago2 phosphorylation of serine 388 is dispensable for Ago2-dependent processes in adult hematopoiesis.



C

		<i>Ago2^{FL/FL}; Mx-Cre</i>	<i>Ago2^{S388A/FL}; Mx-Cre</i>
RBC	10 ⁶ /μl	9.55±1.07	10.50±0.48
Hb	g/dL	14.36±1.92	15.01±0.55
HCT	%	47.98±7.67	49.26±2.00
MCV	fL	50.06±3.19	46.91±0.38
MCH	pg	15.03±0.41	14.30±0.16
MCHC	g/dL	30.05±1.35	30.49±0.32
RDW	%	18.90±0.98	19.11±0.67

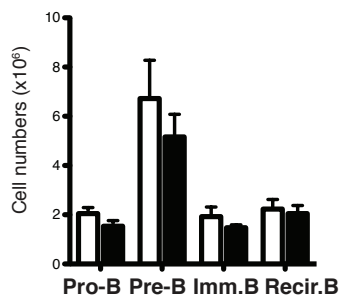
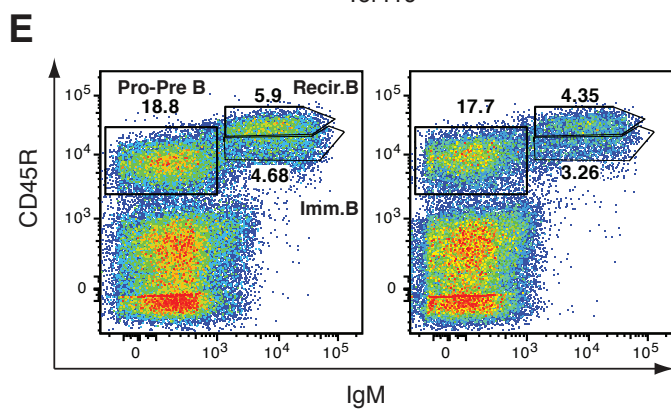
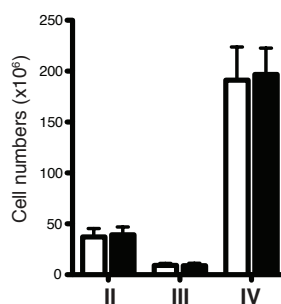
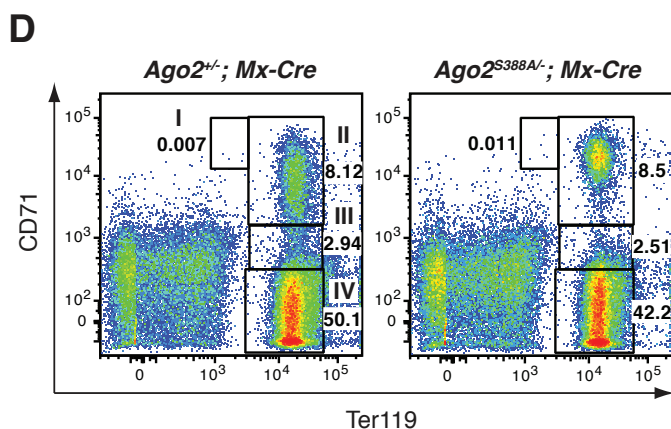
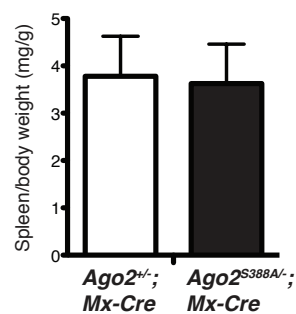
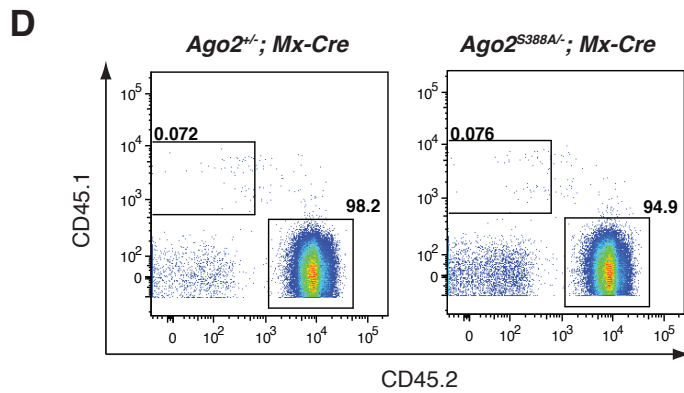
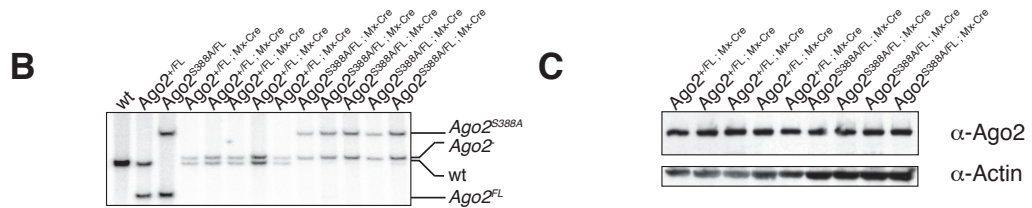
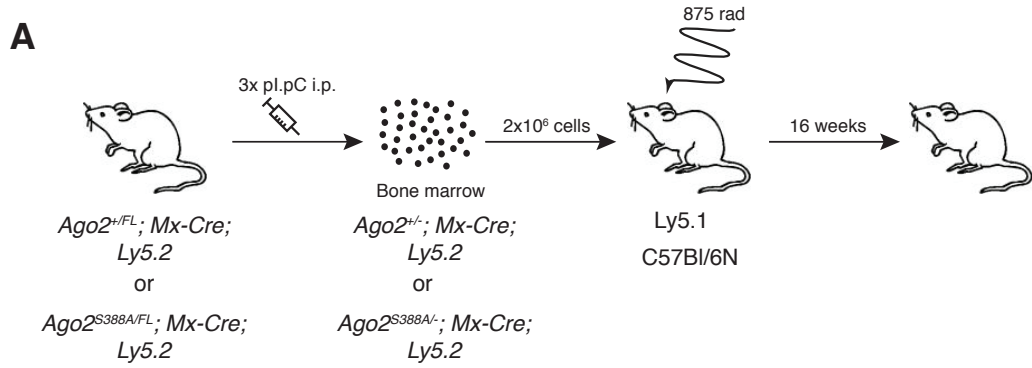


Figure 8. No defects in adult hematopoietic development in *Ago2*^{S388A/FL}; *Mx-Cre* mice upon Cre-induction.

(A) Outline of experimental procedure. Control *Ago2*^{+/FL}; *Mx-Cre* and experimental *Ago2*^{S388A/FL}; *Mx-Cre* animals in a mixed 129P2xC57Bl/6N genetic background were injected with poly I:C to activate the Cre-mediated recombination of the *Ago2*^{FL} alleles in hematopoietic tissues. Four weeks after poly I:C administration the animals were sacrificed for the analysis of hematopoietic lineages. (B) The efficiency of recombination after Cre induction was verified from bone marrow-derived DNA by PCR reaction. (C) Mean \pm s.d. of peripheral blood values from *Ago2*^{+/FL}; *Mx-Cre* and *Ago2*^{S388A/FL}; *Mx-Cre* animals are shown in the table. Graph shows the mean \pm s.d. of spleen to body weight ratio between control and experimental animals (n=4). RBC= red blood cell count; Hb= hemoglobin; HCT= haematocrit; MCV= mean cell volume; MCH= mean cell hemoglobin; MCHC= mean corpuscular hemoglobin concentration; RDW= red blood cell distribution width. (D) Representative flow cytometry analysis of erythroid progenitor cells from spleen of control *Ago2*^{+/FL}; *Mx-Cre* and experimental *Ago2*^{S388A/FL}; *Mx-Cre* mice. The graph represents the mean \pm s.e.m. of cell numbers of erythroid populations as estimated from flow cytometry percentages (n=4). Roman numerals indicate the identity of cells of the developmentally defined subpopulations (Socolovsky, 2001). I) Pro-erythroblasts, II) Basophilic erythroblasts, III) Polychromatophilic erythroblasts and IV) Orthochromatophilic erythroblasts. (E) Representative flow cytometry analysis of B cell progenitors from bone marrow of control *Ago2*^{+/FL}; *Mx-Cre* and experimental *Ago2*^{S388A/FL}; *Mx-Cre* mice. Numbers represent percentages of the gated cells. Bars represent mean values of cell numbers estimated from flow cytometry data, error bars indicate standard deviation of the mean (n=4). Progenitor B (pro-B, CD45R⁺ CD43⁺ IgM⁻), precursor B (pre-B, CD45R⁺ CD43⁻ IgM⁻), immature B (CD45R⁺ CD43⁻ IgM⁺) and recirculating B cells (CD45R^{hi} CD43⁻ IgM⁺) were gated as previously described (Mecklenbrauker, 2002). The data shown are representative of three independent experiments.

The induction of the Mx-Cre through poly I:C injections mediates the deletion of the *Ago2*^{FL} allele not only in the hematopoietic system, but also in other tissues such as liver (Kuhn, 1995). In addition, these injections elicit an interferon response that can alter the homeostasis of hematopoietic development, skewing progenitors cells to differentiate into myeloid cells. As a result, subtle differences between control *Ago2*^{+/FL}; *Mx-Cre* and experimental *Ago2*^{S388A/FL}; *Mx-Cre* mice can be underestimated or even compensated in a non-cell-autonomous fashion. To confirm the data collected, I decided to transplant bone marrow cells from previously characterized mice into lethally irradiated recipients. This approach allows to identify any defects in hematopoiesis due to lack of Ago2 S388

phosphorylation in hematopoietic cells that are developing in a wild type environment. In addition, I take advantage of the presence of two distinct CD45 alleles (*Ly5.1-Ly5.2*) (Miller, 1985; Shen, 1985; Spangrude, 1988) that can be distinguished by antibody staining to evaluate the contribution of transplanted bone marrow to the hematopoietic lineages analysed (Fig. 9A). DNA collected from bone marrow of recipients confirmed the efficiency of recombination (Fig. 9B). In addition, Western Blot analysis of Ago2 levels from bone marrow of transplanted animals showed no differences in protein levels, demonstrating that Ago2-S388A protein is stable (Fig. 9C). Discrimination between donor-derived and recipient-derived cells from the hematopoietic tissues analysed confirmed that more than 95% of cells originated from the transplanted bone marrow, highlighting no differences in homing capacity and engraftment between wild type and phosphomutant cells (Fig. 9D). Peripheral blood values and flow cytometry demonstrated the absence of anaemic phenotype in mice transplanted with *Ago2^{S388A/-}; Mx-Cre* cells (Fig. 9E). Furthermore, no defects in B cell progenitors nor in more mature B cell populations in the periphery were present (Fig. 10A-B). Analysis of T cells and myeloid lineages in transplanted mice showed the lack of any alteration in recipients transplanted with control or experimental bone marrow (Fig. 10C-D). Collectively, these data prove that Ago2 S388A phosphorylation is dispensable for adult hematopoietic development in a mixed 129P2xC57Bl/6N genetic background.



E

		<i>Ago2</i> ^{+/FL} ; <i>Mx-Cre</i>	<i>Ago2</i> ^{S388A/FL} ; <i>Mx-Cre</i>
RBC	10 ⁶ /μl	12.24±0.29	12.83±0.81
Hb	g/dL	12.08±0.31	12.54±0.31
HCT	%	58.02±1.09	59.36±3.46
MCV	fL	47.42±0.74	46.26±0.76
MCH	pg	9.86±0.21	9.78±0.44
MCHC	g/dL	20.84±0.53	21.16±0.90
RDW	%	18.50±0.68	19.14±0.32

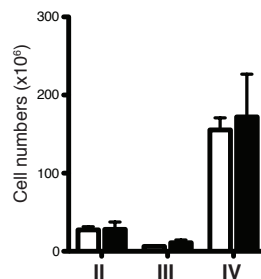
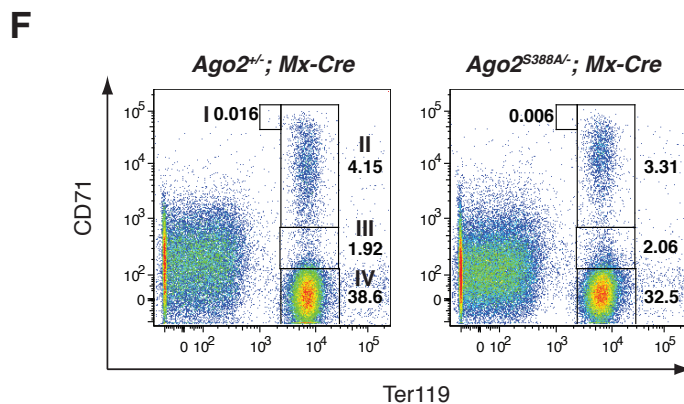
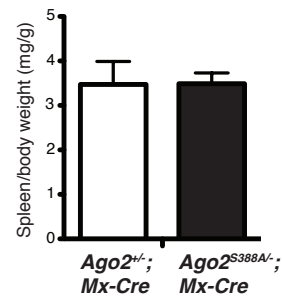


Figure 9. Ago2 S388 phosphorylation is not necessary for erythroid development in a cell-autonomous fashion.

(A) Outline of experimental setup. Control *Ago2*^{+/*FL*}; *Mx-Cre*; *Ly5.2* and experimental *Ago2*^{S388A/*FL*}; *Mx-Cre*; *Ly5.2* animals were injected with poly I:C to activate the Cre-mediated recombination of the *Ago2*^{*FL*} allele in hematopoietic tissues. Five weeks after drug administration, bone marrow cells were isolated and 2 million cells were used to transplant lethally irradiated *Ly5.1* recipients. Hematopoietic development was analysed 16 weeks after reconstitution. (B) Southern blot analysis of control and experimental animals from bone marrow-derived DNA confirmed the efficiency of Cre-mediated conversion of the *Ago2*^{*FL*} allele into a non-functional *Ago2*⁻ allele. (C) S388A mutation of Ago2 has no impact on the stability of the protein. Ago2 protein levels were evaluated in extracts from bone marrow of reconstituted recipients with an anti-Ago2 antibody by Western Blot. Actin was used as loading control. (D) Representative flow cytometry analysis of thymic cells from animals reconstituted with *Ago2*^{+/*FL*}; *Mx-Cre*; *Ly5.2* and experimental *Ago2*^{S388A/*FL*}; *Mx-Cre*; *Ly5.2* bone marrow cells. Number represents the percentages of endogenous *Ly5.1*⁺ and donor-derived *Ly5.2*⁺ cells. Data are indicative of a complete reconstitution of the peripheral hematopoietic organs by transplanted cells. (E) Mean \pm s.d. of peripheral blood values from *Ago2*^{+/*FL*}; *Mx-Cre*; *Ly5.2* and *Ago2*^{S388A/*FL*}; *Mx-Cre*; *Ly5.2* transplanted animals are shown in the table. Graph shows the mean \pm s.d. of spleen to body weight ratio between control and experimental animals (n=5). RBC= red blood cell count; Hb= hemoglobin; HCT= haematocrit; MCV= mean cell volume; MCH= mean cell hemoglobin; MCHC= mean corpuscular hemoglobin concentration; RDW= red blood cell distribution width. (F) Representative flow cytometry analysis of erythroid progenitor cells from spleen of control *Ago2*^{+/*FL*}; *Mx-Cre*; *Ly5.2* and experimental *Ago2*^{S388A/*FL*}; *Mx-Cre*; *Ly5.2* reconstituted animals. The graph represents the mean \pm s.e.m. of cell numbers of erythroid populations as estimated from flow cytometry percentages (n=5). Roman numerals indicate the identity of cells of the developmentally defined subpopulations (Socolovsky, 2001). I) Pro-erythroblasts, II) Basophilic erythroblasts, III) Polychromatophilic erythroblasts and IV) Orthochromatophilic erythroblasts. The data shown are representative of two independent experiments.

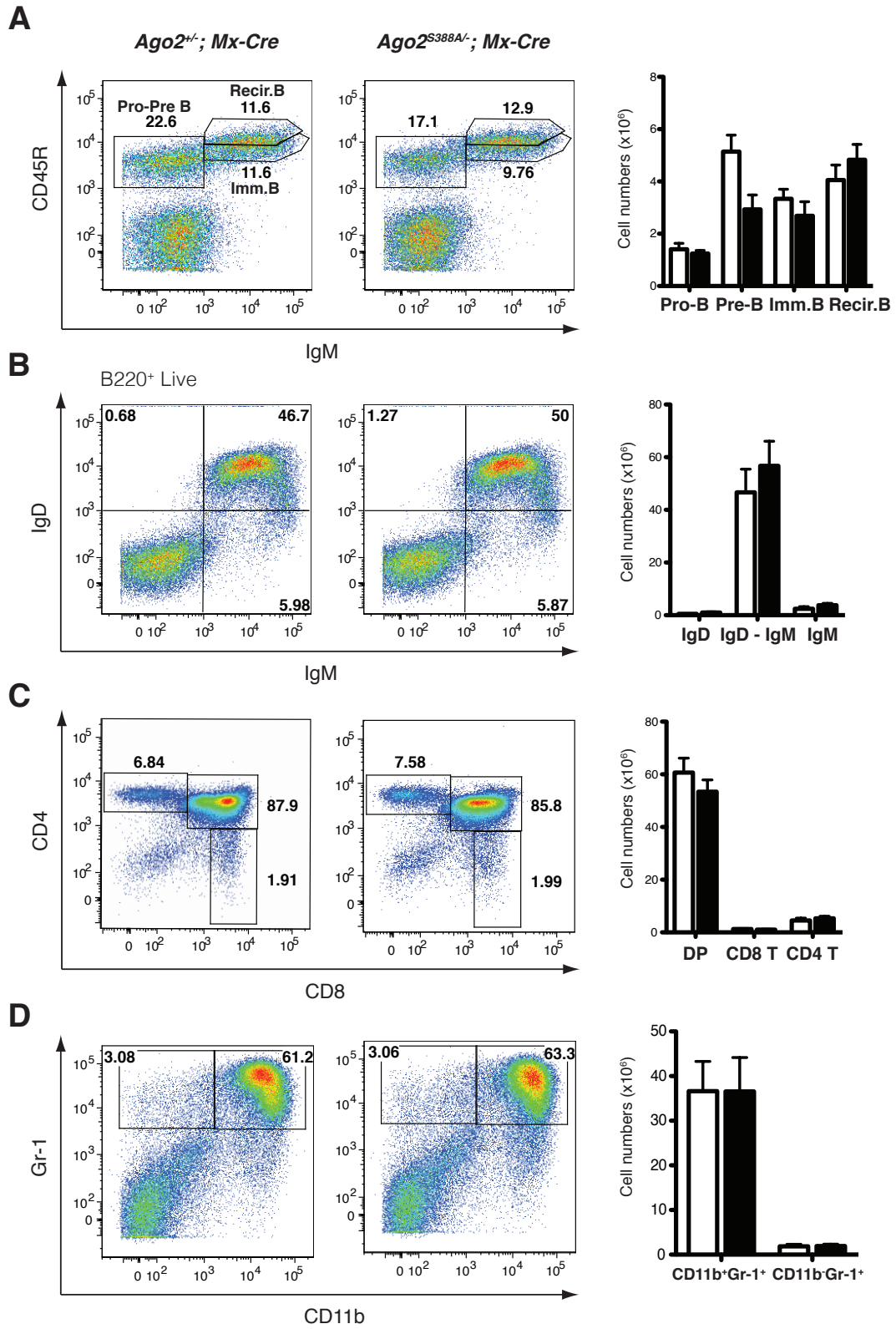


Figure 10. Ago2 S388 phosphorylation is not necessary for lymphoid and myeloid development in a cell-autonomous fashion.

Analysis of lymphoid and myeloid development from transplanted mice as in Fig. 9A. For the flow cytometry analysis, only Ly5.2⁺ cells were gated for further analysis. (A-B) Representative flow cytometry analysis of B cell progenitors and mature B cells from bone marrow (A) and spleen (B) of transplanted animals. Numbers represent percentages of the gated cells. Bars represent mean values of cell numbers estimated from flow cytometry data, error bars indicate standard deviation of the mean (n=5). Progenitor B (pro-B, CD45R⁺ CD43⁺ IgM⁻), precursor B (pre-B, CD45R⁺ CD43⁻ IgM⁻), immature B (CD45R⁺ CD43⁻ IgM⁺) and recirculating B cells (CD45R^{hi} CD43⁻ IgM⁺) were gated as previously described (Mecklenbrauker, 2002). (C) Representative flow cytometry image of the percentages of T cells from thymus of animals reconstituted with *Ago2*^{+FL}; *Mx-Cre*; *Ly5.2* and *Ago2*^{S388A/FL}; *Mx-Cre*; *Ly5.2* bone marrow cells. Numbers in the FACS plot represent percentages. Graph shows mean ±s.e.m. of cell numbers estimated from flow cytometry data (n=5). DP= CD4⁺ CD8⁺ double-positive T cells. (D) Typical FACS analysis is shown for myeloid cells from bone marrow of transplanted animals. Numbers represent percentages of the gated cells. Bars represent mean values of cell numbers estimated from flow cytometry data, error bars indicate standard deviation of the mean (n=5). The data shown are representative of two independent experiments.

3.1.4 Ago2 S388 phosphorylation is dispensable for female fertility

Small non-coding RNA pathway has an important role during oogenesis: conditional deletion of Ago2 or Dicer in early stages of oocyte development induces a block on metaphase II of the meiotic process due to spindle defects (Murchison, 2007; Tang, 2007; Kaneda, 2009). Interestingly, even though both mature miRNAs and endogenous siRNAs (endo-siRNAs) are present in this cell type, only endo-siRNAs seem to be active, since loss of DGCR8 and miRNA pathway do not affect oocyte maturation (Watanabe, 2006; Tang, 2008; Watanabe, 2008; Ma, 2010; Suh, 2010). These data insinuate a differential regulation of miRNA- and siRNA-mediated silencing in oogenesis at the level of Ago2, the only Argonaute family member with the capability to slice target mRNAs (Liu, 2004; Meister, 2004; Song, 2004). I hypothesized that phosphorylation of serine 388 might control a switch between miRNA-based and siRNA-based Ago2 silencing activity. To pursue this hypothesis, I made use of a conditional loss-of-function approach by combining the *Ago2*^{FL} allele with a female-

specific *Zp3-Cre* mouse line (De Vries, 2000; Murchison, 2007; Tang, 2007; Kaneda, 2009). Control *Ago2*^{+/*FL*}; *Zp3-Cre* and experimental *Ago2*^{*Neo-S388A/FL*}; *Zp3-Cre* females were mated with wild type males of known fertility and the number of pups per pregnancy was evaluated (Fig. 11A). No differences in litter size were evident between control and experimental mice (7.88±1.36 and 7.50±2.65 pups per litter for *Ago2*^{*Neo-S388A/FL*}; *Zp3-Cre* and *Ago2*^{+/*FL*}; *Zp3-Cre* animals, respectively) (Fig. 11B). Genotype of pups confirmed the high efficiency of recombination in all tested animals (Fig. 11C). I can conclude that Ago2 phosphorylation of serine 388 is not essential for female fertility and oogenesis. Furthermore, lack of Ago2 S388 modification does not affect the RNA interference pathway, which is active during oocyte development.

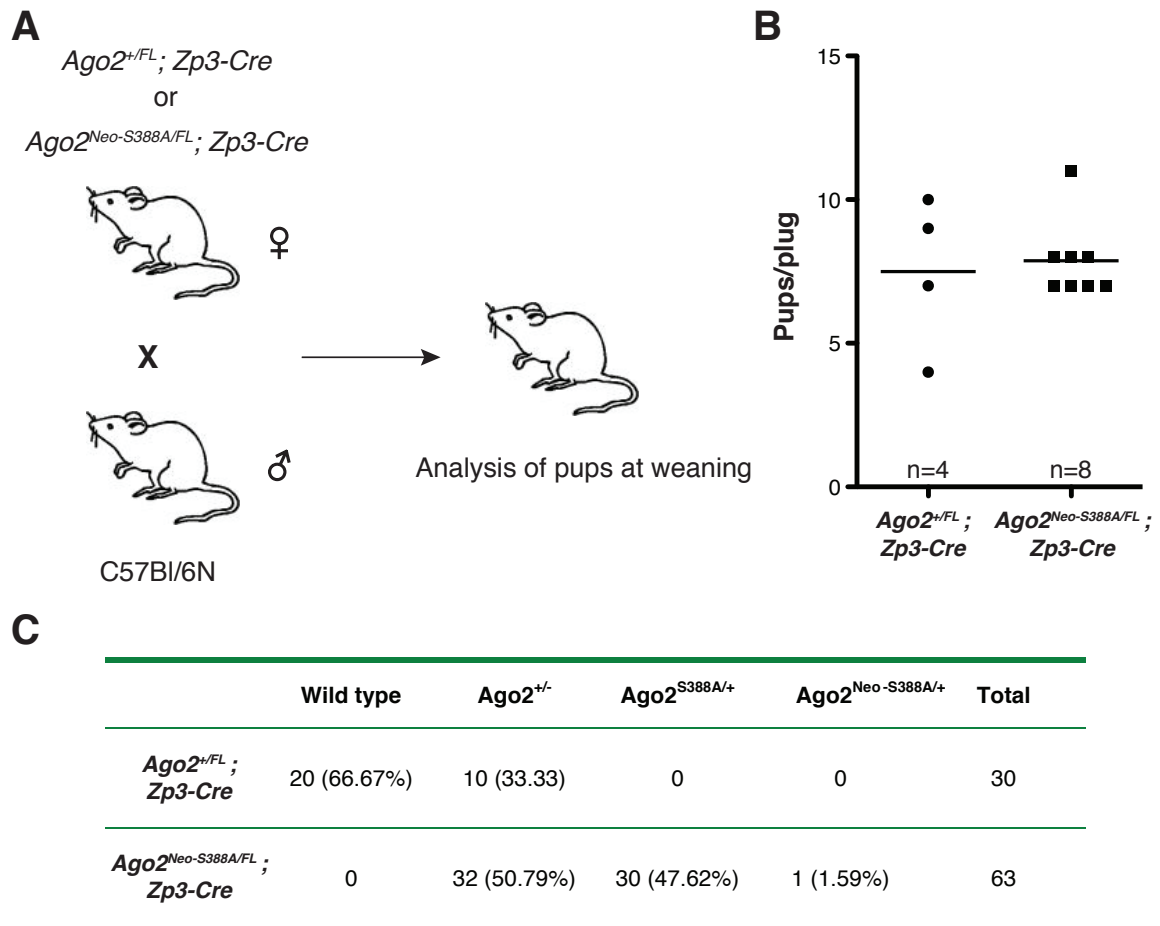


Figure 11. Ago2 S388 phosphorylation is dispensable for oogenesis.

(A) Outline of experimental design. *Ago2*^{+/*FL*}; *Zp3-Cre* and *Ago2*^{*Neo-S388A/FL*}; *Zp3-Cre* females were mated with wild type C57Bl/6N males of known fertility. Male mice were

removed from the cage after the appearance of a vaginal plug. The size of each litter was evaluated after weaning. (B) No significant decrease in the fertility of *Ago2*^{Neo-S388A/FL}; *Zp3-Cre* females was seen compared to control animals. Graph shows the mean of litter size at weaning from *Ago2*^{+/FL}; *Zp3-Cre* and *Ago2*^{Neo-S388A/FL}; *Zp3-Cre* females. The number of animals used for each genotype is indicated in the graph. (C) Genotype of pups at weaning confirmed the high efficiency of recombination in both control and experimental animals.

3.1.5 Ago2 S388 phosphorylation is not necessary for Ago2-dependent processes in the C57Bl/6N genetic background

The use of this novel *Ago2*^{S388A} phospho-incompetent allele has shown that this phosphorylation event is necessary for early stages of mouse embryonic development, while it is dispensable for further adult processes. The previous data were collected in a 129P2xC57Bl/6N mixed genetic background, raising the possibility of the presence of one or more modifier alleles that affect the phenotypic outcome of Ago2 mutation. To address this problem, I mated heterozygous *Ago2*^{S388A/+} mice for 8 generations with C57Bl/6N animals, to reach theoretically 99.6% of the genome from this inbred strain (Fig. 6) (Markel, 1997). Heterozygous individuals were then intercrossed and the pups were genotyped at weaning. Surprisingly, homozygous mutant mice were born accordingly to the expected Mendelian ratios in a C57Bl/6N genetic background (Fig. 12A). This result strongly supports the hypothesis of a background effect, suggesting that one or more allelic variants present in the C57Bl/6N inbred strain are capable of complementing the lack of S388 phosphorylation of Ago2.

The survival of *Ago2*^{S388A/S388A} animals prompted me to further test these animals in the respect of Ago2-dependent processes, such as oocyte and hematopoietic development. Homozygous male and female are fertile, since no appreciable differences between wild type and homozygous animals were seen in litter size (Fig. 12B). Analysis of peripheral blood values and spleen weight show no signs of anaemia in homozygous phosphomutant compared to wild type controls (Fig. 13A-B). Further flow cytometry analysis of several hematopoietic lineages confirms the absence of any relevant defect in *Ago2*^{S388A/S388A} compared to wild type animals (Fig. 13C-F).

A

	Matings	Wild type	<i>Ago2</i> ^{S388A/+}	<i>Ago2</i> ^{S388A/S388A}	Total
At weaning	21	88 (23.47%)	196 (52.27%)	91 (24.26%)	375
	Expected	94	187	94	

B

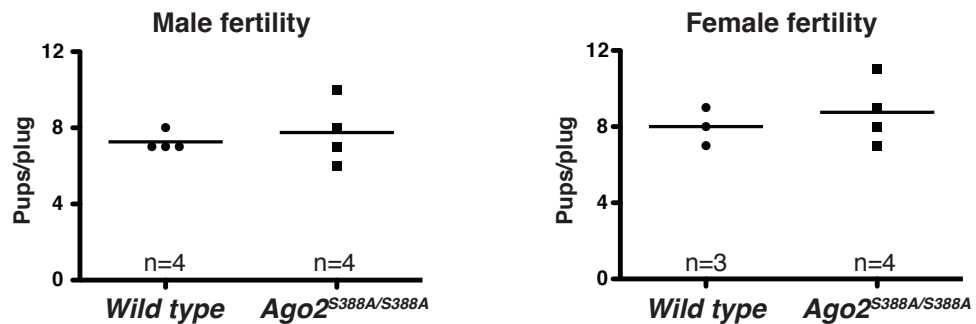
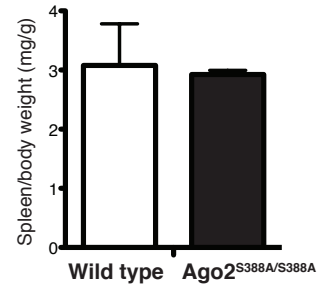
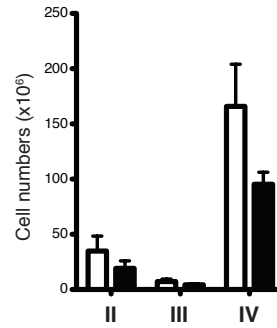
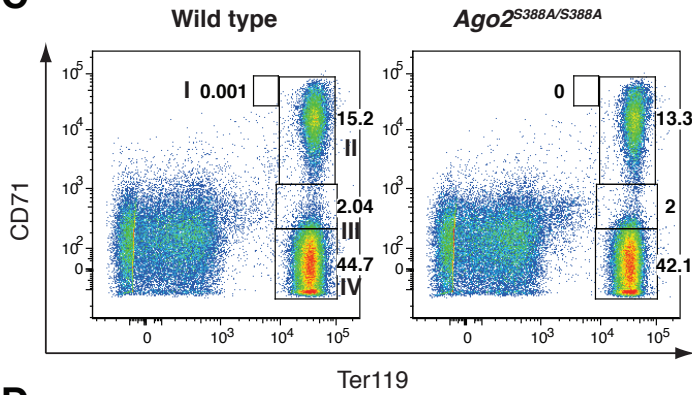
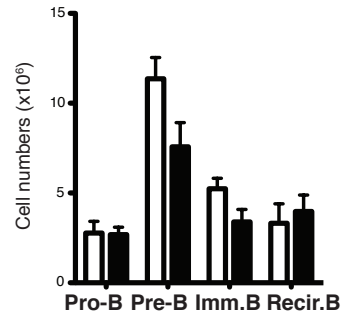
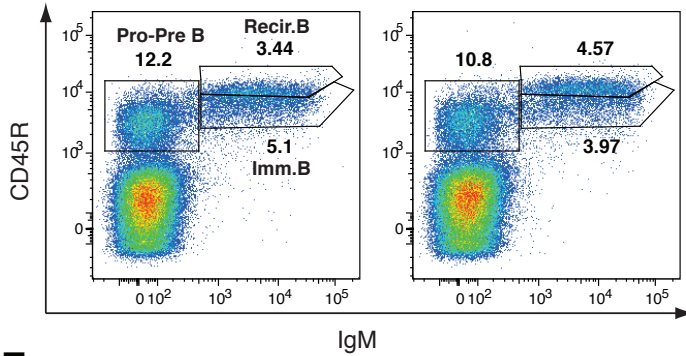
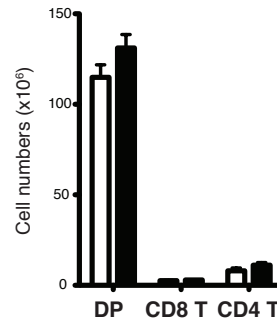
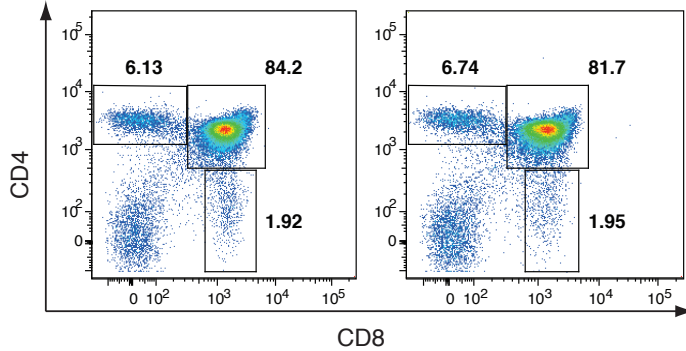


Figure 12. *Ago2*^{S388A/S388A} animals are viable and fertile in a C57Bl/6N genetic background.

(A) *Ago2*^{S388A/+} animals were intercrossed after 8 generation of mating with inbred C57Bl/6N animals. The numbers and percentages of pups at weaning and the expected Mendelian numbers of animals per genotype are shown. The data indicate the absence of lethality for *Ago2*^{S388A/S388A} homozygous mice in this genetic background. (B-C) Male and female *Ago2*^{S388A/S388A} animals were mated with wild type C57Bl/6N mice of known fertility. Males were separated from the female after the appearance of vaginal plug. The graphs represent the mean size of a litter for wild type and *Ago2*^{S388A/S388A} littermates at weaning. No statistically significant differences were evident between control and experimental mice. The number of animals used for each genotype is indicated in the graph.

A

		Wild type	<i>Ago2</i> ^{S388A/S388A}
RBC	10 ⁶ /μl	10.41±1.00	10.51±1.48
Hb	g/dL	13.08±0.79	12.98±1.87
HCT	%	60.98±6.22	62.45±7.34
MCV	fL	58.56±0.75	58.28±1.42
MCH	pg	12.62±0.58	12.10±0.62
MCHC	g/dL	21.54±1.21	20.75±1.20
RDW	%	17.28±0.34	16.98±0.68

B**C****D****E**

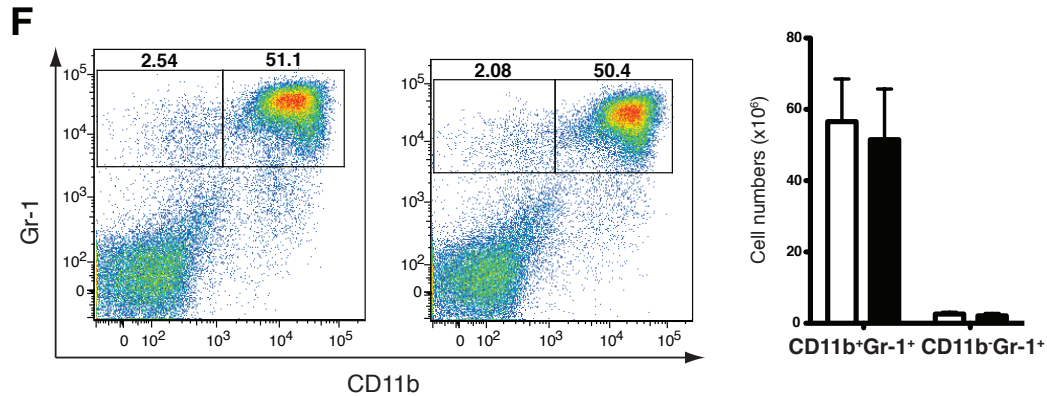


Figure 13. No defects in adult hematopoietic development in *Ago2*^{S388A/S388A} animals in a C57Bl/6N genetic background.

(A) Mean \pm s.d. of peripheral blood values from wild type and *Ago2*^{S388A/S388A} littermates are shown in the table (n=5). No signs of anaemia are present in phosphomutant homozygotes. RBC= red blood cell count; Hb= hemoglobin; HCT= haematocrit; MCV= mean cell volume; MCH= mean cell hemoglobin; MCHC= mean corpuscular hemoglobin concentration; RDW= red blood cell distribution width. (B) Graph shows the mean \pm s.d. of spleen to body weight ratio between control and experimental animals (n=5). No significant differences are visible between wild type and *Ago2*^{S388A/S388A} mutants. (C) Representative flow cytometry analysis of erythroid progenitor cells from spleen of wild type and experimental *Ago2*^{S388A/S388A} littermates. The graph represents the mean \pm s.e.m. of cell numbers of erythroid populations as estimated from flow cytometry percentages (n=5). Roman numerals indicate the identity of cells of the developmentally defined subpopulations (Socolovsky, 2001). I) Pro-erythroblasts, II) Basophilic erythroblasts, III) Poly-chromatophilic erythroblasts and IV) Orthochromatophilic erythroblasts. (D) Representative flow cytometry analysis of B cell progenitors from bone marrow of wild type and phosphomutant mice. Numbers represent percentages of the gated cells. Bars represent mean values of cell numbers estimated from flow cytometry data, error bars indicate standard deviation of the mean (n=5). Progenitor B (pro-B, CD45R⁺ CD43⁺ IgM⁻), precursor B (pre-B, CD45R⁺ CD43⁻ IgM⁻), immature B (CD45R⁺ CD43⁻ IgM⁺) and recirculating B cells (CD45R^{hi} CD43⁻ IgM⁺) were gated as previously described (Mecklenbrauker, 2002). (E) Representative flow cytometry image of the percentages of T cells from thymus of wild type and *Ago2*^{S388A/S388A} mice. Numbers in the FACS plot represent percentages. Graph shows mean \pm s.e.m. of cell numbers estimated from flow cytometry data (n=5). DP= CD4⁺ CD8⁺ double-positive T cells. (F) Typical FACS analysis is shown for myeloid cells from bone marrow of wild type and phosphomutant animals. Numbers represent percentages of the gated cells. Bars represent mean values of cell numbers estimated from flow cytometry data, error bars indicate standard deviation of the mean (n=5). The data shown are representative of two independent experiments.

Since Ago2 S388 phosphorylation is catalysed by the MK2 protein kinase, I decided to deepen the analysis on hematopoietic progenitor populations. Indeed, in a C57Bl/6N genetic background mice lacking MK2 present a reduction of long-term hematopoietic stem cells (LT-HSCs) with a concomitant increase of multiple progenitor cells (MPPs) (Schwermann, 2009). In homozygous *Ago2*^{S388A/S388A} animals no recognizable difference was present in percentages and cell numbers of LT-HSC (Lin⁻ c-Kit⁺ Sca-1⁺ CD150⁺ Flk3⁻) and lymphoid-primed multipotent progenitor cells (LMPPs) (Lin⁻ c-Kit⁺ Sca-1⁺ CD150⁻ Flk3⁺) compared to wild type littermates (Fig. 14A). Analysis of early B cells and megakaryocyte-erythroid precursors also shows no significant defects between control and experimental animals (Fig. 14B-C). I can conclude that Ago2 S388 phosphorylation is dispensable for MK2-dependent regulation of HSC pool. In addition, collective data from C57Bl/6N animals suggest that S388 post-translational modification is not essential for Ago2 function in this genetic background.

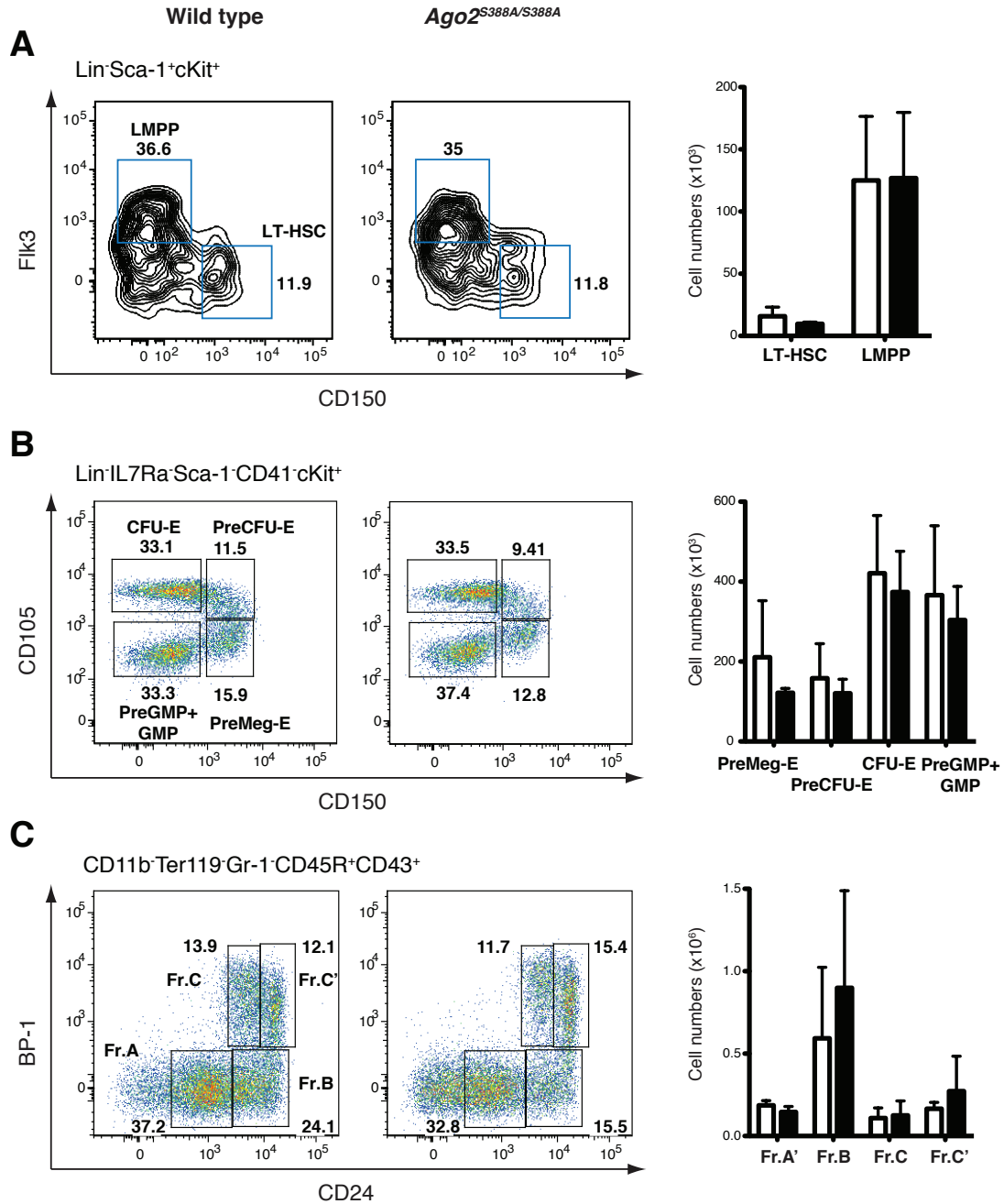


Figure 14. No defects in HSC and early hematopoietic progenitors in *Ago2*^{S388A/S388A} animals in a C57Bl/6N genetic background.

(A) Representative flow cytometry plot of hematopoietic stem cell and early progenitor populations in wild type and *Ago2*^{S388A/S388A} littermates. The panel shows Lin⁻ c-Kit⁺ Sca-1⁺ cells stained for CD150 and Flk3. LT-HSC (Lin⁻ c-Kit⁺ Sca-1⁺ CD150⁺ Flk3⁻) and LMPP (Lin⁻ c-Kit⁺ Sca-1⁺ CD150⁻ Flk3⁺) populations are defined as previously described (Kiel, 2005; Adolfsson, 2005). Numbers indicate percentages of the gated populations. Graph represents mean \pm s.e.m. of total cell numbers inferred from the flow

cytometry data (n=3). (B) Representative FACS analysis is shown for the c-kit-positive erythroid progenitors in the bone marrow of wild type and *Ago2*^{S388A/S388A} mice. The gates illustrate following developmentally defined subpopulations: Pre-colony forming unit erythroid precursor (Pre-CFU-E), colony forming unit erythroid (CFU-E), premegakaryocyte/erythroid precursor (Pre-MegE), granulo monocyte precursor (GMP) and pre-granulo monocyte precursor (Pre-GM) (Pronk, 2007). Bars indicate the mean of cell numbers evicted from flow cytometry percentages, error bars show the standard deviation of the mean (n=3). (C) Indicative FACS plot representing different subpopulations of early progenitor B cell populations is shown. The panel presents CD11b⁻ Ter119⁻ Gr-1⁻ CD45R⁺ CD43⁺ cells stained with antibodies against BP-1 and CD24. Fraction A' is composed of CD93⁺ cells from Fraction A. The different progenitor B cells were analysed according to published works (Hardy, 1991; Li, 1996). Graph shows mean \pm s.e.m. of total cell numbers inferred from the flow cytometry data (n=3). The data shown are representative of two independent experiments.

3.1.6 Ago2 S388 phosphorylation is dispensable for endotoxic stress response

The data presented so far investigated the physiological importance of Ago2 S388 phosphorylation event in resting conditions. It has been demonstrated that phosphorylation levels of S387 of the human Ago2 are enhanced after stress stimuli that activate the p38-MK2 pathways (Zeng, 2008; Horman, 2013). *MK2*^{-/-} animals are viable and fertile, but they are resistant to lethal doses of lipopolysaccharide (LPS) due to a decrease in the production of TNF- α and other proinflammatory cytokines (Kotlyarov, 1999). It is then conceivable that *Ago2*^{S388A/S388A} mice also withstand high doses of LPS compared to wild type littermates. In order to test this hypothesis, I challenged wild type and homozygous mutant mice in a C57Bl/6N genetic background with lethal doses of LPS together with D-galactose (D-gal) and evaluate the kinetics of survival in both groups. D-gal was used as an adjuvant to increase the innate response since it is present on the surface of many bacterial species. Homozygous *Ago2*^{S388A/S388A} mice die with similar percentages and kinetics as wild type littermates (Fig. 15A). To prove that this response it is not dependent upon the genetic background used, we transplanted lethally irradiated recipients with bone marrow from *Ago2*^{+/*FL*}; *Mx-Cre* and *Ago2*^{S388A/*FL*}; *Mx-Cre* donors upon Cre induction. In addition, this experimental strategy allowed us to

evaluate the cell-autonomous effect of Ago2 S388 phosphorylation on macrophages and dendritic cells, which are the principal responders to LPS injections. LPS+D-gal were administered 12 weeks after reconstitution, and the survival rate of the two groups was monitored for 24 hours post-injection (Fig. 15B). As for the previous experiment, no differences in kinetics or percentage of survivors were evident between control and experimental animals (Fig. 15B). These data demonstrate that Ago2 S388 phosphorylation is not participating in the MK2-dependent regulation of endotoxic response *in vivo*.

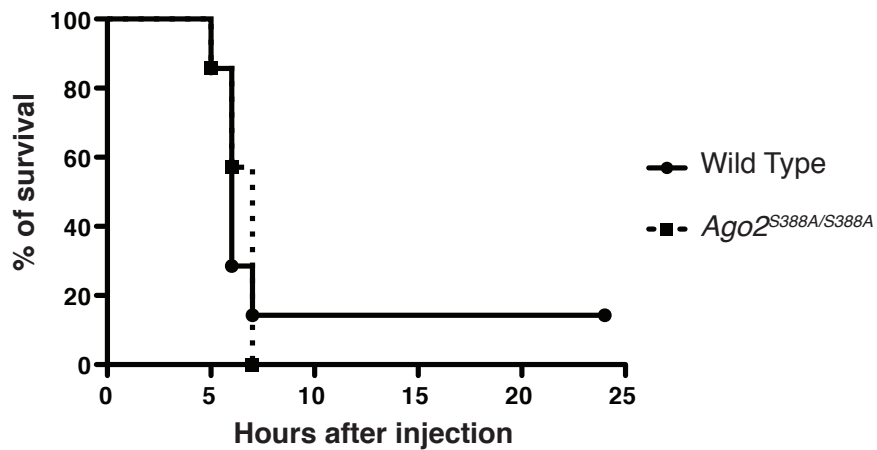
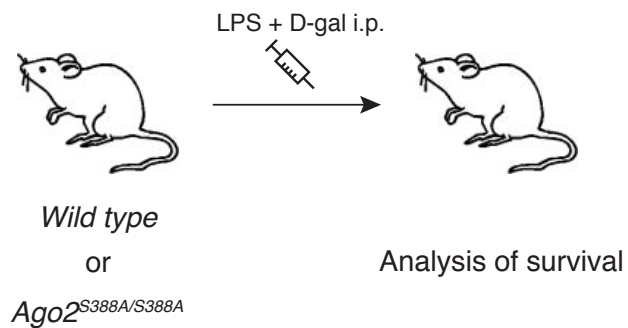
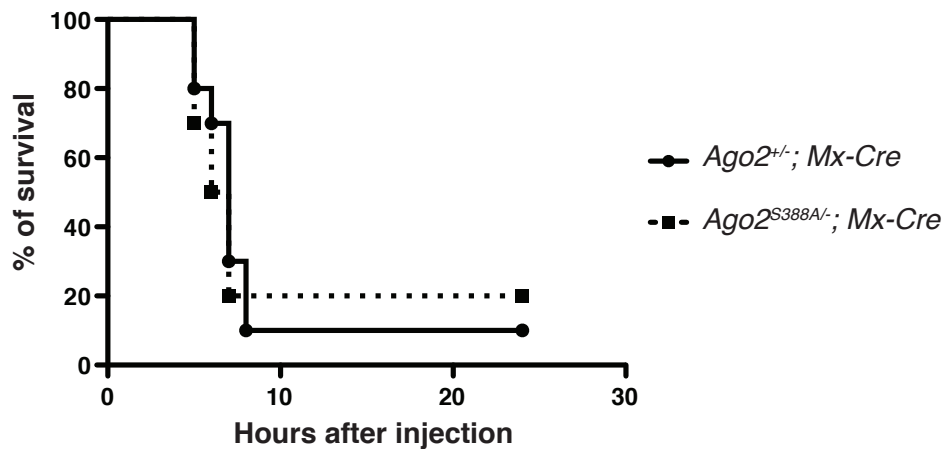
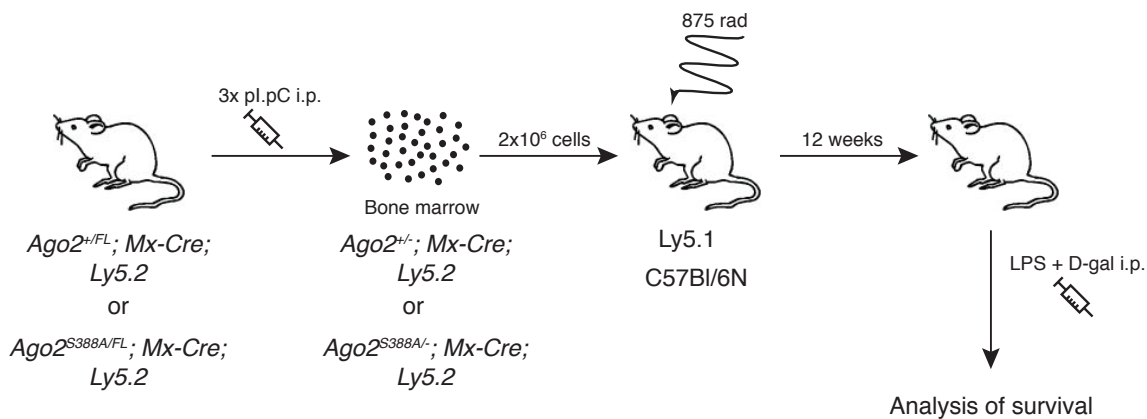
A**B**

Figure 15. Ago2 phosphorylation at S388 is not necessary for MK2-dependent endotoxic response.

(A) Adult wild type and *Ago2*^{S388A/S388A} mutant littermates in a C57Bl/6N genetic background were injected with 30µg of LPS together with 800mg/Kg D-gal and monitored for 24 hours after injection. Kaplan-Meier plot of survival after injection shows no significant differences neither in the kinetics of response nor in the survival ratio between wild type and homozygous phosphomutant mice (n=7). (B) *Ago2*^{+FL}; *Mx-Cre*; *Ly5.2* and *Ago2*^{S388A/FL}; *Mx-Cre*; *Ly5.2* animals were injected with poly I:C to activate the Cre-mediated recombination of the *Ago2*^{FL} alleles in hematopoietic tissues. Five weeks after drug administration, bone marrow cells were isolated and 2 million cells were used to transplant lethally irradiated *Ly5.1* recipients. After 12 weeks from bone marrow transplantation, a lethal dose of LPS+D-gal was administered intraperitoneally and the survival of mice was monitored for 24 hours. Kaplan-Meier graph of survival percentages indicate the absence of any phenotypic difference due to the lack of Ago2 S388 phosphorylation (n=10).

3.1.7 Ago2 S388 phosphorylation is necessary for embryonic development in the 129S2 genetic background

The idea of a genetic background-dependent lethality of *Ago2*^{S388A/S388A} homozygous mice is supported by the results of heterozygote intercrosses in a mixed 129P2xC57Bl/6N and pure C57Bl/6N genetic background. To provide conclusive proof of this phenomenon, I mated heterozygote *Ago2*^{S388A/+} animals with wild type 129S2 for 8 generations in order to create a second congenic 129S2 mouse line (Fig. 6). The number of *Ago2*^{S388A/S388A} animals at weaning is much lower compared to the expected 25% Mendelian ratio: only 5 animals of the 32 expected were born and survived until adulthood (Fig. 16A). In addition, intercrosses of *Ago2*^{S388A/+} mice in the 129S2 strain give similar ratios of homozygous mutants as shown for a 129P2xC57Bl/6N mixed genetic background (compare Fig. 7A and 16A). A subtle reduction of *Ago2*^{S388A/+} mice at weaning was also displayed in a 129S2 genetic background (Fig. 16A). These data strongly support the hypothesis of a strong genetic background effect on the phenotypic outcome of Ago2 S388 phosphorylation. I next sought to determine at which embryonic stage *Ago2* homozygous mutant animals die. Analysis of deciduas at E7.5 shows a percentage of *Ago2*^{S388A/S388A} embryos with no obvious morphological defects similar to

the percentage of these pups at weaning. Furthermore, empty deciduas with no embryonic structure visible were present with a percentage close to the expected one for mutant homozygotes (Fig. 16B). However, isolation and genotype of blastocysts at E3.5 showed a Mendelian number of *Ago2*^{S388A/S388A} embryos (Fig. 16B). No morphological differences were visible between wild type and mutant blastocysts at this stage of development (Fig. 16C). Furthermore, no differences in the Ago2 protein levels were seen by immunofluorescence staining between wild type and *Ago2*^{S388A/S388A} blastocysts (Fig. 16C). Together, the data show that Ago2 S388 phosphorylation is necessary for embryonic development at peri-implantation in the 129S2 genetic background. Secondly, these results prove for the first time the presence of a strong genetic background effect for a post-translational modification site mutation.

A

	Matings	Wild type	<i>Ago2</i> ^{S388A/+}	<i>Ago2</i> ^{S388A/S388A}	Total
At weaning	11	50 (39.68%)	71 (56.35%)	5 (3.97%)	126
	Expected	32	63	32	

B

	Wild type	<i>Ago2</i> ^{S388A/+}	<i>Ago2</i> ^{S388A/S388A}	Resorption	Total
E7.5	20 (29.41%)	28 (41.18%)	3 (4.41%)	19 (27.94%)	68
E3.5	19 (26.39%)	29 (40.28%)	24 (33.33%)	0	72

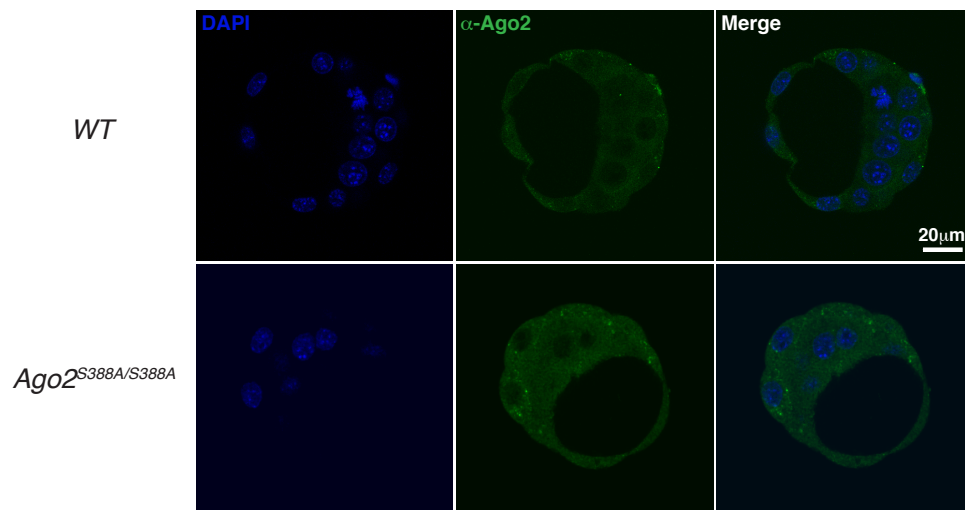
C

Figure 16. *Ago2*^{S388A/S388A} homozygous mutants are lethal in 129S2 genetic background.

(A) *Ago2*^{S388A/+} animals were intercrossed after 8 generation of mating with inbred 129S2 animals. The numbers and percentages of pups at weaning and the expected Mendelian numbers of animals per genotype are shown. The data indicate the presence of a strong selection against homozygous mutant mice in this co-isogenic line ($X^2 < 0.002$, chi-square test). (B) The table shows the number of embryos isolated at embryonic day E3.5-E7.5 from *Ago2*^{S388A/+} intercrosses for each genotype. The number and percentage of abnormal deciduas isolated at E7.5 is also indicated. The discrepancy in the percentage of *Ago2*^{S388A/S388A} mutants between E3.5 and E7.5 embryos suggests a peri-implantation lethality of these animals. (C) Immunofluorescence staining of

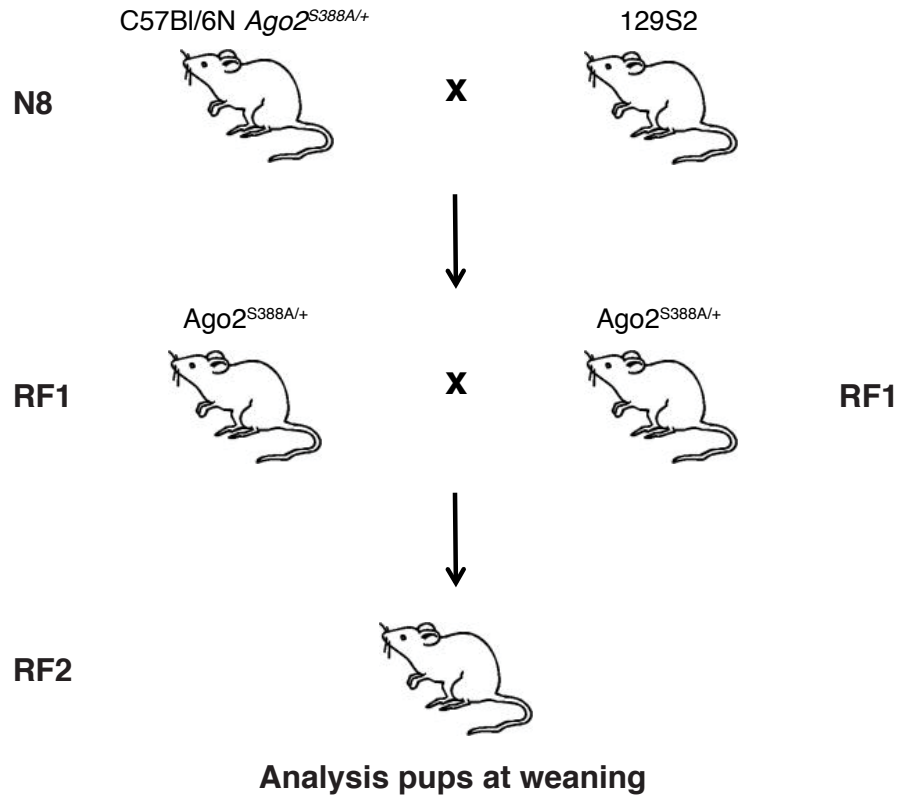
blastocysts isolated at E3.5 from *Ago2*^{S388A/+} intercrosses in a 129S2 genetic background. An anti-Ago2 antibody was used to detect the Ago2 protein in both wild type and phosphomutant homozygous embryos. Nuclei are stained with DAPI. Bar = 20µm. Data presented in this figure were collected and elaborated in collaboration with Maria Placentino.

3.1.8 Differential phenotype of Ago2 S388 mutation between C57Bl/6N and 129S2 genetic backgrounds depends on loci close to the Ago2 locus

During the process of backcrossing into an inbred mouse strain (i.e. C57Bl/6N) that differs from the mESC parental strain (i.e. 129), the genome of the parental strain is gradually replaced by the genomic regions of the inbred strain chosen. However, the creation of a co-isogenic line is based on the principle that only the individuals heterozygous for the mutation of interest are then used for the next step of backcrossing. With this method the chromosomal region close to the mutation of interest is selectively retained from the parental strain of origin, and it gets smaller at each backcrossing step. In the case of the *Ago2*^{S388A} mutant allele, the absence of embryonic lethality in the C57Bl/6N co-isogenic strain indicates the presence of one or more genetic variants that can complement the lack of Ago2 phosphorylation. To shed light on the location of these genetic components, *Ago2*^{S388A/+} heterozygotes in a C57Bl/6N background were first crossed for one generation with 129S2 animals, and the resulting reverse F₁ (RF₁) generation was intercrossed to evaluate the presence of homozygous mice at weaning (Fig. 17A). The presence of *Ago2*^{S388A/S388A} animals at the expected Mendelian ratios would suggest a linkage between the point mutation and the modifier alleles, reflecting genomic vicinity. On the other hand, a negative selection against mutant homozygotes would indicate random segregation of the modifier alleles compared to the Ago2 locus. The data presented in Fig. 17B demonstrate that *Ago2*^{S388A/S388A} homozygous mutants are born at the expected Mendelian ratios as wild types. The lack of lethality in a reverse F₂ (RF₂) clearly points to the presence of modifier alleles in genetic linkage to the Ago2 locus, suggesting proximity in the mouse genome. Indeed, in the RF₁ intercrosses the recombination of 129S2 and C57Bl/6N genomes is not sufficient to separate the point mutation from the modifier alleles derived from the C57Bl/6N strain. Since the Ago2

locus resides in chromosome 15, it is conceivable to hypothesize the C57Bl/6N variants are located in the same chromosome. These data would help to identify the modifier alleles in the C57Bl/6N inbred strain responsible for $Ago2^{S388A/S388A}$ survival.

A



B

	Matings	Wild type	$Ago2^{S388A/+}$	$Ago2^{S388A/S388A}$	Total
At weaning	14	39 (27.67%)	69 (48.93%)	33 (23.40%)	141
	Expected	35	71	35	

Figure 17. $Ago2^{S388A/S388A}$ homozygous mutants are viable in a reverse F₂ genetic background.

(A) Outline of breeding strategy. $Ago2^{S388A/+}$ heterozygotes bred for 8 generations with C57Bl/6N mice were crossed for 1 generation with wild type 129S2 animals. The resultant $Ago2^{S388A/+}$ RF₁ generation was further intercrossed to test the lethality of

homozygous mutants. The absence of a lethal phenotype for *Ago2*^{S388A/S388A} pups may indicate the presence of a genetic linkage between the phospho-incompetent Ago2 locus and the modifier alleles. (B) The table shows the numbers and percentages of pups at weaning and the expected Mendelian numbers of animals per genotype from the RF₁ intercross. No selection against *Ago2*^{S388A/S388A} animals was present in the RF₂ generation.

3.1.9 Development of an Ago2 phospho-serine 388 specific antibody

The discrepancy in phenotype between the C57Bl/6N and 129S2 co-isogenic lines I created could be ascribed to differential levels of Ago2 S388 phosphorylation in the two genetic backgrounds. I decided to develop a phospho-specific antibody that recognizes endogenous levels of Ago2 phosphorylation of Serine 388. Mice were immunized with a peptide encompassing a phosphorylated S388 and subsequently purified a monoclonal antibody (Fig. 18A). I verified the specificity of the antibody by Western blot with a phosphorylated and unphosphorylated S388 from Ago2 L2 linker domain (Fig. 18B). The phospho-specific antibody is able to recognize only the linker domain carrying a phosphorylated S388, but has no reactivity against the unphosphorylated and the S388A mutant peptide. Overexpression of murine wild type and S388A Ago2 proteins in HEK293T cells demonstrate that this antibody is able to recognize phosphorylated levels of Ago2 in resting and stress culture conditions by Western Blot and immunofluorescence (Fig. 18C-D). Importantly, Ago2 S388 phosphorylation levels are greatly increased after treatment with sodium arsenite as described previously (Zeng, 2008).

Since *Ago2*^{S388A/S388A} mutant animals die at peri-implantation in a 129S2 genetic background, I isolated E3.5 blastocysts from wild type C57Bl/6N and 129S2 matings and performed an immunofluorescence analysis using both an anti-Ago2 and the anti-pS388 antibody (Fig. 18E). No differences in Ago2 localization were visible between C57Bl/6N and 129S2 embryos (data not shown). In addition, the signal from the anti-pS388 phospho-specific antibody is really weak and diffused, indicating the inability of this antibody to recognize phosphorylation levels under endogenous Ago2 expression (Fig. 18E). Indeed, the signal for phosphorylated Ago2 is really weak even upon

overexpression of the protein in HEK293T cells without stress (Fig. 18C). These data suggest that no differences in Ago2 activity between the two inbred strains are present at this embryonic stage due to similar cellular localization. The development of a more powerful phospho-specific antibody would allow us to verify if differential phosphorylation levels of serine 388 might explain the diverse phenotypic outcomes between the two co-isogenic lines.

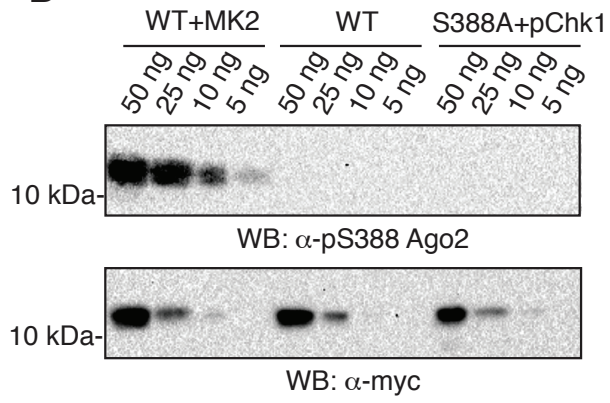
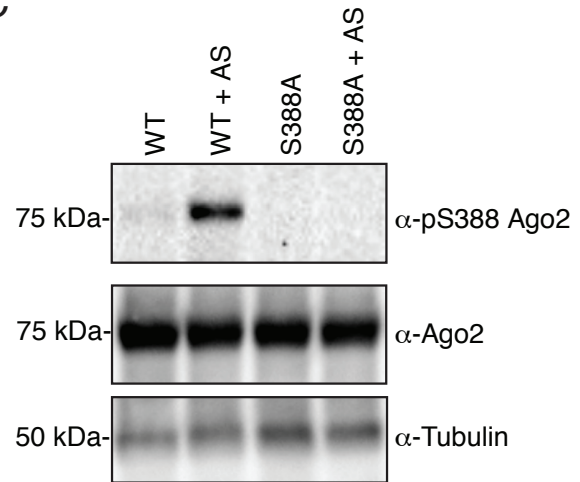
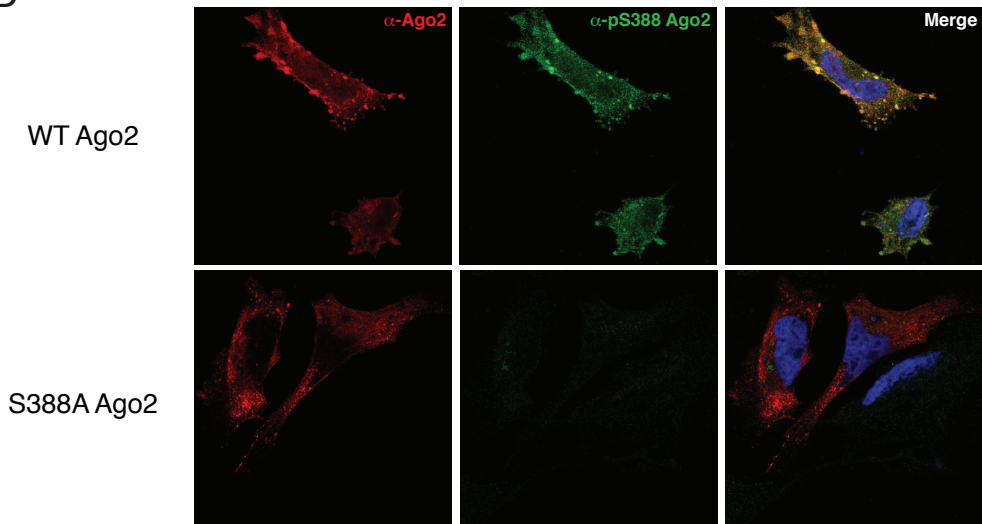
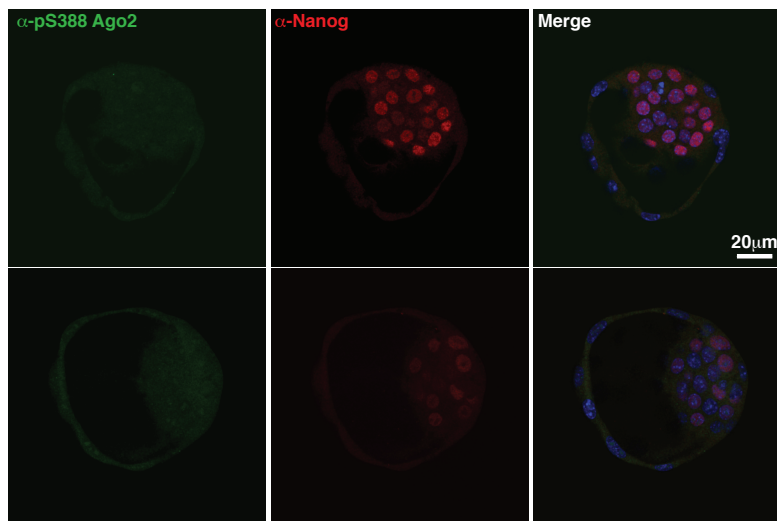
AResidues 382-393: KLMRSAS**F**NNTDP**B****C****D****E**

Figure 18. No differences in phosphorylation levels of Ago2 S388 between 129S2 and C57Bl/6N at blastocyst stage.

(A) The sequence of the peptide encompassing residue 382-393 of murine Ago2 protein used for the development of the phospho-specific S388 antibody is shown. The phosphorylated serine 388 is highlighted in red. (B) Western blot using a synthetic myc-tagged L2 linker domain containing a serine 388 (WT) or S388A mutation from murine Ago2 and probed with a phospho-specific S388 and an anti-myc antibodies. The WT and S388A linker domain was incubated overnight with MK2 to induce the phosphorylation of serine 388 where indicated. (C) Western blot analysis of protein lysates from HEK293T cells transfected with wild type or S388A mutant mouse Ago2, untreated or treated with 250 μ M sodium arsenite (As) for 90 minutes. The samples were assayed with S388 phospho-specific and an anti-Ago2 antibodies. Tubulin was used as loading control. (D) Immunofluorescence analysis of Ago2 localization in HeLa cells transfected with murine wild type and S388A mutant Ago2 protein treated with 250 μ M sodium arsenite for 90 minutes. A phospho-specific S388 (green) and an anti-Ago2 (red) antibodies were used. (E) Immunofluorescence staining of two blastocysts isolated at E3.5 derived from 129S2 wild type matings. An anti-pS388 phospho-specific antibody and an anti-Nanog antibody were used to detect the phosphorylated Ago2 protein in embryos. Nuclei are stained with DAPI. Bar = 20 μ m. The data presented in this figure were made in collaboration with Maria Placentino.

3.2 Discussion

3.2.1 Ago2 S388 phosphorylation and hematopoietic development

Hematopoietic development is a hierarchical system in which terminally differentiated cells, such as white blood cells and erythrocytes, derive from the mitotic division of a hematopoietic stem cell (Goldsby, 2003). Hematopoietic stem cells divide asymmetrically to give rise to a daughter cell, which retain the ability to self-renew, and a second daughter cell that is instead committed for differentiation. Several progenitors have been identified in the past, with a lineage potential that becomes restricted during the differentiation process (Goldsby, 2003). miRNAs have been discovered to play essential roles during hematopoietic development (Chen, 2004b; Li, 2007; Xiao, 2007; Johnnidis, 2008; Ventura, 2008; Xiao, 2008; Rasmussen, 2010; Sangokoya, 2010; Yu, 2010). For example, genetic ablation of miR-223 triggers an increase in granulocytes number, which in turn lead to an aggressive inflammatory response after endotoxic stimuli (Johnnidis, 2008). In addition, miR-150 and miR-17-92 clusters have been implicated in B cell progenitor differentiation (Xiao, 2007; Ventura, 2008; Xiao, 2008). Furthermore, miR-181a expression is instrumental for B and T cell lineage decisions as well as well to modulate T cell response (Chen, 2004b; Li, 2007). Finally, miR-451 is necessary for the differentiation of erythroid progenitors (Rasmussen, 2010; Sangokoya, 2010; Yu, 2010).

Global reduction of miRNA pathway functionality through ablation of the biogenetic factor Dicer or the effector factor Ago2 augmented the number of hematopoietic processes that are under miRNA regulation. Since Dicer and Ago2 conventional knockout mice are lethal (Bernstein, 2003; Liu, 2004; Alisch, 2007; Morita, 2007), combination of conditional alleles with several hematopoietic-specific recombinase carriers were employed to characterize their role in different hematopoietic lineages (Cobb, 2005; Muljo, 2005; Cobb, 2006; O'Carroll, 2007; Koralov, 2008; Belver, 2010; Xu, 2011; Alemdehy, 2012; Buza-Vidas, 2012). Indeed, Dicer ablation during T cell development causes several defects, such as reduction of T cell progenitors, cytotoxic

and regulatory T cells, as well as biased CD4 T cell differentiation (Cobb, 2005; Muljo, 2005; Cobb, 2006). In addition, B cells development is severely blocked at the pro-B-to-pre-B transition stage when Dicer is ablated in B cell progenitors (Koralov, 2008). Furthermore, Dicer inactivation in early hematopoietic progenitors and granulocyte-macrophage progenitors reduces erythroid and myeloid differentiation, respectively (Alemdehy, 2012; Buza-Vidas, 2012).

Ago2 deletion in hematopoietic stem cells results in the impairment of erythroid and B-cell development (O'Carroll, 2007). Bone marrow transplantations demonstrated that these defects are cell-autonomous and do not depend upon Ago2 inactivation in other tissues. In particular, a partial arrest of B cell development was seen at the pro-B-to-pre-B transition, similarly to Dicer inactivation (O'Carroll, 2007; Koralov, 2008). Furthermore, animals transplanted with *Ago2*^{-/-} cells present a severe anaemia with reduced red blood cell and haematocrit values in peripheral blood and splenomegaly. This is due to a defective erythroid differentiation: orthochromatophilic erythroblasts are reduced, while early basophilic erythroblasts are increased in numbers (O'Carroll, 2007). The red blood cell defect is in part ascribed to the loss of miR-451, which biogenesis has been shown to depend on Ago2 endonuclease activity (Cheloufi, 2010; Cifuentes, 2010; Rasmussen, 2010; Yang, 2010). Given the possibility that phosphorylation at serine 388 regulates Ago2 endonuclease activity (Horman, 2013), I aimed to uncover the importance of this modification during hematopoiesis. Furthermore, analysis of protein phosphorylation by mass spectrometry from several mouse tissues discovered very low amount of Ago2 phosphorylation at serine 388 in spleen, suggesting a role in this primary lymphoid organ (Huttlin, 2010). A strategy using a conditional *Ago2*^{FL} and a nonphosphorylatable *Ago2*^{S388A} alleles in combination with an inducible *MxCre* recombinase allowed us to induce the expression of only a mutant Ago2 protein in hematopoietic cells (Fig. 8A-B). Analysis of peripheral blood parameters in mice after Cre induction failed to detect any signs of anaemia or splenomegaly (Fig. 8C). Analysis of erythroid and B cell development by flow cytometry did not reveal any impairment in progenitor differentiation in these two lineages (Fig. 8D-E). Similar results were achieved after bone marrow transplantation of *Ago2*^{S388A/-}; *MxCre* cells in wild type recipients, demonstrating that S388

phosphorylation does not affect Ago2 function in a cell-autonomous manner (Fig. 9-10). Previous results are further reinforced by the absence of any hematopoietic defects in homozygous mutant mice in a defined C57Bl/6N genetic background (Fig. 13). As such, the data presented prove that lack of S388 phosphorylation has no impact on Ago2 functionality in the hematopoietic system. This is suggestive that Ago2 phosphomutant protein is capable to execute miRNA-dependent silencing as well as contribute to miR-451 maturation through its slicing activity. However, a recent report showed that Ago2 phosphomutant protein presents a lower miRNA-dependent silencing activity compared to wild type (Horman, 2013). In addition, phosphomutant protein displays a reduced localization to P-bodies, sites where miRNA silencing is believed to take place (Anderson, 2006; Zeng, 2008; Horman, 2013). Differences between the data presented in here and in the mentioned works could be ascribed to the expression levels and on the particular cellular system used, since Ago2 variants were overexpressed in HeLa and H1299 cell lines (Zeng, 2008; Horman, 2013). In addition, the use of luciferase construct with binding sites for an endogenous miRNA showed no differences in the activity between wild type and Ago2 mutant (Horman, 2013). The analysis of the lack of Ago2 phosphorylation from the endogenous Ago2 locus during developmental processes possesses a much greater physiological meaning compared to the aforementioned studies. As such, it is likely that Ago2 phosphorylation does not affect miRNA activity per se in unperturbed conditions, as suggested by the data presented in this thesis.

3.2.2 Ago2 S388 phosphorylation significance during oocyte maturation

The meiotic process consists of two successive cell divisions with only one replication of the genome for the generation of haploid cells. In mammals, oocyte development starts prenatally, but it stops at the end of prophase I of the first meiotic division. After the pubertal period, hormones stimulate the entry of resting oocytes into the second meiotic division (Solter, 2004). Strikingly, transcription is blocked from early oocyte stages, referred to as growing oocytes, up to the mid-S phase in the 1-cell zygote (Solter, 2004). As such, the entire meiotic process as well as the first mitotic division of the embryo relies on the mRNA transcripts stored in the female egg (Solter, 2004). MiRNA

silencing represents a likely candidate to regulate post-transcriptionally the genetic program in maturing oocytes. In fact, in zebrafish maternally derived miR-430 is necessary for clearance of maternal transcripts and proper embryonic formation (Giraldez, 2005; Giraldez, 2006).

Expression studies in growing and fully mature oocytes demonstrated that various classes of miRNAs are highly expressed in murine female germ cells, and 1-cell zygotes inherited a miRNA pool from the egg cell (Watanabe, 2006; Murchison, 2007; Tang, 2007; Tam, 2008; Watanabe, 2008). In addition, deep sequencing of small RNA libraries derived from fully grown oocytes blocked at prophase I of the meiotic division showed that other RNA classes are expressed in these cells (Watanabe, 2006; Tam, 2008; Watanabe, 2008). Aside from a small fraction of piRNAs, endogenous siRNAs (endo-siRNAs) are derived from naturally occurring dsRNA molecules. Transcripts derived from pseudogenes can form complex secondary structures, which can be recognized and cut by Dicer (Watanabe, 2008). In addition, dsRNA can be formed by transcription of overlapping genes oriented in opposite direction, or by the annealing of coding genes transcripts with complementary regions in pseudogenes (Tam, 2008; Watanabe, 2008). However, the majority of endo-siRNAs are derived from retrotransposons, suggesting a role in the silencing of these genetic elements (Watanabe, 2006; Tam, 2008; Watanabe, 2008). In fact, conditional deletion of Dicer in growing oocytes by the use of the specific Zp3-Cre transgene (de Vries, 2000) renders female animals sterile: oocyte development is blocked at the level of metaphase I due to spindle arrangement and chromosomal defects (Murchison, 2007; Tang, 2007). Furthermore, RNA levels of some transposable elements, like mouse transcript (MT) and short interspersed repetitive sequence (SINE), are increased upon Dicer ablation (Murchison, 2007; Tang, 2008; Watanabe, 2008). Consistent with the notion that Ago2 is the only Ago-like protein with endonuclease activity in mammals (Liu, 2004; Meister, 2004; Song, 2004), loss of Ago2 in growing oocytes resulted in a similar phenotype of Dicer ablation (Kaneda, 2009). Indeed, female mice are infertile, and oocytes are blocked at metaphase II of the second meiotic division (Kaneda, 2009).

Even though miRNA are abundantly expressed in mouse oocytes, search for short sequences on the 3' UTR of upregulated genes on Dicer-deficient cells and Ago2-

deficient cells did not reveal any significant miRNA seeds (Murchison, 2007; Tang, 2007; Ma, 2010; Suh, 2010). Strikingly, a clear enrichment for endo-siRNA motifs on the 3' UTR of upregulated transcripts was recognized, suggesting that these molecules are fundamental for oocyte maturation (Ma, 2010; Suh, 2010). To prove this hypothesis, luciferase reporter assays were employed to verify miRNA- and endo-siRNA-mediated silencing (Ma, 2010). A reporter containing one perfectly complementary site for an endogenous miRNA on its 3' UTR was silenced all along oocyte maturation stages, with a comparable decrease of both mRNA and protein levels. A reporter with several bulged sites for endogenous miRNAs instead had almost complete abolition in silencing activity in mature oocytes compared to growing oocytes: this action is dependent mainly on translational inhibition (Ma, 2010). In addition, P-bodies, which are sites of mRNA degradation, are not present during oocyte maturation (Anderson, 2006; Flemr, 2010). Further supporting data were obtained from the analysis of Drosha conditional ablation in growing oocytes (Suh, 2010). Indeed, loss of the Microprocessor component DGCR8 does not impact on egg maturation: *DGCR8^{FL}; Zp3-Cre* females are fertile (Suh, 2010). In addition, no abnormal spindle assembly nor gene expression perturbation were detected upon DGCR8 deletion in mature oocytes, even though canonical miRNA levels were greatly reduced (Suh, 2010). Since the Microprocessor is involved in the biogenesis of the major part of miRNAs but not in siRNA production, the absence of any phenotype in DGCR8 conditional mice points to the fact that endo-siRNAs are important for oocyte development, while miRNA contribution is negligible.

Since both mature miRNAs and endo-siRNAs are detectable in mature oocytes (Watanabe, 2006; Murchison, 2007; Tang, 2007; Tang, 2008; Watanabe, 2008), why are miRNAs not participating to gene expression regulation? Two possible answers could be proposed: the presence of other RNA binding proteins that mask the 3' UTR to miRNA-loaded RISC complex; differential regulation of miRNA and siRNA activity at level of RISC function. It has been shown that RNA binding proteins can relieve miRNA-mediated silencing for a subset of miRNAs (Bhattacharyya, 2006; Kedde, 2007; Takeda, 2009). However, this masking activity should prevent miRNA-binding at a global level. It is more plausible that a modification of one of the RISC components is accountable for the differential activity of miRNA and endo-siRNA pools. Ago2 meets this criterion:

it is the only Ago-like protein in mammals with a functional endonuclease activity and its loss impairs oocyte development (Liu, 2004; Meister, 2004; Song, 2004; Kaneda, 2009). I then investigated if phosphorylation on serine 388 is necessary for the endo-siRNA pathway during female oogenesis. I employed a conditional strategy in which, upon Zp3-Cre activation in growing oocyte, Ago2 activity derives exclusively from the phosphomutant allele (Fig. 11A). Experimental females presented a fertility and fecundity rate similar to control littermates (Fig. 11B). Except for 1 case out of 63 pups examined, recombination was successfully achieved *in vivo* (Fig. 11C). In addition, analysis of *Ago2*^{S388A/S388A} homozygous females in a C57Bl/6N genetic background confirmed the absence of any issue with female fertility (Fig. 12B). As such, the data collectively prove that serine 388 phosphorylation is dispensable for oocyte development. Furthermore, the nonphosphorylatable Ago2 protein is shown to efficiently perform siRNA-mediated regulation of gene expression during oocyte development. As such, it is unlikely that modification of serine 388 represents a way to control Ago2 activity between miRNA and siRNA pathways in female egg maturation. Other modifications of the Ago2 protein or of the RISC complex can then be responsible for the differential regulation of miRNAs and siRNAs in this cellular system.

3.2.3 Ago2 S388 phosphorylation in embryonic development: a background-dependent effect

3.2.3.1 Lack of Ago2 phosphorylation at serine 388 causes embryonic defects at the peri-implantation stage

Embryogenesis is a complex developmental process that consists in the formation of all tissues and structures starting from a fertilized egg, the zygote. In mammals this process takes place in the uterus of the mother. In mice, the entire gestation period is around ~19 days. The zygote first divides symmetrically for 3 times to form an 8-cell embryo, which is then compacted, becoming morula at embryonic day E2.5. The blastocyst is formed at E3.5 through proliferation and reorganization of the blastomeres: the outer cells will form the trophoectoderm, a monolayer of cells located beside the zona pellucida; the

inner cells instead will give rise to the inner cell mass (ICM). A cavity, called blastocoele, is present at the centre of the blastocyst. The blastocyst implants onto the uterine wall around embryonic day E4.5: the zona pellucida, a membrane derived from the oocyte that physically protected the embryo during early stages, breaks down, allowing the attachment to the uterus. At E6.5, gastrulation process begins through the formation of the primitive streak from the posterior side of the embryo: this process will give rise to all three germ layers. At mid-gestation (E9.5) the whole body plan and body axes are defined. Organogenesis continues throughout the remaining gestation, and some tissues proceed their maturation even after birth (Nagy, 2003).

During embryonic development, several differentiation and migration processes require a tightly regulated genetic program. MiRNAs have been recently appreciated to be part of such complex networks: germline loss of single miRNAs or miRNA clusters can lead to embryonic lethality (Zhao, 2007; Kuhnert, 2008; Liu, 2008; Ventura, 2008; Wang, 2008; Medeiros, 2011). The physiological relevance of overall miRNA activity was further investigated by the deletion of specific miRNA biogenetic factors in mice (Bernstein, 2003; Harfe, 2005; Yang, 2005; Wang, 2007; Suh, 2010). Indeed, deletion of the Droscha cofactor DGCR8 causes malformations of homozygous mutants at embryonic day E6.5 (Wang, 2007; Suh, 2010). No defects in DGCR8-deficient embryos were detected at blastocyst level, suggesting a role for miRNAs at the peri-implantation stage (Suh, 2010). On the other hand, germline ablation of Dicer induces a more severe phenotypic outcome (Bernstein, 2003; Harfe, 2005). About half of Dicer-null embryos are lost before embryonic day E7.5; the surviving embryos are smaller and display a very low expression of Oct4 and Brachyury transcripts compared to wild type embryos (Bernstein, 2003). On the other hand, a hypomorphic Dicer allele was created by the insertion of a neomycin resistant cassette at the beginning of the gene, replacing exon 1 and 2 (Yang, 2005). Transcripts are produced from exon 3 of the Dicer locus in this hypomorphic allele, producing a shorter protein, which is only partially functional. Mice homozygous for this Dicer allele die around embryonic day E12.5-E14.5 due to angiogenic defects in both the embryo and the yolk sac (Yang, 2005).

Loss of RISC key components should present a similar phenotypic outcome of DGCR8 and Dicer germline depletion in embryonic development. Ablation of Ago1, Ago3 and

Ago4 does not impair embryogenesis, since mice are viable (O'Carroll, 2007; Modzelewski, 2012; Van Stry, 2012). On the other hand, three independent studies have shown that Ago2 is essential for embryonic development (Liu, 2004; Alisch, 2007; Morita, 2007). The first Ago2 null allele was created by the introduction of a puromycin selection cassette and the duplication of exons 3 to 6 of the Ago2 gene (Liu, 2004). Homozygous mutant mice present an abnormal morphology at embryonic day E9.5, with heart swelling and several neural tube defects (Liu, 2004). In addition, Ago2-deficient embryos are smaller compared to wild type littermates, suggesting the presence of placental deficiency (Liu, 2004). Subsequently, a second Ago2 knockout allele was created by the insertion of a gene trap cassette between exon 12 and 13 of the mouse locus: the presence of a splice acceptor site at the 5' end and of a strong polyadenylation signal at the 3' end of the inserted cassette impedes the production of the Ago2 protein (Alisch, 2007). This study revealed a more severe phenotype compared to the work of Liu *et al.* In fact, only a small fraction of Ago2-deficient embryos are present at E9.5, displaying similar neural and placental defects; the major part of these embryos instead dies after E7.5 (Alisch, 2007). At E7.5, homozygous embryos are smaller and present an expanded expression profile for Brachyury and other markers of the primitive streak. These data pointed to a second function of Ago2 in the control of mesodermal genes during gastrulation (Alisch, 2007). A third work from Morita *et al.* created a mutant Ago2 allele by insertion of a gene-trap cassette after exon 1 of the Ago2 gene (Morita, 2007). At E7.5, Ago2 knockout embryos were smaller compared to wild type littermates: *in situ* hybridization data revealed no differences in the expression of Oct4, a marker of epiblast cells, but a reduction and mislocalization of the Brachyury expression (Morita, 2007). In addition, Ago2-deficient embryos presented an abnormal morphology already at embryonic day E5.5 (Morita, 2007). Taken together, the aforementioned studies demonstrated that Ago2 is essential for embryonic development, but there are some important differences that need to be noted. In fact, in the work of Liu *et al.* Ago2-deficient embryos die later than in the following studies (Liu, 2004; Alisch, 2007; Morita, 2007). This could be ascribed to the fact that the Ago2 null allele created is instead a hypomorphic one. In fact, the entire Ago2 coding capacity still exists in the locus: no messenger RNA for Ago2 was detected from homozygous embryos and cell

lines by RT-PCR, but Ago2 protein levels were never assessed (Liu, 2004). On the other hand, there is a clear disagreement about Brachyury expression patterns upon Ago2 loss in embryos at E7.5 between the study from Alisch *et al.* and Morita *et al.* (Alisch, 2007; Morita, 2007). Even if the two Ago2 alleles were employed on two different genetic backgrounds, these opposing data might derive from the use of different antisense probes for the Brachyury transcript (Alisch, 2007; Morita, 2007).

I sought to determine if phosphorylation at serine 388 is necessary for Ago2 function during embryonic development. Homozygous phosphomutant embryos are partially lethal in two different genetic backgrounds (Fig. 7 and Fig. 16). In a mixed 129P2xC57Bl/6N6N genetic background, phospho-deficient homozygotes present an abnormal morphology at E6.5: they are smaller compared to wild type and heterozygous littermates, with a reduced extraembryonic part (Fig. 7C). Conversely, in a defined 129S2 genetic background, no morphologically malformed embryos were isolated at E7.5, but a number of empty decidua close to the expected mendelian ratios for homozygous mutants was collected (Fig. 16B). Collection of blastocysts at E3.5 does not reveal any difference in the morphology nor in the localization of the Ago2 protein between wild type and phospho-deficient animals (Fig. 16C). As such, in both genetic backgrounds, Ago2 phosphorylation is necessary during peri-implantation. The phenotype described for Ago2 phosphomutant displays similarity with the arrest of development in DGCR8- and Dicer-null embryos (Bernstein, 2003; Harfe, 2005; Wang, 2006; Suh, 2010). In addition, the phospho-deficient embryos isolated at E6.5 in a mixed genetic background show similar morphological features as Ago2-deficient embryos from Alisch *et al.* and Morita *et al.* (Alisch, 2007; Morita, 2007). It is important to note that in a defined 129S2 genetic background, lack of Ago2 phosphorylation triggers a more severe phenotype, since I found a significant percentage of empty decidua as early as E7.5. Alisch *et al.* backcrossed for 10 generation the Ago2-null allele into C57Bl/6 mice, while Morita *et al.* used a mixed 129xC57Bl6 genetic background similar to the first set of experiments presented here (Alisch, 2007; Morita, 2007). As such, this study is readily comparable to the one from Morita *et al.*: Ago2-null and phospho-deficient embryos present similar morphological defects, suggesting that serine 388 phosphorylation is critical for Ago2 function at the peri-implantation stage (Morita,

2007). However, lack of serine 388 phosphorylation does not simply phenocopy Ago2 loss by inactivating the protein. In fact, the phosphomutant allele is able to sustain normal hematopoietic and oocyte development in a mixed 129P2xC57Bl/6N genetic background (Fig. 8-11). Furthermore, in a C57Bl/6N genetic background, phosphomutant homozygotes are viable, fertile and present no haematological pathology (Fig. 12-14). Finally, phosphomutant animals that survive to adulthood do not show any gross morphological abnormalities. It is conceivable that serine 388 phosphorylation is fundamental for Ago2 function at a specific time point during early embryonic development, but it is dispensable in later developmental stages. Fluctuation in environmental stimuli or in gene expression might help to overcome the requirement for serine 388 phosphorylation at this early embryonic stage. Conversely, one or more genetic determinants might be responsible for the different phenotypic outcome in 129S2 and C57Bl/6N genetic backgrounds.

3.2.3.2 Mutation of Ago2 serine 388 reveals the importance of genetic background on the phenotypic consequences of post-translational modification site mutations

Functional studies on the gene function are accessible in mice thanks to the possibility to specifically target embryonic stem cells to ablate or modify almost any locus of interest. Nonetheless, mouse genetics first began with the selection of numerous diverse mouse strains accordingly to specific physiological characteristic. In particular, generation of inbred mouse strains contributed enormously to genetic studies in the mouse model. An inbred mouse strain is created by brother-sister mating for at least 20 generations: this allows to have approximately 98.6% of all loci in homozygosity. Different strains are indeed more amenable for particular studies: C57Bl/6 animals are used for studies on substance preferences, while BALB/c and C3H mice are employed for ethyl nitrosurea mutagenesis programs due to their sensitivity to this compound. In addition, 129 inbred strain is widely used for the production of targeted ESC clones since several ESC lines are available. However, recent works revealed an extensive variability in 129 substrains (Simpson, 1997; Threadgill, 1997). As a consequence, a revised nomenclature for 129 substrains was defined: Parental (129P1-3), substrains were derived from the original

129 colony; Steel (129S1-8) substrains originated from an outcross with the C3H strain and harbor a mutation in the *c-Kit* gene; Ter (129T1-2) substrains were created by a mating with a hybrid WCxC57Bl/6 line and are susceptible to teratoma formation due to a mutation in the *Ter* gene; genetically-contaminated X strain (129X1) which harbors several unique polymorphic loci (Simpson, 1997; Festing, 1999).

The genomic heterogeneity present in the 129 substrains from which ESC lines have been derived is not the only source of variability in the analysis of loss of function mice. In fact, inbred mouse strains do not only harbor in homozygosity allelic variants that make them suitable for specific physiological studies, but also other variants that can interfere with the phenotypic outcome of any targeted gene loss. This is a well-known effect and is referred to as genetic background effect (reviewed in Gerlai, 1996; Wolfer, 2002). Several examples have been reported in the literature about the influence of modifier alleles on gene-specific loss of function analysis (Shull, 1992; Kulkarni, 1993; Veis, 1993; Dickson, 1995; Sibilia, 1995; Threadgill, 1995; Bonyadi, 1997; Casademunt, 1999; Kallapur, 1999; LeCouter, 1998a-b; Benzel, 2001; Bilovocky, 2003; Strunk, 2004; Lin, 2012). For example, germline deletion of epidermal growth factor receptor (EGFR) causes embryonic or postnatal lethality depending on the genetic background (Sibilia, 1995; Threadgill, 1995; Strunk, 2004). In fact, three distinguished phenotypes have been described for EGFR-null animals: peri-implantation lethality, due to ICM proliferation defects; growth arrest at E11.5-12.5 because of abnormalities in the placental spongiotrophoblast and labyrinthine layers; postnatal lethality before PND 20 thanks to severe developmental defects in various organs (Sibilia, 1995; Threadgill, 1995). A mixed genetic background of 129xCF-1 and 129xFVB/N inbred strains favour embryonic lethality at early implantation stages in EGFR-deficient embryos. On the other hand, congenic 129 mice and mixed 129xC57Bl/6 EGFR homozygous mutants die at mid-gestation, while crosses with outbred MF-1 or the inbred ALS/Ltj strains allow survival up to term (Sibilia, 1995; Threadgill, 1995; Strunk, 2004). A similar genetic background effect has been described for loss of TGF β 1 protein (Shull, 1992; Kulkarni, 1993; Dickson, 1995; Bonyadi, 1997; Kallapur, 1999). 50% of *TGF β 1*^{-/-} animals and 25% of *TGF β 1*^{+/-} die around E11.5 in mixed 129xC57Bl/6J genetic background due to defects in vasculogenesis and erythroid development in the yolk sac. Surviving TGF β 1-

null embryos die before PND 20 from an aggressive inflammatory disease (Shull, 1992; Kulkarni, 1993; Dickson, 1995). However, most of the mice in a 129S2xC57Bl/6J mixed and prevalent C57Bl/6J genetic background stop to develop before E7.5, and present defects in morula formation (Bonyadi, 1997; Kallapur, 1999). Furthermore, upon mating for 4 generations with NIH-Ola inbred animals, more than 80% of the expected TGF β 1-deficient mice survive up to birth (Bonyadi, 1997). Genomic analysis of polymorphic markers from F₂ C57Bl/6JxNIH-Ola pups revealed the association of a region at chromosome 5 with the ability to survive to birth (Bonyadi, 1997).

EGF- and TGF β 1-deletion interests numerous developmental processes during embryogenesis, and the employment of several inbred mouse strains shed light to possible modifier alleles (Bonyadi, 1997; Strunk, 2004). On the other hand, a differential phenotype between two mouse strains could involve only one specific developmental process. In fact, deletion of NRIF, a cytoplasmic interactor of the neurotrophic receptor, leads to embryonic lethality in a C57Bl/6J genetic background, while mice are viable in both mixed 129S2xC57Bl/6J and 129S2 genetic backgrounds (Casademunt, 1999; Benzel, 2001). In addition, germline loss of ARIH2, an E3 ubiquitin ligase, causes the death of mutant mice in a pure C57Bl/6 genetic background due to defects in fetal liver functionality (Lin, 2012). Conversely, in a mixed 129P2xC57Bl/6 genetic background ARIH2 homozygous null animals were born at the expected mendelian ratios (Lin, 2012). The presence of a milder phenotype in mixed genetic backgrounds is generally ascribed to a phenomenon called “hybrid vigour”. Indeed, the presence of genetic variants from two different inbred strains complement for the deleterious alleles that both strains harbor in homozygosity. Nonetheless, exceptions to this general principle exist. For example, germline deletion of the Engrailed 1, which is important for the establishment of midbrain/hindbrain region in the developing brain, causes perinatal lethality due to loss of cerebellum in 129 and 129xC57Bl/6J mixed genetic backgrounds, but not in a C57Bl/6J genetic background (Bilovocky, 2003).

Since genetic background can strongly affect the outcome of targeted mutations, the Banbury Conference on Genetic Background in Mice proposed simple recommendations on the breeding and maintenance strategy for newly targeted mice. They proposed to maintain the targeted mutation in two different mouse strains, creating two congenic

lines by several backcrosses. They suggested to employ 129 and C57Bl/6 mouse strains since 129-derived ESC lines are widely used for gene targeting and C57Bl/6 is a commonly used inbred strain (Mice, 1997). Phenotypic analysis of gene knockout in both congenic lines might reveal the presence of genetic background effects. In this breeding strategy I followed these recommendations (Fig. 6). A 129P2-derived ESC line, IB10 (Robanus-Maandag, 1998), was used to create an *Ago2*^{S388A} nonphosphorylatable allele in the endogenous *Ago2* locus, and I mated chimeric mice with C57Bl/6N animals to first induce the recombination of the neomycin resistance cassette and second to segregate away the Cre transgene. I then established two congenic mouse lines by backcrossing heterozygous phosphomutants with 129S2 and C57Bl/6N strains for at least 8 generations. I showed that *Ago2* phosphomutant animals are prevalently lethal at peri-implantation stage in mixed 129P2xC57Bl/6N and 129S2, but not C57Bl/6N, genetic backgrounds (Fig. 7, 12 and 16). These data strongly support the presence of allelic variants that are able to mask the lack of *Ago2* serine 388 phosphorylation during early development in the C57Bl/6N strain. Surprisingly, only a partial hybrid vigour effect was visible in a mixed 129P2xC57Bl/6N background compared to a defined 129S2 genetic background, since abnormal *Ago2*^{S388A/S388A} embryos could be readily isolated at E7.5. I investigated this phenomenon by mating heterozygous mutants in a C57Bl/6N background with wild type 129S2 animals in order to create a “reverse F₁” (RF₁) generation (Fig. 17) (Wolfer, 2002). This strategy allowed us to evaluate the effects of genes flanking the *Ago2* locus on *Ago2*^{S388A/S388A} survival. These data demonstrate that no embryonic lethality is present upon RF₁ intercrosses for homozygous mutants, pointing to the presence of one or more modifying alleles that are in close proximity to the *Ago2* locus. However, this genetic strategy does not permit to identify precisely which area of mouse chromosome 15 near to the *Ago2* gene is modifying homozygous mutant phenotype. A combination of genome sequencing and breeding with other inbred strains could be useful to get insights on the modifier alleles. The effect of genetic background on genetic studies using loss-of-function alleles has been widely described in the past years (reviewed in Gerlai, 1996; Wolfer, 2002). The data presented here represent the first example of a background effect onto a post-translational modification site. Secondly, lack of phosphorylation of serine 388 does not

impair the functionality of the Ago2 protein since phosphomutant homozygotes are viable in a C57Bl/6N genetic background. In addition, *Ago2*^{S388A} allele is able to sustain hematopoietic and oocyte development in both mixed 129P2xC57Bl6N and C57Bl/6N backgrounds. This work is of broad interest, since it establishes for the first time the presence of genetic interaction between a post-translational modification site and other genomic variants in the mouse genome. This is of fundamental importance for studies of complex human diseases. In the past decade, the onset of genome-wide association studies (GWAS) initiated to investigate the genetic bases of human diseases derived from complex traits. Previously, linkage analysis was used to identify causative genetic mutations for human traits by the analysis of the co-segregation of the putative gene with the phenotype. With the availability of a high quality reference genome and advanced sequencing techniques, GWAS analyse the correlation of millions of polymorphic markers in the genome between large cohorts of control individuals and individuals with the phenotype of interest (reviewed in Stranger, 2011). Collaborative projects such as International HapMap Consortium and the 1000 Genomes Project were created to identify and catalogue single nucleotide polymorphisms (SNPs) and copy number variants (CNVs) and group them in single haplotypes (International HapMap Consortium, 2003; Genomes Project Consortium, 2010). As such, GWAS are able to map hypothetical causative variants to narrow regions of the genome. However, the polymorphic markers that associate with the trait study unlikely represent the causative genetic variants of the phenotypic trait (Graham, 2007; Dideberg, 2007; Yeager, 2007; Musunuru, 2010; Teslovich, 2010). They instead help to define the haplotype that harbors the causative variant. The genomic region is further analysed for the presence of annotated genes and sequenced for the identification of possible functional variants (Graham, 2007; Dideberg, 2007; Musunuru, 2010; Teslovich, 2010). In this context, this study points to the importance of the analysis of allelic variants that alter post-translational modification sites. In addition, it posits the possibility of epistatic relationships with other genomic regions, which may or not have been associated to a specific trait of interest in the same GWAS. In conclusion, the data presented in this thesis have important implications for the interpretation of genetic variation of post-translational modification sites in relation to genotype-phenotype association studies.

3.2.3.3 Embryonic lethality of Ago2 S388A mutants points to other kinases involved in Ago2 phosphorylation

Ago2 phosphorylation at serine 387 was first discovered in human cell lines under homeostatic conditions (Zeng, 2008; Horman, 2013). The phosphorylation levels are increased upon cellular stress, and treatment of cells with the p38-MAPK inhibitor SB203580 reduced stress-induced phosphorylation (Zeng, 2008). *In vitro* kinase assays revealed that the MK2 kinase downstream of p38 MAPK is responsible for Ago2 phosphorylation at human serine 387 (Zeng, 2008). A more recent study used a combination of RNAi silencing and biochemical assays to show that PKB/Akt protein kinases are also able to phosphorylates Ago2 (Horman, 2013).

The p38-MAPK pathway is activated upon several stress stimuli, ranging from UV irradiation, bacterial endotoxins and genotoxic stress (Rouse, 1994; Freshney, 1994; Manke, 2007; reviewed in Ono, 2000). To date, 4 isoforms of the p38 kinase (p38 α / β / γ / δ) are encoded in the mammalian cells from four separate loci (Ono, 2000). p38 activity is stimulated by external and cellular stimuli through phosphorylation of key amino acid residues by the upstream MAP kinase kinase MKK3/6 (Xia, 1995; Raingeaud, 1996; Ono, 2000). Upon activation, the p38 kinase amplifies the signaling cascade through phosphorylation of downstream kinases and it regulates gene expression and translational activity through phosphorylation of transcription and initiation factors (Raingeaud, 1996; Wang, 1998; Ono, 2000). Among the downstream kinases, p38 is known to activate the MAPKAPK protein family, which consists of three members (MK2, MK3 and MK5) (Stokoe, 1992; Sithanandam, 1996; New, 1998; reviewed in Gaestel, 2006). MK2 and MK3 associates with p38 α / β isoforms and are activated exclusively by these two isoforms (Clifton, 1996; Ben-Levy, 1998; Allen, 2000). After p38 α / β activation, the associated MK2 is phosphorylated and a nuclear export signal is uncovered, mediating the cytoplasmic export of the entire complex (Ben-Levy, 1998). The physiological relevance of the upstream p38 isoforms and of the three downstream MK proteins was investigated with the use of loss-of-function alleles. Germline deletion of the p38 α isoform causes embryonic lethality at embryonic day E10.5 due to placental defects; some homozygous embryos survive up to E16.5, but die

later due to anaemia (Mudgett, 2000; Tamura, 2000). Surprisingly, single p38 $\beta/\gamma/\delta$ and double p38 γ/δ mouse knockouts are viable and fertile (Beardmore, 2005; Sabio, 2005). Similarly, deletion of MK2, MK3 and MK5 alone or MK2/3 double ablation do not affect embryonic development in mice (Kotlyarov, 1999; Shi, 2003; Ronkina, 2007). These results are in evident contrast with the phenotype described here for Ago2 phosphomutant embryos in a mixed 129P2xC57Bl/6N and 129S2 defined background (Fig. 7 and 16). MK2 and MK3 single as well as double knockout animals were first analysed in a 129xC57Bl/6 genetic background (Kotlyarov, 1999; Ronkina, 2007). Furthermore, germline depletion of p38 α gives similar phenotypic results in F₂ generations derived from matings of original 129 chimeric animals with 4 different mouse strains (Mudgett, 2000; Tamura, 2000). It is conceivable that Ago2 phosphorylation during peri-implantation might not be dependent only upon MK2 activity. Alternatively, compensatory mechanisms masking the lack of Ago2 phosphorylation can derive by the broad effectors that the p38-MK2 axis regulates.

p38 MAPK has been shown to be important in hematopoietic stem cell maintenance as well as erythroid and myeloid differentiation (Tamura, 2000; Kirito, 2003; Ito, 2006; reviewed in Geest, 2009). Furthermore, ablation of MK2 in stem cells reduces HSC numbers and ability to reconstitute lethally irradiated recipients (Schwermann, 2009). In addition, both MK2 and MK3 participate in the production of pro-inflammatory cytokines upon endotoxic stress. Ablation of MK2 alone or in combination with MK3 reduces the levels of inflammatory cytokines like tumour necrosis factor α (TNF- α) and interleukin 6 (IL-6), rendering homozygous mice more resistant to lethal doses of LPS (Kotlyarov, 1999; Ronkina, 2007). I first verified if Ago2 phosphomutant mice present any impairment in hematopoietic development in homeostatic conditions. The data included here show that both in a mixed 129P2xC57Bl/6N and C57Bl/6N genetic backgrounds lack of serine 388 phosphorylation does not impair HSC numbers nor differentiation (Fig 8-10 and 13). In addition, I tested if mutation on serine 388 confers resistance to lethal doses of LPS endotoxin as described for MK2 ablation (Kotlyarov, 1999). I demonstrated that the absence of phosphorylation does not influence the sensitivity to LPS in both mixed 129P2xC57Bl/6N and C57Bl/6N genetic background

(Fig. 15). Taken together, these data prove that Ago2 phosphorylation at serine 388 is dispensable for p38-MK2 functions in the hematopoietic system.

A recent study demonstrated that PKB/Akt protein kinases have the ability to phosphorylate human Ago2 at serine 387 in addition to MK2 (Horman, 2013). The PKB/Akt protein family consists of three members in mammals, PKB α /Akt1, PKB β /Akt2 and PKB γ /Akt3 (reviewed in Hers, 2011 and Polak, 2012). Akt proteins are downstream of the phosphatidylinositide 3-kinases (PI3K): PI3K produces phosphatidylinositol 3,4,5 triphosphate [PI(3,4,5)P₃] from a biphosphate precursor found in the plasma membranes of cells (Hers, 2011; Polak, 2012). Inactive Akt kinases relocate from the cytoplasm to the cell membrane by binding of [PI(3,4,5)P₃] molecules, triggering a conformational change that recruits PDK1 protein and mTORC2 kinase complex. PDK1 and mTORC2 phosphorylates threonine 308 and serine 473 on Akt, respectively, in order to activate the protein kinase domain (Alessi, 1996; Frias, 2006; Jacinto, 2006; Calleja, 2007; Hers, 2011). Compelling evidences demonstrated the importance of the Akt signaling in a plethora of physiological and disease processes, including cancer and diabetes (reviewed in Hers, 2011). Deletion of the three Akt isoforms in mice revealed that the different isoforms have distinct functional roles. Indeed, germline ablation of Akt1 showed a partial perinatal lethality, and surviving animals are smaller and present a reduce growth rate compared to wild type littermates (Chen, 2001; Cho, 2001a). Furthermore, *Akt1*^{-/-} adult animals have a higher degree of apoptosis in several tissues, such as the thymus and the testis, in both homeostatic and stress conditions (Chen, 2001). Further studies showed that Akt1 deletion affects vasculogenesis, muscle fibre formation, thymic development and spermatogenesis in mice (Chen, 2005; Fayard, 2007; Goncalves, 2010; Kim, 2012). On the other hand, germline ablation of Akt2 impairs glucose metabolism: homozygous mice are diabetic due to impaired insulin-dependent glucose uptake in peripheral tissues (Cho, 2001b; Garofalo, 2003). Finally, *Akt3*^{-/-} mice are viable, but present a reduction of 20% of brain mass (Easton, 2005). Recent work showed that Akt3 is important for platelet activation and thrombosis *in vivo* (O'Brien, 2011). Combined deletion of Akt1/2 and Akt1/3 causes much more severe phenotype compared to ablation of single Akt isoforms. Akt1/2 double knockout mice die shortly after birth for several developmental defects

on adipose, bone, muscle and skin development (Peng, 2003). In addition, analysis of hematopoietic progenitors from fetal liver of *Akt1*^{-/-}; *Akt2*^{-/-} embryos revealed a role of these cells in HSC homeostasis and T and B lymphocyte development (Juntilla, 2007; Calamito, 2010; Juntilla, 2010). On the other hand, simultaneous deletion of Akt1 and Akt3 triggers embryonic lethality at mid-gestation due to reduced vasculogenesis in placenta and in the embryos as well as increased apoptosis in brain (Yang, 2005).

Analysis on embryonic development of mice lacking Ago2 phosphorylation showed that in a mixed 129P2xC57Bl/6N and 129S2 homozygous mutant prevalently die at the peri-implantation stage (Fig. 7 and 16). It is evident that even deletion of two Akt isoforms could not trigger such an early arrest in embryogenesis (Peng, 2003; Yang, 2005). It is important to note that Akt3 showed a much higher kinase activity towards Ago2 serine phosphorylation than the other Akt family members, but *Akt3*^{-/-} mice are born in the expected Mendelian ratios (Easton, 2005; Horman, 2013). As such, Akt3 might not be the kinase responsible for Ago2 phosphorylation at this early embryonic stage. Together with the data derived from MK2 knockout animals, I hypothesize that a yet unknown protein kinase might be involved in Ago2 serine 388 phosphorylation in the peri-implantation period. Nonetheless, since both Akt3 and MK2 proteins could modify Ago2 *in vitro*, it is conceivable that both PI3K-Akt and p38-MK2 pathways are cooperating to regulate Ago2 function at this developmental stage. Hence, loss of Akt3 would be compensated by MK2 activity, and vice versa. It would be interesting to test this hypothesis by the analysis of Akt3-MK2 double mutant mice in light of the data presented in this thesis work. These results would either corroborate or confute the hypothesis of a third kinase that regulates Ago2 function in early mouse development.

3.3 Conclusions and future plans

Compelling efforts have been recently focused on the discovery and characterization of post-translational modification of Ago2 protein to understand how miRNA and siRNA pathways are regulated (Qi, 2008; Zeng, 2008; Rybak, 2009; Leung, 2011; Rudel, 2011; Wu, 2011; Horman, 2013; Shen, 2013). We created a nonphosphorylatable *Ago2*^{S388A} allele by inserting two point mutations in the endogenous Ago2 locus in murine ESCs to investigate the physiological role of this phosphorylation event. Our data showed that Ago2 phosphorylation at serine 388 is dispensable for Ago2 functions during hematopoietic development in a mixed 129P2xC57Bl/6N and C57Bl/6N background (Fig. 8-10 and 13-14). In addition, we proved that modification of serine 388 is not important for siRNA-mediated function of Ago2 during oocyte development using both homozygous *Ago2*^{S388A/S388A} females as well as a conditional deletion approach (Fig. 11-12). Finally, we were able to demonstrate that lack of Ago2 phosphorylation on serine 388 shows an almost complete lethality in mixed 129P2xC57Bl/6N and defined 129S2 genetic backgrounds, but not in the widely used C57Bl/6N background (Fig. 7, 12 and 16). Isolation of mouse embryos from heterozygote intercrosses allowed us to pinpoint Ago2 phosphomutant animals die at the peri-implantation stage (Fig. 7 and 16). Therefore, we demonstrated for the first time that post-translational modifications of Ago2 might be important at the organismal levels for some but not all Ago2 functions. In addition, we first proved the existence of a genetic background effect on a protein post-translational modification site, which has major implications for the investigation of causative genes in human pathologies and diseases using GWAS studies.

The lethality seen in the mixed 129P2xC57Bl/6N and the 129S2 genetic backgrounds appeared to be incompletely penetrant (Fig. 7 and 16). In addition, the analysis of reverse F₂ offspring allowed us to hypothesize that the modifier variants responsible for the differential effects of *Ago2*^{S388A} phosphomutant allele in the genetic background tested are likely in the vicinity of the Ago2 locus (Fig. 17). The identification of such genomic variants could not depend only between the comparison of C57Bl/6N and 129S2 genomes. In fact, a recent work presented the sequence of 17 mouse genomes, including the genomes of C57Bl/6NJ and three 129 strains (Keane, 2011). The

comparison of C57Bl/6NJ and the three 129 strains revealed the presence of 4 million SNPs and 0.8 million insertions/deletions, uncovering an enormous genetic variation between these mouse strains (Keane, 2011). Hence, to pinpoint the modifier allele(s) accountable for the differences between 129S2 and C57Bl/6N background, we would need to sequence the genome of *Ago2*^{S388A/S388A} survivor animals in a 129S2 background with wild type animals of the same genetic background. The comparison of these two datasets could reveal the presence of any common variant derived from the C57Bl/6N genome that is still segregating with the *Ago2*^{S388A} allele and allows the survival of such animals. Alternatively, we could take advantage of the identified linkage disequilibrium present between the endogenous *Ago2* locus and the genomic variant(s). We could then backcrossed heterozygotes animals in a 129S2 background with C57Bl/6N wild type mice: intercross of the offspring during each generation will verify the presence of any lethality against homozygous mutants. When the *Ago2*^{S388A} allele segregates away from the modifier allele(s), *Ago2*^{S388A/S388A} homozygotes will be vital and sequencing of these animals will reveal the genomic area in the C57Bl/6N genome that accounts for the rescue of this lethality. In parallel, a similar experiment could be conducted by mating heterozygote mutants from the C57Bl/6N background with wild type 129S2 animals and screen these animals for the appearance of any lethal phenotype against homozygotes. The identification of genetic variant(s) that modifies the output of *Ago2* phosphomutant allele would shed light on the molecular function of this post-translational modification. The partial lethal phenotype that *Ago2* phosphomutant animals demonstrated do not mimic the effects of germline deletions of the kinase which are possibly responsible for *Ago2* modification (Kotlyarov, 1999; Mudgett, 2000; Tamura, 2000; Chen, 2001; Cho, 2001a-b; Garofalo, 2003; Shi, 2003; Peng, 2003; Easton, 2005; Yang, 2005; Ronkina, 2007; Zeng, 2008; Horman, 2013). Indeed, ablation of MK2 alone or in combination with MK3 does not lead to embryonic lethality (Kotlyarov, 1999; Shi, 2003; Ronkina, 2007). Furthermore, deletion of Akt isoforms alone or in combination could be lethal, but always after mid-gestation (Chen, 2001; Cho, 2001a-b; Garofalo, 2003; Peng, 2003; Easton, 2005; Yang, 2005). It could be interesting to understand if the combination of MK2 and Akt3 null alleles would then be able to phenotypically copy the absence of *Ago2* serine 388 phosphorylation, regarding the peri-implantation lethality as well as the

genetic background effect. Furthermore, we were able to raise and purify a specific antibody against phosphorylated serine 388 of the mouse Ago2 protein (Fig. 18). Even though the antibody is not able to recognize phosphorylation levels of the endogenous protein, it is a promising tool to identify other kinases, which could be responsible for Ago2 phosphorylation. Indeed, we could evaluate the effects of a broad range of stimuli together with specific kinase inhibitors by using our phosphoantibody on cell lines overexpressing the Ago2 protein. The discovery of other protein kinase(s) might link Ago2 function with other signaling pathways, thus potentially clarifying the phenotypic outcome of *Ago2*^{S388A/S388A} in the 129S2 strain.

The physiological relevance of Ago2 has been studied using conditional deletion approaches to overcome the lethality of Ago2 germline ablation (Liu, 2004; Alish, 2007; Morita, 2007; O'Carroll, 2007; Kaneda, 2009; Schaefer, 2011; Wang, 2012). We investigated the importance of phosphorylation of serine 388 for Ago2 function during embryonic, hematopoietic and oocyte development. Nonetheless, lack of Ago2 in dopaminergic neurons increases the self-administration of cocaine in mice (Schaefer, 2011). Furthermore, ablation of Ago1 and Ago2 in the developing skin causes gross morphological abnormalities in the epidermis (Wang, 2012). *Ago2*^{S388A/S388A} adult animals in both 129S2 and C57Bl/6N were not tested for any behavioural abnormalities. Therefore, a more thorough testing for cocaine addiction would be useful to understand if lack of phosphorylation is necessary for Ago2 function in this system. Furthermore, combination of the *Ago2*^{S388A} mutant allele with the *Ago1*^{-/-} allele is needed to demonstrate a possible role of Ago2 serine 388 phosphorylation during skin development. In conclusion, phenotypic characterization of Ago2 phosphorylation at serine 388 might reveal new physiological systems in which it regulates the functionality of the Ago2 protein.

Chapter 4: Miwi2 expression marks a population of spermatogonia with stem cell characteristics

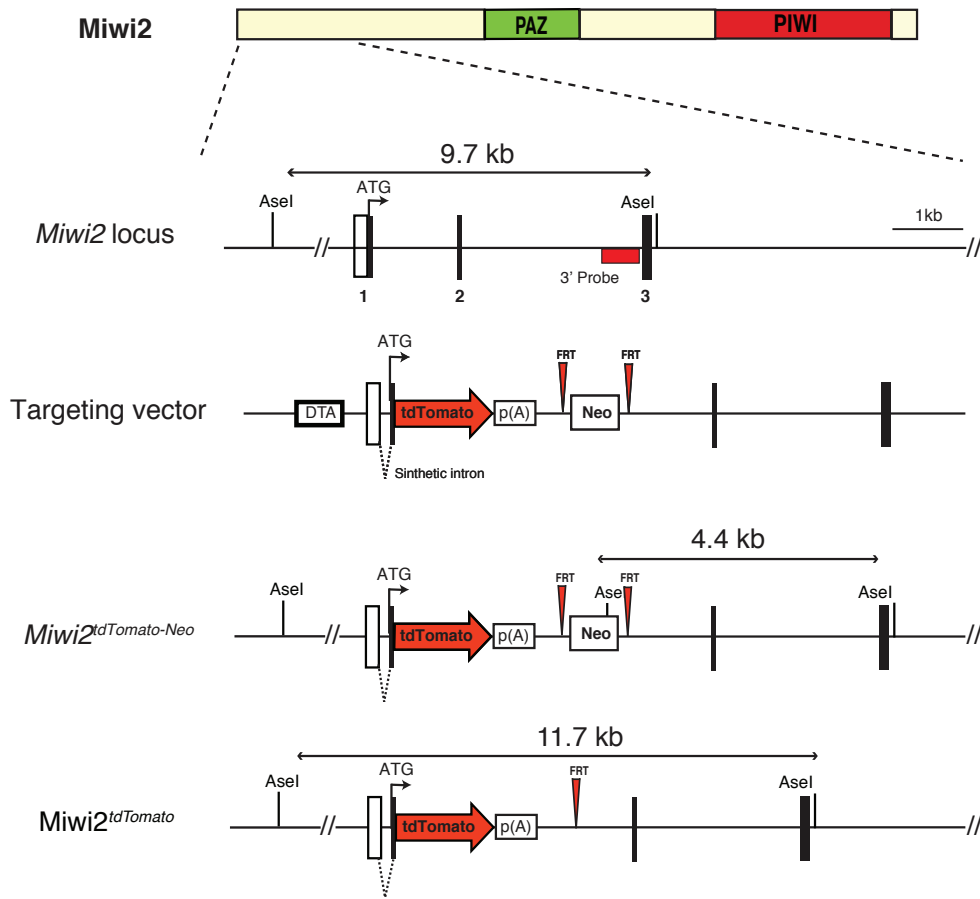
4.1 Results

4.1.2 Generation of reporter allele to mark Miwi2-expressing cells *in vivo*

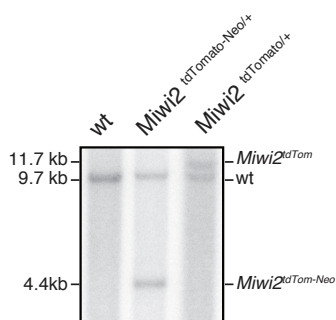
The Piwi-like subclade of Argonaute proteins plays an essential role in the maintenance of transposon silencing in the mouse male germ line (Deng, 2002; Kuramochi-Miyagawa, 2004; Carmell, 2007; De Fazio, 2011; Reuter, 2011; Di Giacomo, 2013). Among this sub-clade, Miwi2 and Mili are necessary for the DNA methylation of transposable elements (Carmell, 2007; Aravin, 2008; Kuramochi-Miyagawa, 2008). Intriguingly, lack of Mili or Miwi2 halts the spermatogenic process in adult animals at the level of meiotic divisions, but only *Miwi2*^{-/-} animals present an accompanying progressive loss of germ cells with age (Carmell, 2007; De Fazio, 2011). This is suggestive of a secondary role of Miwi2 protein in the stem cell compartment in adult animals. Since the precise identity of spermatogonial stem cell (SSC) is not known, I hypothesize that Miwi2 could be a useful marker for the isolation of this elusive cell type. To this end, I generated a *Miwi2*^{tdTomato} allele to fluorescently label Miwi2-expressing cells. I targeted the Miwi2 locus by electroporating mESC from a mixed 129xC57Bl/6 genetic background (A9 cells) (kind gift of A. Wutz) with a construct that would insert in the endogenous Miwi2 locus a cassette encoding for the tdTomato protein and the neomycin resistance, the latter flanked at the 5' and 3' end with FRT sites (Fig. 19A). The positive clones were then used to generate ESCs mice by injection at the morula stage. ESC mice were then crossed to a Flp-expressing mouse strain (Farley, 2000) to remove the neo cassette *in vivo*: Southern blot analysis confirmed the excision of the neo from the Miwi2 locus (Fig 19B). The overlap of Miwi2 and tdTomato proteins was verified in fetal testis isolated from wild type and *Miwi2*^{tdTomato/+}

embryos at E16.5 by immunofluorescence (Fig. 19C). *Miwi2^{tdTomato/+}*; *Tg^{FLP}* mice were backcrossed one generation with C57Bl/6N animals to remove the FLP recombinase before being used for further experiments.

A



B



C

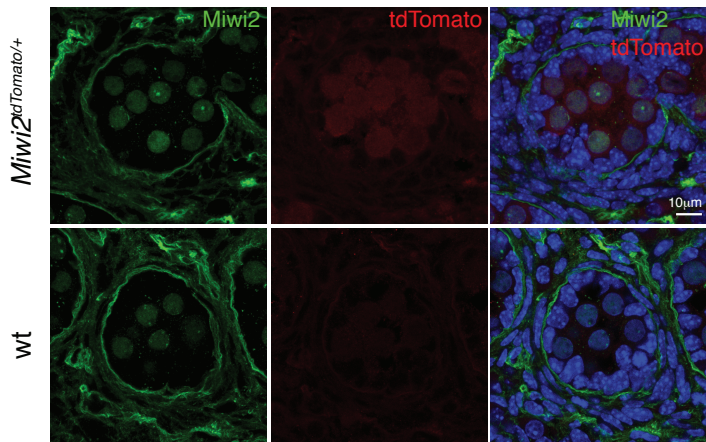


Figure 19. Targeting strategy and validation of the *Miwi2*^{tdTomato} allele.

(A) Schematic representation of the *Miwi2* locus and the targeting strategy for the formation of a *Miwi2*^{tdTomato} allele. Squared boxes indicate the *neomycin* (*neo*) and *Diphtheria Toxin A* (*pDTA*) resistance cassettes for the selection of embryonic stem

cells. Red triangles represent FRT sites at both sides of the *neo* resistance to allow a FLP-mediated excision of this cassette. A synthetic intron was introduced between the 3' untranslated region of exon 1 and the starting codon of the endogenous *Miwi2* locus, which is then followed by the ORF for the fluorescent tdTomato protein. *AseI* sites used for the Southern blot screen of positive clones are indicated along with the size of the fragments recognized by a 3' probe. (B) Representative Southern blot image of genomic DNA isolated from the tail of mice of the indicated genotype. A correct targeting of the *Miwi2* locus and recombination of the *neo* resistance confirmed the formation of a functional *Miwi2^{tdTomato}* allele *in vivo*. (C) Immunofluorescent analysis of *Miwi2* and tdTomato localization from fetal E16.5 testis from wild type and *Miwi2^{tdTomato/+}* embryos using antibodies specific for *Miwi2* and tdTomato proteins. Both *Miwi2* and tdTomato localized in the gonocytes present at the centre of the tubule but not in the external Sertoli cells. The data presented in B-C of this figures were made in collaboration with Dr. Claudia Carrieri.

4.1.2 The *Miwi2^{tdTomato}* allele labels two distinct populations of germ cells in juvenile mice

Several efforts were made in order to identify bona fide SSC markers in mice using flow cytometry (Brinster, 1994a-b; Shinohara, 2000 and 2001; Kubota, 2003; Hobbs, 2010). Recently, Hobbs *et al.* used testis isolated from mice at postnatal day 10-14 (PND 10-14) to identify a population of CD45⁻ CD51⁻ Thy-1^{lo} c-Kit⁻ spermatogonia with a high repopulating capability (Hobbs, 2010). I undertook a similar approach by analysing the juvenile wild type and *Miwi2^{tdTomato/+}* testis at PND 14 by flow cytometry. First, I selected CD45⁻ CD51⁻ cells to exclude hematopoietic and endothelial cells from the analysis (Fig. 20). Second, I searched for tdTomato-positive (tdTom⁺) cells in correlation with c-Kit expression, using a wild type mouse as negative control for tdTomato signal. I identified 2 separate populations: tdTom⁺ c-Kit⁻ cells, that represent around 3-4% of the CD45⁻ CD51⁻ fraction, and tdTom⁺ c-Kit⁺ cells, which represent 8-10% of CD45⁻ CD51⁻ subpopulation (Fig. 20). I estimated that there are about 35 thousand tdTom⁺ c-Kit⁻ and 72 thousand tdTom⁺ c-Kit⁺ per testis in juvenile PND 14 testis.

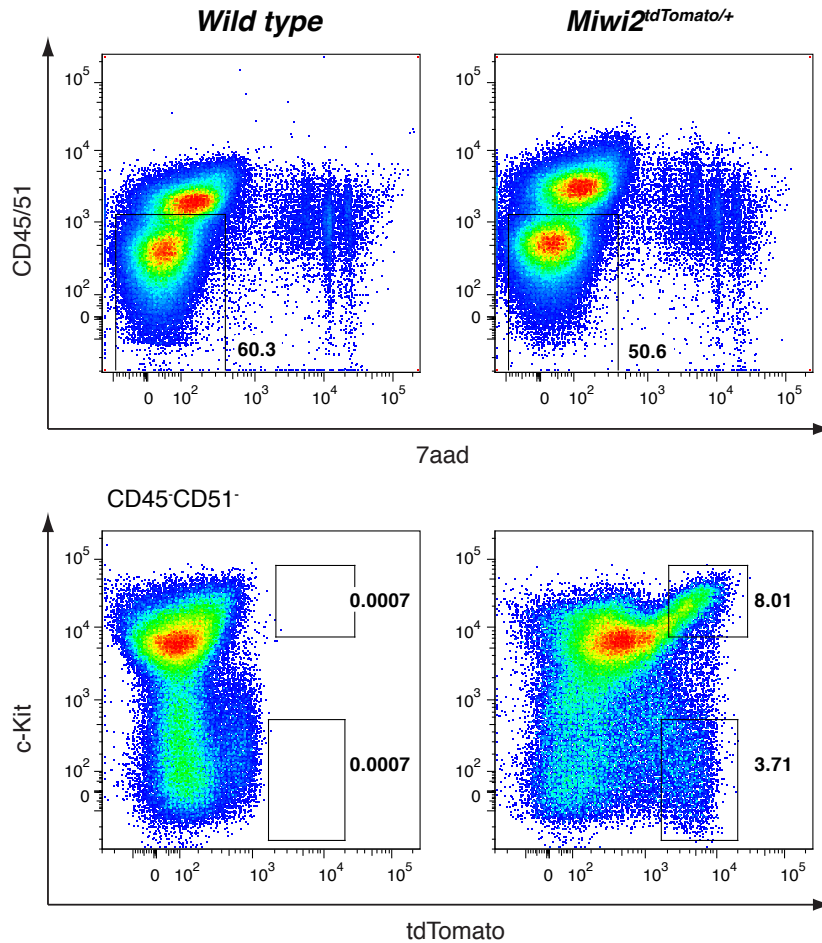


Figure 20. *Miwi2* expression marks two populations of spermatogonia in juvenile mouse testis.

Representative flow cytometry graphs of testis cells isolated from PND 14 wild type and *Miwi2*^{tdTomato/+} males are shown. CD45⁻ CD51⁻ live cells were first selected (upper panels) and plotted for c-Kit and tdTomato protein levels (lower panels). Numbers represent the percentages of gated cells. Two distinct populations of tdTom⁺ c-Kit⁻ and tdTom⁺ c-Kit⁺ cells are distinguishable from the flow cytometry analysis. The data presented are representative of four independent experiments.

Since the expression of c-Kit correlates with the differentiation of spermatogonia during the mitotic phase of the spermatogenic cycle (Yoshinaga, 1991; Shinohara, 1999), I believe that tdTom⁺ c-Kit⁺ cells derive from the commitment of tdTom⁺ c-Kit⁻ population. To further characterize these two populations, I tested the expression of multiple surface antigens that have been used alone or in combination to enrich or deplete for stem cell activity (Shinohara, 1999 and 2000; Kubota, 2003; Kanatsu-

Shinohara, 2004; Kubota, 2004; Hobbs, 2010; Kanatsu-Shinohara, 2011). Indeed, MHC-I⁺ Thy-1⁺ c-Kit⁻ cell population sorted from adult animals showed a 25 fold enrichment of repopulating activity compared to unsorted cells (Kubota, 2003). In addition, this population shares with the HSC population the expression of integrin α 6 (CD49f) and CD24 but no other surface markers (Kubota, 2003). Selection of CD9⁺ cells alone also enriched for stem cell activity from adult rat and mouse testis cells (Kanatsu-Shinohara, 2004). The tdTom⁺ c-Kit⁻ cells present low side scatter and a Thy-1^{lo} CD9^{Hi} CD24⁺ CD49f⁺ CD29⁺ EpCAM^{lo} CD34⁻ Sca-1⁻ MHC-I^{lo} marker profile, which is suggestive of a stem cell population (Fig. 21). tdTom⁺ c-Kit⁺ cells present similar surface profile, but with lower protein levels of Thy-1 and CD9 and a broader forward scatter profile, indicating a more differentiated population (Fig. 22). On the other hand, tdTom⁺ c-Kit⁺ cells show higher surface levels of EpCAM protein, which is known to mark more differentiated progenitor cells (Fig. 21-22) (Kanatsu-Shinohara, 2011). Collectively, these data demonstrate the potential existence of two Miwi2-expressing cell populations in the testis, with the tdTom⁺ c-Kit⁻ fraction likely to be a high-ranked stem cell population in the spermatogenic hierarchy.

Miwi2^{tdTomato/+}

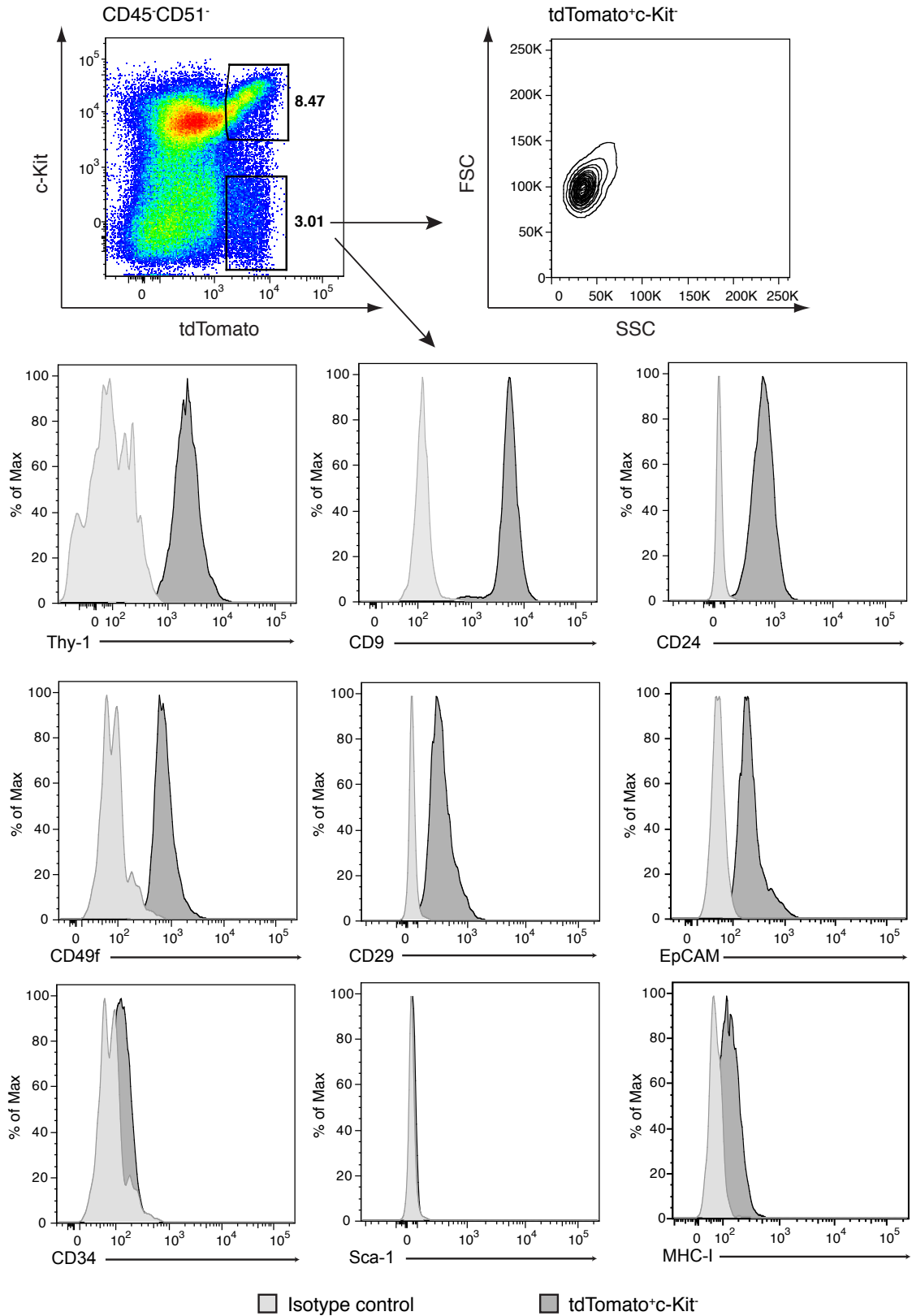


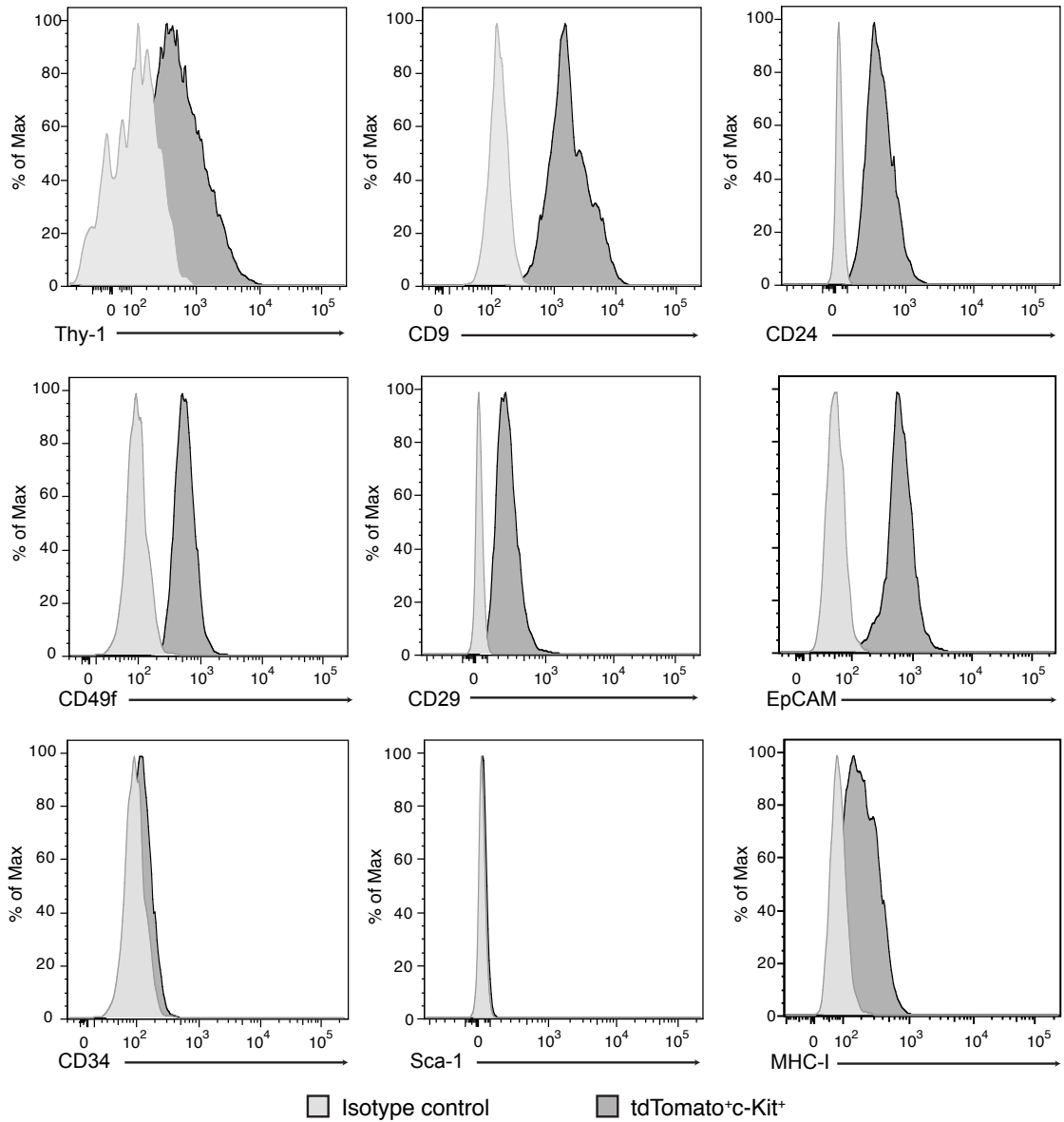
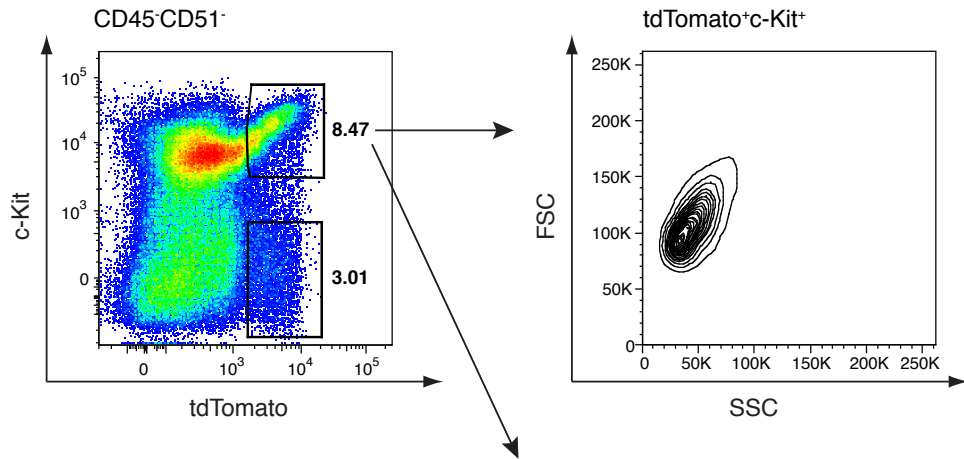
Figure 21. TdTomato⁺ c-Kit⁻ cell population possesses a surface marker profile reminiscent of SSCs.

Representative flow cytometry analysis of surface marker expression from juvenile *Miwi2^{tdTomato/+}* male testis is depicted. TdTom⁺ c-Kit⁻ cells were gated and stained with specific antibodies against Thy-1, CD9, CD24, CD49f, CD29, EpCAM, CD34, Sca-1 and MHC-I. The forward and side scatter profile of this selected population is also reported in the upper right panel. TdTom⁺ c-Kit⁻ cell pool expresses all the markers employed to enrich for stem cell activity, suggesting that these cells represent a highly stem cell population. The data presented are representative of two independent experiments employing 3 different *Miwi2^{tdTomato/+}* individuals.

Figure 22. TdTomato⁺ c-Kit⁺ cell population possesses a surface marker profile of more differentiated spermatogonia. (next page)

Representative flow cytometry analysis of surface marker expression from juvenile *Miwi2^{tdTomato/+}* male testis is depicted. TdTom⁺ c-Kit⁺ cells were gated and stained with specific antibodies against Thy-1, CD9, CD24, CD49f, CD29, EpCAM, CD34, Sca-1 and MHC-I. The forward and side scatter profile of this selected population is also reported in the upper right panel. TdTom⁺ c-Kit⁺ subset represents a more differentiated population of spermatogonia cells for the higher expression of c-Kit and EpCAM and a concomitant reduction of Thy-1 and CD9 protein levels. The data presented are representative of two independent experiments employing 3 different *Miwi2^{tdTomato/+}* individuals.

Miwi2^{tdTomato/+}



4.1.3 The tdTomato⁺ c-Kit⁻ cellular fraction has cell cycle and gene-expression profile typical of a stem cell population

The stem cell theory postulates a hierarchical structure in the differentiation process of adult tissues: the stem cell atop of the hierarchy divides slowly to form a pool of multipotent progenitor cells, that highly proliferate in order to amplify the number of differentiated cells produced for each stem cell division. Indeed, low cycling activity has been proven to inversely correlate with stem cell activity (Clermont, 1968; Dym, 1970; de Rooij, 1973; Stingl, 2006; Orford, 2008; Wilson, 2008). I analysed the cell cycle profile of both tdTomato⁺ c-Kit⁻ and tdTomato⁺ c-Kit⁺ cells in testis from PND 14 animals. tdTomato⁺ c-Kit⁻ cells are mainly in the G₀/G₁ phase of the cell cycle, with only ~10% of the total cell population in the S- and G₂-M phases (Fig. 23). Conversely, tdTomato⁺ c-Kit⁺ cells show a high rate of proliferation, coherent with this population representing a transit-amplifying set of spermatogonia (Fig. 23).

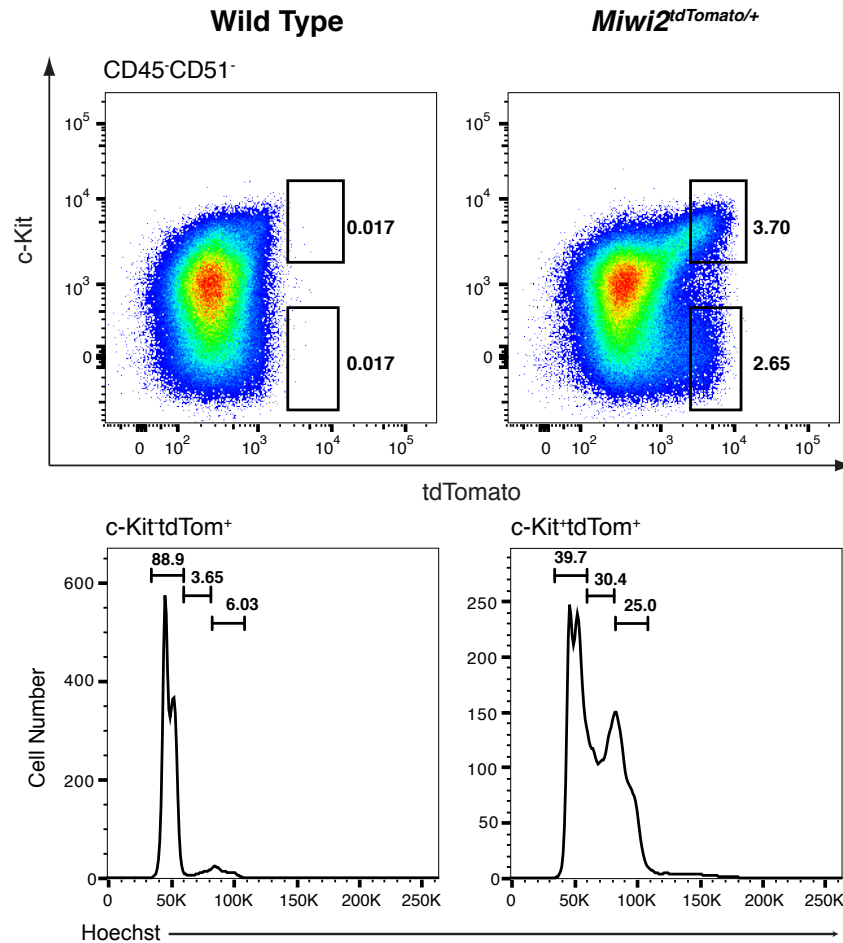


Figure 23. Cell cycle profile of tdTomato⁺ c-Kit⁻ and tdTomato⁺ c-Kit⁺ cells.

Representative flow cytometry analysis of tdTomato⁺ cell populations from wild type and *Miwi2*^{tdTomato/+} juvenile testis is shown. Cells were gated according to tdTomato and c-Kit protein levels (upper panel), and the DNA content of tdTom⁺ c-Kit⁻ and tdTom⁺ c-Kit⁺ cells was analysed using Hoechst 33342 incorporation (lower panels). Numbers indicate percentages of cells in the indicated gates. Only a small fraction of tdTom⁺ c-Kit⁻ cells is actively cycling, while tdTom⁺ c-Kit⁺ cells are mostly in active division. The data presented are representative of three independent experiments employing 2 different *Miwi2*^{tdTomato/+} individuals.

I further isolated live tdTom⁺ cells from juvenile testis by cell sorting to study the expression levels of genes previously used to mark SSCs in the testis. The expression of glial cell line-derived neurotrophic factor family receptor alpha-1 (GFRA1) is commonly used to define a population of As spermatogonia, which are believe to represent a population of SSCs in the testis (Hofmann, 2005; Tokuda, 2007; Suzuki, 2009). In

addition, several transcription factors, such as PLZF and Oct4, and RNA-Binding proteins, like Nanos2 and Lin28a, have proven to mark undifferentiated spermatogonia cells (Yoshimizu, 1999; Ohbo, 2003; Buaas, 2004; Costoya, 2004; Sada, 2009; Zheng 2009). Since Thy-1 expression is decreasing in tdTom⁺ c-Kit⁺ cell fraction (Fig. 21-22), I decided to subdivide this population in Thy-1^{lo} and Thy-1⁻ cells to have a better insight of the transition step during the loss of Miwi2 expression (Fig. 24A). RT-PCR analysis revealed that tdTom⁺ c-Kit⁻ cells express higher levels of SSC-enriched genes such as Lin28, GFRA1, Oct4 and PLZF (Fig. 24B). In addition, the mRNA levels of c-Kit and EpCAM reflects the flow cytometry data presented in Fig. 21-22, confirming that tdTom⁺ c-Kit⁺ cells are more differentiated progenitor cells (Fig. 24B). It is important to note that Miwi2 expression levels present similar profiles to the other stemness-related genes, decreasing of 75% between tdTom⁺ c-Kit⁻ and tdTom⁺ c-Kit⁺ Thy-1^{lo} cell populations (Fig. 24B). Altogether, the cell cycle and gene expression profiles of tdTom⁺ c-Kit⁻ cells indicate that this population could define a bona-fide spermatogonial stem cell population.

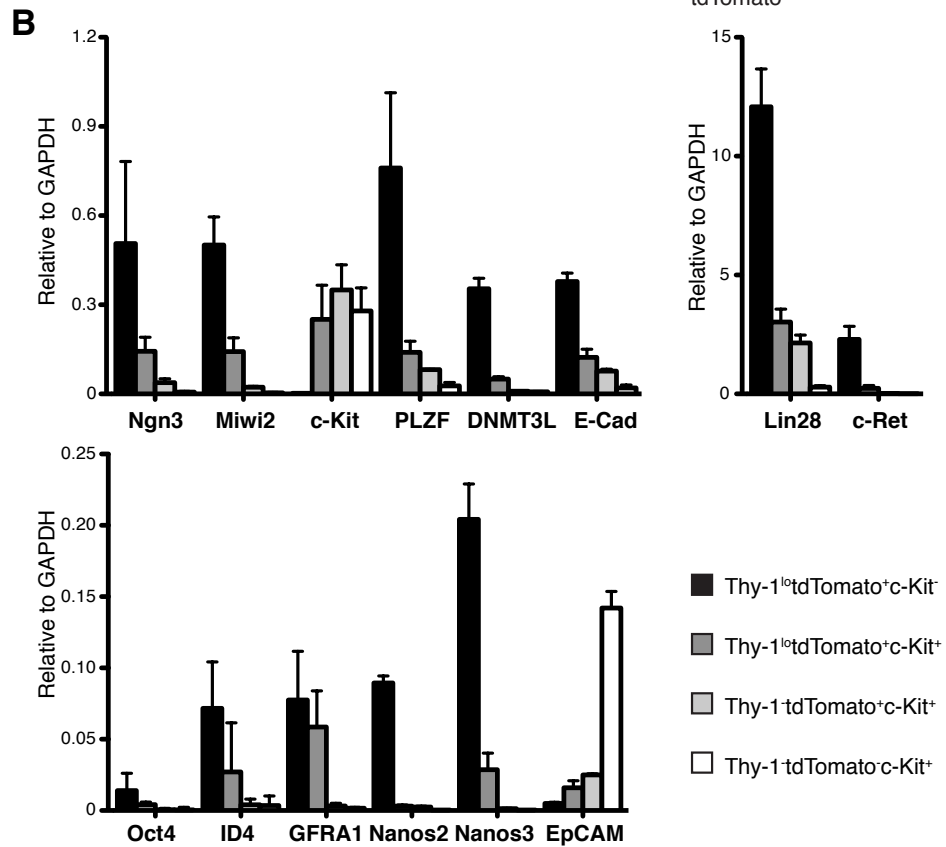
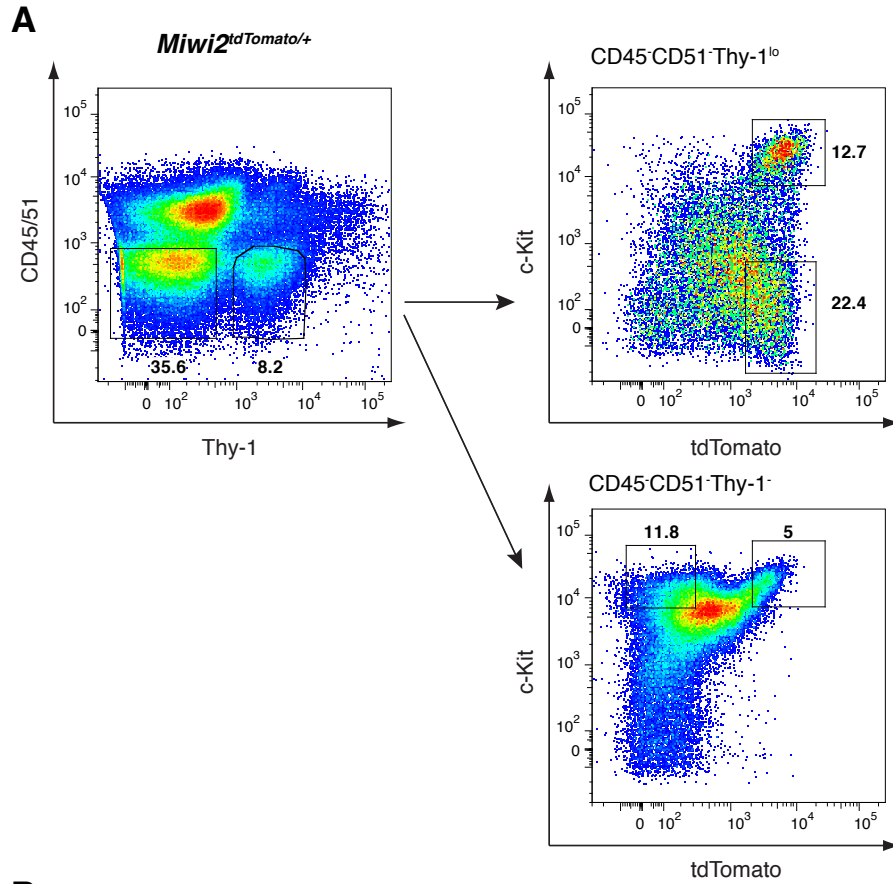


Figure 24. Expression profile of tdTomato⁺ c-Kit⁻ reveals a stem cell signature.

(A) Representative flow cytometry plots show the strategy to obtain tdTom⁺ c-Kit⁻ Thy-1^{lo}, tdTom⁺ c-Kit⁺ Thy-1^{lo}, tdTom⁺ c-Kit⁺ Thy-1⁻ and tdTom⁻ c-Kit⁺ Thy-1⁻ populations for RNA extraction from *Miwi2^{tdTomato/+}* PND 14 testis by fluorescent-activated cell sorting. Numbers indicate percentages of gated cells. Cells were first selected for CD45/51 and Thy-1 expression, and then gated according to tdTomato and c-Kit staining. (B) Real-time PCR reactions were carried out using primer specific for the indicated genes. The mRNA levels of the tested genes are normalized according to GAPDH expression. Graphs show the mean \pm s.e.m from three independent biological samples.

4.1.4 Comparison of tdTomato⁺ c-Kit⁻ cellular fraction from adult and juvenile testis shows similar surface marker profile

Stem cells in adult and young animals are known to have diverse differentiation capacity and cologenic potential. Indeed, fetal HSCs derived from E14.5 embryos tend to give rise to innate-like lymphocyte subsets and outcompete adult HSCs in the repopulation of lethally irradiated mice (Morrison, 1995; Bowie, 2007). In the testis, analysis of colonization capacity revealed that cells derived from juvenile mice have a higher stem cell potential compared to adult testis cells after transplantation (Brinster, 1994b; Shinohara, 2001; McLean, 2003). This differential colonization ability could be ascribed to differences in the percentage of SSCs between juvenile and adult cell preparations or to intrinsic differences between adult and juvenile SSCs. To test this hypothesis, I made use of the *Miwi2^{tdTomato}* allele to compare the surface marker profiles from tdTom⁺ c-Kit⁻ cells isolated from pre-pubertal and adult mice. Flow cytometry analysis shows that tdTom⁺ c-Kit⁻ fraction is present in lower percentage in adult samples compared to juvenile testis (Fig. 25): I estimated that there are ~8000 tdTom⁺ c-Kit⁻ cells per million of testis cells in juvenile mice, while only ~1500 in adult mice. However, adult and juvenile tdTom⁺ c-Kit⁻ pools present very similar surface marker profiles, with the only exception of Thy-1, which is expressed at higher levels in juvenile cells (Fig. 25). Therefore, the elevated expression level of Thy-1 in juvenile cells could be indicative of a higher stem cell potential compared to adult counterparts.

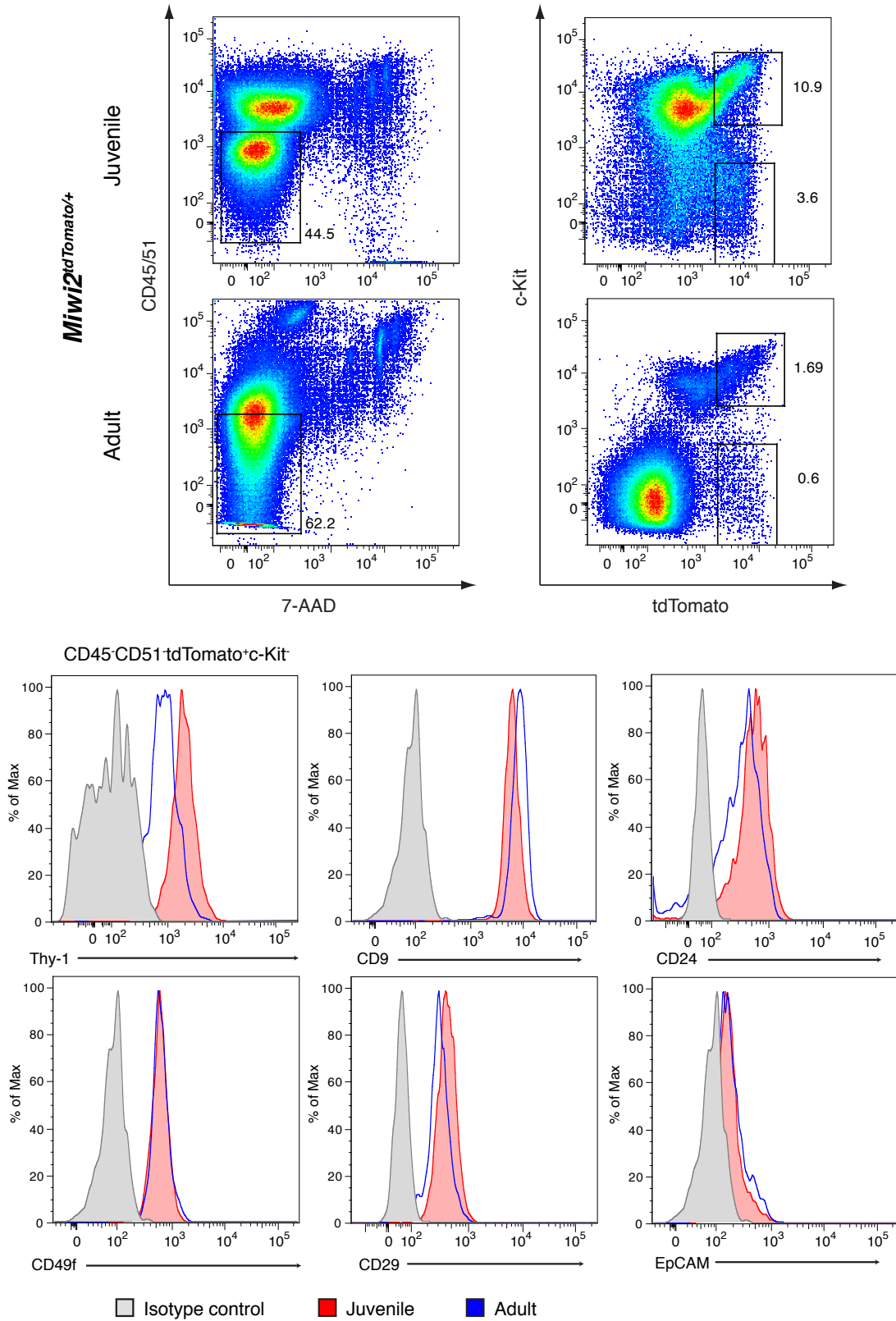


Figure 25. Adult and juvenile tdTomato⁺ c-Kit⁻ cells share similar surface marker expression profiles.

Representative flow cytometry analysis of adult and juvenile testis cells from *Miwi2^{tdTomato/+}* males. Numbers represent percentages of the gated cells. CD45⁻ CD51⁻ live cells were first selected (upper left panels), and then analysed according to tdTomato and c-Kit protein levels (upper right panels). TdTom⁺ c-Kit⁻ populations from adult and PND 14 testis were stained with antibody specific for Thy-1, CD9, CD24, CD49f, CD29 and EpCAM. Adult and juvenile gated cells differ only for the surface levels of Thy-1. The data shown are representative of three independent experiments.

4.2 Discussion

4.2.1 Miwi2 is expressed in the testis of juvenile male mice

In the mouse, three PIWI-like protein exists: Mili, Miwi and Miwi2 (Cerutti, 2006; Hutvagner, 2008). These proteins are expressed mainly in the germ cell lineage, even though recent studies showed the presence of PIWI-related proteins in the brain of mouse and *Aplysia* (Kuramochi-Miyagawa, 2001; Deng, 2002; Kuramochi-Miyagawa, 2004; Carmell, 2007; Aravin, 2008; Kuramochi-Miyagawa, 2008; De Fazio, 2011; Lee, 2011; Rajasethupathy, 2012; Di Giacomo, 2013). Miwi protein is detected only in adult testis, and its expression is restricted to late spermatocytes and spermatids (Kuramochi-Miyagawa, 2001; Deng, 2002; Kuramochi-Miyagawa, 2004; Di Giacomo, 2013). Mili initiates to be expressed in both female and male germ cells as early as embryonic day E12.5, and it is further expressed in spermatogonia and in spermatocytes at the pachytene-diplotene stages (Kuramochi-Miyagawa, 2001; Kuramochi-Miyagawa, 2004; Aravin, 2008; De Fazio, 2011; Di Giacomo, 2013).

The detection of Miwi2 protein has been more challenging due to the absence of good antibodies specific to this protein. First characterization by semiquantitative RT-PCR revealed that *Miwi2* transcripts are present in male testis starting from E15.5 up to 10 days after birth (PND 10) (Carmell, 2007; Kuramochi-Miyagawa, 2008). Later, detection of Miwi2 protein by antibody staining and fluorescently labeled Miwi2 protein in transgenic mice confirmed the narrow window of Miwi2 expression (Aravin, 2008). Surprisingly, Miwi2 transcript could be detected in testis from adult mutant W/W^v animals (Carmell, 2007). W/W^v male mice harbors a mutation in the *c-Kit* gene that create an hypomorphic allele, blocking the differentiation of spermatogonia cells. Homozygous mutant testes contain undifferentiated spermatogonia cells and somatic cells in the seminiferous tubules (Silvers, 1979). Furthermore, analysis of *Miwi2*^{-/-} testis revealed an age-related loss of germ cells, which begins at 3 months after birth (Carmell, 2007). These observations suggested the possibility of a functional role of Miwi2 in the adult SSC compartment.

In order to understand if *Miwi2* is expressed after early postnatal days, I created a *Miwi2^{tdTomato}* transcriptional reporter allele by inserting the expression cassette for the tdTomato fluorescent protein in the endogenous *Miwi2* locus (Fig. 19). I first verified that tdTomato protein expression mirrors *Miwi2* expression in fetal testis by immunofluorescence (Fig. 19). Further analysis of tdTomato fluorescence by flow cytometry revealed that in both pre-pubertal and adult mice two distinct populations of testicular cells are fluorescently labeled, tdTom⁺ c-Kit⁻ and tdTom⁺ c-Kit⁺ (Fig. 20 and 25). Quantitative RT-PCR from RNA isolated from tdTom⁺ c-Kit⁻ and tdTom⁺ c-Kit⁺ population as well as tdTom⁻ c-Kit⁺ control cells confirmed that *Miwi2* transcript is selectively present in tdTomato-expressing cells (Fig. 24). Taken together, the data presented demonstrated that *Miwi2* is indeed expressed in juvenile and adult testis, corroborating the hypothesis that *Miwi2* is indeed required for adult spermatogenesis.

4.2.2 The *Miwi2^{tdTomato}* allele marks a population of germ cells presenting several stem cell properties

Identification of stem cell population in the mouse testis is based on data derived from morphological studies as well as transplantation assays. Since mouse spermatogenesis takes place in highly ordered manner inside the seminiferous tubules, pioneering studies used morphological, positional and cell cycle kinetics information to define the SSC population in testis (Clermont, 1968; Dym, 1970; Huckin, 1971a-b, Oakberg, 1971, de Rooij, 1973; Clermont, 1975; Erickson, 1978; Lok, 1983). The population of A_s spermatogonia was hypothesized to possess the self-renewal capacity in mouse testis since they do not present any intercellular bridge and divide rarely (Clermont, 1968; Dym, 1970; Huckins, 1971a-b; de Rooij, 1973; Lok, 1983). Efforts were thus concentrated to discover markers specific for the undifferentiated spermatogonia cells, and in particular for the A_s population. The GFRA1 receptor and the receptor kinase c-Ret were first identified as possible stem cell markers (Meng, 2000; Kanatsu-Shinohara, 2003; Kubota, 2004; Buageaw, 2005; Hofmann, 2005; Naughton, 2006; He, 2007; Tokuda, 2007). Indeed, deletion of one of the two *GFRA1* alleles in mice leads to degeneration of seminiferous tubule due to lack of germ cells. Conversely,

overexpression of GFRA1 leads to the accumulation of undifferentiated spermatogonial cells in the testis lumen, with a consequent block in formation of differentiated cells (Meng, 2000). In addition, GFRA1 is necessary for the maintenance of SSC culture *in vitro* (Kanatsu-Shinohara, 2003; Kubota, 2004). Immunofluorescence experiments demonstrated that GFRA1 is expressed in A_s and A_{pr} cell population in the mouse testis (Tokuda, 2007; Suzuki, 2009). In addition to GFRA1, transcription regulators such as PLZF, Oct4, Neurogenin 3 (Ngn3) and Id4 were identified as spermatogonia markers (Buaas, 2004; Costoya, 2004; Yoshida, 2004; He, 2007; Oatley, 2011). Genetic deletion of PLZF induces increased apoptosis and an age-related loss of germ cells (Buaas, 2004; Costoya, 2004). Similarly, ablation of Id4 causes a progressive but not complete depletion of germ cells (Oatley, 2011). PLZF and Ngn3 expression marks all type A spermatogonia, from A_s to A_{al}, while Id4 expression seems to be specific for A_s cells (Tokuda, 2007; Suzuki, 2009; Oatley, 2011). Further efforts revealed that the RNA binding proteins Nanos2, Nanos3 and Lin28a are expressed in undifferentiated spermatogonia (Sada, 2009; Zheng, 2009; Suzuki, 2009; Nakagawa, 2010). Nonetheless, immunofluorescence studies on whole-mount seminiferous tubules show that the A_s population is quite heterogeneous in the respects of the expression of the aforementioned markers (Tokuda, 2007; Sada, 2009; Suzuki, 2009; Nakagawa, 2010). The heterogeneity of A_s protein expression points to the limitations on morphological studies alone to define SSC population. The identification of *bona fide* stem cell population requires the assessment of the ability to differentiate into all the cell lineages present in the tissue of origin. This ability has been tested in testis as well as other physiological systems through transplantation procedures (Spangrude, 1988; Brinster, 1994a-b; Stingl, 2006; Shackleton, 2006). FACS-based purification of raw testis preparation was used to enrich for stem cell activity using particular surface markers. The first studies employed single antibody staining against integrin $\alpha 6$ (CD49f) or integrin $\beta 1$ (CD29) to enrich for stem cell population, while expression of c-Kit or integrin αv (CD51) was discovered to deplete for stem cell activity (Shinohara, 2000; Shinohara, 2001). In addition, selection of small cells, evaluated by low forward and side scatters, by flow cytometry enhances stem cell potential in sorted cells (Shinohara, 2001). Isolation of MHC-I⁺ Thy-1⁺ CD49f⁺ from cryptorchid mouse testis revealed a

higher enrichment for stem cells, with an estimated stem cell concentration of 1 out of 15 cells (Kubota, 2003). Further analysis of these cell population revealed that it expresses CD24, but not the known HSC stem cell markers Sca-1 and CD34 (Spangrude, 1988; Osawa, 1996; Kubota, 2003). Similar to flow cytometry based cell purification, Magnetic-Activated cell sorting (MACS) was employed for enrichment of stem cell activity. Selection for GFRA1-positive cells enriches for stem cell activity from both pups and adult testis cell preparations compared to GFRA1-negative cells (Buageaw, 2005; Ebata, 2005; Grisanti, 2009). In addition, enrichment for Thy-1, E-cadherin and CD9 expressing cells improves the repopulating capacity of transplanted cells compared to depleted fractions, while enrichment for EpCAM expression inversely correlates with stem cell potential (Kubota, 2004; Kanatsu-Shinohara, 2004; Tokuda, 2007; Kanatsu-Shinohara, 2011).

Several of the markers used to define undifferentiated spermatogonia are present inside the cells. These markers are not accessible for antibody staining for FACS- or MACS-sorting. To overcome this issue, transgenic mice expressing fluorescent protein markers under the regulatory elements of these genes could be extremely useful. The first example is represented by a transgenic animal that expresses the GFP protein under a genomic fragment encompassing Oct4 promoter and enhancer sequences (Yoshimizu, 1999; Ohbo, 2003). Oct4, a POU domain transcription factor known to be necessary for ESC self-renewal, is expressed in PGCs during early embryonic development and in undifferentiated spermatogonia after birth (Ovitt, 1998; Pesce, 1998). The analysis of Oct4-GFP transgenic mice demonstrated that GFP-expressing cells are present in testis cells up to PND10, and immunofluorescence studies confirmed that Oct4 and GFRA1 are co-express in a population of type A spermatogonia at PND 6 (Yoshimizu, 1999; Ohbo, 2003; Hofmann, 2005; He, 2007). Flow cytometry analysis of testis cells at PND 7.5 revealed that two populations of GFP-expressing cells exist: GFP⁺ c-Kit⁻ and GFP⁺ c-Kit⁺ fractions (Ohbo, 2003). GFP⁺ c-Kit⁻ population expresses integrin β 1/CD29 and in transplantation assays have an higher capacity to repopulate recipient testis than GFP⁺ c-Kit⁺ fraction (Ohbo, 2003).

A recent work studied the surface marker profile and repopulating capability of PLZF⁺ cells in juvenile testis between PND 10-14 (Hobbs, 2010). Flow cytometry analysis

revealed that PLZF-expressing cells are all CD45⁻ CD51⁻ Thy-1⁺, while resulting both positive and negative for c-Kit surface expression. The CD45⁻ CD51⁻ Thy-1⁺ c-Kit⁻ fraction also expresses CD9, CD49f and CD29 markers, and are mainly in the G₀/G₁ phase of the cell cycle (Hobbs, 2010). Transplantation assay demonstrated that CD45⁻ CD51⁻ Thy-1⁺ c-Kit⁻ population has 25-fold enrichment on stem cell activity compared to unsorted cells when transplanted into adult recipient testis (Hobbs, 2010).

I sought to employ a similar approach to characterize the two tdTom⁺ cell populations I identified in *Miwi2*^{tdTomato/+} juvenile testis. I showed that tdTom⁺ c-Kit⁻ cells present low side scatter and a CD45⁻ CD51⁻ Thy-1^{lo} CD9^{Hi} CD24⁺ CD49f⁺ CD29⁺ EpCAM^{lo} CD34⁻ Sca-1⁻ MHC-I^{-/lo} marker profile, which is suggestive of a stem cell population (Fig. 21). Comparison between the two tdTomato-expressing populations showed that tdTom⁺ c-Kit⁺ fraction expresses higher levels of the adhesion molecule EpCAM and lower levels of Thy-1 (Fig. 21-22). To my knowledge, this is the first example of such a detailed expression profile, which combines all the surface markers previously used in the literature to enrich or deplete for stem cell activity. Cell cycle analysis also demonstrates that more than 80% of the tdTom⁺ c-Kit⁻ cells are not actively dividing, while the tdTom⁺ c-Kit⁺ fraction possesses a high proliferation rate (Fig. 23). Finally, I evaluated the gene expression profile of tdTom⁺ c-Kit⁻ cells by quantitative RT-PCR to test the expression levels of type A spermatogonia markers. These cells express high levels of GFRA1, c-Ret, Lin28a, Nanos2, Nanos3, Ngn3 and Oct-4 compared to tdTom⁺ c-Kit⁺ and tdTom⁻ c-Kit⁺ populations (Fig. 24). Conversely, both c-Kit and EpCAM expression levels are increased in c-Kit⁺ populations, in accordance with flow cytometry data (Fig. 21-22 and 24). On the other hand, tdTom⁺ c-Kit⁺ cells are likely to be more committed transit-amplifying progenitor cells. Nonetheless, the levels of the *Miwi2* transcript are gradually decreasing from tdTom⁺ c-Kit⁻ to tdTom⁺ Thy1⁺ c-Kit⁺ and tdTom⁺ Thy1⁻ c-Kit⁺ fractions, implying that these cells do not express any *Miwi2* protein. The fact that these cells have comparable tdTomato fluorescence levels might depend on the high stability of this dimeric protein. A similar phenomenon has been described previously for intestinal stem cells marked by a GFP marker from the *Lgr5* endogenous locus. Indeed, progenitor cells derived from GFP^{Hi} intestinal stem cells still maintain low levels of GFP protein, and can be readily isolated by flow cytometry (Sato, 2009).

In conclusion, the tdTom⁺ c-Kit⁻ population possesses three important properties believed to be present in SSCs. First, they express surface markers used to enrich for stem cell activity, such as CD49f, CD29, Thy-1 and CD9, and are devoid of markers present in more differentiating spermatogonia, such as c-Kit and EpCAM (Shinohara, 2000; Shinohara, 2001; Kubota, 2003; Kanatsu-Shinohara, 2004; Hobbs, 2010; Kanatsu-Shinohara, 2011). Second, a high percentage of tdTom⁺ c-Kit⁻ cells are quiescent. Stem cells in other tissues also divide only rarely and a high mitotic rate inversely correlates with stem cell activity (Clermont, 1968; Dym, 1970; Huckins, 1971a-b; de Rooij, 1973; Stingl, 2006; Orford, 2008; Wilson, 2008). Third, tdTom⁺ c-Kit⁻ cells express higher levels of type A spermatogonia markers, like Lin28a, Nanos2, GFRA1 and c-Ret (Meng, 2000; Kanatsu-Shinohara, 2003; Buaas, 2004; Costoya, 2004; Kubota, 2004; Yoshida, 2004; Buageaw, 2005; Hofmann, 2005; Naughton, 2006; He, 2007; Tokuda, 2007; Sada, 2009; Zheng, 2009; Suzuki, 2009; Hobbs, 2010; Nakagawa, 2010; Oatley, 2011). Collectively these data suggest that tdTom⁺ c-Kit⁻ population represents a potential *bona fide* SSC population. Transplantation assay is needed to test the self-renewal ability and reconstitution capacity of these cells. Alternatively, the creation of a mouse line expressing the Cre-Ert2 transgene under the control of Miwi2 regulatory regions would allow us to trace the progeny of Miwi2-expressing cells after pulse labeling in homeostatic conditions. These future experiments will be pivotal to consolidate the hypothesis that tdTom⁺ c-Kit⁻ population comprehends a potential SSC population.

4.2.3 Miwi2 marks two similar cell populations in both adult and juvenile mouse testes

Early transplantation assays of testis cell preparation aimed to understand when the SSCs population is established in neonatal and juvenile testis as well as compared the repopulating capacity of stem cells at different ages (Brinster, 1994b; Shinohara, 2001; McLean, 2003). A first analysis demonstrated that testicular cell preparations from pups (PND 5-12) have a much higher repopulation capacity compared to neonatal (PND 0-2) and almost adult (PND 21-28) cell preparations (Brinster, 1994b). Subsequently, a more detailed analysis revealed that transplantation of cells from juvenile PND 10-12 mice

produces a greater number and larger colonies compared to both neonatal and adult donor (McLean, 2003). Similar studies were conducted between fetal HSCs derived from the fetal liver of E14.5-15.5 embryos and adult HSCs isolated from bone marrow (Morrison, 1995; Bowie, 2007; Yuan, 2012; Copley, 2013). Fetal HSCs have a lower capacity to engraft when transplanted in lethally irradiated adult recipients, but they present a higher proliferation and repopulating capacity than adult HSCs (Morrison, 1995; Bowie, 2007). Recent studies compared the expression profiles from purified adult and fetal HSCs population and discovered that Lin28b is highly expressed in fetal cells while it is completely absent in adult counterparts (Yuan, 2012; Copley, 2013). Overexpression of Lin28b alone is able to convert adult bone marrow-derive HSCs to self-renewal potential and hematopoietic differentiation patterns similar to fetal HSCs (Yuan, 2012; Copley, 2013). The let-7-HMGA2 axis seems to be necessary for this reprogramming: Lin28b reduces mature let-7 miRNA levels in fetal cells, thus increasing HMGA2 expression (Yuan, 2012; Copley, 2013).

Transplantation of unfractionated testis cells revealed that cell preparations from juvenile testis show a greater repopulating capacity compared to cells isolated from adult mice (McLean, 2003). However, this could depend on a higher stem cell potential of juvenile SSCs, as it happens for fetal HSCs, or on a higher percentage of stem cells in juvenile testis. Indeed, differentiated spermatocytes and haploid spermatids accumulate gradually during the first wave of spermatogenesis in a time-dependent manner (Sapford, 1962; Kluin, 1982; Sung, 1986; Vergouwen, 1991). Hence, the percentage of spermatogonia cells in adult testis will be lower compared to pre-pubertal mice, where haploid cells are not yet present. In support to this idea, single cell suspensions from cryptorchid mice, where undifferentiated spermatogonia represent the only germ cell type in the seminiferous tubules, are more enriched for stem cell activity compared to juvenile cells (Shinohara, 2001; Kubota, 2004). I decided to further test these two hypothesis by comparing surface marker expression in tdTom⁺ c-Kit⁻ population in adult and pre-pubertal PND 14 *Miwi2*^{tdTomato/+} male animals. I did not observe significant differences in the expression levels of CD9, CD24, CD29, CD49f and EpCAM. Conversely, Thy-1 expression results to be higher in juvenile cells compared to adult cells (Fig. 25). This difference could be suggestive of a differential self-renewal

capacity. In fact, Thy-1 is widely used for the enrichment of stem cell potential from adult testis preparations prior to transplantation (Kubota, 2004; Oatley, 2006; Hobbs, 2010). Nonetheless, in order to prove a differential cell intrinsic capacity of juvenile versus adult testis preparations, sorted tdTom⁺ c-Kit⁻ cells from adult and juvenile mice need to be transplanted in recipient testis. Number of colonies as well as the area colonized by transplanted cells will allow us to quantitatively compare the repopulating capacity of these two populations, similarly to what has been previously done for fetal and adult HSCs (Morrison, 1995; Bowie, 2007; Yuan, 2012; Copley, 2013).

4.3 Conclusions and future plans

The creation of a new *Miwi2*^{tdTomato} transcriptional reporter allele allowed me to discover that *Miwi2* is expressed in two populations of spermatogonia in prepubertal testis (Fig. 19-20). Flow cytometry analysis showed that one of these two populations, the tdTom⁺ c-Kit⁻ population, is defined by the expression of surface markers that enrich for stem cell activity, while it is depleted of differentiation markers (Fig. 21). Furthermore, these cells are mainly quiescent, a characteristic which positively correlates with stem cell potential (Fig. 23). Finally, tdTom⁺ c-Kit⁻ cells possess a transcriptional profile suggestive of a population highly enriched for stem cells (Fig. 24). Collectively, our data represent the first proof that *Miwi2* is expressed in a subpopulation of spermatogonia cells in juvenile testis. Furthermore, *Miwi2* expression might be used for the isolation of *bona fide* SSC population from the adult testis.

Transplantation assay is recognized as the golden standard to test the regenerative capacity of stem cell population in several tissues (Spangrude, 1988; Brinster, 1994a-b; Stingl, 2006; Shackleton, 2006). Hence, we will use tdTom⁺ c-Kit⁻ cells purified by flow cytometry to reconstitute insulted testis and compare the repopulating capacity of this population compared to bulk testis cells. We are currently crossing the *Miwi2*^{tdTomato} allele with a reporter allele that will help us to identify the colonies derived from donor cells in the recipient testis. As an alternative, stem cell potential can be assessed through lineage tracing technology (Sada, 2009; Nakagawa, 2010). An inducible recombineering enzyme, often the Cre recombinase fused with a mutated estrogen receptor (Cre-Ert2), is posed under the control of the regulatory regions of the gene of interest. The combination with a reporter gene activated after Cre induction allows to follow the progeny of cells that expressed the Cre at the moment of the induction. We are now developing a transgenic strategy in which the Cre-Ert2 transgene is inserted in the mouse genome by Bacterial Artificial Chromosome (BAC) technology with the regulatory regions of the *Miwi2* locus. We will then couple this with an inducible fluorescent marker to monitor the fate of *Miwi2*-expressing cells and their progeny. The combination of these two approaches will further strengthen our hypothesis that *Miwi2*-expression is an important marker for the isolation of SSCs in mouse testis.

The first transplantation studies using testis cell preparations revealed that cells isolated from juvenile males possess a higher stem cell potential compared to neonatal and adult preparations (Brinster, 1994b; Shinohara, 2001; McLean, 2003). We therefore compared the surface marker profile of tdTom⁺ c-Kit⁻ cells from juvenile and adult *Miwil2^{tdTomato/+}* males, and discovered only a difference in the expression of Thy-1 marker (Fig. 25). Since Thy-1 is widely used to enrich for stem cell activity (Kubota, 2004; Oatley, 2006; Hobbs, 2010), we speculate that the lower expression level detected in adult cells could implicate an intrinsically lower stem cell capacity of adult cells compared to the juvenile population, as it has been shown for fetal and adult HSC (Morrison, 1995; Bowie, 2007; Yuan, 2012; Copley, 2013). To prove this, it is needed to transplant tdTom⁺ c-Kit⁻ cells isolated from adult and juvenile *Miwil2^{tdTomato/+}* testis in adult recipients and compared the cologenic capacity of these two populations. In addition, we are planning to compare the gene expression profile of sorted tdTom⁺ c-Kit⁻ cells from juvenile and adult males by microarray to identify any other interesting candidate that is differentially regulated with age. These further experiments will clarify if the greater stem cell potential of juvenile testis preparations in transplantation assay depends on a superior intrinsic self-renewal capacity or a higher concentration of stem cells compared to adult samples.

Bibliography

- Aboobaker, A. A., P. Tomancak, N. Patel, G. M. Rubin and E. C. Lai (2005). "Drosophila microRNAs exhibit diverse spatial expression patterns during embryonic development." Proc Natl Acad Sci U S A **102**(50): 18017-18022.
- Addo-Quaye, C., T. W. Eshoo, D. P. Bartel and M. J. Axtell (2008). "Endogenous siRNA and miRNA targets identified by sequencing of the Arabidopsis degradome." Curr Biol **18**(10): 758-762.
- Adolfsson, J., R. Mansson, N. Buza-Vidas, A. Hultquist, K. Liuba, C. T. Jensen, D. Bryder, L. Yang, O. J. Borge, L. A. Thoren, K. Anderson, E. Sitnicka, Y. Sasaki, M. Sigvardsson and S. E. Jacobsen (2005). "Identification of Flt3⁺ lympho-myeloid stem cells lacking erythro-megakaryocytic potential a revised road map for adult blood lineage commitment." Cell **121**(2): 295-306.
- Alemdehy, M. F., N. G. van Boxtel, H. W. de Looper, I. J. van den Berge, M. A. Sanders, T. Cupedo, I. P. Touw and S. J. Erkeland (2012). "Dicer1 deletion in myeloid-committed progenitors causes neutrophil dysplasia and blocks macrophage/dendritic cell development in mice." Blood **119**(20): 4723-4730.
- Alessi, D. R., M. Andjelkovic, B. Caudwell, P. Cron, N. Morrice, P. Cohen and B. A. Hemmings (1996). "Mechanism of activation of protein kinase B by insulin and IGF-1." EMBO J **15**(23): 6541-6551.
- Alisch, R. S., P. Jin, M. Epstein, T. Caspary and S. T. Warren (2007). "Argonaute2 is essential for mammalian gastrulation and proper mesoderm formation." PLoS Genet **3**(12): e227.
- Allen, E., Z. Xie, A. M. Gustafson and J. C. Carrington (2005). "microRNA-directed phasing during trans-acting siRNA biogenesis in plants." Cell **121**(2): 207-221.
- Allen, M., L. Svensson, M. Roach, J. Hambor, J. McNeish and C. A. Gabel (2000). "Deficiency of the stress kinase p38alpha results in embryonic lethality: characterization of the kinase dependence of stress responses of enzyme-deficient embryonic stem cells." J Exp Med **191**(5): 859-870.
- Altuvia, Y., P. Landgraf, G. Lithwick, N. Elefant, S. Pfeffer, A. Aravin, M. J. Brownstein, T. Tuschl and H. Margalit (2005). "Clustering and conservation patterns of human microRNAs." Nucleic Acids Res **33**(8): 2697-2706.
- Ameres, S. L. and P. D. Zamore (2013). "Diversifying microRNA sequence and function." Nat Rev Mol Cell Biol **14**(8): 475-488.
- Anantharaman, V., E. V. Koonin and L. Aravind (2002). "Comparative genomics and evolution of proteins involved in RNA metabolism." Nucleic Acids Res **30**(7): 1427-1464.
- Anderson, P. and N. Kedersha (2006). "RNA granules." J Cell Biol **172**(6): 803-808.
- Aravin, A., D. Gaidatzis, S. Pfeffer, M. Lagos-Quintana, P. Landgraf, N. Iovino, P. Morris, M. J. Brownstein, S. Kuramochi-Miyagawa, T. Nakano, M. Chien, J. J. Russo, J. Ju, R. Sheridan, C. Sander, M. Zavolan and T. Tuschl (2006). "A novel class of small RNAs bind to MILI protein in mouse testes." Nature **442**(7099): 203-207.
- Aravin, A. A., N. M. Naumova, A. V. Tulin, V. V. Vagin, Y. M. Rozovsky and V. A. Gvozdev (2001). "Double-stranded RNA-mediated silencing of genomic tandem repeats and transposable elements in the D. melanogaster germline." Curr Biol **11**(13): 1017-1027.
- Aravin, A. A., R. Sachidanandam, D. Bourc'his, C. Schaefer, D. Pezic, K. F. Toth, T. Bestor and G. J. Hannon (2008). "A piRNA pathway primed by individual transposons is linked to de novo DNA methylation in mice." Mol Cell **31**(6): 785-799.

Aravin, A. A., R. Sachidanandam, A. Girard, K. Fejes-Toth and G. J. Hannon (2007). "Developmentally regulated piRNA clusters implicate MILI in transposon control." Science **316**(5825): 744-747.

Aravin, A. A., G. W. van der Heijden, J. Castaneda, V. V. Vagin, G. J. Hannon and A. Bortvin (2009). "Cytoplasmic compartmentalization of the fetal piRNA pathway in mice." PLoS Genet **5**(12): e1000764.

Asselin-Labat, M. L., M. Shackleton, J. Stingl, F. Vaillant, N. C. Forrest, C. J. Eaves, J. E. Visvader and G. J. Lindeman (2006). "Steroid hormone receptor status of mouse mammary stem cells." J Natl Cancer Inst **98**(14): 1011-1014.

Azuma-Mukai, A., H. Oguri, T. Mituyama, Z. R. Qian, K. Asai, H. Siomi and M. C. Siomi (2008). "Characterization of endogenous human Argonautes and their miRNA partners in RNA silencing." Proc Natl Acad Sci U S A **105**(23): 7964-7969.

Babiarz, J. E., J. G. Ruby, Y. Wang, D. P. Bartel and R. Blelloch (2008). "Mouse ES cells express endogenous shRNAs, siRNAs, and other Microprocessor-independent, Dicer-dependent small RNAs." Genes Dev **22**(20): 2773-2785.

Baek, D., J. Villen, C. Shin, F. D. Camargo, S. P. Gygi and D. P. Bartel (2008). "The impact of microRNAs on protein output." Nature **455**(7209): 64-71.

Bagga, S., J. Bracht, S. Hunter, K. Massirer, J. Holtz, R. Eachus and A. E. Pasquinelli (2005). "Regulation by let-7 and lin-4 miRNAs results in target mRNA degradation." Cell **122**(4): 553-563.

Baguna, J., E. Salo and R. Romero (1989). "Effects of activators and antagonists of the neuropeptides substance P and substance K on cell proliferation in planarians." Int J Dev Biol **33**(2): 261-266.

Bartel, D. P. (2004). "MicroRNAs: genomics, biogenesis, mechanism, and function." Cell **116**(2): 281-297.

Bartel, D. P. (2009). "MicroRNAs: target recognition and regulatory functions." Cell **136**(2): 215-233.

Bartmanska, J. and Y. Clermont (1983). "Renewal of type A spermatogonia in adult rats." Cell Tissue Kinet **16**(2): 135-143.

Baskerville, S. and D. P. Bartel (2005). "Microarray profiling of microRNAs reveals frequent coexpression with neighboring miRNAs and host genes." RNA **11**(3): 241-247.

Baulcombe, D. (2004). "RNA silencing in plants." Nature **431**(7006): 356-363.

Bazzini, A. A., M. T. Lee and A. J. Giraldez (2012). "Ribosome profiling shows that miR-430 reduces translation before causing mRNA decay in zebrafish." Science **336**(6078): 233-237.

Beardmore, V. A., H. J. Hinton, C. Eftychi, M. Apostolaki, M. Armaka, J. Darragh, J. McIlrath, J. M. Carr, L. J. Armit, C. Clacher, L. Malone, G. Kollias and J. S. Arthur (2005). "Generation and characterization of p38beta (MAPK11) gene-targeted mice." Mol Cell Biol **25**(23): 10454-10464.

Behm-Ansmant, I., J. Rehwinkel, T. Doerks, A. Stark, P. Bork and E. Izaurralde (2006). "mRNA degradation by miRNAs and GW182 requires both CCR4:NOT deadenylase and DCP1:DCP2 decapping complexes." Genes Dev **20**(14): 1885-1898.

Bellve, A. R., J. C. Cavicchia, C. F. Millette, D. A. O'Brien, Y. M. Bhatnagar and M. Dym (1977). "Spermatogenic cells of the prepuberal mouse. Isolation and morphological characterization." J Cell Biol **74**(1): 68-85.

Belver, L., V. G. de Yébenes and A. R. Ramiro (2010). "MicroRNAs prevent the generation of autoreactive antibodies." Immunity **33**(5): 713-722.

- Ben-Levy, R., S. Hooper, R. Wilson, H. F. Paterson and C. J. Marshall (1998). "Nuclear export of the stress-activated protein kinase p38 mediated by its substrate MAPKAP kinase-2." Curr Biol **8**(19): 1049-1057.
- Benzel, I., Y. A. Barde and E. Casademunt (2001). "Strain-specific complementation between NRIF1 and NRIF2, two zinc finger proteins sharing structural and biochemical properties." Gene **281**(1-2): 19-30.
- Berezikov, E., G. van Tetering, M. Verheul, J. van de Belt, L. van Laake, J. Vos, R. Verloop, M. van de Wetering, V. Guryev, S. Takada, A. J. van Zonneveld, H. Mano, R. Plasterk and E. Cuppen (2006). "Many novel mammalian microRNA candidates identified by extensive cloning and RAKE analysis." Genome Res **16**(10): 1289-1298.
- Bernstein, E., A. A. Caudy, S. M. Hammond and G. J. Hannon (2001). "Role for a bidentate ribonuclease in the initiation step of RNA interference." Nature **409**(6818): 363-366.
- Bernstein, E., S. Y. Kim, M. A. Carmell, E. P. Murchison, H. Alcorn, M. Z. Li, A. A. Mills, S. J. Elledge, K. V. Anderson and G. J. Hannon (2003). "Dicer is essential for mouse development." Nat Genet **35**(3): 215-217.
- Bhattacharyya, S. N., R. Habermacher, U. Martine, E. I. Closs and W. Filipowicz (2006). "Stress-induced reversal of microRNA repression and mRNA P-body localization in human cells." Cold Spring Harb Symp Quant Biol **71**: 513-521.
- Bilovocky, N. A., R. R. Romito-DiGiacomo, C. L. Murcia, S. M. Maricich and K. Herrup (2003). "Factors in the genetic background suppress the engrailed-1 cerebellar phenotype." J Neurosci **23**(12): 5105-5112.
- Blevins, T., R. Rajeswaran, P. V. Shivaprasad, D. Beknazariants, A. Si-Ammour, H. S. Park, F. Vazquez, D. Robertson, F. Meins, Jr., T. Hohn and M. M. Pooggin (2006). "Four plant Dicers mediate viral small RNA biogenesis and DNA virus induced silencing." Nucleic Acids Res **34**(21): 6233-6246.
- Bohmert, K., I. Camus, C. Bellini, D. Bouchez, M. Caboche and C. Benning (1998). "AGO1 defines a novel locus of Arabidopsis controlling leaf development." EMBO J **17**(1): 170-180.
- Boland, A., F. Tritzschler, S. Heimstadt, E. Izaurrealde and O. Weichenrieder (2010). "Crystal structure and ligand binding of the MID domain of a eukaryotic Argonaute protein." EMBO Rep **11**(7): 522-527.
- Bonyadi, M., S. A. Rusholme, F. M. Cousins, H. C. Su, C. A. Biron, M. Farrall and R. J. Akhurst (1997). "Mapping of a major genetic modifier of embryonic lethality in TGF beta 1 knockout mice." Nat Genet **15**(2): 207-211.
- Bourc'his, D. and T. H. Bestor (2004). "Meiotic catastrophe and retrotransposon reactivation in male germ cells lacking Dnmt3L." Nature **431**(7004): 96-99.
- Bowie, M. B., D. G. Kent, B. Dykstra, K. D. McKnight, L. McCaffrey, P. A. Hoodless and C. J. Eaves (2007). "Identification of a new intrinsically timed developmental checkpoint that reprograms key hematopoietic stem cell properties." Proc Natl Acad Sci U S A **104**(14): 5878-5882.
- Brennecke, J., A. A. Aravin, A. Stark, M. Dus, M. Kellis, R. Sachidanandam and G. J. Hannon (2007). "Discrete small RNA-generating loci as master regulators of transposon activity in Drosophila." Cell **128**(6): 1089-1103.
- Brennecke, J., D. R. Hipfner, A. Stark, R. B. Russell and S. M. Cohen (2003). "bantam encodes a developmentally regulated microRNA that controls cell proliferation and regulates the proapoptotic gene hid in Drosophila." Cell **113**(1): 25-36.
- Brennecke, J., A. Stark, R. B. Russell and S. M. Cohen (2005). "Principles of microRNA-target recognition." PLoS Biol **3**(3): e85.

- Brinster, R. L. and M. R. Avarbock (1994b). "Germline transmission of donor haplotype following spermatogonial transplantation." Proc Natl Acad Sci U S A **91**(24): 11303-11307.
- Brinster, R. L. and J. W. Zimmermann (1994a). "Spermatogenesis following male germ-cell transplantation." Proc Natl Acad Sci U S A **91**(24): 11298-11302.
- Brodersen, P., L. Sakvarelidze-Achard, M. Bruun-Rasmussen, P. Dunoyer, Y. Y. Yamamoto, L. Sieburth and O. Voinnet (2008). "Widespread translational inhibition by plant miRNAs and siRNAs." Science **320**(5880): 1185-1190.
- Brown, E. H. and R. C. King (1962). "Oogonial and spermatogonial differentiation within a mosaic gonad of *Drosophila melanogaster*." Growth **26**: 53-69.
- Brown, E. H. and R. C. King (1964). "Studies on the Events Resulting in the Formation of an Egg Chamber in *Drosophila Melanogaster*." Growth **28**: 41-81.
- Brown, F. D., E. L. Keeling, A. D. Le and B. J. Swalla (2009). "Whole body regeneration in a colonial ascidian, *Botrylloides violaceus*." J Exp Zool B Mol Dev Evol **312**(8): 885-900.
- Buaas, F. W., A. L. Kirsh, M. Sharma, D. J. McLean, J. L. Morris, M. D. Griswold, D. G. de Rooij and R. E. Braun (2004). "Plzf is required in adult male germ cells for stem cell self-renewal." Nat Genet **36**(6): 647-652.
- Buageaw, A., M. Sukhwani, A. Ben-Yehudah, J. Ehmcke, V. Y. Rawe, C. Pholpramool, K. E. Orwig and S. Schlatt (2005). "GDNF family receptor alpha1 phenotype of spermatogonial stem cells in immature mouse testes." Biol Reprod **73**(5): 1011-1016.
- Buhler, M., A. Verdel and D. Moazed (2006). "Tethering RITS to a nascent transcript initiates RNAi- and heterochromatin-dependent gene silencing." Cell **125**(5): 873-886.
- Buza-Vidas, N., V. B. Cismasiu, S. Moore, A. J. Mead, P. S. Woll, M. Lutteropp, L. Melchiori, S. Luc, T. Bouriez-Jones, D. Atkinson, D. O'Carroll, S. E. Jacobsen and C. Nerlov (2012). "Dicer is selectively important for the earliest stages of erythroid development." Blood **120**(12): 2412-2416.
- Cai, X., C. H. Hagedorn and B. R. Cullen (2004). "Human microRNAs are processed from capped, polyadenylated transcripts that can also function as mRNAs." RNA **10**(12): 1957-1966.
- Calamito, M., M. M. Juntilla, M. Thomas, D. L. Northrup, J. Rathmell, M. J. Birnbaum, G. Koretzky and D. Allman (2010). "Akt1 and Akt2 promote peripheral B-cell maturation and survival." Blood **115**(20): 4043-4050.
- Calleja, V., D. Alcor, M. Laguerre, J. Park, B. Vojnovic, B. A. Hemmings, J. Downward, P. J. Parker and B. Larijani (2007). "Intramolecular and intermolecular interactions of protein kinase B define its activation in vivo." PLoS Biol **5**(4): e95.
- Carmell, M. A., A. Girard, H. J. van de Kant, D. Bourc'his, T. H. Bestor, D. G. de Rooij and G. J. Hannon (2007). "MIWI2 is essential for spermatogenesis and repression of transposons in the mouse male germline." Dev Cell **12**(4): 503-514.
- Carswell, S. and J. C. Alwine (1989). "Efficiency of utilization of the simian virus 40 late polyadenylation site: effects of upstream sequences." Mol Cell Biol **9**(10): 4248-4258.
- Carthew, R. W. and E. J. Sontheimer (2009). "Origins and Mechanisms of miRNAs and siRNAs." Cell **136**(4): 642-655.
- Casademunt, E., B. D. Carter, I. Benzel, J. M. Frade, G. Dechant and Y. A. Barde (1999). "The zinc finger protein NRIF interacts with the neurotrophin receptor p75(NTR) and participates in programmed cell death." EMBO J **18**(21): 6050-6061.

- Cerutti, H. and J. A. Casas-Mollano (2006). "On the origin and functions of RNA-mediated silencing: from protists to man." Curr Genet **50**(2): 81-99.
- Cerutti, L., N. Mian and A. Bateman (2000). "Domains in gene silencing and cell differentiation proteins: the novel PAZ domain and redefinition of the Piwi domain." Trends Biochem Sci **25**(10): 481-482.
- Cheloufi, S., C. O. Dos Santos, M. M. Chong and G. J. Hannon (2010). "A dicer-independent miRNA biogenesis pathway that requires Ago catalysis." Nature **465**(7298): 584-589.
- Chen, C. Z., L. Li, H. F. Lodish and D. P. Bartel (2004b). "MicroRNAs modulate hematopoietic lineage differentiation." Science **303**(5654): 83-86.
- Chen, J., P. R. Somanath, O. Razorenova, W. S. Chen, N. Hay, P. Bornstein and T. V. Byzova (2005). "Akt1 regulates pathological angiogenesis, vascular maturation and permeability in vivo." Nat Med **11**(11): 1188-1196.
- Chen, W. S., P. Z. Xu, K. Gottlob, M. L. Chen, K. Sokol, T. Shiyanova, I. Roninson, W. Weng, R. Suzuki, K. Tobe, T. Kadowaki and N. Hay (2001). "Growth retardation and increased apoptosis in mice with homozygous disruption of the Akt1 gene." Genes Dev **15**(17): 2203-2208.
- Chen, X. (2004a). "A microRNA as a translational repressor of APETALA2 in Arabidopsis flower development." Science **303**(5666): 2022-2025.
- Chendrimada, T. P., R. I. Gregory, E. Kumaraswamy, J. Norman, N. Cooch, K. Nishikura and R. Shiekhattar (2005). "TRBP recruits the Dicer complex to Ago2 for microRNA processing and gene silencing." Nature **436**(7051): 740-744.
- Chi, S. W., G. J. Hannon and R. B. Darnell (2012). "An alternative mode of microRNA target recognition." Nat Struct Mol Biol **19**(3): 321-327.
- Chiang, H. R., L. W. Schoenfeld, J. G. Ruby, V. C. Auyeung, N. Spies, D. Baek, W. K. Johnston, C. Russ, S. Luo, J. E. Babiarz, R. Blelloch, G. P. Schroth, C. Nusbaum and D. P. Bartel (2010). "Mammalian microRNAs: experimental evaluation of novel and previously annotated genes." Genes Dev **24**(10): 992-1009.
- Chiquoine, A. D. (1954). "The identification, origin, and migration of the primordial germ cells in the mouse embryo." Anat Rec **118**(2): 135-146.
- Cho, H., J. Mu, J. K. Kim, J. L. Thorvaldsen, Q. Chu, E. B. Crenshaw, 3rd, K. H. Kaestner, M. S. Bartolomei, G. I. Shulman and M. J. Birnbaum (2001b). "Insulin resistance and a diabetes mellitus-like syndrome in mice lacking the protein kinase Akt2 (PKB beta)." Science **292**(5522): 1728-1731.
- Cho, H., J. L. Thorvaldsen, Q. Chu, F. Feng and M. J. Birnbaum (2001a). "Akt1/PKBalpha is required for normal growth but dispensable for maintenance of glucose homeostasis in mice." J Biol Chem **276**(42): 38349-38352.
- Choi, S. Y., P. Huang, G. M. Jenkins, D. C. Chan, J. Schiller and M. A. Frohman (2006). "A common lipid links Mfn-mediated mitochondrial fusion and SNARE-regulated exocytosis." Nat Cell Biol **8**(11): 1255-1262.
- Christodoulou, F., F. Raible, R. Tomer, O. Simakov, K. Trachana, S. Klaus, H. Snyman, G. J. Hannon, P. Bork and D. Arendt (2010). "Ancient animal microRNAs and the evolution of tissue identity." Nature **463**(7284): 1084-1088.
- Chu, Y., X. Yue, S. T. Younger, B. A. Janowski and D. R. Corey (2010). "Involvement of argonaute proteins in gene silencing and activation by RNAs complementary to a non-coding transcript at the progesterone receptor promoter." Nucleic Acids Res **38**(21): 7736-7748.

- Cifuentes, D., H. Xue, D. W. Taylor, H. Patnode, Y. Mishima, S. Cheloufi, E. Ma, S. Mane, G. J. Hannon, N. D. Lawson, S. A. Wolfe and A. J. Giraldez (2010). "A novel miRNA processing pathway independent of Dicer requires Argonaute2 catalytic activity." *Science* **328**(5986): 1694-1698.
- Clermont, Y. and E. Bustos-Obregon (1968). "Re-examination of spermatogonial renewal in the rat by means of seminiferous tubules mounted "in toto"." *Am J Anat* **122**(2): 237-247.
- Clermont, Y. and L. Hermo (1975). "Spermatogonial stem cells in the albino rat." *Am J Anat* **142**(2): 159-175.
- Clermont, Y. and B. Perey (1957). "Quantitative study of the cell population of the seminiferous tubules in immature rats." *Am J Anat* **100**(2): 241-267.
- Clifton, A. D., P. R. Young and P. Cohen (1996). "A comparison of the substrate specificity of MAPKAP kinase-2 and MAPKAP kinase-3 and their activation by cytokines and cellular stress." *FEBS Lett* **392**(3): 209-214.
- Cobb, B. S., A. Hertweck, J. Smith, E. O'Connor, D. Graf, T. Cook, S. T. Smale, S. Sakaguchi, F. J. Livesey, A. G. Fisher and M. Merkenschlager (2006). "A role for Dicer in immune regulation." *J Exp Med* **203**(11): 2519-2527.
- Cobb, B. S., T. B. Nesterova, E. Thompson, A. Hertweck, E. O'Connor, J. Godwin, C. B. Wilson, N. Brockdorff, A. G. Fisher, S. T. Smale and M. Merkenschlager (2005). "T cell lineage choice and differentiation in the absence of the RNase III enzyme Dicer." *J Exp Med* **201**(9): 1367-1373.
- Cogoni, C., J. T. Irelan, M. Schumacher, T. J. Schmidhauser, E. U. Selker and G. Macino (1996). "Transgene silencing of the *al-1* gene in vegetative cells of *Neurospora* is mediated by a cytoplasmic effector and does not depend on DNA-DNA interactions or DNA methylation." *EMBO J* **15**(12): 3153-3163.
- Cogoni, C. and G. Macino (1999). "Posttranscriptional gene silencing in *Neurospora* by a RecQ DNA helicase." *Science* **286**(5448): 2342-2344.
- Copley, M. R., S. Babovic, C. Benz, D. J. Knapp, P. A. Beer, D. G. Kent, S. Wohrer, D. Q. Treloar, C. Day, K. Rowe, H. Mader, F. Kuchenbauer, R. K. Humphries and C. J. Eaves (2013). "The Lin28b-let-7-Hmga2 axis determines the higher self-renewal potential of fetal haematopoietic stem cells." *Nat Cell Biol* **15**(8): 916-925.
- Corcoran, D. L., K. V. Pandit, B. Gordon, A. Bhattacharjee, N. Kaminski and P. V. Benos (2009). "Features of mammalian microRNA promoters emerge from polymerase II chromatin immunoprecipitation data." *PLoS One* **4**(4): e5279.
- Costoya, J. A., R. M. Hobbs, M. Barna, G. Cattoretti, K. Manova, M. Sukhwani, K. E. Orwig, D. J. Wolgemuth and P. P. Pandolfi (2004). "Essential role of *Plzf* in maintenance of spermatogonial stem cells." *Nat Genet* **36**(6): 653-659.
- Cougot, N., S. Babajko and B. Seraphin (2004). "Cytoplasmic foci are sites of mRNA decay in human cells." *J Cell Biol* **165**(1): 31-40.
- Cox, D. N., A. Chao, J. Baker, L. Chang, D. Qiao and H. Lin (1998). "A novel class of evolutionarily conserved genes defined by *piwi* are essential for stem cell self-renewal." *Genes Dev* **12**(23): 3715-3727.
- Cox, D. N., A. Chao and H. Lin (2000). "*piwi* encodes a nucleoplasmic factor whose activity modulates the number and division rate of germline stem cells." *Development* **127**(3): 503-514.
- Dalmay, T., A. Hamilton, S. Rudd, S. Angell and D. C. Baulcombe (2000). "An RNA-dependent RNA polymerase gene in *Arabidopsis* is required for posttranscriptional gene silencing mediated by a transgene but not by a virus." *Cell* **101**(5): 543-553.

- DaRocha, W. D., K. Otsu, S. M. Teixeira and J. E. Donelson (2004). "Tests of cytoplasmic RNA interference (RNAi) and construction of a tetracycline-inducible T7 promoter system in *Trypanosoma cruzi*." Mol Biochem Parasitol **133**(2): 175-186.
- Darricarrere, N., N. Liu, T. Watanabe and H. Lin (2013). "Function of Piwi, a nuclear Piwi/Argonaute protein, is independent of its slicer activity." Proc Natl Acad Sci U S A **110**(4): 1297-1302.
- Davis, B. N., A. C. Hilyard, G. Lagna and A. Hata (2008). "SMAD proteins control DROSHA-mediated microRNA maturation." Nature **454**(7200): 56-61.
- Davis, T. L., J. M. Trasler, S. B. Moss, G. J. Yang and M. S. Bartolomei (1999). "Acquisition of the H19 methylation imprint occurs differentially on the parental alleles during spermatogenesis." Genomics **58**(1): 18-28.
- De Fazio, S., N. Bartonicek, M. Di Giacomo, C. Abreu-Goodger, A. Sankar, C. Funaya, C. Antony, P. N. Moreira, A. J. Enright and D. O'Carroll (2011). "The endonuclease activity of Mili fuels piRNA amplification that silences LINE1 elements." Nature **480**(7376): 259-263.
- De Mulder, K., D. Pfister, G. Kuales, B. Egger, W. Salvenmoser, M. Willems, J. Steger, K. Fauster, R. Micura, G. Borgonie and P. Ladurner (2009). "Stem cells are differentially regulated during development, regeneration and homeostasis in flatworms." Dev Biol **334**(1): 198-212.
- de Rooij, D. G. (1973). "Spermatogonial stem cell renewal in the mouse. I. Normal situation." Cell Tissue Kinet **6**(3): 281-287.
- de Rooij, D. G. and L. D. Russell (2000). "All you wanted to know about spermatogonia but were afraid to ask." J Androl **21**(6): 776-798.
- de Vries, W. N., L. T. Binns, K. S. Fancher, J. Dean, R. Moore, R. Kemler and B. B. Knowles (2000). "Expression of Cre recombinase in mouse oocytes: a means to study maternal effect genes." Genesis **26**(2): 110-112.
- Deleris, A., J. Gallego-Bartolome, J. Bao, K. D. Kasschau, J. C. Carrington and O. Voinnet (2006). "Hierarchical action and inhibition of plant Dicer-like proteins in antiviral defense." Science **313**(5783): 68-71.
- Deng, W. and H. Lin (2002). "miwi, a murine homolog of piwi, encodes a cytoplasmic protein essential for spermatogenesis." Dev Cell **2**(6): 819-830.
- Denker, E., M. Manuel, L. Leclere, H. Le Guyader and N. Rabet (2008). "Ordered progression of nematogenesis from stem cells through differentiation stages in the tentacle bulb of *Clytia hemisphaerica* (Hydrozoa, Cnidaria)." Dev Biol **315**(1): 99-113.
- Denli, A. M., B. B. Tops, R. H. Plasterk, R. F. Ketting and G. J. Hannon (2004). "Processing of primary microRNAs by the Microprocessor complex." Nature **432**(7014): 231-235.
- Di Giacomo, M., S. Comazzetto, H. Saini, S. De Fazio, C. Carrieri, M. Morgan, L. Vasiliauskaite, V. Benes, A. J. Enright and D. O'Carroll (2013). "Multiple epigenetic mechanisms and the piRNA pathway enforce LINE1 silencing during adult spermatogenesis." Mol Cell **50**(4): 601-608.
- Dickson, M. C., J. S. Martin, F. M. Cousins, A. B. Kulkarni, S. Karlsson and R. J. Akhurst (1995). "Defective haematopoiesis and vasculogenesis in transforming growth factor-beta 1 knock out mice." Development **121**(6): 1845-1854.
- Dideberg, V., G. Kristjansdottir, L. Milani, C. Libioulle, S. Sigurdsson, E. Louis, A. C. Wiman, S. Vermeire, P. Rutgeerts, J. Belaiche, D. Franchimont, A. Van Gossum, V. Bours and A. C. Syvanen (2007). "An insertion-deletion polymorphism in the interferon regulatory Factor 5 (IRF5) gene confers risk of inflammatory bowel diseases." Hum Mol Genet **16**(24): 3008-3016.

- Diederichs, S. and D. A. Haber (2007). "Dual role for argonautes in microRNA processing and posttranscriptional regulation of microRNA expression." Cell **131**(6): 1097-1108.
- Djikeng, A., H. Shi, C. Tschudi and E. Ullu (2001). "RNA interference in *Trypanosoma brucei*: cloning of small interfering RNAs provides evidence for retroposon-derived 24-26-nucleotide RNAs." RNA **7**(11): 1522-1530.
- Doench, J. G. and P. A. Sharp (2004). "Specificity of microRNA target selection in translational repression." Genes Dev **18**(5): 504-511.
- Dore, L. C., J. D. Amigo, C. O. Dos Santos, Z. Zhang, X. Gai, J. W. Tobias, D. Yu, A. M. Klein, C. Dorman, W. Wu, R. C. Hardison, B. H. Paw and M. J. Weiss (2008). "A GATA-1-regulated microRNA locus essential for erythropoiesis." Proc Natl Acad Sci U S A **105**(9): 3333-3338.
- Drumond, A. L., M. L. Meistrich and H. Chiarini-Garcia (2011). "Spermatogonial morphology and kinetics during testis development in mice: a high-resolution light microscopy approach." Reproduction **142**(1): 145-155.
- Dueck, A., C. Ziegler, A. Eichner, E. Berezikov and G. Meister (2012). "microRNAs associated with the different human Argonaute proteins." Nucleic Acids Res **40**(19): 9850-9862.
- Dunoyer, P., C. H. Lecellier, E. A. Parizotto, C. Himber and O. Voinnet (2004). "Probing the microRNA and small interfering RNA pathways with virus-encoded suppressors of RNA silencing." Plant Cell **16**(5): 1235-1250.
- Dym, M. and D. W. Fawcett (1970). "The blood-testis barrier in the rat and the physiological compartmentation of the seminiferous epithelium." Biol Reprod **3**(3): 308-326.
- Easton, R. M., H. Cho, K. Roovers, D. W. Shineman, M. Mizrahi, M. S. Forman, V. M. Lee, M. Szabolcs, R. de Jong, T. Oltersdorf, T. Ludwig, A. Efstratiadis and M. J. Birnbaum (2005). "Role for Akt3/protein kinase Bgamma in attainment of normal brain size." Mol Cell Biol **25**(5): 1869-1878.
- Ebata, K. T., X. Zhang and M. C. Nagano (2005). "Expression patterns of cell-surface molecules on male germ line stem cells during postnatal mouse development." Mol Reprod Dev **72**(2): 171-181.
- Eddy, E. M. (2002). "Male germ cell gene expression." Recent Prog Horm Res **57**: 103-128.
- Elbashir, S. M., W. Lendeckel and T. Tuschl (2001). "RNA interference is mediated by 21- and 22-nucleotide RNAs." Genes Dev **15**(2): 188-200.
- Elkayam, E., C. D. Kuhn, A. Tocilj, A. D. Haase, E. M. Greene, G. J. Hannon and L. Joshua-Tor (2012). "The structure of human argonaute-2 in complex with miR-20a." Cell **150**(1): 100-110.
- Emery, J. F., S. K. Floyd, J. Alvarez, Y. Eshed, N. P. Hawker, A. Izhaki, S. F. Baum and J. L. Bowman (2003). "Radial patterning of Arabidopsis shoots by class III HD-ZIP and KANADI genes." Curr Biol **13**(20): 1768-1774.
- English, J. J., E. Mueller and D. C. Baulcombe (1996). "Suppression of Virus Accumulation in Transgenic Plants Exhibiting Silencing of Nuclear Genes." Plant Cell **8**(2): 179-188.
- Erickson, B. H. (1978). "Effect of continuous gamma-radiation on the stem and differentiating spermatogonia of the adult rat." Mutat Res **52**(1): 117-128.
- Erickson, B. H. (1981). "Survival and renewal of murine stem spermatogonia following ⁶⁰Co gamma radiation." Radiat Res **86**(1): 34-51.
- Eulalio, A., I. Behm-Ansmant, D. Schweizer and E. Izaurralde (2007). "P-body formation is a consequence, not the cause, of RNA-mediated gene silencing." Mol Cell Biol **27**(11): 3970-3981.

- Eulalio, A., E. Huntzinger and E. Izaurralde (2008). "GW182 interaction with Argonaute is essential for miRNA-mediated translational repression and mRNA decay." Nat Struct Mol Biol **15**(4): 346-353.
- Eun, C., Z. J. Lorkovic, U. Naumann, Q. Long, E. R. Havecker, S. A. Simon, B. C. Meyers, A. J. Matzke and M. Matzke (2011). "AGO6 functions in RNA-mediated transcriptional gene silencing in shoot and root meristems in *Arabidopsis thaliana*." PLoS One **6**(10): e25730.
- Faehnle, C. R., E. Elkayam, A. D. Haase, G. J. Hannon and L. Joshua-Tor (2013). "The making of a slicer: activation of human Argonaute-1." Cell Rep **3**(6): 1901-1909.
- Farh, K. K., A. Grimson, C. Jan, B. P. Lewis, W. K. Johnston, L. P. Lim, C. B. Burge and D. P. Bartel (2005). "The widespread impact of mammalian MicroRNAs on mRNA repression and evolution." Science **310**(5755): 1817-1821.
- Farley, F. W., P. Soriano, L. S. Steffen and S. M. Dymecki (2000). "Widespread recombinase expression using FLPeR (flipper) mice." Genesis **28**(3-4): 106-110.
- Fawcett, D. W., S. Ito and D. Slautterback (1959). "The occurrence of intercellular bridges in groups of cells exhibiting synchronous differentiation." J Biophys Biochem Cytol **5**(3): 453-460.
- Fayard, E., J. Gill, M. Paolino, D. Hynx, G. A. Hollander and B. A. Hemmings (2007). "Deletion of PKBalpha/Akt1 affects thymic development." PLoS One **2**(10): e992.
- Festing, M. F., E. M. Simpson, M. T. Davisson and L. E. Mobraaten (1999). "Revised nomenclature for strain 129 mice." Mamm Genome **10**(8): 836.
- Fire, A., S. Xu, M. K. Montgomery, S. A. Kostas, S. E. Driver and C. C. Mello (1998). "Potent and specific genetic interference by double-stranded RNA in *Caenorhabditis elegans*." Nature **391**(6669): 806-811.
- Flemr, M., J. Ma, R. M. Schultz and P. Svoboda (2010). "P-body loss is concomitant with formation of a messenger RNA storage domain in mouse oocytes." Biol Reprod **82**(5): 1008-1017.
- Forman, J. J., A. Legesse-Miller and H. A. Collier (2008). "A search for conserved sequences in coding regions reveals that the let-7 microRNA targets Dicer within its coding sequence." Proc Natl Acad Sci U S A **105**(39): 14879-14884.
- Frank, F., M. R. Fabian, J. Stepinski, J. Jemielity, E. Darzynkiewicz, N. Sonenberg and B. Nagar (2011). "Structural analysis of 5'-mRNA-cap interactions with the human AGO2 MID domain." EMBO Rep **12**(5): 415-420.
- Frank, F., N. Sonenberg and B. Nagar (2010). "Structural basis for 5'-nucleotide base-specific recognition of guide RNA by human AGO2." Nature **465**(7299): 818-822.
- Freshney, N. W., L. Rawlinson, F. Guesdon, E. Jones, S. Cowley, J. Hsuan and J. Saklatvala (1994). "Interleukin-1 activates a novel protein kinase cascade that results in the phosphorylation of Hsp27." Cell **78**(6): 1039-1049.
- Frias, M. A., C. C. Thoreen, J. D. Jaffe, W. Schroder, T. Sculley, S. A. Carr and D. M. Sabatini (2006). "mSin1 is necessary for Akt/PKB phosphorylation, and its isoforms define three distinct mTORC2s." Curr Biol **16**(18): 1865-1870.
- Funayama, N., M. Nakatsukasa, K. Mohri, Y. Masuda and K. Agata (2010). "Piwi expression in archeocytes and choanocytes in demosponges: insights into the stem cell system in demosponges." Evol Dev **12**(3): 275-287.
- Gaestel, M. (2006). "MAPKAP kinases - MKs - two's company, three's a crowd." Nat Rev Mol Cell Biol **7**(2): 120-130.

Garofalo, R. S., S. J. Orena, K. Rafidi, A. J. Torchia, J. L. Stock, A. L. Hildebrandt, T. Coskran, S. C. Black, D. J. Brees, J. R. Wicks, J. D. McNeish and K. G. Coleman (2003). "Severe diabetes, age-dependent loss of adipose tissue, and mild growth deficiency in mice lacking Akt2/PKB beta." J Clin Invest **112**(2): 197-208.

Geest, C. R. and P. J. Coffey (2009). "MAPK signaling pathways in the regulation of hematopoiesis." J Leukoc Biol **86**(2): 237-250.

Genomes Project, C., G. R. Abecasis, D. Altshuler, A. Auton, L. D. Brooks, R. M. Durbin, R. A. Gibbs, M. E. Hurles and G. A. McVean (2010). "A map of human genome variation from population-scale sequencing." Nature **467**(7319): 1061-1073.

Gerlai, R. (1996). "Gene-targeting studies of mammalian behavior: is it the mutation or the background genotype?" Trends Neurosci **19**(5): 177-181.

Ginsburg, M., M. H. Snow and A. McLaren (1990). "Primordial germ cells in the mouse embryo during gastrulation." Development **110**(2): 521-528.

Giraldez, A. J., R. M. Cinalli, M. E. Glasner, A. J. Enright, J. M. Thomson, S. Baskerville, S. M. Hammond, D. P. Bartel and A. F. Schier (2005). "MicroRNAs regulate brain morphogenesis in zebrafish." Science **308**(5723): 833-838.

Giraldez, A. J., Y. Mishima, J. Rihel, R. J. Grocock, S. Van Dongen, K. Inoue, A. J. Enright and A. F. Schier (2006). "Zebrafish MiR-430 promotes deadenylation and clearance of maternal mRNAs." Science **312**(5770): 75-79.

Girard, A., R. Sachidanandam, G. J. Hannon and M. A. Carmell (2006). "A germline-specific class of small RNAs binds mammalian Piwi proteins." Nature **442**(7099): 199-202.

Goldsby, R.A., T.J. Kindt, B.A. Osborne, and J. Kuby (2003). "Immunology". Fifth Edition, W. H. Freeman and Company.

Goncalves, M. D., E. E. Pistilli, A. Balduzzi, M. J. Birnbaum, J. Lachey, T. S. Khurana and R. S. Ahima (2010). "Akt deficiency attenuates muscle size and function but not the response to ActRIIB inhibition." PLoS One **5**(9): e12707.

Graham, R. R., C. Kyogoku, S. Sigurdsson, I. A. Vlasova, L. R. Davies, E. C. Baechler, R. M. Plenge, T. Koeuth, W. A. Ortmann, G. Hom, J. W. Bauer, C. Gillett, N. Burt, D. S. Cunninghame Graham, R. Onofrio, M. Petri, I. Gunnarsson, E. Svenungsson, L. Ronnblom, G. Nordmark, P. K. Gregersen, K. Moser, P. M. Gaffney, L. A. Criswell, T. J. Vyse, A. C. Syvanen, P. R. Bohjanen, M. J. Daly, T. W. Behrens and D. Altshuler (2007). "Three functional variants of IFN regulatory factor 5 (IRF5) define risk and protective haplotypes for human lupus." Proc Natl Acad Sci U S A **104**(16): 6758-6763.

Gregory, R. I., K. P. Yan, G. Amuthan, T. Chendrimada, B. Doratotaj, N. Cooch and R. Shiekhattar (2004). "The Microprocessor complex mediates the genesis of microRNAs." Nature **432**(7014): 235-240.

Grewal, S. I. (2010). "RNAi-dependent formation of heterochromatin and its diverse functions." Curr Opin Genet Dev **20**(2): 134-141.

Grey, F., R. Tirabassi, H. Meyers, G. Wu, S. McWeeney, L. Hook and J. A. Nelson (2010). "A viral microRNA down-regulates multiple cell cycle genes through mRNA 5'UTRs." PLoS Pathog **6**(6): e1000967.

Grimson, A., K. K. Farh, W. K. Johnston, P. Garrett-Engele, L. P. Lim and D. P. Bartel (2007). "MicroRNA targeting specificity in mammals: determinants beyond seed pairing." Mol Cell **27**(1): 91-105.

- Grimson, A., M. Srivastava, B. Fahey, B. J. Woodcroft, H. R. Chiang, N. King, B. M. Degnan, D. S. Rokhsar and D. P. Bartel (2008). "Early origins and evolution of microRNAs and Piwi-interacting RNAs in animals." *Nature* **455**(7217): 1193-1197.
- Grisanti, L., I. Falciatori, M. Grasso, L. Dovere, S. Fera, B. Muciaccia, A. Fuso, V. Berno, C. Boitani, M. Stefanini and E. Vicini (2009). "Identification of spermatogonial stem cell subsets by morphological analysis and prospective isolation." *Stem Cells* **27**(12): 3043-3052.
- Grishok, A., A. E. Pasquinelli, D. Conte, N. Li, S. Parrish, I. Ha, D. L. Baillie, A. Fire, G. Ruvkun and C. C. Mello (2001). "Genes and mechanisms related to RNA interference regulate expression of the small temporal RNAs that control *C. elegans* developmental timing." *Cell* **106**(1): 23-34.
- Grivna, S. T., E. Beyret, Z. Wang and H. Lin (2006). "A novel class of small RNAs in mouse spermatogenic cells." *Genes Dev* **20**(13): 1709-1714.
- Gu, S., L. Jin, F. Zhang, P. Sarnow and M. A. Kay (2009). "Biological basis for restriction of microRNA targets to the 3' untranslated region in mammalian mRNAs." *Nat Struct Mol Biol* **16**(2): 144-150.
- Guang, S., A. F. Bochner, D. M. Pavelec, K. B. Burkhardt, S. Harding, J. Lachowicz and S. Kennedy (2008). "An Argonaute transports siRNAs from the cytoplasm to the nucleus." *Science* **321**(5888): 537-541.
- Guil, S. and J. F. Caceres (2007). "The multifunctional RNA-binding protein hnRNP A1 is required for processing of miR-18a." *Nat Struct Mol Biol* **14**(7): 591-596.
- Gunawardane, L. S., K. Saito, K. M. Nishida, K. Miyoshi, Y. Kawamura, T. Nagami, H. Siomi and M. C. Siomi (2007). "A slicer-mediated mechanism for repeat-associated siRNA 5' end formation in *Drosophila*." *Science* **315**(5818): 1587-1590.
- Guo, H., N. T. Ingolia, J. S. Weissman and D. P. Bartel (2010). "Mammalian microRNAs predominantly act to decrease target mRNA levels." *Nature* **466**(7308): 835-840.
- Haase, A. D., S. Fenoglio, F. Muerdter, P. M. Guzzardo, B. Czech, D. J. Pappin, C. Chen, A. Gordon and G. J. Hannon (2010). "Probing the initiation and effector phases of the somatic piRNA pathway in *Drosophila*." *Genes Dev* **24**(22): 2499-2504.
- Hafner, M., M. Landthaler, L. Burger, M. Khorshid, J. Hausser, P. Berninger, A. Rothballer, M. Ascano, Jr., A. C. Jungkamp, M. Munschauer, A. Ulrich, G. S. Wardle, S. Dewell, M. Zavolan and T. Tuschl (2010). "Transcriptome-wide identification of RNA-binding protein and microRNA target sites by PAR-CLIP." *Cell* **141**(1): 129-141.
- Hagan, J. P., E. Piskounova and R. I. Gregory (2009). "Lin28 recruits the TUTase Zcchc11 to inhibit let-7 maturation in mouse embryonic stem cells." *Nat Struct Mol Biol* **16**(10): 1021-1025.
- Hamilton, A. J. and D. C. Baulcombe (1999). "A species of small antisense RNA in posttranscriptional gene silencing in plants." *Science* **286**(5441): 950-952.
- Hammell, C. M., I. Lubin, P. R. Boag, T. K. Blackwell and V. Ambros (2009). "nhl-2 Modulates microRNA activity in *Caenorhabditis elegans*." *Cell* **136**(5): 926-938.
- Hammond, S. M., E. Bernstein, D. Beach and G. J. Hannon (2000). "An RNA-directed nuclease mediates post-transcriptional gene silencing in *Drosophila* cells." *Nature* **404**(6775): 293-296.
- Hammond, S. M., S. Boettcher, A. A. Caudy, R. Kobayashi and G. J. Hannon (2001). "Argonaute2, a link between genetic and biochemical analyses of RNAi." *Science* **293**(5532): 1146-1150.
- Han, J., Y. Lee, K. H. Yeom, Y. K. Kim, H. Jin and V. N. Kim (2004). "The Drosha-DGCR8 complex in primary microRNA processing." *Genes Dev* **18**(24): 3016-3027.

- Han, J., Y. Lee, K. H. Yeom, J. W. Nam, I. Heo, J. K. Rhee, S. Y. Sohn, Y. Cho, B. T. Zhang and V. N. Kim (2006). "Molecular basis for the recognition of primary microRNAs by the Drosha-DGCR8 complex." Cell **125**(5): 887-901.
- Han, J., J. S. Pedersen, S. C. Kwon, C. D. Belair, Y. K. Kim, K. H. Yeom, W. Y. Yang, D. Haussler, R. Blelloch and V. N. Kim (2009). "Posttranscriptional crossregulation between Drosha and DGCR8." Cell **136**(1): 75-84.
- Hardy, R. R., C. E. Carmack, S. A. Shinton, J. D. Kemp and K. Hayakawa (1991). "Resolution and characterization of pro-B and pre-pro-B cell stages in normal mouse bone marrow." J Exp Med **173**(5): 1213-1225.
- Harfe, B. D., M. T. McManus, J. H. Mansfield, E. Hornstein and C. J. Tabin (2005). "The RNaseIII enzyme Dicer is required for morphogenesis but not patterning of the vertebrate limb." Proc Natl Acad Sci U S A **102**(31): 10898-10903.
- Harris, A. N. and P. M. Macdonald (2001). "Aubergine encodes a Drosophila polar granule component required for pole cell formation and related to eIF2C." Development **128**(14): 2823-2832.
- Hauptmann, J., A. Dueck, S. Harlander, J. Pfaff, R. Merkl and G. Meister (2013). "Turning catalytically inactive human Argonaute proteins into active slicer enzymes." Nat Struct Mol Biol **20**(7): 814-817.
- Havecker, E. R., L. M. Wallbridge, T. J. Hardcastle, M. S. Bush, K. A. Kelly, R. M. Dunn, F. Schwach, J. H. Doonan and D. C. Baulcombe (2010). "The Arabidopsis RNA-directed DNA methylation argonautes functionally diverge based on their expression and interaction with target loci." Plant Cell **22**(2): 321-334.
- He, L., X. He, L. P. Lim, E. de Stanchina, Z. Xuan, Y. Liang, W. Xue, L. Zender, J. Magnus, D. Ridzon, A. L. Jackson, P. S. Linsley, C. Chen, S. W. Lowe, M. A. Cleary and G. J. Hannon (2007). "A microRNA component of the p53 tumour suppressor network." Nature **447**(7148): 1130-1134.
- He, Z., J. Jiang, M. C. Hofmann and M. Dym (2007). "Gfra1 silencing in mouse spermatogonial stem cells results in their differentiation via the inactivation of RET tyrosine kinase." Biol Reprod **77**(4): 723-733.
- Helwak, A., G. Kudla, T. Dudnakova and D. Tollervey (2013). "Mapping the human miRNA interactome by CLASH reveals frequent noncanonical binding." Cell **153**(3): 654-665.
- Hendrickson, D. G., D. J. Hogan, H. L. McCullough, J. W. Myers, D. Herschlag, J. E. Ferrell and P. O. Brown (2009). "Concordant regulation of translation and mRNA abundance for hundreds of targets of a human microRNA." PLoS Biol **7**(11): e1000238.
- Heo, I., M. Ha, J. Lim, M. J. Yoon, J. E. Park, S. C. Kwon, H. Chang and V. N. Kim (2012). "Mono-uridylation of pre-microRNA as a key step in the biogenesis of group II let-7 microRNAs." Cell **151**(3): 521-532.
- Heo, I., C. Joo, J. Cho, M. Ha, J. Han and V. N. Kim (2008). "Lin28 mediates the terminal uridylation of let-7 precursor MicroRNA." Mol Cell **32**(2): 276-284.
- Heo, I., C. Joo, Y. K. Kim, M. Ha, M. J. Yoon, J. Cho, K. H. Yeom, J. Han and V. N. Kim (2009). "TUT4 in concert with Lin28 suppresses microRNA biogenesis through pre-microRNA uridylation." Cell **138**(4): 696-708.
- Herr, A. J., M. B. Jensen, T. Dalmay and D. C. Baulcombe (2005). "RNA polymerase IV directs silencing of endogenous DNA." Science **308**(5718): 118-120.
- Hers, I., E. E. Vincent and J. M. Tavaré (2011). "Akt signalling in health and disease." Cell Signal **23**(10): 1515-1527.

- Hertel, J., M. Lindemeyer, K. Missal, C. Fried, A. Tanzer, C. Flamm, I. L. Hofacker, P. F. Stadler and a. Students of Bioinformatics Computer Labs (2006). "The expansion of the metazoan microRNA repertoire." BMC Genomics **7**: 25.
- Hobbs, R. M., M. Seandel, I. Falciatori, S. Rafii and P. P. Pandolfi (2010). "Plzf regulates germline progenitor self-renewal by opposing mTORC1." Cell **142**(3): 468-479.
- Hofmann, M. C., L. Braydich-Stolle and M. Dym (2005). "Isolation of male germ-line stem cells; influence of GDNF." Dev Biol **279**(1): 114-124.
- Horman, S. R., M. M. Janas, C. Litterst, B. Wang, I. J. MacRae, M. J. Sever, D. V. Morrissey, P. Graves, B. Luo, S. Umesalma, H. H. Qi, L. J. Miraglia, C. D. Novina and A. P. Orth (2013). "Akt-mediated phosphorylation of argonaute 2 downregulates cleavage and upregulates translational repression of MicroRNA targets." Mol Cell **50**(3): 356-367.
- Hornstein, E., J. H. Mansfield, S. Yekta, J. K. Hu, B. D. Harfe, M. T. McManus, S. Baskerville, D. P. Bartel and C. J. Tabin (2005). "The microRNA miR-196 acts upstream of Hoxb8 and Shh in limb development." Nature **438**(7068): 671-674.
- Houwing, S., L. M. Kamminga, E. Berezikov, D. Cronembold, A. Girard, H. van den Elst, D. V. Filippov, H. Blaser, E. Raz, C. B. Moens, R. H. Plasterk, G. J. Hannon, B. W. Draper and R. F. Ketting (2007). "A role for Piwi and piRNAs in germ cell maintenance and transposon silencing in Zebrafish." Cell **129**(1): 69-82.
- Huang, H., Q. Gao, X. Peng, S. Y. Choi, K. Sarma, H. Ren, A. J. Morris and M. A. Frohman (2011). "piRNA-associated germline nuage formation and spermatogenesis require MitoPLD profusogenic mitochondrial-surface lipid signaling." Dev Cell **20**(3): 376-387.
- Huang, X. A., H. Yin, S. Sweeney, D. Raha, M. Snyder and H. Lin (2013). "A major epigenetic programming mechanism guided by piRNAs." Dev Cell **24**(5): 502-516.
- Huckins, C. (1971a). "The spermatogonial stem cell population in adult rats. I. Their morphology, proliferation and maturation." Anat Rec **169**(3): 533-557.
- Huckins, C. (1971b). "The spermatogonial stem cell population in adult rats. II. A radioautographic analysis of their cell cycle properties." Cell Tissue Kinet **4**(4): 313-334.
- Huckins, C. (1978). "Spermatogonial intercellular bridges in whole-mounted seminiferous tubules from normal and irradiated rodent testes." Am J Anat **153**(1): 97-121.
- Huckins, C. and Y. Clermont (1968). "Evolution of gonocytes in the rat testis during late embryonic and early post-natal life." Arch Anat Histol Embryol **51**(1): 341-354.
- Humphreys, D. T., B. J. Westman, D. I. Martin and T. Preiss (2005). "MicroRNAs control translation initiation by inhibiting eukaryotic initiation factor 4E/cap and poly(A) tail function." Proc Natl Acad Sci U S A **102**(47): 16961-16966.
- Huttlin, E. L., M. P. Jedrychowski, J. E. Elias, T. Goswami, R. Rad, S. A. Beausoleil, J. Villen, W. Haas, M. E. Sowa and S. P. Gygi (2010). "A tissue-specific atlas of mouse protein phosphorylation and expression." Cell **143**(7): 1174-1189.
- Hutvagner, G., J. McLachlan, A. E. Pasquinelli, E. Balint, T. Tuschl and P. D. Zamore (2001). "A cellular function for the RNA-interference enzyme Dicer in the maturation of the let-7 small temporal RNA." Science **293**(5531): 834-838.
- Hutvagner, G. and M. J. Simard (2008). "Argonaute proteins: key players in RNA silencing." Nat Rev Mol Cell Biol **9**(1): 22-32.

- Hutvagner, G. and P. D. Zamore (2002). "A microRNA in a multiple-turnover RNAi enzyme complex." Science **297**(5589): 2056-2060.
- Ingelfinger, D., D. J. Arndt-Jovin, R. Luhrmann and T. Achsel (2002). "The human LSM1-7 proteins colocalize with the mRNA-degrading enzymes Dcp1/2 and Xrn1 in distinct cytoplasmic foci." RNA **8**(12): 1489-1501.
- International HapMap, C. (2003). "The International HapMap Project." Nature **426**(6968): 789-796.
- Ipsaro, J. J., A. D. Haase, S. R. Knott, L. Joshua-Tor and G. J. Hannon (2012). "The structural biochemistry of Zucchini implicates it as a nuclease in piRNA biogenesis." Nature **491**(7423): 279-283.
- Ishizu, H., H. Siomi and M. C. Siomi (2012). "Biology of PIWI-interacting RNAs: new insights into biogenesis and function inside and outside of germlines." Genes Dev **26**(21): 2361-2373.
- Ito, K., A. Hirao, F. Arai, K. Takubo, S. Matsuoka, K. Miyamoto, M. Ohmura, K. Naka, K. Hosokawa, Y. Ikeda and T. Suda (2006). "Reactive oxygen species act through p38 MAPK to limit the lifespan of hematopoietic stem cells." Nat Med **12**(4): 446-451.
- Jacinto, E., V. Facchinetti, D. Liu, N. Soto, S. Wei, S. Y. Jung, Q. Huang, J. Qin and B. Su (2006). "SIN1/MIP1 maintains rictor-mTOR complex integrity and regulates Akt phosphorylation and substrate specificity." Cell **127**(1): 125-137.
- Jackson, A. L., S. R. Bartz, J. Schelter, S. V. Kobayashi, J. Burchard, M. Mao, B. Li, G. Cavet and P. S. Linsley (2003). "Expression profiling reveals off-target gene regulation by RNAi." Nat Biotechnol **21**(6): 635-637.
- Janowski, B. A., K. E. Huffman, J. C. Schwartz, R. Ram, R. Nordsell, D. S. Shames, J. D. Minna and D. R. Corey (2006). "Involvement of AGO1 and AGO2 in mammalian transcriptional silencing." Nat Struct Mol Biol **13**(9): 787-792.
- Jinek, M. and J. A. Doudna (2009). "A three-dimensional view of the molecular machinery of RNA interference." Nature **457**(7228): 405-412.
- Johnnidis, J. B., M. H. Harris, R. T. Wheeler, S. Stehling-Sun, M. H. Lam, O. Kirak, T. R. Brummelkamp, M. D. Fleming and F. D. Camargo (2008). "Regulation of progenitor cell proliferation and granulocyte function by microRNA-223." Nature **451**(7182): 1125-1129.
- Johnston, R. J. and O. Hobert (2003). "A microRNA controlling left/right neuronal asymmetry in *Caenorhabditis elegans*." Nature **426**(6968): 845-849.
- Joshua-Tor, L. and G. J. Hannon (2011). "Ancestral roles of small RNAs: an Ago-centric perspective." Cold Spring Harb Perspect Biol **3**(10): a003772.
- Juliano, C., J. Wang and H. Lin (2011). "Uniting germline and stem cells: the function of Piwi proteins and the piRNA pathway in diverse organisms." Annu Rev Genet **45**: 447-469.
- Juntilla, M. M., V. D. Patil, M. Calamito, R. P. Joshi, M. J. Birnbaum and G. A. Koretzky (2010). "AKT1 and AKT2 maintain hematopoietic stem cell function by regulating reactive oxygen species." Blood **115**(20): 4030-4038.
- Juntilla, M. M., J. A. Wofford, M. J. Birnbaum, J. C. Rathmell and G. A. Koretzky (2007). "Akt1 and Akt2 are required for alphabeta thymocyte survival and differentiation." Proc Natl Acad Sci U S A **104**(29): 12105-12110.
- Kallapur, S., I. Ormsby and T. Doetschman (1999). "Strain dependency of TGFbeta1 function during embryogenesis." Mol Reprod Dev **52**(4): 341-349.

- Kamminga, L. M., M. J. Luteijn, M. J. den Broeder, S. Redl, L. J. Kaaij, E. F. Roovers, P. Ladurner, E. Berezikov and R. F. Ketting (2010). "Hen1 is required for oocyte development and piRNA stability in zebrafish." *EMBO J* **29**(21): 3688-3700.
- Kanatsu-Shinohara, M., N. Ogonuki, K. Inoue, H. Miki, A. Ogura, S. Toyokuni and T. Shinohara (2003). "Long-term proliferation in culture and germline transmission of mouse male germline stem cells." *Biol Reprod* **69**(2): 612-616.
- Kanatsu-Shinohara, M., S. Takashima, K. Ishii and T. Shinohara (2011). "Dynamic changes in EPCAM expression during spermatogonial stem cell differentiation in the mouse testis." *PLoS One* **6**(8): e23663.
- Kanatsu-Shinohara, M., S. Toyokuni and T. Shinohara (2004). "CD9 is a surface marker on mouse and rat male germline stem cells." *Biol Reprod* **70**(1): 70-75.
- Kaneda, M., M. Okano, K. Hata, T. Sado, N. Tsujimoto, E. Li and H. Sasaki (2004). "Essential role for de novo DNA methyltransferase Dnmt3a in paternal and maternal imprinting." *Nature* **429**(6994): 900-903.
- Kaneda, M., F. Tang, D. O'Carroll, K. Lao and M. A. Surani (2009). "Essential role for Argonaute2 protein in mouse oogenesis." *Epigenetics Chromatin* **2**(1): 9.
- Karginov, F. V., S. Cheloufi, M. M. Chong, A. Stark, A. D. Smith and G. J. Hannon (2010). "Diverse endonucleolytic cleavage sites in the mammalian transcriptome depend upon microRNAs, Drosha, and additional nucleases." *Mol Cell* **38**(6): 781-788.
- Kawahara, Y., B. Zinshteyn, T. P. Chendrimada, R. Shiekhattar and K. Nishikura (2007). "RNA editing of the microRNA-151 precursor blocks cleavage by the Dicer-TRBP complex." *EMBO Rep* **8**(8): 763-769.
- Kawaoka, S., N. Izumi, S. Katsuma and Y. Tomari (2011). "3' end formation of PIWI-interacting RNAs in vitro." *Mol Cell* **43**(6): 1015-1022.
- Keane, T. M., L. Goodstadt, P. Danecek, M. A. White, K. Wong, B. Yalcin, A. Heger, A. Agam, G. Slater, M. Goodson, N. A. Furlotte, E. Eskin, C. Nellaker, H. Whitley, J. Cleak, D. Janowitz, P. Hernandez-Pliego, A. Edwards, T. G. Belgard, P. L. Oliver, R. E. McIntyre, A. Bhomra, J. Nicod, X. Gan, W. Yuan, L. van der Weyden, C. A. Steward, S. Bala, J. Stalker, R. Mott, R. Durbin, I. J. Jackson, A. Czechanski, J. A. Guerra-Assuncao, L. R. Donahue, L. G. Reinholdt, B. A. Payseur, C. P. Ponting, E. Birney, J. Flint and D. J. Adams (2011). "Mouse genomic variation and its effect on phenotypes and gene regulation." *Nature* **477**(7364): 289-294.
- Kedde, M., M. J. Strasser, B. Boldajipour, J. A. Oude Vrielink, K. Slanchev, C. le Sage, R. Nagel, P. M. Voorhoeve, J. van Duijse, U. A. Orom, A. H. Lund, A. Perrakis, E. Raz and R. Agami (2007). "RNA-binding protein Dnd1 inhibits microRNA access to target mRNA." *Cell* **131**(7): 1273-1286.
- Kedersha, N., S. Chen, N. Gilks, W. Li, I. J. Miller, J. Stahl and P. Anderson (2002). "Evidence that ternary complex (eIF2-GTP-tRNA(i)(Met))-deficient preinitiation complexes are core constituents of mammalian stress granules." *Mol Biol Cell* **13**(1): 195-210.
- Ketting, R. F., S. E. Fischer, E. Bernstein, T. Sijen, G. J. Hannon and R. H. Plasterk (2001). "Dicer functions in RNA interference and in synthesis of small RNA involved in developmental timing in *C. elegans*." *Genes Dev* **15**(20): 2654-2659.
- Khvorova, A., A. Reynolds and S. D. Jayasena (2003). "Functional siRNAs and miRNAs exhibit strand bias." *Cell* **115**(2): 209-216.
- Kiel, M. J., O. H. Yilmaz, T. Iwashita, O. H. Yilmaz, C. Terhorst and S. J. Morrison (2005). "SLAM family receptors distinguish hematopoietic stem and progenitor cells and reveal endothelial niches for stem cells." *Cell* **121**(7): 1109-1121.

- Kim, D. H., L. M. Villeneuve, K. V. Morris and J. J. Rossi (2006). "Argonaute-1 directs siRNA-mediated transcriptional gene silencing in human cells." Nat Struct Mol Biol **13**(9): 793-797.
- Kim, E. K., S. J. Yun, J. M. Ha, Y. W. Kim, I. H. Jin, D. H. Woo, S. H. Song, H. K. Ha, Y. S. Choi, T. G. Lee and S. S. Bae (2012). "Loss of Akt1 evokes epithelial-mesenchymal transition by autocrine regulation of transforming growth factor-beta1." Adv Biol Regul **52**(1): 88-96.
- Kim, Y. K., I. Heo and V. N. Kim (2010). "Modifications of small RNAs and their associated proteins." Cell **143**(5): 703-709.
- Kimball, S. R., R. L. Horetsky, D. Ron, L. S. Jefferson and H. P. Harding (2003). "Mammalian stress granules represent sites of accumulation of stalled translation initiation complexes." Am J Physiol Cell Physiol **284**(2): C273-284.
- Kiriakidou, M., G. S. Tan, S. Lamprinaki, M. De Planell-Saguer, P. T. Nelson and Z. Mourelatos (2007). "An mRNA m7G cap binding-like motif within human Ago2 represses translation." Cell **129**(6): 1141-1151.
- Kirito, K., N. Fox and K. Kaushansky (2003). "Thrombopoietin stimulates Hoxb4 expression: an explanation for the favorable effects of TPO on hematopoietic stem cells." Blood **102**(9): 3172-3178.
- Klenov, M. S., O. A. Sokolova, E. Y. Yakushev, A. D. Stolyarenko, E. A. Mikhaleva, S. A. Lavrov and V. A. Gvozdev (2011). "Separation of stem cell maintenance and transposon silencing functions of Piwi protein." Proc Natl Acad Sci U S A **108**(46): 18760-18765.
- Kluin, P. M. and D. G. de Rooij (1981). "A comparison between the morphology and cell kinetics of gonocytes and adult type undifferentiated spermatogonia in the mouse." Int J Androl **4**(4): 475-493.
- Kluin, P. M., M. F. Kramer and D. G. de Rooij (1982). "Spermatogenesis in the immature mouse proceeds faster than in the adult." Int J Androl **5**(3): 282-294.
- Knight, S. W. and B. L. Bass (2001). "A role for the RNase III enzyme DCR-1 in RNA interference and germ line development in *Caenorhabditis elegans*." Science **293**(5538): 2269-2271.
- Koralov, S. B., S. A. Muljo, G. R. Galler, A. Krek, T. Chakraborty, C. Kanellopoulou, K. Jensen, B. S. Cobb, M. Merckenschlager, N. Rajewsky and K. Rajewsky (2008). "Dicer ablation affects antibody diversity and cell survival in the B lymphocyte lineage." Cell **132**(5): 860-874.
- Kotlyarov, A., A. Neininger, C. Schubert, R. Eckert, C. Birchmeier, H. D. Volk and M. Gaestel (1999). "MAPKAP kinase 2 is essential for LPS-induced TNF-alpha biosynthesis." Nat Cell Biol **1**(2): 94-97.
- Krek, A., D. Grun, M. N. Poy, R. Wolf, L. Rosenberg, E. J. Epstein, P. MacMenamin, I. da Piedade, K. C. Gunsalus, M. Stoffel and N. Rajewsky (2005). "Combinatorial microRNA target predictions." Nat Genet **37**(5): 495-500.
- Krutzfeldt, J., N. Rajewsky, R. Braich, K. G. Rajeev, T. Tuschl, M. Manoharan and M. Stoffel (2005). "Silencing of microRNAs in vivo with 'antagomirs'." Nature **438**(7068): 685-689.
- Kubota, H., M. R. Avarbock and R. L. Brinster (2003). "Spermatogonial stem cells share some, but not all, phenotypic and functional characteristics with other stem cells." Proc Natl Acad Sci U S A **100**(11): 6487-6492.
- Kubota, H., M. R. Avarbock and R. L. Brinster (2004). "Culture conditions and single growth factors affect fate determination of mouse spermatogonial stem cells." Biol Reprod **71**(3): 722-731.
- Kuchen, S., W. Resch, A. Yamane, N. Kuo, Z. Li, T. Chakraborty, L. Wei, A. Laurence, T. Yasuda, S. Peng, J. Hu-Li, K. Lu, W. Dubois, Y. Kitamura, N. Charles, H. W. Sun, S. Muljo, P. L. Schwartzberg, W.

- E. Paul, J. O'Shea, K. Rajewsky and R. Casellas (2010). "Regulation of microRNA expression and abundance during lymphopoiesis." *Immunity* **32**(6): 828-839.
- Kuhn, R., F. Schwenk, M. Aguet and K. Rajewsky (1995). "Inducible gene targeting in mice." *Science* **269**(5229): 1427-1429.
- Kuhnert, F., M. R. Mancuso, J. Hampton, K. Stankunas, T. Asano, C. Z. Chen and C. J. Kuo (2008). "Attribution of vascular phenotypes of the murine *Egfl7* locus to the microRNA miR-126." *Development* **135**(24): 3989-3993.
- Kulkarni, A. B., C. G. Huh, D. Becker, A. Geiser, M. Lyght, K. C. Flanders, A. B. Roberts, M. B. Sporn, J. M. Ward and S. Karlsson (1993). "Transforming growth factor beta 1 null mutation in mice causes excessive inflammatory response and early death." *Proc Natl Acad Sci U S A* **90**(2): 770-774.
- Kuramochi-Miyagawa, S., T. Kimura, T. W. Ijiri, T. Isobe, N. Asada, Y. Fujita, M. Ikawa, N. Iwai, M. Okabe, W. Deng, H. Lin, Y. Matsuda and T. Nakano (2004). "Mili, a mammalian member of piwi family gene, is essential for spermatogenesis." *Development* **131**(4): 839-849.
- Kuramochi-Miyagawa, S., T. Watanabe, K. Gotoh, Y. Totoki, A. Toyoda, M. Ikawa, N. Asada, K. Kojima, Y. Yamaguchi, T. W. Ijiri, K. Hata, E. Li, Y. Matsuda, T. Kimura, M. Okabe, Y. Sakaki, H. Sasaki and T. Nakano (2008). "DNA methylation of retrotransposon genes is regulated by Piwi family members MILI and MIWI2 in murine fetal testes." *Genes Dev* **22**(7): 908-917.
- Kwak, P. B. and Y. Tomari (2012). "The N domain of Argonaute drives duplex unwinding during RISC assembly." *Nat Struct Mol Biol* **19**(2): 145-151.
- Lagos-Quintana, M., R. Rauhut, W. Lendeckel and T. Tuschl (2001). "Identification of novel genes coding for small expressed RNAs." *Science* **294**(5543): 853-858.
- Lal, A., F. Navarro, C. A. Maher, L. E. Maliszewski, N. Yan, E. O'Day, D. Chowdhury, D. M. Dykxhoorn, P. Tsai, O. Hofmann, K. G. Becker, M. Gorospe, W. Hide and J. Lieberman (2009). "miR-24 Inhibits cell proliferation by targeting E2F2, MYC, and other cell-cycle genes via binding to "seedless" 3'UTR microRNA recognition elements." *Mol Cell* **35**(5): 610-625.
- Landthaler, M., A. Yalcin and T. Tuschl (2004). "The human DiGeorge syndrome critical region gene 8 and its D. melanogaster homolog are required for miRNA biogenesis." *Curr Biol* **14**(23): 2162-2167.
- Lanet, E., E. Delannoy, R. Sormani, M. Floris, P. Brodersen, P. Crete, O. Voinnet and C. Robaglia (2009). "Biochemical evidence for translational repression by Arabidopsis microRNAs." *Plant Cell* **21**(6): 1762-1768.
- Lau, N. C., L. P. Lim, E. G. Weinstein and D. P. Bartel (2001). "An abundant class of tiny RNAs with probable regulatory roles in *Caenorhabditis elegans*." *Science* **294**(5543): 858-862.
- Lau, N. C., A. G. Seto, J. Kim, S. Kuramochi-Miyagawa, T. Nakano, D. P. Bartel and R. E. Kingston (2006). "Characterization of the piRNA complex from rat testes." *Science* **313**(5785): 363-367.
- Lawson, K. A. and R. A. Pedersen (1992). "Clonal analysis of cell fate during gastrulation and early neurulation in the mouse." *Ciba Found Symp* **165**: 3-21; discussion 21-26.
- Le Thomas, A., A. K. Rogers, A. Webster, G. K. Marinov, S. E. Liao, E. M. Perkins, J. K. Hur, A. A. Aravin and K. F. Toth (2013). "Piwi induces piRNA-guided transcriptional silencing and establishment of a repressive chromatin state." *Genes Dev* **27**(4): 390-399.
- LeCouter, J. E., B. Kablar, W. R. Hardy, C. Ying, L. A. Megeney, L. L. May and M. A. Rudnicki (1998). "Strain-dependent myeloid hyperplasia, growth deficiency, and accelerated cell cycle in mice lacking the Rb-related p107 gene." *Mol Cell Biol* **18**(12): 7455-7465.

- LeCouter, J. E., B. Kablar, P. F. Whyte, C. Ying and M. A. Rudnicki (1998). "Strain-dependent embryonic lethality in mice lacking the retinoblastoma-related p130 gene." *Development* **125**(23): 4669-4679.
- Lee, E. J., S. Banerjee, H. Zhou, A. Jammalamadaka, M. Arcila, B. S. Manjunath and K. S. Kosik (2011). "Identification of piRNAs in the central nervous system." *RNA* **17**(6): 1090-1099.
- Lee, R. C. and V. Ambros (2001). "An extensive class of small RNAs in *Caenorhabditis elegans*." *Science* **294**(5543): 862-864.
- Lee, R. C., R. L. Feinbaum and V. Ambros (1993). "The *C. elegans* heterochronic gene *lin-4* encodes small RNAs with antisense complementarity to *lin-14*." *Cell* **75**(5): 843-854.
- Lee, Y., C. Ahn, J. Han, H. Choi, J. Kim, J. Yim, J. Lee, P. Provost, O. Radmark, S. Kim and V. N. Kim (2003). "The nuclear RNase III Droscha initiates microRNA processing." *Nature* **425**(6956): 415-419.
- Lee, Y., M. Kim, J. Han, K. H. Yeom, S. Lee, S. H. Baek and V. N. Kim (2004). "MicroRNA genes are transcribed by RNA polymerase II." *EMBO J* **23**(20): 4051-4060.
- Leung, A. K., J. M. Calabrese and P. A. Sharp (2006). "Quantitative analysis of Argonaute protein reveals microRNA-dependent localization to stress granules." *Proc Natl Acad Sci U S A* **103**(48): 18125-18130.
- Leung, A. K., S. Vyas, J. E. Rood, A. Bhutkar, P. A. Sharp and P. Chang (2011). "Poly(ADP-ribose) regulates stress responses and microRNA activity in the cytoplasm." *Mol Cell* **42**(4): 489-499.
- Levy, C., M. Khaled, K. C. Robinson, R. A. Veguilla, P. H. Chen, S. Yokoyama, E. Makino, J. Lu, L. Larue, F. Beermann, L. Chin, M. Bosenberg, J. S. Song and D. E. Fisher (2010). "Lineage-specific transcriptional regulation of DICER by MITF in melanocytes." *Cell* **141**(6): 994-1005.
- Lewis, B. P., C. B. Burge and D. P. Bartel (2005). "Conserved seed pairing, often flanked by adenosines, indicates that thousands of human genes are microRNA targets." *Cell* **120**(1): 15-20.
- Lewis, B. P., I. H. Shih, M. W. Jones-Rhoades, D. P. Bartel and C. B. Burge (2003). "Prediction of mammalian microRNA targets." *Cell* **115**(7): 787-798.
- Li, C., V. V. Vagin, S. Lee, J. Xu, S. Ma, H. Xi, H. Seitz, M. D. Horwich, M. Syrzycka, B. M. Honda, E. L. Kittler, M. L. Zapp, C. Klattenhoff, N. Schulz, W. E. Theurkauf, Z. Weng and P. D. Zamore (2009). "Collapse of germline piRNAs in the absence of Argonaute3 reveals somatic piRNAs in flies." *Cell* **137**(3): 509-521.
- Li, H., W. X. Li and S. W. Ding (2002). "Induction and suppression of RNA silencing by an animal virus." *Science* **296**(5571): 1319-1321.
- Li, Q. J., J. Chau, P. J. Ebert, G. Sylvester, H. Min, G. Liu, R. Braich, M. Manoharan, J. Soutschek, P. Skare, L. O. Klein, M. M. Davis and C. Z. Chen (2007). "miR-181a is an intrinsic modulator of T cell sensitivity and selection." *Cell* **129**(1): 147-161.
- Li, X. Z., C. K. Roy, X. Dong, E. Bolcun-Filas, J. Wang, B. W. Han, J. Xu, M. J. Moore, J. C. Schimenti, Z. Weng and P. D. Zamore (2013). "An ancient transcription factor initiates the burst of piRNA production during early meiosis in mouse testes." *Mol Cell* **50**(1): 67-81.
- Li, Y. S., R. Wasserman, K. Hayakawa and R. R. Hardy (1996). "Identification of the earliest B lineage stage in mouse bone marrow." *Immunity* **5**(6): 527-535.
- Lim, L. P., N. C. Lau, P. Garrett-Engele, A. Grimson, J. M. Schelter, J. Castle, D. P. Bartel, P. S. Linsley and J. M. Johnson (2005). "Microarray analysis shows that some microRNAs downregulate large numbers of target mRNAs." *Nature* **433**(7027): 769-773.

- Lin, A. E., G. Ebert, Y. Ow, S. P. Preston, J. G. Toe, J. P. Cooney, H. W. Scott, M. Sasaki, S. D. Saibil, D. Dissanayake, R. H. Kim, A. Wakeham, A. You-Ten, A. Shahinian, G. Duncan, J. Silvester, P. S. Ohashi, T. W. Mak and M. Pellegrini (2013). "ARIH2 is essential for embryogenesis, and its hematopoietic deficiency causes lethal activation of the immune system." *Nat Immunol* **14**(1): 27-33.
- Lin, H. and A. C. Spradling (1993). "Germline stem cell division and egg chamber development in transplanted *Drosophila* germaria." *Dev Biol* **159**(1): 140-152.
- Lin, H. and A. C. Spradling (1997). "A novel group of pumilio mutations affects the asymmetric division of germline stem cells in the *Drosophila* ovary." *Development* **124**(12): 2463-2476.
- Lindbo, J. A. and W. G. Dougherty (1992). "Untranslatable transcripts of the tobacco etch virus coat protein gene sequence can interfere with tobacco etch virus replication in transgenic plants and protoplasts." *Virology* **189**(2): 725-733.
- Lingel, A., B. Simon, E. Izaurralde and M. Sattler (2004). "Nucleic acid 3'-end recognition by the Argonaute2 PAZ domain." *Nat Struct Mol Biol* **11**(6): 576-577.
- Liu, J., M. A. Carmell, F. V. Rivas, C. G. Marsden, J. M. Thomson, J. J. Song, S. M. Hammond, L. Joshua-Tor and G. J. Hannon (2004). "Argonaute2 is the catalytic engine of mammalian RNAi." *Science* **305**(5689): 1437-1441.
- Liu, J., F. V. Rivas, J. Wohlschlegel, J. R. Yates, 3rd, R. Parker and G. J. Hannon (2005). "A role for the P-body component GW182 in microRNA function." *Nat Cell Biol* **7**(12): 1261-1266.
- Liu, N., S. Bezprozvannaya, A. H. Williams, X. Qi, J. A. Richardson, R. Bassel-Duby and E. N. Olson (2008). "microRNA-133a regulates cardiomyocyte proliferation and suppresses smooth muscle gene expression in the heart." *Genes Dev* **22**(23): 3242-3254.
- Liu, Y., X. Ye, F. Jiang, C. Liang, D. Chen, J. Peng, L. N. Kinch, N. V. Grishin and Q. Liu (2009). "C3PO, an endoribonuclease that promotes RNAi by facilitating RISC activation." *Science* **325**(5941): 750-753.
- Livak, K. J. and T. D. Schmittgen (2001). "Analysis of relative gene expression data using real-time quantitative PCR and the 2(-Delta Delta C(T)) Method." *Methods* **25**(4): 402-408.
- Llave, C., Z. Xie, K. D. Kasschau and J. C. Carrington (2002). "Cleavage of Scarecrow-like mRNA targets directed by a class of Arabidopsis miRNA." *Science* **297**(5589): 2053-2056.
- Lok, D. and D. G. de Rooij (1983). "Spermatogonial multiplication in the Chinese hamster. III. Labelling indices of undifferentiated spermatogonia throughout the cycle of the seminiferous epithelium." *Cell Tissue Kinet* **16**(1): 31-40.
- Long, D., R. Lee, P. Williams, C. Y. Chan, V. Ambros and Y. Ding (2007). "Potent effect of target structure on microRNA function." *Nat Struct Mol Biol* **14**(4): 287-294.
- Lu, R., M. Maduro, F. Li, H. W. Li, G. Broitman-Maduro, W. X. Li and S. W. Ding (2005). "Animal virus replication and RNAi-mediated antiviral silencing in *Caenorhabditis elegans*." *Nature* **436**(7053): 1040-1043.
- Luteijn, M. J. and R. F. Ketting (2013). "PIWI-interacting RNAs: from generation to transgenerational epigenetics." *Nat Rev Genet* **14**(8): 523-534.
- Ma, J., M. Flemr, P. Stein, P. Berninger, R. Malik, M. Zavolan, P. Svoboda and R. M. Schultz (2010). "MicroRNA activity is suppressed in mouse oocytes." *Curr Biol* **20**(3): 265-270.
- Ma, J. B., K. Ye and D. J. Patel (2004). "Structural basis for overhang-specific small interfering RNA recognition by the PAZ domain." *Nature* **429**(6989): 318-322.

Ma, J. B., Y. R. Yuan, G. Meister, Y. Pei, T. Tuschl and D. J. Patel (2005). "Structural basis for 5'-end-specific recognition of guide RNA by the *A. fulgidus* Piwi protein." *Nature* **434**(7033): 666-670.

MacRae, I. J., E. Ma, M. Zhou, C. V. Robinson and J. A. Doudna (2008). "In vitro reconstitution of the human RISC-loading complex." *Proc Natl Acad Sci U S A* **105**(2): 512-517.

Macrae, I. J., K. Zhou, F. Li, A. Repic, A. N. Brooks, W. Z. Cande, P. D. Adams and J. A. Doudna (2006). "Structural basis for double-stranded RNA processing by Dicer." *Science* **311**(5758): 195-198.

Malone, C. D., J. Brennecke, M. Dus, A. Stark, W. R. McCombie, R. Sachidanandam and G. J. Hannon (2009). "Specialized piRNA pathways act in germline and somatic tissues of the *Drosophila* ovary." *Cell* **137**(3): 522-535.

Maniataki, E. and Z. Mourelatos (2005). "A human, ATP-independent, RISC assembly machine fueled by pre-miRNA." *Genes Dev* **19**(24): 2979-2990.

Manke, I. A., A. Nguyen, D. Lim, M. Q. Stewart, A. E. Elia and M. B. Yaffe (2005). "MAPKAP kinase-2 is a cell cycle checkpoint kinase that regulates the G2/M transition and S phase progression in response to UV irradiation." *Mol Cell* **17**(1): 37-48.

Markel, P., P. Shu, C. Ebeling, G. A. Carlson, D. L. Nagle, J. S. Smutko and K. J. Moore (1997). "Theoretical and empirical issues for marker-assisted breeding of congenic mouse strains." *Nat Genet* **17**(3): 280-284.

Maroney, P. A., Y. Yu, J. Fisher and T. W. Nilsen (2006). "Evidence that microRNAs are associated with translating messenger RNAs in human cells." *Nat Struct Mol Biol* **13**(12): 1102-1107.

Martinez, J., A. Patkaniowska, H. Urlaub, R. Luhrmann and T. Tuschl (2002). "Single-stranded antisense siRNAs guide target RNA cleavage in RNAi." *Cell* **110**(5): 563-574.

Martinez, J. and T. Tuschl (2004). "RISC is a 5' phosphomonoester-producing RNA endonuclease." *Genes Dev* **18**(9): 975-980.

Mathonnet, G., M. R. Fabian, Y. V. Svitkin, A. Parsyan, L. Huck, T. Murata, S. Biffo, W. C. Merrick, E. Darzynkiewicz, R. S. Pillai, W. Filipowicz, T. F. Duchaine and N. Sonenberg (2007). "MicroRNA inhibition of translation initiation in vitro by targeting the cap-binding complex eIF4F." *Science* **317**(5845): 1764-1767.

Matranga, C., Y. Tomari, C. Shin, D. P. Bartel and P. D. Zamore (2005). "Passenger-strand cleavage facilitates assembly of siRNA into Ago2-containing RNAi enzyme complexes." *Cell* **123**(4): 607-620.

McGuinness, M. P. and J. M. Orth (1992). "Reinitiation of gonocyte mitosis and movement of gonocytes to the basement membrane in testes of newborn rats in vivo and in vitro." *Anat Rec* **233**(4): 527-537.

McLean, D. J., P. J. Friel, D. S. Johnston and M. D. Griswold (2003). "Characterization of spermatogonial stem cell maturation and differentiation in neonatal mice." *Biol Reprod* **69**(6): 2085-2091.

Mecklenbrauker, I., K. Saijo, N. Y. Zheng, M. Leitges and A. Tarakhovsky (2002). "Protein kinase Cdelta controls self-antigen-induced B-cell tolerance." *Nature* **416**(6883): 860-865.

Medeiros, L. A., L. M. Dennis, M. E. Gill, H. Houbaviy, S. Markoulaki, D. Fu, A. C. White, O. Kirak, P. A. Sharp, D. C. Page and R. Jaenisch (2011). "Mir-290-295 deficiency in mice results in partially penetrant embryonic lethality and germ cell defects." *Proc Natl Acad Sci U S A* **108**(34): 14163-14168.

Meister, G. (2013). "Argonaute proteins: functional insights and emerging roles." *Nat Rev Genet* **14**(7): 447-459.

- Meister, G., M. Landthaler, A. Patkaniowska, Y. Dorsett, G. Teng and T. Tuschl (2004). "Human Argonaute2 mediates RNA cleavage targeted by miRNAs and siRNAs." *Mol Cell* **15**(2): 185-197.
- Meister, G., M. Landthaler, L. Peters, P. Y. Chen, H. Urlaub, R. Luhrmann and T. Tuschl (2005). "Identification of novel argonaute-associated proteins." *Curr Biol* **15**(23): 2149-2155.
- Melnyk, C. W., A. Molnar and D. C. Baulcombe (2011). "Intercellular and systemic movement of RNA silencing signals." *EMBO J* **30**(17): 3553-3563.
- Meng, X., M. Lindahl, M. E. Hyvonen, M. Parvinen, D. G. de Rooij, M. W. Hess, A. Raatikainen-Ahokas, K. Sainio, H. Rauvala, M. Lakso, J. G. Pichel, H. Westphal, M. Saarma and H. Sariola (2000). "Regulation of cell fate decision of undifferentiated spermatogonia by GDNF." *Science* **287**(5457): 1489-1493.
- Mice, B. C. o. G. B. i. (1997). "Mutant mice and neuroscience: recommendations concerning genetic background. Banbury Conference on genetic background in mice." *Neuron* **19**(4): 755-759.
- Michlewski, G., S. Guil, C. A. Semple and J. F. Caceres (2008). "Posttranscriptional regulation of miRNAs harboring conserved terminal loops." *Mol Cell* **32**(3): 383-393.
- Miller, B. A., G. Antognetti and T. A. Springer (1985). "Identification of cell surface antigens present on murine hematopoietic stem cells." *J Immunol* **134**(5): 3286-3290.
- Miyoshi, K., H. Tsukumo, T. Nagami, H. Siomi and M. C. Siomi (2005). "Slicer function of Drosophila Argonautes and its involvement in RISC formation." *Genes Dev* **19**(23): 2837-2848.
- Mlotshwa, S., G. J. Pruss and V. Vance (2008). "Small RNAs in viral infection and host defense." *Trends Plant Sci* **13**(7): 375-382.
- Modzelewski, A. J., R. J. Holmes, S. Hilz, A. Grimson and P. E. Cohen (2012). "AGO4 regulates entry into meiosis and influences silencing of sex chromosomes in the male mouse germline." *Dev Cell* **23**(2): 251-264.
- Morita, S., T. Horii, M. Kimura, Y. Goto, T. Ochiya and I. Hatada (2007). "One Argonaute family member, Eif2c2 (Ago2), is essential for development and appears not to be involved in DNA methylation." *Genomics* **89**(6): 687-696.
- Morrison, S. J., H. D. Hemmati, A. M. Wandycz and I. L. Weissman (1995). "The purification and characterization of fetal liver hematopoietic stem cells." *Proc Natl Acad Sci U S A* **92**(22): 10302-10306.
- Motamedi, M. R., A. Verdel, S. U. Colmenares, S. A. Gerber, S. P. Gygi and D. Moazed (2004). "Two RNAi complexes, RITS and RDCR, physically interact and localize to noncoding centromeric RNAs." *Cell* **119**(6): 789-802.
- Mourrain, P., C. Beclin, T. Elmayan, F. Feuerbach, C. Godon, J. B. Morel, D. Jouette, A. M. Lacombe, S. Nikic, N. Picault, K. Remoue, M. Sanial, T. A. Vo and H. Vaucheret (2000). "Arabidopsis SGS2 and SGS3 genes are required for posttranscriptional gene silencing and natural virus resistance." *Cell* **101**(5): 533-542.
- Mudgett, J. S., J. Ding, L. Guh-Siesel, N. A. Chartrain, L. Yang, S. Gopal and M. M. Shen (2000). "Essential role for p38alpha mitogen-activated protein kinase in placental angiogenesis." *Proc Natl Acad Sci U S A* **97**(19): 10454-10459.
- Muljo, S. A., K. M. Ansel, C. Kanellopoulou, D. M. Livingston, A. Rao and K. Rajewsky (2005). "Aberrant T cell differentiation in the absence of Dicer." *J Exp Med* **202**(2): 261-269.
- Murchison, E. P., P. Stein, Z. Xuan, H. Pan, M. Q. Zhang, R. M. Schultz and G. J. Hannon (2007). "Critical roles for Dicer in the female germline." *Genes Dev* **21**(6): 682-693.

- Musunuru, K., A. Strong, M. Frank-Kamenetsky, N. E. Lee, T. Ahfeldt, K. V. Sachs, X. Li, H. Li, N. Kuperwasser, V. M. Ruda, J. P. Pirruccello, B. Muchmore, L. Prokunina-Olsson, J. L. Hall, E. E. Schadt, C. R. Morales, S. Lund-Katz, M. C. Phillips, J. Wong, W. Cantley, T. Racie, K. G. Ejebe, M. Orho-Melander, O. Melander, V. Koteliansky, K. Fitzgerald, R. M. Krauss, C. A. Cowan, S. Kathiresan and D. J. Rader (2010). "From noncoding variant to phenotype via SORT1 at the 1p13 cholesterol locus." *Nature* **466**(7307): 714-719.
- Nagano, R., S. Tabata, Y. Nakanishi, S. Ohsako, M. Kurohmaru and Y. Hayashi (2000). "Reproliferation and relocation of mouse male germ cells (gonocytes) during prespermatogenesis." *Anat Rec* **258**(2): 210-220.
- Nagy, A., M. Gertsenstein, K. Vintersten, R. Behringer (2003). "Manipulating the mouse embryo: a laboratory manual." (Third Edition) Cold Spring Harbor Laboratory Press
- Nakagawa, T., Y. Nabeshima and S. Yoshida (2007). "Functional identification of the actual and potential stem cell compartments in mouse spermatogenesis." *Dev Cell* **12**(2): 195-206.
- Nakagawa, T., M. Sharma, Y. Nabeshima, R. E. Braun and S. Yoshida (2010). "Functional hierarchy and reversibility within the murine spermatogenic stem cell compartment." *Science* **328**(5974): 62-67.
- Nakanishi, K., M. Ascano, T. Gogakos, S. Ishibe-Murakami, A. A. Serganov, D. Briskin, P. Morozov, T. Tuschl and D. J. Patel (2013). "Eukaryote-specific insertion elements control human ARGONAUTE slicer activity." *Cell Rep* **3**(6): 1893-1900.
- Nakanishi, K., D. E. Weinberg, D. P. Bartel and D. J. Patel (2012). "Structure of yeast Argonaute with guide RNA." *Nature* **486**(7403): 368-374.
- Napoli, C., C. Lemieux and R. Jorgensen (1990). "Introduction of a Chimeric Chalcone Synthase Gene into Petunia Results in Reversible Co-Suppression of Homologous Genes in trans." *Plant Cell* **2**(4): 279-289.
- Naughton, C. K., S. Jain, A. M. Strickland, A. Gupta and J. Milbrandt (2006). "Glial cell-line derived neurotrophic factor-mediated RET signaling regulates spermatogonial stem cell fate." *Biol Reprod* **74**(2): 314-321.
- New, L., Y. Jiang, M. Zhao, K. Liu, W. Zhu, L. J. Flood, Y. Kato, G. C. Parry and J. Han (1998). "PRAK, a novel protein kinase regulated by the p38 MAP kinase." *EMBO J* **17**(12): 3372-3384.
- Newman, M. A., J. M. Thomson and S. M. Hammond (2008). "Lin-28 interaction with the Let-7 precursor loop mediates regulated microRNA processing." *RNA* **14**(8): 1539-1549.
- Newmark, P. A., P. W. Reddien, F. Cebria and A. Sanchez Alvarado (2003). "Ingestion of bacterially expressed double-stranded RNA inhibits gene expression in planarians." *Proc Natl Acad Sci U S A* **100** **Suppl 1**: 11861-11865.
- Newmark, P. A. and A. Sanchez Alvarado (2002). "Not your father's planarian: a classic model enters the era of functional genomics." *Nat Rev Genet* **3**(3): 210-219.
- Nielsen, C. B., N. Shomron, R. Sandberg, E. Hornstein, J. Kitzman and C. B. Burge (2007). "Determinants of targeting by endogenous and exogenous microRNAs and siRNAs." *RNA* **13**(11): 1894-1910.
- Nishida, K. M., K. Saito, T. Mori, Y. Kawamura, T. Nagami-Okada, S. Inagaki, H. Siomi and M. C. Siomi (2007). "Gene silencing mechanisms mediated by Aubergine piRNA complexes in Drosophila male gonad." *RNA* **13**(11): 1911-1922.

- Nishimasu, H., H. Ishizu, K. Saito, S. Fukuhara, M. K. Kamatani, L. Bonnefond, N. Matsumoto, T. Nishizawa, K. Nakanaga, J. Aoki, R. Ishitani, H. Siomi, M. C. Siomi and O. Nureki (2012). "Structure and function of Zucchini endoribonuclease in piRNA biogenesis." Nature **491**(7423): 284-287.
- Noma, K., T. Sugiyama, H. Cam, A. Verdel, M. Zofall, S. Jia, D. Moazed and S. I. Grewal (2004). "RITS acts in cis to promote RNA interference-mediated transcriptional and post-transcriptional silencing." Nat Genet **36**(11): 1174-1180.
- Nottrott, S., M. J. Simard and J. D. Richter (2006). "Human let-7a miRNA blocks protein production on actively translating polyribosomes." Nat Struct Mol Biol **13**(12): 1108-1114.
- Nykanen, A., B. Haley and P. D. Zamore (2001). "ATP requirements and small interfering RNA structure in the RNA interference pathway." Cell **107**(3): 309-321.
- O'Brien, K. A., A. Stojanovic-Terpo, N. Hay and X. Du (2011). "An important role for Akt3 in platelet activation and thrombosis." Blood **118**(15): 4215-4223.
- O'Carroll, D., I. Mecklenbrauker, P. P. Das, A. Santana, U. Koenig, A. J. Enright, E. A. Miska and A. Tarakhovsky (2007). "A Slicer-independent role for Argonaute 2 in hematopoiesis and the microRNA pathway." Genes Dev **21**(16): 1999-2004.
- Oakberg, E. F. (1971). "Spermatogonial stem-cell renewal in the mouse." Anat Rec **169**(3): 515-531.
- Oatley, J. M. and R. L. Brinster (2006). "Spermatogonial stem cells." Methods Enzymol **419**: 259-282.
- Oatley, M. J., A. V. Kaucher, K. E. Racicot and J. M. Oatley (2011). "Inhibitor of DNA binding 4 is expressed selectively by single spermatogonia in the male germline and regulates the self-renewal of spermatogonial stem cells in mice." Biol Reprod **85**(2): 347-356.
- Ohbo, K., S. Yoshida, M. Ohmura, O. Ohneda, T. Ogawa, H. Tsuchiya, T. Kuwana, J. Kehler, K. Abe, H. R. Scholer and T. Suda (2003). "Identification and characterization of stem cells in prepubertal spermatogenesis in mice small star, filled." Dev Biol **258**(1): 209-225.
- Ohinata, Y., B. Payer, D. O'Carroll, K. Ancelin, Y. Ono, M. Sano, S. C. Barton, T. Obukhanych, M. Nussenzweig, A. Tarakhovsky, M. Saitou and M. A. Surani (2005). "Blimp1 is a critical determinant of the germ cell lineage in mice." Nature **436**(7048): 207-213.
- Ohrt, T., J. Mutze, W. Staroske, L. Weinmann, J. Hock, K. Crell, G. Meister and P. Schwillle (2008). "Fluorescence correlation spectroscopy and fluorescence cross-correlation spectroscopy reveal the cytoplasmic origination of loaded nuclear RISC in vivo in human cells." Nucleic Acids Res **36**(20): 6439-6449.
- Okamura, K., J. W. Hagen, H. Duan, D. M. Tyler and E. C. Lai (2007). "The mirtron pathway generates microRNA-class regulatory RNAs in Drosophila." Cell **130**(1): 89-100.
- Olivieri, D., M. M. Sykora, R. Sachidanandam, K. Mechtler and J. Brennecke (2010). "An in vivo RNAi assay identifies major genetic and cellular requirements for primary piRNA biogenesis in Drosophila." EMBO J **29**(19): 3301-3317.
- Ono, K. and J. Han (2000). "The p38 signal transduction pathway: activation and function." Cell Signal **12**(1): 1-13.
- Onodera, Y., J. R. Haag, T. Ream, P. Costa Nunes, O. Pontes and C. S. Pikaard (2005). "Plant nuclear RNA polymerase IV mediates siRNA and DNA methylation-dependent heterochromatin formation." Cell **120**(5): 613-622.
- Orban, T. I. and E. Izaurralde (2005). "Decay of mRNAs targeted by RISC requires XRN1, the Ski complex, and the exosome." RNA **11**(4): 459-469.

- Orford, K. W. and D. T. Scadden (2008). "Deconstructing stem cell self-renewal: genetic insights into cell-cycle regulation." Nat Rev Genet **9**(2): 115-128.
- Ovitt, C. E. and H. R. Scholer (1998). "The molecular biology of Oct-4 in the early mouse embryo." Mol Hum Reprod **4**(11): 1021-1031.
- Ozsolak, F., L. L. Poling, Z. Wang, H. Liu, X. S. Liu, R. G. Roeder, X. Zhang, J. S. Song and D. E. Fisher (2008). "Chromatin structure analyses identify miRNA promoters." Genes Dev **22**(22): 3172-3183.
- Pal-Bhadra, M., U. Bhadra and J. A. Birchler (2002). "RNAi related mechanisms affect both transcriptional and posttranscriptional transgene silencing in Drosophila." Mol Cell **9**(2): 315-327.
- Pal-Bhadra, M., U. Bhadra and J. A. Birchler (2004). "Interrelationship of RNA interference and transcriptional gene silencing in Drosophila." Cold Spring Harb Symp Quant Biol **69**: 433-438.
- Palakodeti, D., M. Smielewska, Y. C. Lu, G. W. Yeo and B. R. Graveley (2008). "The PIWI proteins SMEDWI-2 and SMEDWI-3 are required for stem cell function and piRNA expression in planarians." RNA **14**(6): 1174-1186.
- Palatnik, J. F., H. Wollmann, C. Schommer, R. Schwab, J. Boisbouvier, R. Rodriguez, N. Warthmann, E. Allen, T. Dezulian, D. Huson, J. C. Carrington and D. Weigel (2007). "Sequence and expression differences underlie functional specialization of Arabidopsis microRNAs miR159 and miR319." Dev Cell **13**(1): 115-125.
- Pane, A., K. Wehr and T. Schupbach (2007). "zucchini and squash encode two putative nucleases required for rasiRNA production in the Drosophila germline." Dev Cell **12**(6): 851-862.
- Parker, J. S., S. M. Roe and D. Barford (2004). "Crystal structure of a PIWI protein suggests mechanisms for siRNA recognition and slicer activity." EMBO J **23**(24): 4727-4737.
- Parker, J. S., S. M. Roe and D. Barford (2005). "Structural insights into mRNA recognition from a PIWI domain-siRNA guide complex." Nature **434**(7033): 663-666.
- Parker, R. and U. Sheth (2007). "P bodies and the control of mRNA translation and degradation." Mol Cell **25**(5): 635-646.
- Paroo, Z., X. Ye, S. Chen and Q. Liu (2009). "Phosphorylation of the human microRNA-generating complex mediates MAPK/Erk signaling." Cell **139**(1): 112-122.
- Pasero, M., M. Giovarelli, G. Bucci, R. Gherzi and P. Briata (2012). "Bone morphogenetic protein/SMAD signaling orients cell fate decision by impairing KSRP-dependent microRNA maturation." Cell Rep **2**(5): 1159-1168.
- Pasquinelli, A. E., B. J. Reinhart, F. Slack, M. Q. Martindale, M. I. Kuroda, B. Maller, D. C. Hayward, E. E. Ball, B. Degan, P. Muller, J. Spring, A. Srinivasan, M. Fishman, J. Finnerty, J. Corbo, M. Levine, P. Leahy, E. Davidson and G. Ruvkun (2000). "Conservation of the sequence and temporal expression of let-7 heterochronic regulatory RNA." Nature **408**(6808): 86-89.
- Peng, X. D., P. Z. Xu, M. L. Chen, A. Hahn-Windgassen, J. Skeen, J. Jacobs, D. Sundararajan, W. S. Chen, S. E. Crawford, K. G. Coleman and N. Hay (2003). "Dwarfism, impaired skin development, skeletal muscle atrophy, delayed bone development, and impeded adipogenesis in mice lacking Akt1 and Akt2." Genes Dev **17**(11): 1352-1365.
- Pesce, M., X. Wang, D. J. Wolgemuth and H. Scholer (1998). "Differential expression of the Oct-4 transcription factor during mouse germ cell differentiation." Mech Dev **71**(1-2): 89-98.
- Pickford, A. S., C. Catalanotto, C. Cogoni and G. Macino (2002). "Quelling in Neurospora crassa." Adv Genet **46**: 277-303.

- Pillai, R. S., C. G. Artus and W. Filipowicz (2004). "Tethering of human Ago proteins to mRNA mimics the miRNA-mediated repression of protein synthesis." *RNA* **10**(10): 1518-1525.
- Pillai, R. S., S. N. Bhattacharyya, C. G. Artus, T. Zoller, N. Cougot, E. Basyuk, E. Bertrand and W. Filipowicz (2005). "Inhibition of translational initiation by Let-7 MicroRNA in human cells." *Science* **309**(5740): 1573-1576.
- Piskounova, E., C. Polytarchou, J. E. Thornton, R. J. LaPierre, C. Pothoulakis, J. P. Hagan, D. Iliopoulos and R. I. Gregory (2011). "Lin28A and Lin28B inhibit let-7 microRNA biogenesis by distinct mechanisms." *Cell* **147**(5): 1066-1079.
- Polak, R. and M. Buitenhuis (2012). "The PI3K/PKB signaling module as key regulator of hematopoiesis: implications for therapeutic strategies in leukemia." *Blood* **119**(4): 911-923.
- Pontes, O., C. F. Li, P. Costa Nunes, J. Haag, T. Ream, A. Vitins, S. E. Jacobsen and C. S. Pikaard (2006). "The Arabidopsis chromatin-modifying nuclear siRNA pathway involves a nucleolar RNA processing center." *Cell* **126**(1): 79-92.
- Prochnik, S. E., D. S. Rokhsar and A. A. Aboobaker (2007). "Evidence for a microRNA expansion in the bilaterian ancestor." *Dev Genes Evol* **217**(1): 73-77.
- Pronk, C. J., D. J. Rossi, R. Mansson, J. L. Attema, G. L. Norddahl, C. K. Chan, M. Sigvardsson, I. L. Weissman and D. Bryder (2007). "Elucidation of the phenotypic, functional, and molecular topography of a myeloerythroid progenitor cell hierarchy." *Cell Stem Cell* **1**(4): 428-442.
- Qi, H. H., P. P. Ongusaha, J. Myllyharju, D. Cheng, O. Pakkanen, Y. Shi, S. W. Lee, J. Peng and Y. Shi (2008). "Prolyl 4-hydroxylation regulates Argonaute 2 stability." *Nature* **455**(7211): 421-424.
- Qi, Y., X. He, X. J. Wang, O. Kohany, J. Jurka and G. J. Hannon (2006). "Distinct catalytic and non-catalytic roles of ARGONAUTE4 in RNA-directed DNA methylation." *Nature* **443**(7114): 1008-1012.
- Raingeaud, J., A. J. Whitmarsh, T. Barrett, B. Derijard and R. J. Davis (1996). "MKK3- and MKK6-regulated gene expression is mediated by the p38 mitogen-activated protein kinase signal transduction pathway." *Mol Cell Biol* **16**(3): 1247-1255.
- Rajasethupathy, P., I. Antonov, R. Sheridan, S. Frey, C. Sander, T. Tuschl and E. R. Kandel (2012). "A role for neuronal piRNAs in the epigenetic control of memory-related synaptic plasticity." *Cell* **149**(3): 693-707.
- Rasmussen, K. D., S. Simmini, C. Abreu-Goodger, N. Bartonicek, M. Di Giacomo, D. Bilbao-Cortes, R. Horos, M. Von Lindern, A. J. Enright and D. O'Carroll (2010). "The miR-144/451 locus is required for erythroid homeostasis." *J Exp Med* **207**(7): 1351-1358.
- Ratcliff, F., B. D. Harrison and D. C. Baulcombe (1997). "A similarity between viral defense and gene silencing in plants." *Science* **276**(5318): 1558-1560.
- Reczko, M., M. Maragkakis, P. Alexiou, I. Grosse and A. G. Hatzigeorgiou (2012). "Functional microRNA targets in protein coding sequences." *Bioinformatics* **28**(6): 771-776.
- Reddien, P. W., N. J. Oviedo, J. R. Jennings, J. C. Jenkin and A. Sanchez Alvarado (2005). "SMEDWI-2 is a PIWI-like protein that regulates planarian stem cells." *Science* **310**(5752): 1327-1330.
- Reinhart, B. J., F. J. Slack, M. Basson, A. E. Pasquinelli, J. C. Bettinger, A. E. Rougvie, H. R. Horvitz and G. Ruvkun (2000). "The 21-nucleotide let-7 RNA regulates developmental timing in *Caenorhabditis elegans*." *Nature* **403**(6772): 901-906.
- Reinhart, B. J., E. G. Weinstein, M. W. Rhoades, B. Bartel and D. P. Bartel (2002). "MicroRNAs in plants." *Genes Dev* **16**(13): 1616-1626.

- Reuter, M., P. Berninger, S. Chuma, H. Shah, M. Hosokawa, C. Funaya, C. Antony, R. Sachidanandam and R. S. Pillai (2011). "Miwi catalysis is required for piRNA amplification-independent LINE1 transposon silencing." Nature **480**(7376): 264-267.
- Rinkevich, Y., A. Rosner, C. Rabinowitz, Z. Lapidot, E. Moiseeva and B. Rinkevich (2010). "Piwi positive cells that line the vasculature epithelium, underlie whole body regeneration in a basal chordate." Dev Biol **345**(1): 94-104.
- Rivas, F. V., N. H. Tolia, J. J. Song, J. P. Aragon, J. Liu, G. J. Hannon and L. Joshua-Tor (2005). "Purified Argonaute2 and an siRNA form recombinant human RISC." Nat Struct Mol Biol **12**(4): 340-349.
- Robanus-Maandag, E., M. Dekker, M. van der Valk, M. L. Carrozza, J. C. Jeanny, J. H. Dannenberg, A. Berns and H. te Riele (1998). "p107 is a suppressor of retinoblastoma development in pRb-deficient mice." Genes Dev **12**(11): 1599-1609.
- Robb, G. B., K. M. Brown, J. Khurana and T. M. Rana (2005). "Specific and potent RNAi in the nucleus of human cells." Nat Struct Mol Biol **12**(2): 133-137.
- Robinson, K. A. and S. M. Beverley (2003). "Improvements in transfection efficiency and tests of RNA interference (RNAi) approaches in the protozoan parasite Leishmania." Mol Biochem Parasitol **128**(2): 217-228.
- Ronkina, N., A. Kotlyarov, O. Dittrich-Breiholz, M. Kracht, E. Hitti, K. Milarski, R. Askew, S. Marusic, L. L. Lin, M. Gaestel and J. B. Telliez (2007). "The mitogen-activated protein kinase (MAPK)-activated protein kinases MK2 and MK3 cooperate in stimulation of tumor necrosis factor biosynthesis and stabilization of p38 MAPK." Mol Cell Biol **27**(1): 170-181.
- Rossi, L., A. Salvetti, A. Lena, R. Batistoni, P. Deri, C. Pugliesi, E. Loreti and V. Gremigni (2006). "DjPiwi-1, a member of the PAZ-Piwi gene family, defines a subpopulation of planarian stem cells." Dev Genes Evol **216**(6): 335-346.
- Rouse, J., P. Cohen, S. Trigon, M. Morange, A. Alonso-Llamazares, D. Zamanillo, T. Hunt and A. R. Nebreda (1994). "A novel kinase cascade triggered by stress and heat shock that stimulates MAPKAP kinase-2 and phosphorylation of the small heat shock proteins." Cell **78**(6): 1027-1037.
- Rozhkov, N. V., M. Hammell and G. J. Hannon (2013). "Multiple roles for Piwi in silencing Drosophila transposons." Genes Dev **27**(4): 400-412.
- Ruby, J. G., C. H. Jan and D. P. Bartel (2007). "Intronic microRNA precursors that bypass Drosha processing." Nature **448**(7149): 83-86.
- Rudel, S., A. Flatley, L. Weinmann, E. Kremmer and G. Meister (2008). "A multifunctional human Argonaute2-specific monoclonal antibody." RNA **14**(6): 1244-1253.
- Rudel, S., Y. Wang, R. Lenobel, R. Korner, H. H. Hsiao, H. Urlaub, D. Patel and G. Meister (2011). "Phosphorylation of human Argonaute proteins affects small RNA binding." Nucleic Acids Res **39**(6): 2330-2343.
- Russell, L. B. (1990). "Patterns of mutational sensitivity to chemicals in poststem-cell stages of mouse spermatogenesis." Prog Clin Biol Res **340C**: 101-113.
- Rybak, A., H. Fuchs, K. Hadian, L. Smirnova, E. A. Wulczyn, G. Michel, R. Nitsch, D. Krappmann and F. G. Wulczyn (2009). "The let-7 target gene mouse lin-41 is a stem cell specific E3 ubiquitin ligase for the miRNA pathway protein Ago2." Nat Cell Biol **11**(12): 1411-1420.

- Rybak, A., H. Fuchs, L. Smirnova, C. Brandt, E. E. Pohl, R. Nitsch and F. G. Wulczyn (2008). "A feedback loop comprising lin-28 and let-7 controls pre-let-7 maturation during neural stem-cell commitment." *Nat Cell Biol* **10**(8): 987-993.
- Sabio, G., J. S. Arthur, Y. Kuma, M. Peggie, J. Carr, V. Murray-Tait, F. Centeno, M. Goedert, N. A. Morrice and A. Cuenda (2005). "p38gamma regulates the localisation of SAP97 in the cytoskeleton by modulating its interaction with GKAP." *EMBO J* **24**(6): 1134-1145.
- Sada, A., A. Suzuki, H. Suzuki and Y. Saga (2009). "The RNA-binding protein NANOS2 is required to maintain murine spermatogonial stem cells." *Science* **325**(5946): 1394-1398.
- Saito, K., S. Inagaki, T. Mituyama, Y. Kawamura, Y. Ono, E. Sakota, H. Kotani, K. Asai, H. Siomi and M. C. Siomi (2009). "A regulatory circuit for piwi by the large Maf gene traffic jam in Drosophila." *Nature* **461**(7268): 1296-1299.
- Saito, K., H. Ishizu, M. Komai, H. Kotani, Y. Kawamura, K. M. Nishida, H. Siomi and M. C. Siomi (2010). "Roles for the Yb body components Armitage and Yb in primary piRNA biogenesis in Drosophila." *Genes Dev* **24**(22): 2493-2498.
- Saito, K., K. M. Nishida, T. Mori, Y. Kawamura, K. Miyoshi, T. Nagami, H. Siomi and M. C. Siomi (2006). "Specific association of Piwi with rasiRNAs derived from retrotransposon and heterochromatic regions in the Drosophila genome." *Genes Dev* **20**(16): 2214-2222.
- Saito, K., Y. Sakaguchi, T. Suzuki, T. Suzuki, H. Siomi and M. C. Siomi (2007). "Pimet, the Drosophila homolog of HEN1, mediates 2'-O-methylation of Piwi-interacting RNAs at their 3' ends." *Genes Dev* **21**(13): 1603-1608.
- Sangokoya, C., M. J. Telen and J. T. Chi (2010). "microRNA miR-144 modulates oxidative stress tolerance and associates with anemia severity in sickle cell disease." *Blood* **116**(20): 4338-4348.
- Sapsford, C. (1962). "Changes in the cells of the Sex Cords and Seminiferous Tubules during the development of the Testis of the rat and mouse." *Australian Journal of Zoology* **10**(2): 178-192.
- Sato, T., R. G. Vries, H. J. Snippert, M. van de Wetering, N. Barker, D. E. Stange, J. H. van Es, A. Abo, P. Kujala, P. J. Peters and H. Clevers (2009). "Single Lgr5 stem cells build crypt-villus structures in vitro without a mesenchymal niche." *Nature* **459**(7244): 262-265.
- Scacheri, P. C., O. Rozenblatt-Rosen, N. J. Caplen, T. G. Wolfsberg, L. Umayam, J. C. Lee, C. M. Hughes, K. S. Shanmugam, A. Bhattacharjee, M. Meyerson and F. S. Collins (2004). "Short interfering RNAs can induce unexpected and divergent changes in the levels of untargeted proteins in mammalian cells." *Proc Natl Acad Sci U S A* **101**(7): 1892-1897.
- Schaefer, A., H. I. Im, M. T. Veno, C. D. Fowler, A. Min, A. Intrator, J. Kjems, P. J. Kenny, D. O'Carroll and P. Greengard (2010). "Argonaute 2 in dopamine 2 receptor-expressing neurons regulates cocaine addiction." *J Exp Med* **207**(9): 1843-1851.
- Schirle, N. T. and I. J. MacRae (2012). "The crystal structure of human Argonaute2." *Science* **336**(6084): 1037-1040.
- Schmidt, A., G. Palumbo, M. P. Bozzetti, P. Tritto, S. Pimpinelli and U. Schafer (1999). "Genetic and molecular characterization of sting, a gene involved in crystal formation and meiotic drive in the male germ line of Drosophila melanogaster." *Genetics* **151**(2): 749-760.
- Schurmann, N., L. G. Trabuco, C. Bender, R. B. Russell and D. Grimm (2013). "Molecular dissection of human Argonaute proteins by DNA shuffling." *Nat Struct Mol Biol* **20**(7): 818-826.
- Schwartz, J. C., S. T. Younger, N. B. Nguyen, D. B. Hardy, B. P. Monia, D. R. Corey and B. A. Janowski (2008). "Antisense transcripts are targets for activating small RNAs." *Nat Struct Mol Biol* **15**(8): 842-848.

Schwarz, D. S., G. Hutvagner, T. Du, Z. Xu, N. Aronin and P. D. Zamore (2003). "Asymmetry in the assembly of the RNAi enzyme complex." Cell **115**(2): 199-208.

Schwarz, D. S., G. Hutvagner, B. Haley and P. D. Zamore (2002). "Evidence that siRNAs function as guides, not primers, in the Drosophila and human RNAi pathways." Mol Cell **10**(3): 537-548.

Schwermann, J., C. Rathinam, M. Schubert, S. Schumacher, F. Noyan, H. Koseki, A. Kotlyarov, C. Klein and M. Gaestel (2009). "MAPKAP kinase MK2 maintains self-renewal capacity of haematopoietic stem cells." EMBO J **28**(10): 1392-1406.

Seggerson, K., L. Tang and E. G. Moss (2002). "Two genetic circuits repress the Caenorhabditis elegans heterochronic gene lin-28 after translation initiation." Dev Biol **243**(2): 215-225.

Seipel, K., N. Yanze and V. Schmid (2004). "The germ line and somatic stem cell gene Cniwi in the jellyfish Podocoryne carnea." Int J Dev Biol **48**(1): 1-7.

Selbach, M., B. Schwanhausser, N. Thierfelder, Z. Fang, R. Khanin and N. Rajewsky (2008). "Widespread changes in protein synthesis induced by microRNAs." Nature **455**(7209): 58-63.

Sempere, L. F., C. N. Cole, M. A. McPeck and K. J. Peterson (2006). "The phylogenetic distribution of metazoan microRNAs: insights into evolutionary complexity and constraint." J Exp Zool B Mol Dev Evol **306**(6): 575-588.

Shackleton, M., F. Vaillant, K. J. Simpson, J. Stingl, G. K. Smyth, M. L. Asselin-Labat, L. Wu, G. J. Lindeman and J. E. Visvader (2006). "Generation of a functional mammary gland from a single stem cell." Nature **439**(7072): 84-88.

Shen, F. W., Y. Saga, G. Litman, G. Freeman, J. S. Tung, H. Cantor and E. A. Boyse (1985). "Cloning of Ly-5 cDNA." Proc Natl Acad Sci U S A **82**(21): 7360-7363.

Sheth, U. and R. Parker (2003). "Decapping and decay of messenger RNA occur in cytoplasmic processing bodies." Science **300**(5620): 805-808.

Shi, Y., A. Kotlyarov, K. Laabeta, A. D. Gruber, E. Butt, K. Marcus, H. E. Meyer, A. Friedrich, H. D. Volk and M. Gaestel (2003). "Elimination of protein kinase MK5/PRAK activity by targeted homologous recombination." Mol Cell Biol **23**(21): 7732-7741.

Shen, J., W. Xia, Y. B. Khotskaya, L. Huo, K. Nakanishi, S. Lim, Y. Du, Y. Wang, W. Chang, C. Chen, J. L. Hsu, Y. Wu, Y. C. Lam, B. P. James, X. Liu, C. Liu, D. Patel and M. C. Hung (2013). "EGFR modulates microRNA maturation in response to hypoxia through phosphorylation of Ago2." Nature **497**(7449): 383-387.

Shin, C., J. W. Nam, K. K. Farh, H. R. Chiang, A. Shkumatava and D. P. Bartel (2010). "Expanding the microRNA targeting code: functional sites with centered pairing." Mol Cell **38**(6): 789-802.

Shinohara, T., M. R. Avarbock and R. L. Brinster (1999). "beta1- and alpha6-integrin are surface markers on mouse spermatogonial stem cells." Proc Natl Acad Sci U S A **96**(10): 5504-5509.

Shinohara, T., K. E. Orwig, M. R. Avarbock and R. L. Brinster (2000). "Spermatogonial stem cell enrichment by multiparameter selection of mouse testis cells." Proc Natl Acad Sci U S A **97**(15): 8346-8351.

Shinohara, T., K. E. Orwig, M. R. Avarbock and R. L. Brinster (2001). "Remodeling of the postnatal mouse testis is accompanied by dramatic changes in stem cell number and niche accessibility." Proc Natl Acad Sci U S A **98**(11): 6186-6191.

Shoji, M., T. Tanaka, M. Hosokawa, M. Reuter, A. Stark, Y. Kato, G. Kondoh, K. Okawa, T. Chujo, T. Suzuki, K. Hata, S. L. Martin, T. Noce, S. Kuramochi-Miyagawa, T. Nakano, H. Sasaki, R. S. Pillai, N.

- Nakatsuji and S. Chuma (2009). "The TDRD9-MIWI2 complex is essential for piRNA-mediated retrotransposon silencing in the mouse male germline." *Dev Cell* **17**(6): 775-787.
- Shull, M. M., I. Ormsby, A. B. Kier, S. Pawlowski, R. J. Diebold, M. Yin, R. Allen, C. Sidman, G. Proetzel, D. Calvin and et al. (1992). "Targeted disruption of the mouse transforming growth factor-beta 1 gene results in multifocal inflammatory disease." *Nature* **359**(6397): 693-699.
- Sibilia, M. and E. F. Wagner (1995). "Strain-dependent epithelial defects in mice lacking the EGF receptor." *Science* **269**(5221): 234-238.
- Sienski, G., D. Donertas and J. Brennecke (2012). "Transcriptional silencing of transposons by Piwi and maelstrom and its impact on chromatin state and gene expression." *Cell* **151**(5): 964-980.
- Sigova, A., N. Rhind and P. D. Zamore (2004). "A single Argonaute protein mediates both transcriptional and posttranscriptional silencing in *Schizosaccharomyces pombe*." *Genes Dev* **18**(19): 2359-2367.
- Silvers, W.K. (1979). "The coat colors of mice (A model for mammalian gene action and interaction)." Springer Verlag.
- Sijen, T., J. Fleenor, F. Simmer, K. L. Thijssen, S. Parrish, L. Timmons, R. H. Plasterk and A. Fire (2001). "On the role of RNA amplification in dsRNA-triggered gene silencing." *Cell* **107**(4): 465-476.
- Silhavy, D., A. Molnar, A. Luciola, G. Szittyta, C. Hornyik, M. Tavazza and J. Burgyan (2002). "A viral protein suppresses RNA silencing and binds silencing-generated, 21- to 25-nucleotide double-stranded RNAs." *EMBO J* **21**(12): 3070-3080.
- Simpson, E. M., C. C. Linder, E. E. Sargent, M. T. Davisson, L. E. Mobraaten and J. J. Sharp (1997). "Genetic variation among 129 substrains and its importance for targeted mutagenesis in mice." *Nat Genet* **16**(1): 19-27.
- Siomi, H. and M. C. Siomi (2010). "Posttranscriptional regulation of microRNA biogenesis in animals." *Mol Cell* **38**(3): 323-332.
- Sithanandam, G., F. Latif, F. M. Duh, R. Bernal, U. Smola, H. Li, I. Kuzmin, V. Wixler, L. Geil and S. Shrestha (1996). "3pK, a new mitogen-activated protein kinase-activated protein kinase located in the small cell lung cancer tumor suppressor gene region." *Mol Cell Biol* **16**(3): 868-876.
- Slack, F. J., M. Basson, Z. Liu, V. Ambros, H. R. Horvitz and G. Ruvkun (2000). "The lin-41 RBCC gene acts in the *C. elegans* heterochronic pathway between the let-7 regulatory RNA and the LIN-29 transcription factor." *Mol Cell* **5**(4): 659-669.
- Smardon, A., J. M. Spoerke, S. C. Stacey, M. E. Klein, N. Mackin and E. M. Maine (2000). "EGO-1 is related to RNA-directed RNA polymerase and functions in germ-line development and RNA interference in *C. elegans*." *Curr Biol* **10**(4): 169-178.
- Socolovsky, M., H. Nam, M. D. Fleming, V. H. Haase, C. Brugnara and H. F. Lodish (2001). "Ineffective erythropoiesis in Stat5a(-/-)5b(-/-) mice due to decreased survival of early erythroblasts." *Blood* **98**(12): 3261-3273.
- Solter, D., T. Hiiragi, A. V. Evsikov, J. Moyer, W. N. De Vries, A. E. Peaston and B. B. Knowles (2004). "Epigenetic mechanisms in early mammalian development." *Cold Spring Harb Symp Quant Biol* **69**: 11-17.
- Song, J. J., S. K. Smith, G. J. Hannon and L. Joshua-Tor (2004). "Crystal structure of Argonaute and its implications for RISC slicer activity." *Science* **305**(5689): 1434-1437.
- Souret, F. F., J. P. Kastanmayer and P. J. Green (2004). "AtXRN4 degrades mRNA in *Arabidopsis* and its substrates include selected miRNA targets." *Mol Cell* **15**(2): 173-183.

- Spangrude, G. J., S. Heimfeld and I. L. Weissman (1988). "Purification and characterization of mouse hematopoietic stem cells." *Science* **241**(4861): 58-62.
- Spradling, A. C. (1993). "Germline cysts: communes that work." *Cell* **72**(5): 649-651.
- Stokoe, D., D. G. Campbell, S. Nakielny, H. Hidaka, S. J. Leever, C. Marshall and P. Cohen (1992). "MAPKAP kinase-2; a novel protein kinase activated by mitogen-activated protein kinase." *EMBO J* **11**(11): 3985-3994.
- Stranger, B. E., E. A. Stahl and T. Raj (2011). "Progress and promise of genome-wide association studies for human complex trait genetics." *Genetics* **187**(2): 367-383.
- Strunk, K. E., V. Amann and D. W. Threadgill (2004). "Phenotypic variation resulting from a deficiency of epidermal growth factor receptor in mice is caused by extensive genetic heterogeneity that can be genetically and molecularly partitioned." *Genetics* **167**(4): 1821-1832.
- Su, H., M. I. Trombly, J. Chen and X. Wang (2009). "Essential and overlapping functions for mammalian Argonautes in microRNA silencing." *Genes Dev* **23**(3): 304-317.
- Sugiyama, T., H. Cam, A. Verdel, D. Moazed and S. I. Grewal (2005). "RNA-dependent RNA polymerase is an essential component of a self-enforcing loop coupling heterochromatin assembly to siRNA production." *Proc Natl Acad Sci U S A* **102**(1): 152-157.
- Suh, N., L. Baehner, F. Moltzahn, C. Melton, A. Shenoy, J. Chen and R. Blelloch (2010). "MicroRNA function is globally suppressed in mouse oocytes and early embryos." *Curr Biol* **20**(3): 271-277.
- Sung, W. K., J. Van't Hof and G. Jagiello (1986). "DNA synthesis studies in pre-meiotic mouse oogenesis." *Exp Cell Res* **163**(2): 370-380.
- Suzuki, H., A. Sada, S. Yoshida and Y. Saga (2009). "The heterogeneity of spermatogonia is revealed by their topology and expression of marker proteins including the germ cell-specific proteins Nanos2 and Nanos3." *Dev Biol* **336**(2): 222-231.
- Suzuki, H. I., K. Yamagata, K. Sugimoto, T. Iwamoto, S. Kato and K. Miyazono (2009). "Modulation of microRNA processing by p53." *Nature* **460**(7254): 529-533.
- Szakmary, A., D. N. Cox, Z. Wang and H. Lin (2005). "Regulatory relationship among piwi, pumilio, and bag-of-marbles in Drosophila germline stem cell self-renewal and differentiation." *Curr Biol* **15**(2): 171-178.
- Takeda, Y., Y. Mishima, T. Fujiwara, H. Sakamoto and K. Inoue (2009). "DAZL relieves miRNA-mediated repression of germline mRNAs by controlling poly(A) tail length in zebrafish." *PLoS One* **4**(10): e7513.
- Tam, O. H., A. A. Aravin, P. Stein, A. Girard, E. P. Murchison, S. Cheloufi, E. Hodges, M. Anger, R. Sachidanandam, R. M. Schultz and G. J. Hannon (2008). "Pseudogene-derived small interfering RNAs regulate gene expression in mouse oocytes." *Nature* **453**(7194): 534-538.
- Tamura, K., T. Sudo, U. Senfleben, A. M. Dadak, R. Johnson and M. Karin (2000). "Requirement for p38alpha in erythropoietin expression: a role for stress kinases in erythropoiesis." *Cell* **102**(2): 221-231.
- Tang, F., M. Kaneda, D. O'Carroll, P. Hajkova, S. C. Barton, Y. A. Sun, C. Lee, A. Tarakhovsky, K. Lao and M. A. Surani (2007). "Maternal microRNAs are essential for mouse zygotic development." *Genes Dev* **21**(6): 644-648.
- Tang, G., B. J. Reinhart, D. P. Bartel and P. D. Zamore (2003). "A biochemical framework for RNA silencing in plants." *Genes Dev* **17**(1): 49-63.

Teslovich, T. M., K. Musunuru, A. V. Smith, A. C. Edmondson, I. M. Stylianou, M. Koseki, J. P. Pirruccello, S. Ripatti, D. I. Chasman, C. J. Willer, C. T. Johansen, S. W. Fouchier, A. Isaacs, G. M. Peloso, M. Barbalic, S. L. Ricketts, J. C. Bis, Y. S. Aulchenko, G. Thorleifsson, M. F. Feitosa, J. Chambers, M. Orho-Melander, O. Melander, T. Johnson, X. Li, X. Guo, M. Li, Y. Shin Cho, M. Jin Go, Y. Jin Kim, J. Y. Lee, T. Park, K. Kim, X. Sim, R. Twee-Hee Ong, D. C. Croteau-Chonka, L. A. Lange, J. D. Smith, K. Song, J. Hua Zhao, X. Yuan, J. Luan, C. Lamina, A. Ziegler, W. Zhang, R. Y. Zee, A. F. Wright, J. C. Witteman, J. F. Wilson, G. Willemsen, H. E. Wichmann, J. B. Whitfield, D. M. Waterworth, N. J. Wareham, G. Waeber, P. Vollenweider, B. F. Voight, V. Vitart, A. G. Uitterlinden, M. Uda, J. Tuomilehto, J. R. Thompson, T. Tanaka, I. Surakka, H. M. Stringham, T. D. Spector, N. Soranzo, J. H. Smit, J. Sinisalo, K. Silander, E. J. Sijbrands, A. Scuteri, J. Scott, D. Schlessinger, S. Sanna, V. Salomaa, J. Saharinen, C. Sabatti, A. Ruokonen, I. Rudan, L. M. Rose, R. Roberts, M. Rieder, B. M. Psaty, P. P. Pramstaller, I. Pichler, M. Perola, B. W. Penninx, N. L. Pedersen, C. Pattaro, A. N. Parker, G. Pare, B. A. Oostra, C. J. O'Donnell, M. S. Nieminen, D. A. Nickerson, G. W. Montgomery, T. Meitinger, R. McPherson, M. I. McCarthy, W. McArdle, D. Masson, N. G. Martin, F. Marroni, M. Mangino, P. K. Magnusson, G. Lucas, R. Luben, R. J. Loos, M. L. Lokki, G. Lettre, C. Langenberg, L. J. Launer, E. G. Lakatta, R. Laaksonen, K. O. Kyvik, F. Kronenberg, I. R. Konig, K. T. Khaw, J. Kaprio, L. M. Kaplan, A. Johansson, M. R. Jarvelin, A. C. Janssens, E. Ingelsson, W. Igl, G. Kees Hovingh, J. J. Hottenga, A. Hofman, A. A. Hicks, C. Hengstenberg, I. M. Heid, C. Hayward, A. S. Havulinna, N. D. Hastie, T. B. Harris, T. Haritunians, A. S. Hall, U. Gyllensten, C. Guiducci, L. C. Groop, E. Gonzalez, C. Gieger, N. B. Freimer, L. Ferrucci, J. Erdmann, P. Elliott, K. G. Ejebe, A. Doring, A. F. Dominiczak, S. Demissie, P. Deloukas, E. J. de Geus, U. de Faire, G. Crawford, F. S. Collins, Y. D. Chen, M. J. Caulfield, H. Campbell, N. P. Burt, L. L. Bonnycastle, D. I. Boomsma, S. M. Boekholdt, R. N. Bergman, I. Barroso, S. Bandinelli, C. M. Ballantyne, T. L. Assimes, T. Quertermous, D. Altshuler, M. Seielstad, T. Y. Wong, E. S. Tai, A. B. Feranil, C. W. Kuzawa, L. S. Adair, H. A. Taylor, Jr., I. B. Borecki, S. B. Gabriel, J. G. Wilson, H. Holm, U. Thorsteinsdottir, V. Gudnason, R. M. Krauss, K. L. Mohlke, J. M. Ordovas, P. B. Munroe, J. S. Kooner, A. R. Tall, R. A. Hegele, J. J. Kastelein, E. E. Schadt, J. I. Rotter, E. Boerwinkle, D. P. Strachan, V. Mooser, K. Stefansson, M. P. Reilly, N. J. Samani, H. Schunkert, L. A. Cupples, M. S. Sandhu, P. M. Ridker, D. J. Rader, C. M. van Duijn, L. Peltonen, G. R. Abecasis, M. Boehnke and S. Kathiresan (2010). "Biological, clinical and population relevance of 95 loci for blood lipids." *Nature* **466**(7307): 707-713.

Threadgill, D. W., A. A. Dlugosz, L. A. Hansen, T. Tennenbaum, U. Lichti, D. Yee, C. LaMantia, T. Mourton, K. Herrup, R. C. Harris and et al. (1995). "Targeted disruption of mouse EGF receptor: effect of genetic background on mutant phenotype." *Science* **269**(5221): 230-234.

Threadgill, D. W., D. Yee, A. Matin, J. H. Nadeau and T. Magnuson (1997). "Genealogy of the 129 inbred strains: 129/SvJ is a contaminated inbred strain." *Mamm Genome* **8**(6): 390-393.

Till, S., E. Lejeune, R. Thermann, M. Bortfeld, M. Hothorn, D. Enderle, C. Heinrich, M. W. Hentze and A. G. Ladurner (2007). "A conserved motif in Argonaute-interacting proteins mediates functional interactions through the Argonaute PIWI domain." *Nat Struct Mol Biol* **14**(10): 897-903.

Tokuda, M., Y. Kadokawa, H. Kurahashi and T. Marunouchi (2007). "CDH1 is a specific marker for undifferentiated spermatogonia in mouse testes." *Biol Reprod* **76**(1): 130-141.

Tomari, Y., T. Du, B. Haley, D. S. Schwarz, R. Bennett, H. A. Cook, B. S. Koppetsch, W. E. Theurkauf and P. D. Zamore (2004). "RISC assembly defects in the Drosophila RNAi mutant armitage." *Cell* **116**(6): 831-841.

Tomari, Y. and P. D. Zamore (2005). "Perspective: machines for RNAi." *Genes Dev* **19**(5): 517-529.

Trabucchi, M., P. Briata, M. Garcia-Mayoral, A. D. Haase, W. Filipowicz, A. Ramos, R. Gherzi and M. G. Rosenfeld (2009). "The RNA-binding protein KSRP promotes the biogenesis of a subset of microRNAs." *Nature* **459**(7249): 1010-1014.

Tretter, E. M., J. P. Alvarez, Y. Eshed and J. L. Bowman (2008). "Activity range of Arabidopsis small RNAs derived from different biogenesis pathways." *Plant Physiol* **147**(1): 58-62.

- Tsuda, M., Y. Sasaoka, M. Kiso, K. Abe, S. Haraguchi, S. Kobayashi and Y. Saga (2003). "Conserved role of nanos proteins in germ cell development." Science **301**(5637): 1239-1241.
- Ullu, E., C. Tschudi and T. Chakraborty (2004). "RNA interference in protozoan parasites." Cell Microbiol **6**(6): 509-519.
- Vagin, V. V., A. Sigova, C. Li, H. Seitz, V. Gvozdev and P. D. Zamore (2006). "A distinct small RNA pathway silences selfish genetic elements in the germline." Science **313**(5785): 320-324.
- Van Stry, M., T. H. Oguin, 3rd, S. Cheloufi, P. Vogel, M. Watanabe, M. R. Pillai, P. Dash, P. G. Thomas, G. J. Hannon and M. Bix (2012). "Enhanced susceptibility of Ago1/3 double-null mice to influenza A virus infection." J Virol **86**(8): 4151-4157.
- Vance, V. and H. Vaucheret (2001). "RNA silencing in plants--defense and counterdefense." Science **292**(5525): 2277-2280.
- Vastenhouw, N. L., S. E. Fischer, V. J. Robert, K. L. Thijssen, A. G. Fraser, R. S. Kamath, J. Ahringer and R. H. Plasterk (2003). "A genome-wide screen identifies 27 genes involved in transposon silencing in *C. elegans*." Curr Biol **13**(15): 1311-1316.
- Veis, D. J., C. M. Sorenson, J. R. Shutter and S. J. Korsmeyer (1993). "Bcl-2-deficient mice demonstrate fulminant lymphoid apoptosis, polycystic kidneys, and hypopigmented hair." Cell **75**(2): 229-240.
- Vella, M. C., K. Reinert and F. J. Slack (2004). "Architecture of a validated microRNA::target interaction." Chem Biol **11**(12): 1619-1623.
- Ventura, A., A. G. Young, M. M. Winslow, L. Lintault, A. Meissner, S. J. Erkeland, J. Newman, R. T. Bronson, D. Crowley, J. R. Stone, R. Jaenisch, P. A. Sharp and T. Jacks (2008). "Targeted deletion reveals essential and overlapping functions of the miR-17 through 92 family of miRNA clusters." Cell **132**(5): 875-886.
- Verdel, A., S. Jia, S. Gerber, T. Sugiyama, S. Gygi, S. I. Grewal and D. Moazed (2004). "RNAi-mediated targeting of heterochromatin by the RITS complex." Science **303**(5658): 672-676.
- Vergouwen, R. P., S. G. Jacobs, R. Huiskamp, J. A. Davids and D. G. de Rooij (1991). "Proliferative activity of gonocytes, Sertoli cells and interstitial cells during testicular development in mice." J Reprod Fertil **93**(1): 233-243.
- Viswanathan, S. R., G. Q. Daley and R. I. Gregory (2008). "Selective blockade of microRNA processing by Lin28." Science **320**(5872): 97-100.
- Voigt, F., M. Reuter, A. Kasaruho, E. C. Schulz, R. S. Pillai and O. Barabas (2012). "Crystal structure of the primary piRNA biogenesis factor Zucchini reveals similarity to the bacterial PLD endonuclease Nuc." RNA **18**(12): 2128-2134.
- Volpe, T. A., C. Kidner, I. M. Hall, G. Teng, S. I. Grewal and R. A. Martienssen (2002). "Regulation of heterochromatic silencing and histone H3 lysine-9 methylation by RNAi." Science **297**(5588): 1833-1837.
- Vourekas, A., Q. Zheng, P. Alexiou, M. Maragkakis, Y. Kirino, B. D. Gregory and Z. Mourelatos (2012). "Mili and Miwi target RNA repertoire reveals piRNA biogenesis and function of Miwi in spermiogenesis." Nat Struct Mol Biol **19**(8): 773-781.
- Wada, T., J. Kikuchi and Y. Furukawa (2012). "Histone deacetylase 1 enhances microRNA processing via deacetylation of DGCR8." EMBO Rep **13**(2): 142-149.
- Wakiyama, M., K. Takimoto, O. Ohara and S. Yokoyama (2007). "Let-7 microRNA-mediated mRNA deadenylation and translational repression in a mammalian cell-free system." Genes Dev **21**(15): 1857-1862.

- Walsh, C. P., J. R. Chaillet and T. H. Bestor (1998). "Transcription of IAP endogenous retroviruses is constrained by cytosine methylation." *Nat Genet* **20**(2): 116-117.
- Wang, D., Z. Zhang, E. O'Loughlin, T. Lee, S. Houel, D. O'Carroll, A. Tarakhovsky, N. G. Ahn and R. Yi (2012). "Quantitative functions of Argonaute proteins in mammalian development." *Genes Dev* **26**(7): 693-704.
- Wang, S., A. B. Aurora, B. A. Johnson, X. Qi, J. McAnally, J. A. Hill, J. A. Richardson, R. Bassel-Duby and E. N. Olson (2008). "The endothelial-specific microRNA miR-126 governs vascular integrity and angiogenesis." *Dev Cell* **15**(2): 261-271.
- Wang, X., A. Flynn, A. J. Waskiewicz, B. L. Webb, R. G. Vries, I. A. Baines, J. A. Cooper and C. G. Proud (1998). "The phosphorylation of eukaryotic initiation factor eIF4E in response to phorbol esters, cell stresses, and cytokines is mediated by distinct MAP kinase pathways." *J Biol Chem* **273**(16): 9373-9377.
- Wang, X. H., R. Aliyari, W. X. Li, H. W. Li, K. Kim, R. Carthew, P. Atkinson and S. W. Ding (2006). "RNA interference directs innate immunity against viruses in adult *Drosophila*." *Science* **312**(5772): 452-454.
- Wang, Y., R. Medvid, C. Melton, R. Jaenisch and R. Blelloch (2007). "DGCR8 is essential for microRNA biogenesis and silencing of embryonic stem cell self-renewal." *Nat Genet* **39**(3): 380-385.
- Wang, Y., G. Sheng, S. Juranek, T. Tuschl and D. J. Patel (2008). "Structure of the guide-strand-containing argonaute silencing complex." *Nature* **456**(7219): 209-213.
- Wassenegger, M. and G. Krczal (2006). "Nomenclature and functions of RNA-directed RNA polymerases." *Trends Plant Sci* **11**(3): 142-151.
- Watanabe, T., S. Chuma, Y. Yamamoto, S. Kuramochi-Miyagawa, Y. Totoki, A. Toyoda, Y. Hoki, A. Fujiyama, T. Shibata, T. Sado, T. Noce, T. Nakano, N. Nakatsuji, H. Lin and H. Sasaki (2011). "MITOPLD is a mitochondrial protein essential for nuage formation and piRNA biogenesis in the mouse germline." *Dev Cell* **20**(3): 364-375.
- Watanabe, T., A. Takeda, T. Tsukiyama, K. Mise, T. Okuno, H. Sasaki, N. Minami and H. Imai (2006). "Identification and characterization of two novel classes of small RNAs in the mouse germline: retrotransposon-derived siRNAs in oocytes and germline small RNAs in testes." *Genes Dev* **20**(13): 1732-1743.
- Watanabe, T., Y. Totoki, A. Toyoda, M. Kaneda, S. Kuramochi-Miyagawa, Y. Obata, H. Chiba, Y. Kohara, T. Kono, T. Nakano, M. A. Surani, Y. Sakaki and H. Sasaki (2008). "Endogenous siRNAs from naturally formed dsRNAs regulate transcripts in mouse oocytes." *Nature* **453**(7194): 539-543.
- Weber, J. E. and L. D. Russell (1987). "A study of intercellular bridges during spermatogenesis in the rat." *Am J Anat* **180**(1): 1-24.
- Webster, K. E., M. K. O'Bryan, S. Fletcher, P. E. Crewther, U. Aapola, J. Craig, D. K. Harrison, H. Aung, N. Phutikanit, R. Lyle, S. J. Meachem, S. E. Antonarakis, D. M. de Kretser, M. P. Hedger, P. Peterson, B. J. Carroll and H. S. Scott (2005). "Meiotic and epigenetic defects in Dnmt3L-knockout mouse spermatogenesis." *Proc Natl Acad Sci U S A* **102**(11): 4068-4073.
- Wee, L. M., C. F. Flores-Jasso, W. E. Salomon and P. D. Zamore (2012). "Argonaute divides its RNA guide into domains with distinct functions and RNA-binding properties." *Cell* **151**(5): 1055-1067.
- Weinmann, L., J. Hock, T. Ivacevic, T. Ohrt, J. Mutze, P. Schwill, E. Kremmer, V. Benes, H. Urlaub and G. Meister (2009). "Importin 8 is a gene silencing factor that targets argonaute proteins to distinct mRNAs." *Cell* **136**(3): 496-507.

- Wierzbicki, A. T., J. R. Haag and C. S. Pikaard (2008). "Noncoding transcription by RNA polymerase Pol IVb/Pol V mediates transcriptional silencing of overlapping and adjacent genes." Cell **135**(4): 635-648.
- Wieschaus, E. and J. Szabad (1979). "The development and function of the female germ line in *Drosophila melanogaster*: a cell lineage study." Dev Biol **68**(1): 29-46.
- Wightman, B., T. R. Burglin, J. Gatto, P. Arasu and G. Ruvkun (1991). "Negative regulatory sequences in the *lin-14* 3'-untranslated region are necessary to generate a temporal switch during *Caenorhabditis elegans* development." Genes Dev **5**(10): 1813-1824.
- Wightman, B., I. Ha and G. Ruvkun (1993). "Posttranscriptional regulation of the heterochronic gene *lin-14* by *lin-4* mediates temporal pattern formation in *C. elegans*." Cell **75**(5): 855-862.
- Wilson, A., E. Laurenti, G. Oser, R. C. van der Wath, W. Blanco-Bose, M. Jaworski, S. Offner, C. F. Dunant, L. Eshkind, E. Bockamp, P. Lio, H. R. Macdonald and A. Trumpp (2008). "Hematopoietic stem cells reversibly switch from dormancy to self-renewal during homeostasis and repair." Cell **135**(6): 1118-1129.
- Wilson, J. E., J. E. Connell and P. M. Macdonald (1996). "aubergine enhances oskar translation in the *Drosophila* ovary." Development **122**(5): 1631-1639.
- Wolfer, D. P., W. E. Crusio and H. P. Lipp (2002). "Knockout mice: simple solutions to the problems of genetic background and flanking genes." Trends Neurosci **25**(7): 336-340.
- Wu, C., J. So, B. N. Davis-Dusenbery, H. H. Qi, D. B. Bloch, Y. Shi, G. Lagna and A. Hata (2011). "Hypoxia potentiates microRNA-mediated gene silencing through posttranslational modification of Argonaute2." Mol Cell Biol **31**(23): 4760-4774.
- Wu, J. and X. Xie (2006). "Comparative sequence analysis reveals an intricate network among REST, CREB and miRNA in mediating neuronal gene expression." Genome Biol **7**(9): R85.
- Wu, L., J. Fan and J. G. Belasco (2008). "Importance of translation and nonnucleolytic ago proteins for on-target RNA interference." Curr Biol **18**(17): 1327-1332.
- Wulczyn, F. G., L. Smirnova, A. Rybak, C. Brandt, E. Kwidzinski, O. Ninnemann, M. Strehle, A. Seiler, S. Schumacher and R. Nitsch (2007). "Post-transcriptional regulation of the *let-7* microRNA during neural cell specification." FASEB J **21**(2): 415-426.
- Xia, Z., M. Dickens, J. Raingeaud, R. J. Davis and M. E. Greenberg (1995). "Opposing effects of ERK and JNK-p38 MAP kinases on apoptosis." Science **270**(5240): 1326-1331.
- Xiao, C., D. P. Calado, G. Galler, T. H. Thai, H. C. Patterson, J. Wang, N. Rajewsky, T. P. Bender and K. Rajewsky (2007). "MiR-150 controls B cell differentiation by targeting the transcription factor *c-Myb*." Cell **131**(1): 146-159.
- Xiao, C., L. Srinivasan, D. P. Calado, H. C. Patterson, B. Zhang, J. Wang, J. M. Henderson, J. L. Kutok and K. Rajewsky (2008). "Lymphoproliferative disease and autoimmunity in mice with increased miR-17-92 expression in lymphocytes." Nat Immunol **9**(4): 405-414.
- Xie, Z., E. Allen, N. Fahlgren, A. Calamar, S. A. Givan and J. C. Carrington (2005). "Expression of Arabidopsis MIRNA genes." Plant Physiol **138**(4): 2145-2154.
- Xie, Z., L. K. Johansen, A. M. Gustafson, K. D. Kasschau, A. D. Lellis, D. Zilberman, S. E. Jacobsen and J. C. Carrington (2004). "Genetic and functional diversification of small RNA pathways in plants." PLoS Biol **2**(5): E104.
- Xu, S., K. Guo, Q. Zeng, J. Huo and K. P. Lam (2012). "The RNase III enzyme Dicer is essential for germinal center B-cell formation." Blood **119**(3): 767-776.

- Yamagata, K., S. Fujiyama, S. Ito, T. Ueda, T. Murata, M. Naitou, K. Takeyama, Y. Minami, B. W. O'Malley and S. Kato (2009). "Maturation of microRNA is hormonally regulated by a nuclear receptor." *Mol Cell* **36**(2): 340-347.
- Yang, J. S., T. Maurin, N. Robine, K. D. Rasmussen, K. L. Jeffrey, R. Chandwani, E. P. Papapetrou, M. Sadelain, D. O'Carroll and E. C. Lai (2010). "Conserved vertebrate mir-451 provides a platform for Dicer-independent, Ago2-mediated microRNA biogenesis." *Proc Natl Acad Sci U S A* **107**(34): 15163-15168.
- Yang, W., T. P. Chendrimada, Q. Wang, M. Higuchi, P. H. Seeburg, R. Shiekhattar and K. Nishikura (2006). "Modulation of microRNA processing and expression through RNA editing by ADAR deaminases." *Nat Struct Mol Biol* **13**(1): 13-21.
- Yang, W. J., D. D. Yang, S. Na, G. E. Sandusky, Q. Zhang and G. Zhao (2005). "Dicer is required for embryonic angiogenesis during mouse development." *J Biol Chem* **280**(10): 9330-9335.
- Yang, Z. Z., O. Tschopp, N. Di-Poi, E. Bruder, A. Baudry, B. Dummler, W. Wahli and B. A. Hemmings (2005). "Dosage-dependent effects of Akt1/protein kinase Balpha (PKBalpha) and Akt3/PKBgamma on thymus, skin, and cardiovascular and nervous system development in mice." *Mol Cell Biol* **25**(23): 10407-10418.
- Ye, X., N. Huang, Y. Liu, Z. Paroo, C. Huerta, P. Li, S. Chen, Q. Liu and H. Zhang (2011). "Structure of C3PO and mechanism of human RISC activation." *Nat Struct Mol Biol* **18**(6): 650-657.
- Yeager, M., N. Orr, R. B. Hayes, K. B. Jacobs, P. Kraft, S. Wacholder, M. J. Minichiello, P. Fearhead, K. Yu, N. Chatterjee, Z. Wang, R. Welch, B. J. Staats, E. E. Calle, H. S. Feigelson, M. J. Thun, C. Rodriguez, D. Albanes, J. Virtamo, S. Weinstein, F. R. Schumacher, E. Giovannucci, W. C. Willett, G. Cancel-Tassin, O. Cussenot, A. Valeri, G. L. Andriole, E. P. Gelmann, M. Tucker, D. S. Gerhard, J. F. Fraumeni, Jr., R. Hoover, D. J. Hunter, S. J. Chanock and G. Thomas (2007). "Genome-wide association study of prostate cancer identifies a second risk locus at 8q24." *Nat Genet* **39**(5): 645-649.
- Yekta, S., I. H. Shih and D. P. Bartel (2004). "MicroRNA-directed cleavage of HOXB8 mRNA." *Science* **304**(5670): 594-596.
- Yeom, K. H., Y. Lee, J. Han, M. R. Suh and V. N. Kim (2006). "Characterization of DGCR8/Pasha, the essential cofactor for Drosha in primary miRNA processing." *Nucleic Acids Res* **34**(16): 4622-4629.
- Yi, R., Y. Qin, I. G. Macara and B. R. Cullen (2003). "Exportin-5 mediates the nuclear export of pre-microRNAs and short hairpin RNAs." *Genes Dev* **17**(24): 3011-3016.
- Yigit, E., P. J. Batista, Y. Bei, K. M. Pang, C. C. Chen, N. H. Tolia, L. Joshua-Tor, S. Mitani, M. J. Simard and C. C. Mello (2006). "Analysis of the *C. elegans* Argonaute family reveals that distinct Argonautes act sequentially during RNAi." *Cell* **127**(4): 747-757.
- Yilmaz, O. H., M. J. Kiel and S. J. Morrison (2006). "SLAM family markers are conserved among hematopoietic stem cells from old and reconstituted mice and markedly increase their purity." *Blood* **107**(3): 924-930.
- Yoshida, S. (2010). "Stem cells in mammalian spermatogenesis." *Dev Growth Differ* **52**(3): 311-317.
- Yoshida, S., A. Takakura, K. Ohbo, K. Abe, J. Wakabayashi, M. Yamamoto, T. Suda and Y. Nabeshima (2004). "Neurogenin3 delineates the earliest stages of spermatogenesis in the mouse testis." *Dev Biol* **269**(2): 447-458.
- Yoshikawa, M., A. Peragine, M. Y. Park and R. S. Poethig (2005). "A pathway for the biogenesis of trans-acting siRNAs in Arabidopsis." *Genes Dev* **19**(18): 2164-2175.

Yoshimizu, T., N. Sugiyama, M. De Felice, Y. I. Yeom, K. Ohbo, K. Masuko, M. Obinata, K. Abe, H. R. Scholer and Y. Matsui (1999). "Germline-specific expression of the Oct-4/green fluorescent protein (GFP) transgene in mice." *Dev Growth Differ* **41**(6): 675-684.

Yoshinaga, K., S. Nishikawa, M. Ogawa, S. Hayashi, T. Kunisada, T. Fujimoto and S. Nishikawa (1991). "Role of c-kit in mouse spermatogenesis: identification of spermatogonia as a specific site of c-kit expression and function." *Development* **113**(2): 689-699.

Yu, D., C. O. dos Santos, G. Zhao, J. Jiang, J. D. Amigo, E. Khandros, L. C. Dore, Y. Yao, J. D'Souza, Z. Zhang, S. Ghaffari, J. Choi, S. Friend, W. Tong, J. S. Orange, B. H. Paw and M. J. Weiss (2010). "miR-451 protects against erythroid oxidant stress by repressing 14-3-3zeta." *Genes Dev* **24**(15): 1620-1633.

Yuan, J., C. K. Nguyen, X. Liu, C. Kanellopoulou and S. A. Muljo (2012). "Lin28b reprograms adult bone marrow hematopoietic progenitors to mediate fetal-like lymphopoiesis." *Science* **335**(6073): 1195-1200.

Yuan, Y. R., Y. Pei, J. B. Ma, V. Kuryavyyi, M. Zhadina, G. Meister, H. Y. Chen, Z. Dauter, T. Tuschl and D. J. Patel (2005). "Crystal structure of A. aeolicus argonaute, a site-specific DNA-guided endoribonuclease, provides insights into RISC-mediated mRNA cleavage." *Mol Cell* **19**(3): 405-419.

Zamore, P. D., T. Tuschl, P. A. Sharp and D. P. Bartel (2000). "RNAi: double-stranded RNA directs the ATP-dependent cleavage of mRNA at 21 to 23 nucleotide intervals." *Cell* **101**(1): 25-33.

Zhang, H., F. A. Kolb, L. Jaskiewicz, E. Westhof and W. Filipowicz (2004). "Single processing center models for human Dicer and bacterial RNase III." *Cell* **118**(1): 57-68.

Zhang, X., G. Wan, F. G. Berger, X. He and X. Lu (2011). "The ATM kinase induces microRNA biogenesis in the DNA damage response." *Mol Cell* **41**(4): 371-383.

Zhao, Y., J. F. Ransom, A. Li, V. Vedantham, M. von Drehle, A. N. Muth, T. Tsuchihashi, M. T. McManus, R. J. Schwartz and D. Srivastava (2007). "Dysregulation of cardiogenesis, cardiac conduction, and cell cycle in mice lacking miRNA-1-2." *Cell* **129**(2): 303-317.

Zheng, K., X. Wu, K. H. Kaestner and P. J. Wang (2009). "The pluripotency factor LIN28 marks undifferentiated spermatogonia in mouse." *BMC Dev Biol* **9**: 38.

Zhou, Y., J. Ferguson, J. T. Chang and Y. Kluger (2007). "Inter- and intra-combinatorial regulation by transcription factors and microRNAs." *BMC Genomics* **8**: 396.

Zilberman, D., X. Cao and S. E. Jacobsen (2003). "ARGONAUTE4 control of locus-specific siRNA accumulation and DNA and histone methylation." *Science* **299**(5607): 716-719.

Zilberman, D., X. Cao, L. K. Johansen, Z. Xie, J. C. Carrington and S. E. Jacobsen (2004). "Role of Arabidopsis ARGONAUTE4 in RNA-directed DNA methylation triggered by inverted repeats." *Curr Biol* **14**(13): 1214-1220.